East Engineering

Journal of Research

of the National Bureau of Standards

NOVEMBER 1963

VOLUME 67 NUMBER 5

U. S. DEPARTMENT OF COMMERCE
Sinclair Weeks, Secretary
NATIONAL BUREAU OF STANDARDS
A. V. Astin, Director

NOVEMBER • 1953
VOLUME • 51
NUMBER • 5

JOURNAL OF RESEARCH

of the

NATIONAL BUREAU OF STANDARDS

PERIODICALS OF THE NATIONAL BUREAU OF STANDARDS

The National Bureau of Standards is engaged in fundamental and applied research in physics, chemistry, mathematics, and engineering. Projects are conducted in thirteen fields: electricity, optics and metrology, heat and power, atomic and radiation physics, chemistry, mechanics, organic and fibrous materials, metallurgy, mineral products, building technology, applied mathematics, electronics, and radio propagation. The Bureau has custody of the national standards of measurement and conducts research leading to the improvement of scientific and engineering standards and of techniques and methods of measurement. Testing methods and instruments are developed; physical constants and properties of materials are determined; and technical processes are investigated.

JOURNAL OF RESEARCH

Internationally known as a leading scientific periodical, the Journal presents research papers by authorities in the specialized fields of physics, mathematics, chemistry, and engineering. Complete details of the work are presented, including laboratory data, experimental procedures, and theoretical and mathematical analyses. Annual subscription: domestic, $5.50; foreign, $6.75.

TECHNICAL NEWS BULLETIN

Summaries of current research at the National Bureau of Standards are published each month in the Technical News Bulletin. The articles are brief, with emphasis on the results of research, chosen on the basis of their scientific or technologic importance. Lists of all Bureau publications during the preceding month are given, including Research Papers, Handbooks, Applied Mathematics Series, Building Materials and Structures Reports, and Circulars. Each issue contains 12 or more two-column pages; illustrated. Annual subscription: domestic, $1.00; foreign, $1.25.

BASIC RADIO PROPAGATION PREDICTIONS

The Predictions provide the information necessary for calculating the best frequencies for communication between any two points in the world at any time during the given month. The data are important to all users of long-range radio communications and navigation, including broadcasting, airline, steamship, and wireless services, as well as to investigators of radio propagation and ionosphere. Each issue, covering a period of one month, is released three months in advance and contains 10 large pages, including pertinent charts, drawings, and tables. Annual subscription: domestic, $1.00; foreign, $1.25.

Order all publications from the Superintendent of Documents
U. S. Government Printing Office, Washington 25, D. C.

The printing of this publication has been approved by the Director of the Bureau of the Budget, May 12, 1953

Journal of Research of the National Bureau of Standards Vol. 51, No. 5, November 1953 Research Paper 2453

Metal Ultrasonic Delay Lines

Russell W. Mebs, John H. Darr, and John D. Grimsley

A study was made of the applicability of a number of metals and alloys for thermally stable ultrasonic delay lines.

A preliminary investigation was made of different types of pressure holders and adhesives for use in crystal transducer attachments and of the influence of specimen length on attenuation for various metals and alloys. The effect of cold-work, annealing, and specimen cross section on attenuation was also determined for a representative isoelastic alloy.

Measurements of temperature variation of signal attenuation, distortion, and delay time on a number of assembled delay lines indicated that an isoelastic alloy employing overcured epoxy-resin crystal attachments gave best over-all transmission characteristics. No correlation was obtainable between strength and sound-transmission characteristics with various cemented joints.

1. Introduction

The ultrasonic delay line has come into wide use in recent years with the development of radar, computers, and other electronic devices [1, 2, 3, 4].[1] It is a means for delaying a signal for a predetermined short period to be accurately reproduced for use at an appropriate later instant. The delay line consists of (a) a transducer for converting the electronic signal to a sound signal, and (b) a suitable medium of appropriate dimensions in contact with the transducer that will transmit the sound signal to a second transducer at the opposite end of the medium, or permit its reflection back to the original transducer; it is then converted to a usable electric signal.

The most common materials now used for delay lines are quartz [1] and mercury [5, 6]. Water, glass, and magnesium alloys have also been used in experimental lines. Where acceleration or changes in temperature of the line may be involved, many of these materials are eliminated from use.

The Metallurgy Division of the National Bureau of Standards was asked by the Ordnance Electronics Division to assist in the search for a more suitable material for delay lines by studies of metals that might be useful for the purpose. Two specific requirements were that it should satisfactorily transmit 10-Mc ultrasonic pulses at temperatures ranging from $-50°$ to $+200°$ C, and possess a negligible temperature coefficient of sound velocity over this temperature range.

2. Elements of High-frequency Sound-Pulse Transmission in Delay Lines

The factors to be considered in the selection of materials for delay lines are (a) the length of delay required, (b) the carrier frequency, pulse length, and pulse shape to be transmitted, (c) the allowable variations in delay time with acceleration or change of temperature to which the line may be submitted, (d) the permitted maximum amounts of pulse attenuation and distortion, and (e) the allowed variations in pulse attenuation and distortion with acceleration or change of temperature.

Only a general survey will be given of the basic theory of ultrasonic transmission as related to delay lines of 50 μsec or less. More comprehensive treatments have been given elsewhere [2, 4, and 5].

2.1 Attenuation

The signals being considered are 10-Mc waves of short pulse length. The attenuation or diminution of the signal in traveling through the delay line is determined by (a) the conversion in the transducers of the electric signal to a sound signal, and vice versa, (b) the efficiency of transfer of the sound signal between transducer and delay line, and (c) the loss in signal strength in passing through the line. Such attenuation is measured in decibels (db) which can be calculated according to formula 1

$$db = 20 \log_{10} \frac{A_o}{A_I}, \tag{1}$$

where A_o and A_I are the output and input signal strengths, respectively. The factors involved in the loss in energy due to conversion between the electric and sound signals in the transducer will not be treated in this discussion.

The efficiency of transmission of the sound wave from the crystal into the delay line, or vice versa, is determined by the intimacy of contact between the crystal and line and by the degree of matching of the acoustic impedances of the crystal and delay line materials. For purposes to be discussed later, the side of the crystal opposite the delay line may be held under pressure by an appropriate material; the acoustic impedance of such material will likewise affect the transmission efficiency of the sound wave between crystal and delay line [2, 4].

The attenuation losses within a metal delay line have been attributed to the elastic hysteresis, the Rayleigh sound scattering, and the sound-diffusion process. The loss due to elastic hysteresis is attributed to an absorption from the sound wave of the energy required for cyclic stressing of the material [7]. This loss is a significant part of the total loss

[1] Figures in brackets refer to the literature references at the end of this paper.

UNIVERSITY OF MICHIGAN LIBRARIES

only at relatively low frequencies in the kilocycle range, being generally proportional to the frequency, whereas the other losses increase much more rapidly.

Sound scattering and diffusion occur only in the megacycle range; they are approximately proportional to the fourth power of the frequency when the grain size of the metal used is somewhat smaller than the sound wavelength and approximately proportional to the square of the frequency when the grain size is somewhat greater than the sound wavelength [8, 9]. Such scattering and diffusion are due to the differences of the elastic coefficients in adjacent grains of the metal in the direction of propagation of the sound wave.

In addition to the principal signal transmitted through the line, there may be echoes caused by reflection of a portion of the signal from line ends and crystal surfaces. These are detected at a later time than the principal signal, and for the proper operation of the delay line in some applications, their amplitude should not exceed a small fraction of the principal signal.

2.2. Distortion

The pulses transmitted through the delay line may not only be attenuated but may also become distorted.

A primary cause of pulse distortion is the superposition upon a weak pulse transmitted directly through the line of additional signals due to portions of the original signal that have been previously scattered and then reflected or refracted to the receiving crystal over a path longer than the direct pulse. Other causes may be attributed to poor contact between crystal and delay line, to improper cutting of the crystals, or to improperly prepared delay lines.

2.3. Effect of Temperature on Delay Time, Attenuation, and Distortion

The velocity of sound within a delay line, and hence the delay time, are determined by the specific physical properties of the material used. The velocities for longitudinal and shear sound waves differ and are expressed as follows:

$$v_{\text{long}}=\sqrt{\frac{E}{\rho}}=\sqrt{\frac{\lambda+2G}{\rho}} \tag{2}$$

$$v_{\text{shear}}=\sqrt{\frac{G}{\rho}}, \tag{3}$$

where E is Young's modulus, λ is the bulk modulus of elasticity, G, the shear modulus, and ρ the density of the material. The longitudinal velocity therefore is greater than the shear velocity.

In the present series of tests, AT and AC cut quartz crystals were used as transducers, and hence only shear waves were produced by the sending crystal. Furthermore, the directly transmitted portion of the signal was normal to the receiving crystal so that there was no transformation to the compressional mode; such transformations are obtained only upon reflection at certain oblique angles.

In the present investigation, emphasis was placed on determining which materials would give the least change in delay time per unit length with change in temperature between −50° and +200° C. The delay time, L_D, of a delay line can be expressed as

$$L_D=\frac{l}{v_{\text{shear}}}, \tag{4}$$

where l is the physical length of the line. From eq (3)

$$L_D=l\sqrt{\frac{\rho}{G}}. \tag{5}$$

Recognizing that l, ρ, and G are all temperature-dependent, and assuming isotropic expansion of a polycrystalline material, it can be shown

$$\frac{1}{L_D}\frac{\partial L_D}{\partial T}+\frac{1}{2l}\frac{\partial l}{\partial T}+\frac{1}{2G}\frac{\partial G}{\partial T}=0. \tag{6}$$

The temperature coefficient of expansion $(1/l)(\partial l/\partial T)$ for most metals is relatively small, and for the alloys of iron and nickel accounts for less than 0.25 percent of the change in delay time over a 250° C range. Thus a satisfactory thermally stable material of this type would be one with nearly zero or small negative temperature coefficient of the modulus $(1/G)(\partial G/\partial T)$ over the required temperature range.

Little study has previously been made of the influence of temperature change on pulse attenuation and distortion. For temperatures ranging up to 200° C, little or no change occurs in the microstructure of many metals. Conversely, cemented crystal attachments may be quite susceptible to temperature change. Therefore, one might expect temperature variation in transducer loss due to change in the nature of the crystal contact with the delay line. In discussing the effect of temperature on attenuation and distortion, a differentiation will be made in this paper between that obtained within the delay line and that obtained at the crystal connections.

3. Test Materials, Specimens, Procedures, and Apparatus

3.1. Materials

The 14 metals and alloys investigated and their compositions and conditions are listed in table 1.

The magnesium alloys were studied as metals known to have good sonic properties and were also employed in the buffer lines to be described later. The high-purity and commercial nickel, Invar, 32 percent-nickel iron and 18:8 chromium-nickel steel were tested to ascertain whether any relationship existed between the nickel content and degree of signal attenuation and distortion obtained. The aluminum single crystal was prepared in the Bureau

TABLE 1. *Chemical composition and condition of the materials used*

Designation	Chemical composition, percentage by weight										Condition
	Fe	Ni	Cr	Mo	Ti	Al	Si	C	Mn	Others	
[illegible] magnesium alloy [a]	0.005 max	0.005 max	----	----	----	2.7	0.3	----	0.3	[b] Mg 95.64 Cu .05 Zn 1.0	Extruded.
[illegible] magnesium alloy [a]	0.005 max	0.005 max	----	----	----	6.5	.3	----	.2	[b] Mg 91.94 Cu .05 Zn 1.0	Extruded.
High-purity nickel [c]	0.032	99.70	----	----	----	----	.10	0.01	.03	Cu .003 S .003	Annealed.
Commercial nickel	0.10	99.49 [b]	----	----	----	----	----	.14	.24	Cu .03	Cold-drawn.
Invar [d]	64.04 [b]	35.96	----	----	----	----	----	----	----	----	Reduced 45 percent in area by cold-drawing.
32-percent-nickel iron [c]	66.35 [b]	31.95	----	----	----	----	.14	.75	.81	----	Reduced 51 percent in area by cold-drawing.
18-8 Cr-Ni steel [a]	72.86 [b]	9.00	18.00	----	----	----	----	.14	----	----	Cold-drawn.
Carbon tool steel [a]	98.4 [b]	----	----	----	----	----	.20	1.20	.20	----	Annealed.
Aluminum	----	----	----	----	----	99.99	----	----	----	----	Single crystal grown by Bridgman method.
Isoelastic A [d]	49.2	41.5	----	9.2	----	----	----	----	.31	----	Reduced 30.5 percent in area by cold-swaging; annealed 1 hr. at 500° C.
Isoelastic B [c]	52.8	36.7	6.8	.56	0.22	----	.62	.096	.45	W .01	Cold-drawn.
Isoelastic C [c]	53.4	37.0	7.0	.06	.18	----	.46	.20	.43	Se .27 W .03	Hot-rolled.
Isoelastic D [d]	47.6	42.79	5.97	----	1.87	.01	.53	----	----	Mg .18	Hot-rolled.
Isoelastic E [c]	51.4	35.6	11.1	----	----	----	----	.11	.17	----	Reduced approximately 50 percent in area by cold-drawing

[a] Type analysis. [b] By difference. [c] Determined by the Analytical Chemistry Section, National Bureau of Standards. [d] Determined by manufacturer.

Metallurgy Division. Of the isoelastic alloys, A was an experimental alloy [10]; B, C, and D were commercial alloys; and E was prepared and cold-rolled in the Metallurgy Division.

3.2. Specimens

Most tests were made on specimens approximately 6 in. long. However, other specimens ranging in physical length from ½ in. to over 6 in. were tested; these permitted the measurement of the attenuation per unit length of a number of materials.

At the beginning of the investigation the specimens used were 0.35 in. in diameter over the central portion, and ½ in. in diameter over a ½-in. length at each end. Pressure holder compression fittings were used with this type specimen for holding quartz crystals directly against the line during test or for mounting cemented crystals before test. Later tests indicated that specimen cross section was of little consequence, providing it exceeded the transducer area. Hence specimens of various sizes were subsequently used, with a ½-in. diameter the most common size.

A special jig was used for specimen preparation. It consisted of a steel cylinder with its two flat ends made effectively parallel by surface grinding. A square hole was carefully machined along its cylinder axis so as to be effectively normal to the end surfaces. Setscrews held the specimen in place during surface grinding and polishing (wet laps). The finished surfaces were flat and parallel within a few ten thousandths of an inch.

3.3. Transducer Assembly

One-quarter-inch square AC and AT cut crystals and ¼-in. round AT cut crystals were used in this investigation [11]. It was found necessary to check all crystals carefully as to uniformity of thickness (a 0.0001-in. variation was permissible) and to indicate the direction of the X-axis. Crystals were obtained with both faces silver-plated.

The compression fitting used for holding a quartz crystal against a line during a test consisted of a laminated plastic pressure holder containing a backing block and a socket-joint screw-tightening arrangement (fig. 1). The backing block was made of lead or steel, with the crystal facing surface being carefully polished. In some tests a 0.0005-in. tinfoil layer was placed between the crystal and specimen. All facing surfaces were refinished between tests. A similar set of compression fittings made of aluminum were found to be unsatisfactory. They added excessive stray capacitance to the circuits.

The following adhesives were used in cementing crystals to the delay lines.

Designation	Type of adhesive
AA	Elevated-temperature thermosetting epoxy cement.
BB	Room- and elevated-temperature thermosetting epoxy cement.
CC	Silver paste.
DD	Silicone.
EE	Bakelite.
FF	Beeswax.

All the adhesives except the beeswax were applied separately to line and crystal and allowed to dry at room temperature or in an oven before assembly. All connections were allowed to set under pressure,

UNIVERSITY OF MICHIGAN LIBRARIES

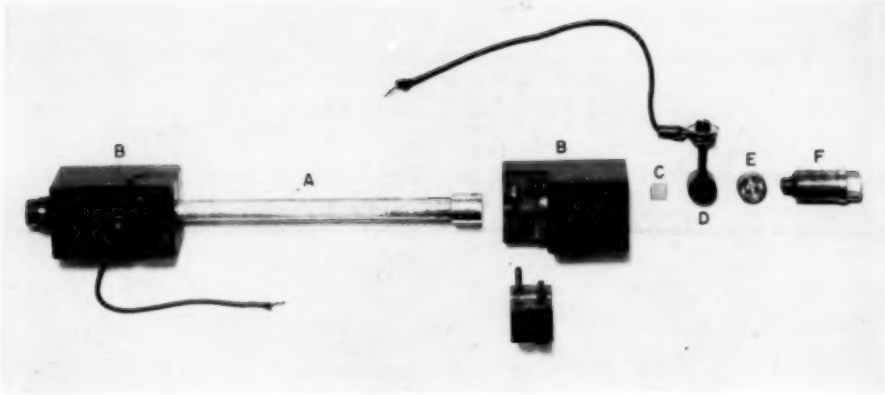

FIGURE 1. *Bakelite compression fittings.*

A, Specimen; B, Bakelite pressure holder; C, crystal; D, backing plate and electrical lead; E, socket plate; F, pressure screw with ball head.

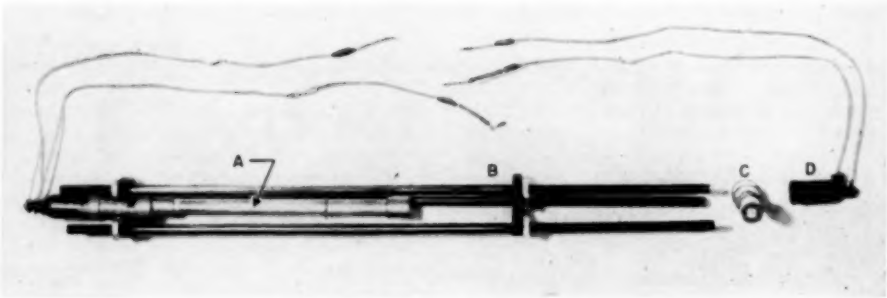

FIGURE 2. *Buffer line assembly.*

A, Specimen; B, clamp holder; C, magnesium-alloy buffer with cement attached crystal; D, shielded brass spring connector with electrical leads.

and additional curing was sometimes given the connection after the pressure was removed. Adhesive AA [12] was set at 170° C or higher before the removal of pressure. Adhesive BB showed a tendency to absorb moisture, which destroyed its sound-transmission qualities. Occasional baking out or storage of the assembly in a desiccator removed this trouble.

Attaching crystals to lines for each test by pressure holders or by cementing was time-consuming. Also after several tests with pressure holders a crystal usually fractured, and cemented crystals could not be salvaged for reuse. Furthermore, transmission efficiency varies with different crystals, and successive tests with compression fittings, using a single pair of crystals, was found to produce sufficient scatter of results to make difficult the measurement of attenuation per unit length on low-loss materials. Hence the buffer technique was developed and used in many tests made at room temperature. This is a modification of the method devised by McSkimin [13]. The two buffers consisted of FS–1 magnesium rods 1½ in. long. The ½-in. length at each end was ½ in. in diameter, and the central portion was 0.35 in. in diameter. Quartz crystals were cemented to one end of each buffer. By means of the special clamp shown in figure 2, the unmounted ends of the two buffers were held under pressure against a specimen of any desired length. It was necessary to lap the ends of the buffers adjacent to the test line between tests, and to regrind these ends whenever erratic test results indicated the need for this operation.

3.4. Electronic Apparatus

Figure 3 is a block diagram of the apparatus used for generating square-wave pulses and for measuring input and output signals for the delay line. A pulse generator capable of producing pulse lengths up to 10 μsec and pulse repetition rates up to 5,000 c/s

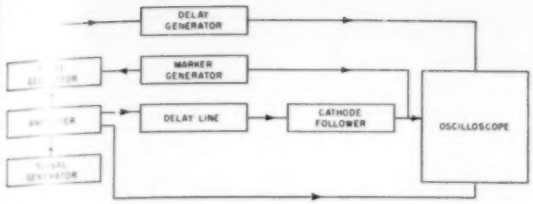

FIGURE 3. *Diagram of test equipment.*

triggered the output of a signal generator adjusted to produce a 10-Mc constant-amplitude wave. The resultant pulsed *hf* (high-frequency) waves were then amplified and fed into the input crystal transducer.

The hf voltage generated in the output crystal transducers was fed through the cathode follower into the cathode-ray oscilloscope where the amplified signal was placed on its vertical plates. The effective output impedence of the delay line is better matched by the input impedence of the cathode follower than by that of the oscilloscope. This permits a more efficient transfer of output energy to the oscilloscope. In some early tests, the cathode follower was not used; a much higher effective signal attenuation thereby was obtained (table 2).

The oscilloscope sweep applied to the horizontal plates is triggered through the delay generator by the pulse generator; the delay generator can be adjusted to retard the sweep by as much as 1,000 μsec. The marker generator, which triggers the pulse generator, also produces small vertical markers every microsecond and larger markers every 10 μsec along the horizontal axis of the oscilloscope screen. An alternate circuit permits placing the input signal on the vertical plates. By accounting for the circuit amplification and attenuation of the various stages, the ratio of output to input signal can be measured by the oscilloscope. A Polaroid-Land camera was used for photographing these signal shapes.

3.5. Measurements at Elevated and Low Temperatures

A nichrome-wound alundum-tube furnace was used. This employed automatic control, providing a temperature that varied less than 5° C over the specimen length as measured by thermocouples attached to the center and ends of the specimen.

Some few tests were made with a shorter 5-in. furnace in which 6-in. test lines had their transducers extending beyond the ends of the furnace. Thus the temperature variation of transmission characteristics of the test material, exclusive of the transducers, could be obtained. All tests were made on specimens with cemented quartz crystals.

In order to obtain subzero temperatures, the test specimen was placed inside and midway as to the length of a thick-walled 1¼-in. copper tube; dry ice was placed around this tube.

The rates of cooling after the application of dry ice and heating upon sublimation of the ice were sufficiently slow to enable accurate measurements of the temperature variation of input and output signal strengths and of delay time. A negligible temperature gradient was obtained along the specimen during these measurements.

4. Effect of Type of Transducer Assembly on the Transmission of Ultrasound in Magnesium Alloy FS–1

Table 2 lists the attenuation values obtained with a 6-in.-long FS–1 magnesium-alloy specimen, using pressure holders or cemented transducers. A torque wrench was used with the pressure holders and the torque adjusted to obtain minimum attenuation; fairly reproducible results were obtained by this method. It is apparent that the use of the cathode follower greatly decreased the attenuation attained.

TABLE 2. *Attenuation at room temperature for various transducer connections on 6-inch-long FS–1 magnesium-alloy lines*

Method of holding crystal against specimens	Pulse length	Attenuation	
		Principal signal	First reflected signal
	μsec	db	db
Steel backing plate	1.0	32.0	42.8
Do	1.0	[a] 53.1	[a] 61.3
Steel backing plate with 0.0005-in. layer of tin foil	1.0	[a] 70.4	------
Lead backing plate	1.0	[a] 57.8	[a] 74.0
Lead backing plate with 0.0005-in. layer of tin foil	1.0	[a] 62.8	[a] 85.8
Adhesive AA	1.0	30.5	36.7
Do	1.0	[a] 47.2	[a] 52.3
Do	2.8	28.4	------
Adhesive AA with lead backing plates and 10-in.-lb torque on pressure holder	1.0	34.1	48.8
Adhesive BB	1.0	[a] 45.8	[a] 58.9
Beeswax FF	1.0	[a] 59.8	[a] 67.8

[a] These lines were tested with output connected directly to oscilloscope, remaining lines were tested with output connected through cathode follower to oscilloscope.

Examination of results indicates that lines cemented with adhesives AA or BB gave the lowest attenuation of the principal pulse. The use of beeswax FF as a crystal adhesive resulted in a fairly large attenuation. Although a fairly high attenuation was obtained with the lead-backed crystals when 0.0005-in. tinfoil was inserted between crystal and line, successive echoes on this line were greatly diminished in comparison with the lines without the foil. The echoes obtained with the line cemented with adhesive AA were somewhat larger than those obtained with any combination of holder and backing plates. Furthermore, when a crystal cemented with adhesive AA was placed in a pressure holder and held with lead backing plates, the attenuation of the principal pulse was increased only a few decibels, whereas the first echo attenuation increased by about 12 db.

Of particular interest in these tests is the effect of transmission on wave shape. There are three general methods of evaluation of this effect, namely, (a) the visible change, as noted on the oscilloscope and which can be photographed; (b) the range of frequencies over which the amplitude of the principal

UNIVERSITY OF MICHIGAN LIBRARIES

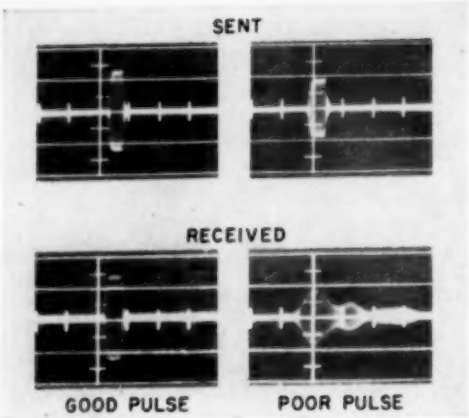

FIGURE 4. *Representative oscillograms for sent and received pulses for good and poor pulse reproduction.*

received pulse does not vary more than a fixed percentage of its maximum value for a given length of pulse; and (c) the minimum pulse length at which the maximum signal strength can be secured. Photographs of satisfactory and unsatisfactory reproductions of transmitted pulses are shown in figure 4.

Qualitatively, the use of lead backing plates on lines with tinfoil between crystal and line gave excellent reproduction. The same combination without tinfoil gave fairly good reproduction. The quality of reproduction was successively poorer in the steel-backed lines, the adhesive AA cemented lines, the adhesive BB cemented lines, and the beeswax FF cemented lines.

In addition to careful control of crystal quality, such factors as cementing technique or design of pressure holders and careful adjustment of pressure were studied in order to secure best sound transmission.

The efficiency of transmission of ultrasound by a given transducer assembly is also dependent on the structure, density, and other physical properties of the delay-line material as well as on the test temperature.

5. Effect of Composition and Specimen Length on the Transmission of Ultrasound

The buffer technique (fig. 2) was employed in this portion of the investigation. The pulse length employed was the minimum that would maintain maximum amplitude of the principal received pulse. This is hereafter referred to as the optimum pulse length.

Figure 5 shows the relationship between attenuation and length for the various materials investigated. The slope of each curve is a measure of the attenuation per unit length of that material. The intersection of each curve with the ordinate axis represents the total attenuation in the two buffers and in the interfaces between the buffers and the

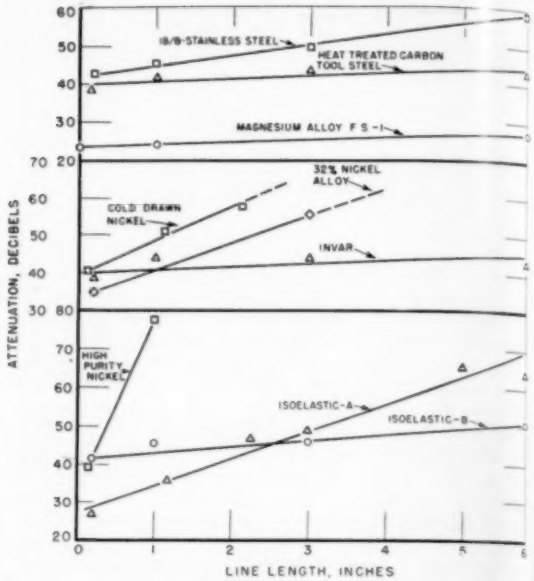

FIGURE 5. *Variation of attenuation with line length for metals and alloys tested by buffer-technique method.*

test material, and is referred to as the buffer loss. It is not the same for all materials due to differences in their physical properties and structure relative to that of the buffer material. Table 3 lists the buffer loss and the attenuation loss per inch length of a number of materials tested.

TABLE 3. *Attenuation at room temperature of various materials as obtained by buffer-line technique*

Material	Attenuation	
	Per inch of length	Buffer
	db	*db*
FS–1 magnesium alloy	0.52	24.0
Annealed high-purity nickel	44.0	33.0
Cold-drawn commercial nickel	16.0	28.2
Invar	0.86	40.0
32-percent-nickel iron	7.2	33.6
18:8 Cr-Ni steel	2.8	42.0
Spheroidized carbon tool steel	3.1	38.7
Quenches and tempered carbon tool steel	0.72	39.8
Isoelastic A	7.1	27.3
Isoelastic B	1.6	41.2
Isoelastic C	3.4	38.0
Isoelastic D	4.7	35.2

The quenched and tempered 1.2-percent-carbon tool steel and Invar provided values of attenuation per unit length similar to magnesium FS–1 alloy, though exhibiting higher buffer losses. Isoelastic alloy B and 18:8 Cr–Ni steel gave greater values of attenuation per unit length with buffer losses comparable to the hardened tool steel and Invar. Commercial cold-drawn nickel, 32-percent-nickel iron, and isoelastic alloy A showed still greater values of attenuation per unit length and also exhibited buffer losses

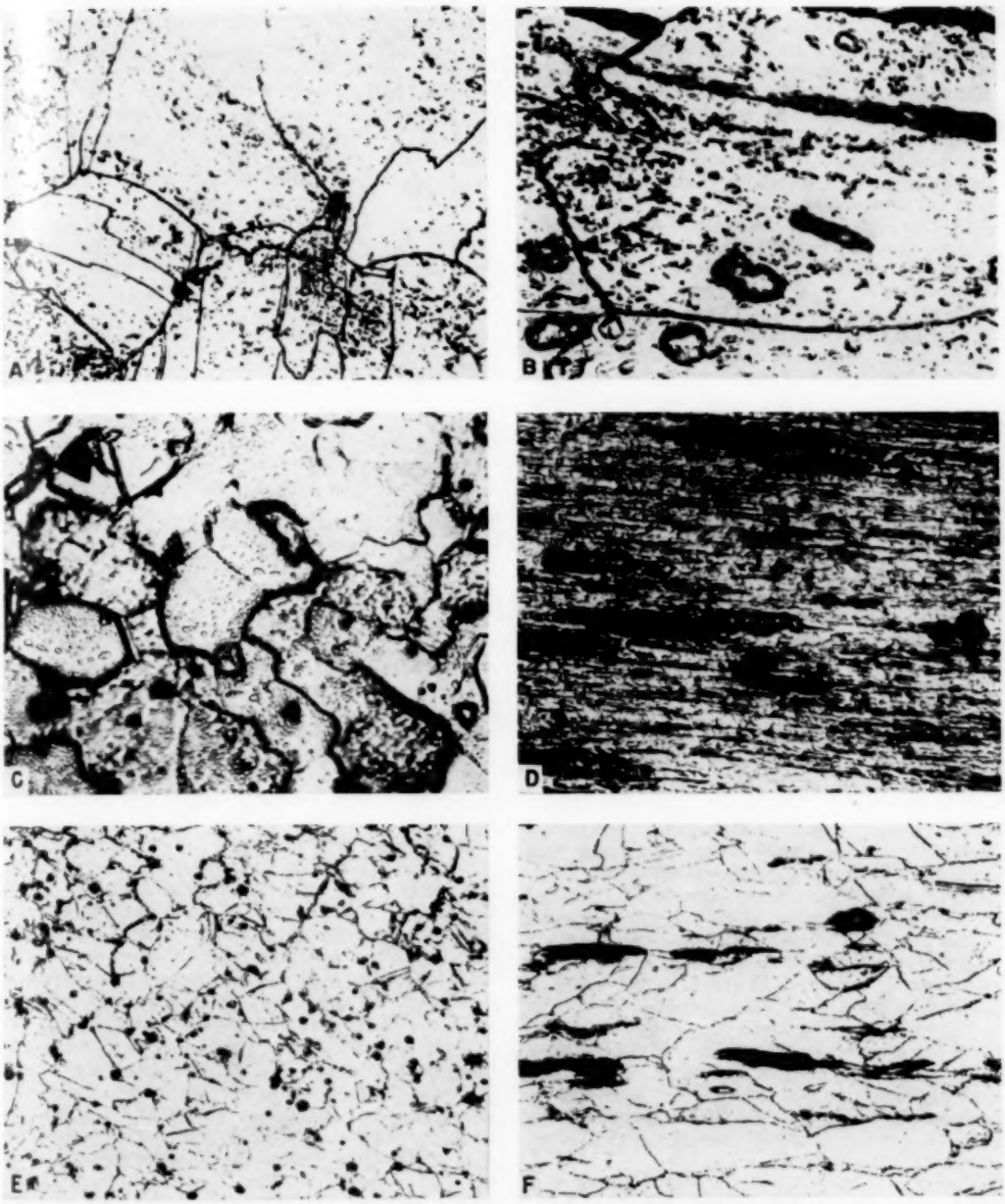

FIGURE 6 *Micrographs of structure of various materials.* ×500

A. Cold-rolled 36% nickel, 12% chromium, 52% iron alloy E, cross section, etched in Precision No. 2 reagent. The rather complex formula and method of preparing this reagent have been described in [14]. B. Cold-rolled 36% nickel, 12% chromium, 52% iron alloy E, longitudinal section, etched in Precision No. 2 reagent. C. Annealed high-purity nickel, longitudinal section etched in 6 parts of nitric (conc.) and 4 parts of glacial acetic acid. D. Cold-drawn isoelastic alloy B, longitudinal section, etched in 1 part of ferric chloride, 10 parts of hydrochloric acid and 20 parts of water. E. Hot-rolled isoelastic alloy C, cross section, etched in Precision No. 2 reagent. F. Hot-rolled isoelastic alloy C, longitudinal section, etched in Precision No. 2 reagent.

UNIVERSITY OF MICHIGAN LIBRARIES

lower than Invar. High-purity nickel was the poorest transmitter of sound of the materials shown, although it did not show a correspondingly high value of buffer loss.

A short length of alloy E was found to give extremely high values of attenuation, as did the single crystal of aluminum. Attenuation per unit length could not be evaluated for these two materials.

A study of figure 5 and table 3 reveals that no general relationship exists between nickel content and attenuation per unit length for the respective metals and alloys. Factors such as other constituents, degree of cold work, and grain structure must also be considered as important. The isoelastic alloy E (fig. 6 A and B) and the high-purity nickel (fig. 6, C) both possessed large grains, which may account, in part, for the high attenuation per unit length obtained. The very low attenuation per unit length of the quenched and tempered carbon tool steel can be attributed to its structure; when annealed, the tool steel was found to give a somewhat higher value. Of the commercial isoelastic alloys tested, alloy B was cold worked a greater amount, with the accompanying refinement of its structure (fig. 6, D), than was alloy C (fig. 6, E and F). This, accordingly, might be presumed to be a prime factor for the low attenuation for alloy B. However, a few tests on another heat of hot-worked alloy C with a structure similar to that of figures 6, E and F, indicated this material to have as low attenuation per unit length as alloy B.

6. Effect of Cold Deformation, Annealing Treatment, and Sound-Path Cross Section on the Attenuation of Ultrasound

A rather extensive study was made of the ultrasonic properties of isoelastic alloy A during this investigation. This material was received in ¼-in.-diameter size, having been cold-reduced 30.5 percent and stress-relief annealed at 500° C during manufacture. This material, as received, possessed a rather large attenuation per unit length and a low buffer loss, as shown in curve 1, figure 7 (also shown in fig. 5). Full annealing of this material tended to raise the attenuation length curve, as show in curve 2. When the as-received material was cold-swaged to 0.165-in. diameter, that is, to a total cold reduction of 70 percent, an appreciable rise occurred in the attenuation values (curve 3). Stress-relief annealing of the swaged material caused a slight lowering of attenuation (curve 4).

In order to determine whether the increase of attenuation was due to the actual cold-working of the material or whether it was due to the reduction effective cross section of the sound path, some of the as-received material was machined to 0.165-in. diameter. Curve 5 for the machined material lies between curves 1 and 4, and thus indicates that the rise in attenuation of the swaged material was partly due to the effect of cold-working and partly to reduction of cross section.

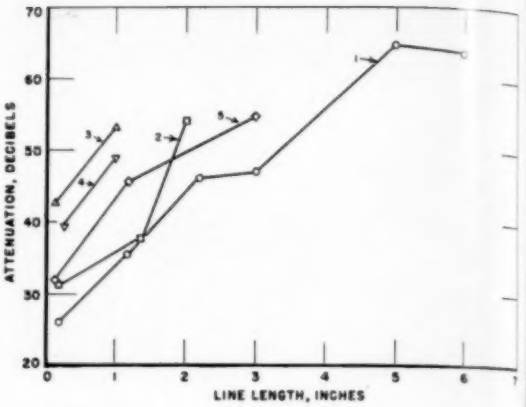

FIGURE 7. *Influence of annealing treatment and additional cold-swaging on the attenuation-length characteristics of isoelastic alloy A.*

Curve 1, as received (cold-swaged to 30.5% reduction of area and stress-relief annealed, 0.250-in. diameter); curve 2, fully annealed (0.250-in. diameter); curve 3, additionally cold-swaged to a total of 70% reduction of area (0.165-in. diameter); curve 4, additionally cold-swaged to a total of 70% reduction of area (0.165-in. diameter) plus stress-annealed at 400° C for 1 hour; curve 5, as received, and machined to 0.165-in. diameter.

It should be noted in this group of curves, however, that all except the curve for the annealed alloy possess nearly the same slope for the portion lying between zero and 1 in. in length, which is the extent of some of the upper curves. Thus the principal difference in attenuation values for these curves can be attributed to a difference in buffer loss. The principal effect of the additional cold-swaging, therefore, exclusive of the effect of reduction of cross section, was its apparent effect on the transmission characteristics of the buffer-specimen interface, i. e., the additional cold-working evidently tended to impede the transmission of sound between such surfaces. The increase in buffer loss by full annealing indicates that optimum sound-energy transfer occurred at the interfaces when this material had been only moderately cold-worked and stress-relief annealed (compare curves 1 and 2).

In the above tests, specimen diameters varied from 0.25 to 0.165 in., thereby affecting somewhat the sound-transmission efficiency, inasmuch as the effective sound-path cross section at the input crystal could be as great as ¼ in. sq. Some tests were therefore made to determine the effect of increasing specimen cross section beyond that of the crystal on the sound-transmission efficiency. One-inch-long specimens of magnesium alloy J–1 were machined to diameters ranging from ¼ to ½ in. and tested between buffer lines. A maximum of only 3-db variation of attenuation was obtained in these tests, with no regular variation with diameter. Therefore, the effect of specimen cross section exceeding the crystal area evidently does not have a significant effect on the efficiency of sound transmission.

7. Effect of Temperature on the Attenuation of Ultrasonic Pulses in Various Materials

Tests were conducted to determine the effect of temperature on both the delay-line material and the transducer connections attached to the delay line. Figures 8 and 9 show the variation of attenuation with temperature of various assembled delay lines. The pulse lengths are indicated in the legend of each figure. With the exception of curve 3 of figure 9, the optimum pulse length was employed.

Figure 8 provides a comparison of various combinations of cements and curing conditions on 6-in.-long alloy B delay lines. In a preliminary test, employing the shorter 5-in. furnace, with transducer connections extending outside the furnace, the attenuation was found to show negligible variation, except for a small decrease at 120° C (curve 1). Thus a temperature change of the delay-line material, in the range shown, caused little variation of attenuation—the transducer connection probably is the chief element affected. Later tests with the shorter furnace on a similar specimen, with cooling air blasts directed at the transducers, indicated a lowering of attenuation by as much as 8 db at the higher temperatures. Such evidence suggests that the attenuation per unit length of the test alloy actually diminishes at higher temperatures.

The remaining curves in these figures were obtained with the entire delay line situated in the longer furnace. When adhesive AA was used with the recommended 200° C curing temperature, a sharp rise of attenuation (curve 2) occurred at elevated test temperatures in contrast to the less abrupt rise obtained after overcuring at 275° C (curve 3).

Curves 4 and 5, obtained with adhesive BB, cured at the optimum temperature [2] of 280° C for this cement, show the variations of attenuation as obtained with the principal signal and the first reflection. Although a small temperature variation of attenuation is secured, the strong reflected signal and the large pulse length required for maximum signal are both deterring factors for satisfactory ultrasonic pulse transmission in such a delay line. Somewhat shorter optimum pulse lengths were obtained with adhesive AA (curves 2 and 3).

Curve 6, obtained with silver-paste adhesive CC, indicates remarkably small variation of attenuation with temperature and a low level of attenuation, although requiring a long pulse length for optimum transmission.

Curves 7 and 8, obtained with silicone adhesive DD, illustrate the flattening of the attenuation-

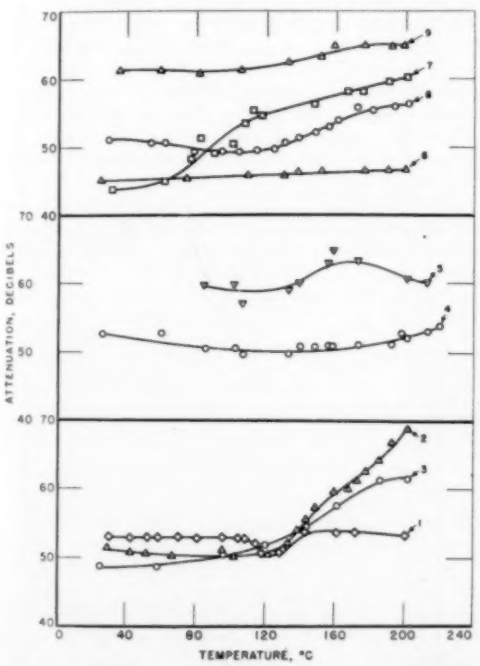

FIGURE 8. *Influence of temperature on attenuation of 10 megacycle ultrasonic pulses in isoelastic alloy B, crystals cemented as indicated. Measurements made for initial received signal with entire line at indicated temperature, except curve 1.*

Curve 1, 6-in. line, adhesive AA, cured 200° C, tested in 5-in. furnace, optimum pulse length exceeds 10 microseconds; curve 2, 6-in. line, adhesive AA, cured 200° C, optimum pulse length 2.5 to 6.8 microseconds; curve 3, 6-in. line, adhesive AA, cured 275° C after test 2, optimum pulse length 2.75 to 5.4 microseconds; curve 4, 5.3-in. line, adhesive BB, cured 280° C, optimum pulse length 5.4 microseconds; curve 5, first reflection of test 4; curve 6, 5.3-in. line, adhesive CC, cured 350° C, optimum pulse length exceeds 10 microseconds; curve 7, 5.3-in. line, adhesive DD, cured 250° C, optimum pulse length exceeds 10 microseconds; curve 8, 5.3-in. line, adhesive DD, cured 350° C after test 7, optimum pulse length exceeds 10 microseconds; curve 9, 5.3-in. line, adhesive EE, optimum pulse length exceeds 10 microseconds.

[2] The optimum temperature for any cement is that minimum curing temperature resulting in the least temperature variation of attenuation.

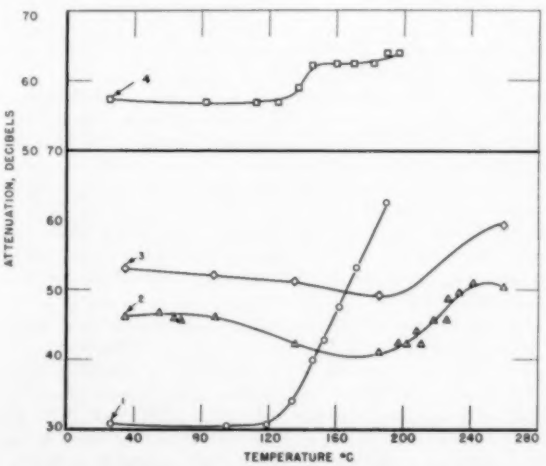

FIGURE 9. *Influence of temperature on attenuation of 10 megacycle ultrasonic pulses of designated length in various delay lines, crystals cemented as indicated. Measurements made for initial received signal with entire line at indicated temperature.*

Curve 1, 6-in. F8-1 magnesium-alloy line, adhesive AA, cured 200° C, optimum pulse length 1 microsecond; curve 2, 6-in. F8-1 magnesium-alloy line, adhesive BB, cured 200° C, optimum pulse length exceeds 10 microseconds; curve 3, same as test 2 with pulse length 3.7 microseconds; curve 4, 6-in. isoelastic-alloy C line, adhesive BB, cured 200° C, pulse varies 0.8 to 1.4 microseconds.

UNIVERSITY OF MICHIGAN LIBRARIES

temperature curve by elevating the curing temperature of this adhesive from 250° to 350° C. However, curve 8 lies somewhat above curve 6 and was obtained with a larger optimum pulse length than was curve 4. The apparent plastic condition of silicone cements, even at elevated temperatures, obviously detracts from their usefulness for transducer connections in delay lines. Curve 9, for Bakelite cement EE, indicates a fairly high attenuation with a low temperature variation. A fairly long pulse length is required.

Figure 9 shows the variation of attenuation with temperature for additional materials. Curves 1, 2, and 3 were obtained with FS–1 magnesium alloy. Adhesive AA cured at 200° C (curve 1) provides a fairly short optimum pulse length, although producing a large variation of attenuation with temperature above 120° C. Adhesive BB, cured at 200° C, gave a smaller variation of attenuation, although it had a somewhat higher room-temperature value. The rise in attenuation produced by shortening the pulse length from its optimum value of 10 μsec (curve 2) to 3.7 μsec is shown in curve 3. Data for these latter two curves were obtained during a single temperature-attenuation test. For this reason, curve 3 between the points at the two highest temperatures is drawn approximately parallel to curve 2.

Curve 4 is for isoelastic alloy C with adhesive BB. A small rise of attenuation occurs at about 150° C.

Additional tests were made on other delay lines with similarly cemented crystals for temperatures ranging to as low as −60° C. Negligible variations in attenuation were noted below room temperature; these curves are not plotted.

It is evident from the above results that perhaps the principal variable in the efficacy of ultrasonic transmission in the isoelastic alloy delay lines is the transducer assembly. It was therefore considered of some interest to determine whether any relationship existed between the mechanical strength and sound-transmission efficiency of the cements for the various curing temperatures employed.

Some mechanical tests were made in which carbon-steel tensile specimens were cut in two, the cut surfaces being carefully polished and rejoined with the various adhesives by the same methods employed in attaching crystals to delay lines. These specimens were then tested in tension.

Maximum tensile strengths were obtained with joints of adhesives AA and BB, when cured at 130° and 150° C, respectively. It will be recalled that the optimum curing temperatures for these cements for best signal transmission were 275° and 280° C, respectively. At these latter temperatures, the mechanical strengths of the joined bars were appreciably lower than maximum. It was also observed that silver-paste adhesive CC, which gave low signal attenuation, possessed quite low mechanical strength at all curing temperatures.

Evidently high strength and optimum signal transmission are not synonymous. The higher curing temperature, though probably causing a more brittle and weaker joint, may provide in such brittleness better signal transmission qualities. Thus the development of good transducer connections becomes purely empirical, inasmuch as the sound and mechanical properties of these elements cannot be correlated.

8. Effect of Temperature on the Delay Time of Ultrasonic Pulses in Various Materials

Figure 10 shows the influence of temperature on delay time, or time of transmission, of 10-Mc ultrasonic pulses in assembled delay lines of various materials. Some of these tests were extended to subzero temperatures. The FS–1 magnesium-alloy line showed the greatest change in delay time with temperature. Of the isoelastic alloys tested, alloy C alone shows no variation in delay time up to the highest test temperature, 194° C. The delay time for alloy B does not change up to 180° C, but rises thereafter. The delay time for alloy D rises gradually with temperature up to 130° C, above which it is nearly constant.

The sensitivity of measurement of delay time in these tests was approximately 0.1 μsec. For a 50-μsec delay line, the limiting variation of the temperature coefficient of delay, measurable over a 200° C range is 10 parts per million. Thus for alloy C, this coefficient evidently is 8 parts per million or smaller. By comparison, the temperature coefficient of delay for the FS–1 magnesium-alloy line averages about 380 parts per million over the test temperature range.

The small change in delay time above 180° C observed with isoelastic alloy B may not be due to an actual change in properties of the alloy. A rather poor received-pulse shape was obtained with this material; it is possible that a change in pulse shape at the upper temperature levels due to some change

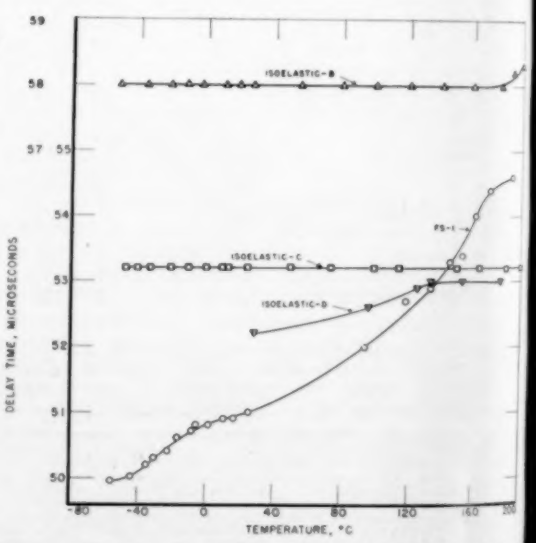

FIGURE 10. *Influence of temperature on delay time for delay lines of various materials.*

in the properties of the adhesive might effect a shift in position of the received-pulse peak and thus effectively change the measured values of delay time.

9. Delay-Line Characteristics

The results of the above tests indicate limitations as to the optimum delay-line characteristics obtainable. Whereas a magnesium delay line may provide satisfactory attenuation and pulse-reproduction characteristics, its delay time varies appreciably with temperature. Constancy of delay time with low attenuation is most nearly fulfilled by isoelastic alloys B and C; alloy C exhibits no measurable temperature variation of delay time. When crystals are attached to an isoelastic alloy C delay line with adhesive BB and cured at 200° C, a reasonably high attenuation is secured (fig. 9, curve 5) that is nearly independent of temperature. In order to obtain a temperature invariant attenuation at a lower loss level, as typified by curves 4, 6, and 8 of figure 8 for isoelastic alloy B, it is necessary to use delay lines that produce greater signal distortion and thus require a greater pulse length for optimum transmission. These tests would indicate that for these alloys a low attenuation is not compatible with a short optimum pulse length.

The number of variables that affect sound transmission make it difficult to provide a simple explanation of the occurrence of the above relationships. Some of these variables are (a) the damping of the crystals by the cements and delay line, (b) the effect of a poorly damped resonating crystal on signal distortion, (c) the relative acoustic impedances of crystals and line materials, and (d) the influence of the cement-layer characteristics on the sound transmission. Possibly other variables affect these relationships, necessitating an empirical study of each crystal, cement, and material combination in order to determine their suitability for use in delay lines.

These tests indicate that the transducer assembly is the greatest variable in obtaining satisfactory delay-line transmission over a wide temperature range.

A primary requirement is a thermally stable cement layer of suitable transmission characteristic. Even with an ideal cement, transmission is limited by the matching of the acoustic impedance of the crystal and delay line.

10. Conclusions

From measurements made of the transmission of 10-Mc ultrasonic pulses in various metals and alloys, the following conclusions may be drawn:

1. The most efficient of the methods employed for conversion of electrical energy into sound energy within a delay line, and vice versa, is to attach quartz crystals to the delay line by an epoxy-type cement. The best reproduction of the principal transmitted signal wave shape, however, was obtained by use of laminated plastic pressure holders in which the quartz crystals were backed up with lead blocks and separated from the line by tinfoil. This latter attachment method also produced the smallest reflected signals.

2. The attenuation per unit length of a material is best measured by the buffer test method. It varies from a very small value for the FS–1 magnesium alloy to very high values for annealed high-purity nickel and a single crystal of aluminum. The buffer loss ranges from small values for the FS–1 magnesium alloy to somewhat higher values for the isoelastic alloys, Invar, and 18:8 Cr-Ni steel.

3. Although very coarse-grained materials presumably give a high attenuation loss, such losses do not show a fixed relationship with grain size for the finer structure commercial isoelastic alloys.

4. Although pure nickel possesses a high attenuation per unit length, there is no regular variation of attenuation with nickel content. Invar, a 36-percent-nickel iron alloy was found to have an attenuation per unit length of the same magnitude as magnesium FS–1 alloy and quenched and tempered 1.2-percent-carbon tool steel.

5. In tests on the effect of cold-work and annealing on one of the isoelastic alloys, it was determined that the attenuation per unit length was not affected; however, the buffer loss was the lowest at an intermediate stage of cold-work.

The increase in buffer loss of the severely swaged isoelastic alloy was due only partly to the change in structure of the material, being also due partly to the reduction in cross section of the material. Where the cross-sectional area of the specimen exceeded that of the crystal, the effect of change of section could not be detected.

6. Of the various metals and alloys tested, two commercial isoelastic alloys, of different manufacture, were found to possess the least variation of delay time with temperature over the range −50° to +200° C. Both alloys contained approximately 36 percent of nickel, 7 to 8 percent of chromium, plus other minor constituents. The variation of over-all attenuation with temperature for these alloys was found to be due primarily to the transducer assembly employed; a small decrease of internal attenuation with rise in temperature was indicated on one of these materials. A negligible variation of attenuation with temperature up to 200° C, at a low attenuation level, was secured by cementing the crystals to the more severely cold-worked of these two alloys with a silver-paste cement or one of the proprietary epoxy-type cements that had been overcured after attachment.

For the isoelastic alloys low attenuation was found to be incompatible with short optimum pulse length for any of the transducer connections tested. The limitations of obtaining good transmission apparently are associated with the characteristics of the cements and the relatively poor impedance match of quartz crystals with isoelastic alloys.

Somewhat higher curing temperatures were necessary for producing cemented joints having best transmission qualities, than for procuring maximum mechanical strength.

7. Although the buffer technique presents a rapid means for determining which metals possess a low

UNIVERSITY OF MICHIGAN LIBRARIES

attenuation per unit length or low transducer losses at room temperature, the more tedious procedure of empirical determination of crystal, cement, and metal delay line combinations tested over the temperature range to which the delay line will be subjected, is necessary for satisfactory development of such lines.

Grateful acknowledgment is extended to W. M. A. Andersen of the Andersen Laboratories, Inc.; to M. E. Fine and W. C. Ellis of the Bell Telephone Laboratories; to W. A. Mudge and E. M. Wise of the International Nickel Co.; and to C. H. Fetter of the American Time Products, Inc., for technical advice and for furnishing some of the isoelastic alloys investigated. The authors are also indebted to W. E. Eberly, Carpenter Steel Co. for cold-drawing the 32-percent-nickel iron alloy and for furnishing the Invar alloy. Many thanks are due the following members of the staff of the National Bureau of Standards: L. T. Sogn, for providing much technical information on quartz crystals; T. E. Orem, for the aluminum single crystal; and R. H. Harwell, for preparing isoelastic alloy E. The authors also acknowledge the extensive assistance and advice provided this work by E. Voznak of the Ordnance Electronics Division, the sponsoring agency.

11. References

[1] David L. Arenberg, Ultrasonic solid delay lines, J. Acous. Soc. Am. **20,** 1 (1948).

[2] Crystal Research Laboratories Interim Engineering Reports, Contract W28–009 and W28–110 (July 1946 to December 1948).

[3] A. G. Emslie and R. L. McConnell, Radar system engineering, **1,** chap. 16 (McGraw-Hill Book Co., Inc., New York, N. Y., 1947).

[4] H. B. Huntington, A. G. Engle, and V. W. Hughes, Ultrasonic delay lines, J. Franklin Inst. **245,** 101 (1948).

[5] A. E. Benfield, A. G. Emslie, and H. B. Huntington, On the theory and performance of liquid delay lines, MIT Radiation Laboratory Report 792 (September 21, 1945).

[6] I. L. Auerbach, J. P. Eckert, R. F. Shaw, and C. B. Sheppard, Mercury delay line memory using a pulse rate of several megacycles, Proc. IRE **37,** 855 (1949).

[7] R. L. Wegel and H. Walther, Internal dissipation in solids for small cyclic strains, Physics **6,** 141 (1935).

[8] W. P. Mason and H. J. McSkimin, Attenuation and scattering of high frequency sound waves in metals and glasses, J. Acous. Soc. Am. **19,** 464–473 (1947).

[9] W. P. Mason and H. J. McSkimin, Energy losses of sound waves in metals due to scattering and diffusion, J. Appl. Phys. **19,** 940–46 (1948).

[10] M. E. Fine and W. C. Ellis, Thermal variation of Young's modulus in some Fe-Ni-Mo alloys, Trans. AIME **191,** 761 (1941).

[11] W. P. Mason, Piezo-electric crystals and their application to ultrasonics, chap. XV (D. Van Nostrand Co., Inc., New York, N. Y., 1950).

[12] A new bonding resin, detailed results of laboratory tests on araldite, Sheet Metal Ind. **26,** 1966–1988 (1949).

[13] H. J. McSkimin, Ultrasonic measurement technique, J. Acous. Soc. Am. **22,** 413–18 (1950).

[14] Charles T. Flachbarth and Chester S. Pondo, Three new etchants for nonferrous metals, Metal Progr. **56,** 688–691 (1949).

WASHINGTON, June 8, 1953.

Journal of Research of the National Bureau of Standards Vol. 51, No. 5, November 1953 Research Paper 2454

A Radio-Frequency Permeameter

Peter H. Haas

An instrument is described, which, in connection with commercially available impedance measuring devices, is capable of measuring the permeability and losses in ferromagnetic toroidal cores. The measurement is made by inserting a toroidal core into the short-circuited secondary of a transformer whose primary is attached to a radio-frequency bridge or Q meter. Equations are derived for the measurements, the accuracy and sensitivity are discussed, and typical construction details are given. Finally, a modification of the device enabling the measurement of permeability temperature coefficients is discussed.

1. Definition of Symbols

L_1 = Input inductance with the top cover removed.
C_1 = Capacitance read on a Q meter, admittance bridge or parallel condenser with the top cover removed.
L_0 = Input inductance with the top cover shorting the secondary.
C_0 = Capacitance with the top cover shorting the secondary.
L_f = Input inductance with the test sample inserted.
C_f = Capacitance with the test sample inserted.
R_1, R_0, R_f = Series resistances corresponding to the above conditions.
G_1, G_0, G_f = Parallel conductances corresponding to the conditions.
Q_1, Q_0, Q_f = Values of the storage factor Q read on a Q meter corresponding to the above conditions.
L_{01}, R_{01}, C_{01} = $-L_1$–L_0, R_0–R_1, C_0–C_1, respectively.
L_{1f}, R_{f1}, C_{f1} = L_1–L_f, R_f–R_1, C_f–C_1, respectively.
L_{f0}, C_{0f} = L_f–L_0 and C_0–C_f, respectively.
V_1 = Voltage applied across the primary terminals of the permeameter.
e_{oc2} = Voltage appearing across the open-circuited secondary with V_1 across the primary.
μ_0' = Initial permeability.
$\tan \delta_m$ = Magnetic dissipation factor. (Note: $\tan \delta_m/\mu_0' = 1/\mu_0' Q$).

The symbols R and L used in the introduction denote the equivalent series resistance and inductance of a core, respectively.

The units used are those defined in the rationalized MKS system, i. e., henries, farads, ohms, and mhos, for inductance, capacitance, resistance, and conductance, respectively.

2. Introduction

With increasing use of magnetic cores at radio frequencies coupled with more stringent demands in communications equipment, it has become more important to accurately evaluate the behavior of core materials in the frequency and temperature range in which they are to be used. At the same time, mass-production methods demand a simple and rapid check for quality-control purposes. In addition to these requirements, some of the newer materials, with their wide spread of permeabilities, have made older testing methods either inaccurate or insensitive. The instrument described was designed to fill the need for a quick testing method of moderate accuracy over the greater part of the range of permeabilities currently available at radio frequencies below 20 Mc/s. With proper caution, this frequency limit may well be exceeded.

It is desired to measure the complex initial permeability

$$\mu_0^* = \mu_0' - j\mu_0'',$$

where μ_0' is the quantity usually called simply the initial permeability, and μ_0''/μ_0' is the initial dissipation factor, $\tan \delta_m$. Initial permeability is that value of μ' measured on a previously demagnetized sample with such low field strengths that no change is noticed when the field is reduced still further. The initial dissipation factor $\tan \delta_m$ is measured under the same conditions. Ideally, it therefore does not contain any losses caused by hysteresis and its resistive component is not a function of the field. It may be noted that Legg's loss factor, L, [1][1] equals [2]

$$\frac{R}{\mu_0' f L} = \frac{2\pi \tan \delta_m}{\mu_0'}.$$

In the past many laboratories have used a method of measurement in which toroidal cores have a number of turns of wire placed upon them. An impedance bridge or Q meter is then used to measure the effective inductance and resistance, and the permeability is calculated from these values and the known geometry of the core. When all the losses not contributed by the core are deducted, one can also calculate the dissipation factor. This method, while cumbersome because of the labor involved in the toroidal winding process, is accurate enough if all the factors contributing to errors are taken into consideration. Some of these factors are:

1. At higher frequencies it is necessary to reduce the number of turns to a minimum, so that the reactance of the ring will fall within the measurable reactance range of an impedance bridge or within the capacitance range of a Q meter. This, in the case of low- and medium-permeability materials, leads to an error because of violation of the uniform-current-sheet assumption.

2. Some of the newer core materials, especially those with high permeabilities, are known to exhibit high dielectric constants as well as high dielectric losses. If the product of permeability and dielectric

[1] Figures in brackets indicate the literature references at the end of this paper.
[2] See appendix III for definitions of symbols.

constant is sufficiently high, a large percentage of a wavelength may exist even at low frequencies in a dimensionally small core. The errors caused by this effect can be very large. This case and the correction of the errors involved are admirably well discussed in the literature [2]. There is, however, even for fairly low dielectric constants, the additional problem caused by displacement currents between windings separated by the core material. This causes the inductance that would actually be present if the material had unity permeability and the dielectric constant found in a ferromagnetic core to differ from the inductance L_a (see appendix II) calculated from the core dimensions and the number of turns.

A simple method used primarily in the powdered-iron fields yields the effective permeability, μ_{eff}, and dissipation factor, $\tan \delta_{eff}$, of slugs. One simply notes the change of inductance or resonating capacitance caused by the insertion of a rod into a standard coil. Although it is sometimes possible to evaluate the true material constants μ_0' and $\tan \delta_m$, given the length to diameter ratio, this ratio must be unreasonably large to obtain satisfactory sensitivity for permeabilities of several hundred and higher.

A third method used at the National Bureau of Standards and other laboratories to obtain the highest accuracies involves the use of thin annular disks accurately ground or machined from the core material. These are inserted into a coaxial line whose impedance changes are measured. From the viewpoint of accuracy this is a highly satisfactory method. The aforementioned errors either do not apply or their elimination or correction is relatively simple. However, the method suffers from a number of drawbacks. As mentioned above, the sample must be prepared with the highest precision. The test is destructive insofar as the sample is not usually of a shape usable in application. Furthermore, special, low-impedance measuring instruments are often required for the measurements.

3. Description of the Radio-Frequency Permeameter

Inasmuch as the requirements for an accurate coaxial line measurement are somewhat stringent, there exists a need for a method of lesser accuracy for use in conjunction with commercially available measuring instruments. The test samples employed should be readily available without any need for accurate shaping and ideally, ought to be usable in applications. It is believed that the method here described meets these requirements. In 1924, G. A. Kelsall developed an instrument to measure the permeability of core materials at power-line and low audiofrequencies [3]. The RF permeameter (fig. 1) described in this paper is essentially of the same construction. Certain changes were made, necessitated by the higher frequencies used. The complete equations, taking losses into consideration, were developed to allow the measurement of the

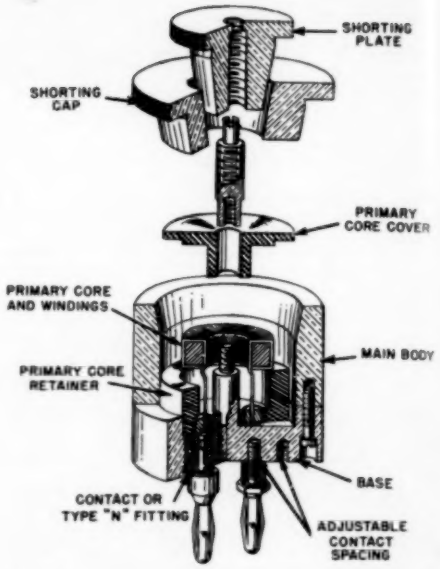

FIGURE 1. *Cutaway view of radio-frequency permeameter with transformer.*

radio-frequency losses in core materials.[3] Additional changes were made to adapt the instrument to the measurement of temperature coefficients of permeability.

4. Analysis

The transformer is represented by the network shown in figure 2. Then the input impedance, Z_{in} at the primary terminals for three conditions in the secondary is

$$Z_1 = R_1 + j\omega L_1 \tag{1}$$

for the secondary open-circuited,

$$Z_0 = R_1 + j\omega L_1 + \frac{\omega^2 M^2}{R_2 + j\omega L_2} \tag{2}$$

for the secondary short-circuited without sample inserted,

$$Z_f = R_1 + j\omega L_1 + \frac{\omega^2 M^2}{(R_2 + R_a) + j\omega(L_2 + L_a)} \tag{3}$$

when the short-circuited secondary impedance has been increased by a quantity $R_\mu + j\omega L_a$ because of the insertion of a ferromagnetic core.

The use of a high Q secondary allows us to make the following assumptions:[4]

[3] At present it appears impossible to use the method described herein for the determination of values of $\mu'' < 0.1$ approximately.

[4] See appendix I.

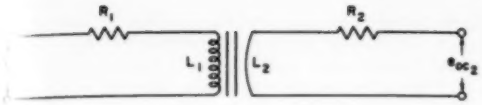

FIGURE 2. *Transformer representation.*

$$R_2^2 \ll \omega^2 L_2^2 \tag{4}$$

$$(R_2+R_u)^2 \ll \omega^2 (L_2+L_u)^2. \tag{5}$$

In the above equations the mutual inductance, M, which is not directly measurable from the input terminals, must be derived.

We note that if the secondary be left open-circuited and a voltage, V_1, be applied to the primary terminals,

$$V_1 = (R_1 + j\omega L_1) i_1 \tag{6}$$

$$e_{oc_2} = j\omega M i_1, \tag{7}$$

and

$$\frac{|V_1|}{|e_{oc_2}|} = \frac{\sqrt{R_1^2+\omega^2 L_1^2}}{\omega M}. \tag{8}$$

The primary coil is selected to have a specially high Q, so that

$$R_1^2 \ll \omega^2 L_1^2. \tag{9}$$

We therefore have

$$\frac{|V_1|}{|e_{oc_2}|} = \frac{L_1}{M}. \tag{10}$$

For convenience, let this ratio be defined

$$\frac{|V_1|}{|e_{oc_2}|} = N.$$

If the leakage inductance is negligible, this is exactly equal to the turns ratio, and for moderate accuracies, this assumption may often be made. We shall discuss this point later in some detail.

Using these conditions we may solve eq (2) and (3) for R_2, L_2, R_u and L_u respectively.

$$Z_0 - Z_1 = R_2 \left(\frac{L_1}{NL_2}\right)^2 - j\,\frac{\omega}{L_2}\left(\frac{L_1}{N}\right)^2 \tag{11}$$

$$L_2 = \left(\frac{L_1}{N}\right)^2 \frac{1}{L_1 - L_0} = \left(\frac{L_1}{N}\right)^2 \frac{1}{L_{10}} \tag{12}$$

$$R_2 = \left(\frac{L_1}{N}\right)^2 \frac{R_0 - R_1}{(L_1 - L_0)^2} = \left(\frac{L_1}{N}\right)^2 \frac{R_{01}}{L_{10}^2}, \tag{13}$$

where

$$L_{10} = L_1 - L_0 \tag{14}$$

$$R_{01} = R_0 - R_1. \tag{15}$$

Furthermore,

$$Zf - Z_1 = \frac{\left(\frac{\omega L_1}{N}\right)^2}{(R_2+R_u) + j\omega(L_2+L_u)} \tag{16}$$

$$R_u = \left(\frac{L_1}{N}\right)^2 \left[\frac{R_{f1}}{L_1 f^2} - \frac{R_{01}}{L_{10}^2}\right] \tag{17}$$

$$L_u = \left(\frac{L_1}{N}\right)^2 \frac{L_{f0}}{L_{1f} L_{10}}, \tag{18}$$

where

$$R_{f1} = R_f - R_1; \quad L_{f0} = L_f - L_0; \quad L_{1f} = L_1 - L_f. \tag{19}$$

We have thus been able to solve for the added inductance and resistance arising from the presence of the ferromagnetic test core in terms of the measured values R_1, L_1, L_0, R_0, R_f, and L_f. It remains then to calculate the permeability, μ', and the dissipation factor, $\tan \delta_m$, from these values.

The value of $L_u/(\mu'-1)$ may be calculated from one of the available formulas (see appendix II). Let this value be called L_a. Thus $\mu' - 1 = L_u/L_a$ and

$$\mu' - 1 = \frac{\left[\left(\frac{L_1}{N}\right)^2 \frac{1}{L_{10}}\right] \frac{L_{f0}}{L_{1f}}}{L_a}. \tag{20}$$

Furthermore, since

$$\frac{R_u}{\omega L_u} = \tan \delta_m, \tag{21}$$

$$\tan \delta_m = \frac{L_{10} L_{1f}}{\omega L_{f0}} \left[\frac{R_{f1}}{L_{1f}^2} - \frac{R_{01}}{L_{10}^2}\right]. \tag{22}$$

It is noteworthy that the bracketed quantity in eq (20) is a constant that may be calibrated. Similarly the last ratio in the brackets and L_{10} in eq (22) are constants. Thus only the differences $L_f - L_0$, $L_1 - L_f$, and $R_f - R_1$ need to be measured for each test core.

The equations (20) and (22) give μ' and $\tan \delta_m$ in terms of series components of resistance and inductance obtainable with a radio-frequency bridge. The extension to other instruments, such as an admittance bridge reading parallel components of conductance and capacitance, or to a Q meter is immediate. The equations are:

(A) Admittance bridge, reading $G + j\omega C$:

$$(\mu' - 1) = \frac{\left[\frac{1}{\omega^2 N^2 C_{01}}\right] \frac{C_{0f}}{C_{f1}}}{L_a}. \tag{23}$$

$$\tan \delta_m = \frac{C_{01} C_{f1}}{\omega C_{0f}} \left[\frac{1}{C_{f1}^2}\left(G_f - \frac{C_f^2}{C_1^2} G_1\right) - \frac{1}{C_{01}^2}\left(G_0 - \frac{C_0^2}{C_1^2} G_1\right)\right]. \tag{24}$$

(B) Q meter, reading resonating capacitance C, and Q:

$\mu'-1$, same as eq (23)

$$(\mu'-1)=\frac{\left[\frac{1}{\omega^2N^2C_{01}}\right]\frac{C_{0f}}{C_{f1}}}{L_a}, \tag{25}$$

$$\tan\delta_m=\frac{C_{01}C_{f1}}{C_{0f}}\left[\frac{1}{C_{f1}^2}\left(\frac{C_f}{Q_f}-\frac{C_f^2C_1}{C_1^2Q_1}\right)-\frac{1}{C_{01}^2}\left(\frac{C_0}{Q_0}-\frac{C_0^2C_1}{C_1^2Q_1}\right)\right]. \tag{26}$$

The choice of instruments will depend on the frequency range to be covered, the desired accuracy and sensitivity, as well as on the construction of the permeameter and its primary transformer. An additional method, capable of high sensitivity in the value of the permeability, especially for the measurement of temperature coefficients, of permeability, uses a radio-frequency impedance bridge, such as General Radio type 916AL, in parallel with a variable capacitor, such as General Radio type 722N. The bridge is balanced with the permeameter connected to its unknown terminals in parallel with the capacitor. The balance is made with the secondary open-circuited and the capacitor set at its lowest value. The rest of the measurements are made as before, except that the reactive portion of the balance is made with the parallel capacitor only. The permeability is given by eq (23), and

$$\tan\delta_m=\frac{R_p}{\omega^2L_1^2}\frac{C_{01}C_{f1}}{\omega C_{0f}}\left\{\frac{1}{C_{f1}^2}\left[\frac{R_f}{R_1}-(1+\omega^2L_1C_{f1})^2\right]-\frac{1}{C_{01}^2}\left[\frac{R_0}{R_1}-(1+\omega^2L_1C_{01})^2\right]\right\}. \tag{27}$$

An additional measurement that needs to be made for the evaluation of $\tan\delta_m$ is one for the primary resistance, R_p, which must be made without the parallel capacitor.

5. Details of Measurements

In general, the measurements are performed in the same manner as any other impedance measurement. Certain precautions, however, will increase the accuracy. Upon examination of eq (20) through (27), it will be noted that in most cases only differences of impedance are required. Many of the bridges used, as well as the Q meter, are provided with vernier capacitors, which may be used to advantage. The short-circuited impedance reading is usually close to the bridge reading with the sample inserted when the latter has low permeability. For high-permeability samples, the difference between the open-circuited impedance reading and that with the sample inserted is usually small. Arranging the order of readings in proper sequence so that a main dial need not be moved, the entire difference reading being taken on the vernier capacitor, usually will increase the accuracy above the quoted accuracy of the bridge. For bridges of the series-impedance type, several transformers are necessary to cover a wide frequency range.

For the measurement of initial permeability and losses, extremely low fields are necessary. In his original article, Kelsall derived the expression for the magnetic field in the sample at the mean radius. The equation shows the field to be proportional to the number of turns on the primary and the total primary current and inversely proportional to the mean diameter, D, of the test core [4].

$$H=\frac{2N_1\,(L_1-L_f)\,I}{5L_1D},$$

where H is in oersteds, and when I is in amperes. For a constant primary voltage, however, the total current is inversely proportional to the input impedance, which is largely inductive. As the primary inductance itself is proportional to N_1^2, the field will be inversely proportional to N_1, the frequency, and the mean diameter, and proportional to the applied voltage. The voltage in practice can be made very low by using sensitive bridge detectors. Thus it can be seen that the conditions favor low magnetic fields and that it is not difficult to make a proper measurement of the initial permeability. In addition to facilitating this measurement, a low voltage is also desirable from the viewpoint of transformer stability and high-input Q because of the reduction of hysteresis losses in the primary circuit. Needless to say, a high Q is very desirable, especially for the measurement of dissipation factor.

6. Accuracy

It is difficult to determine the exact accuracy of the permeameter because too many indeterminate factors are involved. We shall discuss some of these to arrive at some estimate of the highest attainable accuracy and also mention some of the shortcomings of the instrument.

The problem of dimensional resonance caused by a high dielectric constant is, of course, not remedied in this instrument any more than if toroidal windings were placed on the core. The permeability and losses measured will simply be the effective values for that particular core. There are, however, only completely negligible disturbing effects caused by capacitance between turns and resulting displacement currents.

The accuracy of the bridge or of the Q meter used will of course be a large factor in the over-all accuracy of the measurement. Obviously all of the corrections to the readings as specified by the instructions for the particular instrument have been made and care has been taken to keep all shunting capacitances at a minimum. By applying such corrections with care,

it easily possible to secure results that are more accurate than the rated accuracy of the instrument when this is used for a single measurement. This is because in most of the measurements only differences of reactance, resistance, or capacitance are required. It is rarely the case that the amount by which a bridge reading will be inaccurate will change drastically between two closely related readings. Unless the particular instrument is equipped with a vernier scale, the lack of large differences between readings will usually be a greater problem than lack of accuracy. The over-all accuracy can be improved by evaluation through a calibration experiment of that portion of the equation that is theoretically a constant. This point will be discussed in a later section.

Equation (26) contains both Q_1 and Q_f, which may differ by little for low-loss samples. If Q_1 is large, a more precise determination of this difference will be possible. The same advantage is implied in the other equations for the dissipation factor.

In order to get some estimate of the accuracy of the measurements, a number of samples having permeabilities between 20 and 850 were tested by ballistic methods by the Magnetic Measurements Section of the National Bureau of Standards. Although these measurements were made with direct current, they afford some comparison with the values obtained at 100 kc/s on the permeameter, as there is rarely much change of the permeability in that frequency range. The differences between the two methods ranged from 1.6 to 2.8 percent. Some comparisons, especially for the values of the dissipation factor, were also made with values obtained on coaxial samples of presumably the same materials. Because of the variations present from batch to batch and at times even in the same piece, this comparison is not altogether conclusive. It may be said, however, that where the permeabilities agreed to better than 5 percent, the agreement between the dissipation factors remained within 10 percent. It is believed that these are reasonably reliable values for the maximum accuracy, provided all possible care has been taken.

The frequency range within which the permeameter may be used is most limited by the decrease in sensitivity and also to some extent by the decreasing accuracy of measuring instruments. Good results have been obtained at the Bureau up to 20 Mc/s. By proper design it should be possible to extend the upper limit.

7. Calibration of the Permeameter

7.1. Voltage Ratio

It is mentioned earlier in connection with eq (10) that the voltage ratio $|V_1|/|e_{0c_2}|$ may be replaced by the turns ratio N if the primary leakage inductance is negligible. This is essentially the case with transformer cores small by comparison to the radial dimensions of the instrument, of medium permeability ($\mu'=60$ or higher), and for turns ratios of the order

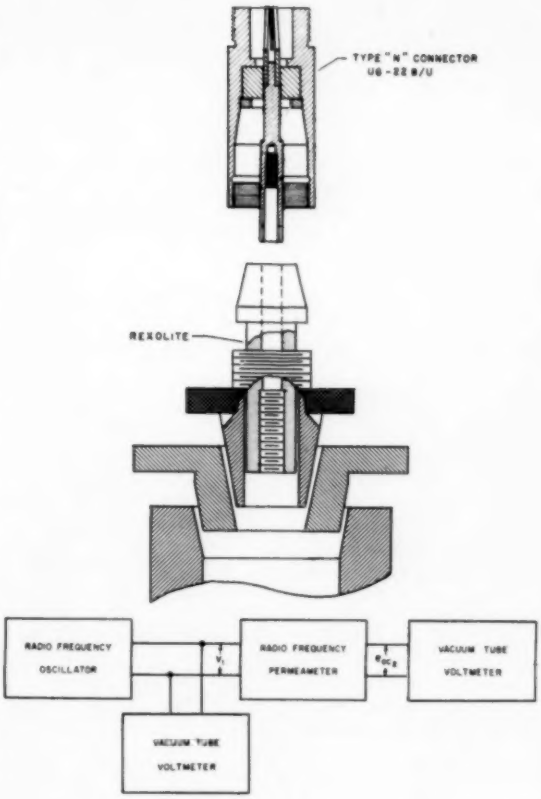

FIGURE 3. *Experimental arrangement for measuring voltage ratio.*

of 100 or greater. It has been found desirable, however, to use low-permeability cores (μ' below 20) for the higher frequency ranges because of the decrease in transformer losses. For best results, it is, therefore, desirable to measure the voltage ratio at several frequencies. For moderate accuracies, a good vacuum-tube voltmeter with a low voltage range (0.01- or at most 0.1-v full scale) will suffice. The experimental arrangement is shown in figure 3, which also shows a top-connection plate replacing the top-shorting plate (shown at the top of fig. 1) for this purpose. A stable radio-frequency generator with a voltage output approximately equal to that used for the permeability measurements is connected to the primary terminals, with provision for a shunting voltmeter close to the terminals. The voltage V_1 is read, and the voltmeter is then connected to the secondary terminals for the reading of e_{0c}. It was found that for input coils with Q of 50 or better over the entire frequency range, the ratio will remain constant within 5 percent from 100 kc/s to 5 Mc/s, increasing at the upper limit. A few cases have been

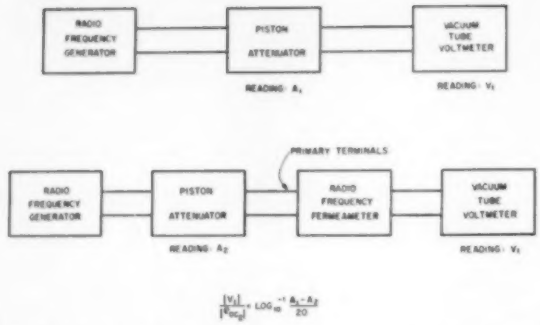

FIGURE 4. *Calibration arrangement, using piston attenuator.*

noted in which the deviations did not exceed 1 percent. It should be kept in mind that this ratio enters the equations as a square, therefore any error in this ratio will cause an error twice as large in the permeability measured.

A more accurate calibration method is shown in figure 4. The piston attenuator is adjusted so that the voltmeter reads a voltage V_1. The permeameter is then inserted between the attenuator and the voltmeter, and the attenuation is reduced until the voltmeter reads a voltage V_1 once more. If the attenuator readings were A_1 and A_2 db, respectively, the voltage ratio is given by

$$\frac{|V_1|}{|e_{0e_2}|} = \log_{10}{}^{-1} \frac{A_1 - A_2}{20}.$$

This method is used at the National Bureau of Standards in conjunction with a standard piston attenuator for calibration of the permeameters. A dissipative attenuator, operating under matched conditions and with sufficient initial attenuation inserted, may also be used with somewhat reduced accuracy. Such an instrument should then have a dial calibrated in hundredths of decibels at least.

7.2. Secondary Inductance

Consider the expression

$$\frac{1}{\omega^2 N^2 C_{01}},$$

which appears as the multiplier of the ratio of the differences in capacitance in eq (23). We note that this is theoretically a constant for a particular permeameter independent of frequency or number of primary turns.

If we define $L_1 = N^2 \mu_1 L_{a1}$, where L_{a1} is the geometrical inductance of the primary core and μ_1 its permeability, it can be shown that

$$\frac{1}{\omega^2 C_{01} N^2} = L_2 - \mu_1 L_{a1}$$
$$= L_{coax} - L_{a1}.$$

Now both L_{coax} and L_{a1} depend on geometry only for wavelengths long as compared with their dimensions, and their values may thus be calculated. The values for L_{coax} and L_{a1} are given by

$$L = (2 \ln b/a)h \times 10^{-7},$$

which is to be calculated for both L_{coax} and L_{a1}. The validity of this calibration constant over a wide range of frequencies, and turns ratios has been experimentally verified to better than one percent. Therefore, it is possible to calibrate the radio frequency permeameter, using physical dimensions only.

8. Measurement of Temperature Coefficients of Permeability

Kelsall originally designed an additional model of his permeameter to measure permeability coefficients of temperature [5]. This instrument is well suited for low frequencies but somewhat large for high-frequency use. A simple modification of the present instrument seemed to be more useful.

Figure 5 shows the modified permeameter for measurement of temperature coefficients of permeability. It is noted that except for an increase in the length of the secondary by the addition of cable the general structure of the instrument remains unchanged and so do the equations and measurement procedures. Because the value of L_2 has been changed, however, a different calibration constant will be obtained. In a convenient experimental setup a number of sample holders (the structure actually enclosing the test sample in fig. 6) are placed in the oven simultaneously. Each one has a cable of identical length leading to a coaxial switch. That portion of the permeameter containing the primary coil may then be connected to any one of the sample holders, one of which may be left empty to facilitate measurement of the short-circuited condition. Individual thermocouples can be connected to each sample to indicate its temperature.

The cables and connectors used in this work must, of course, be able to withstand high temperatures. Coaxial cable and connectors with Teflon dielectric are now available for this purpose and will operate satisfactorily up to 250° C. The importance of this measurement is enhanced by the increasing need for core materials in military miniaturization work where temperatures up to 200° C are prevalent. This portion of the developmental work on the radiofrequency permeameter was sponsored by a miniaturization project at the National Bureau of Standards.

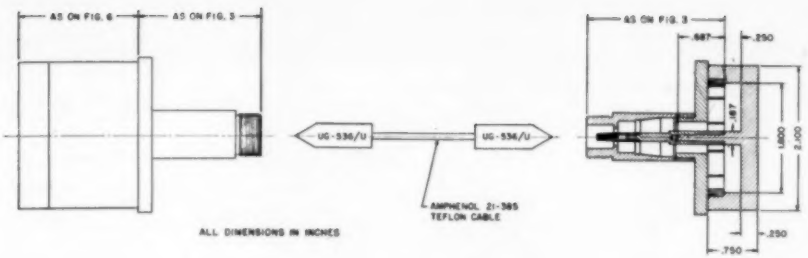

FIGURE 5. *Modified radio-frequency permeameter for measuring temperature coefficient of samples.*

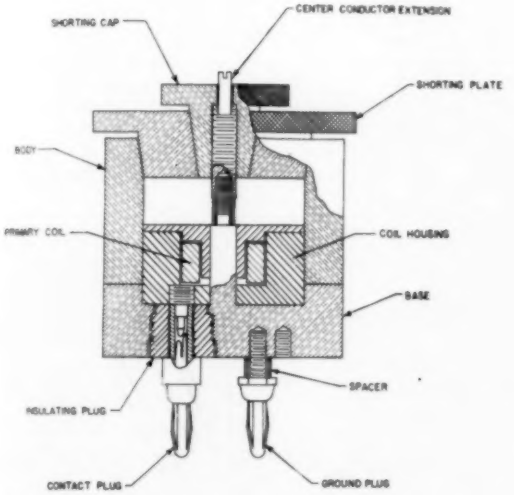

FIGURE 6. *Cutaway view of radio-frequency permeameter.*

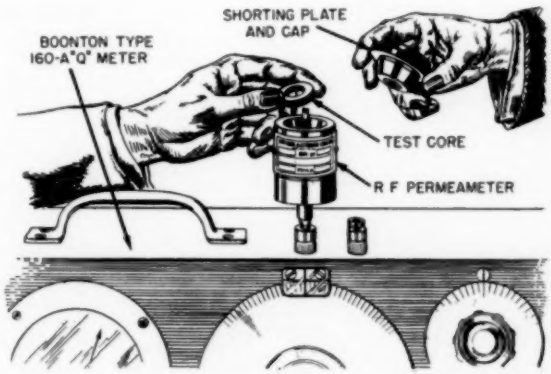

FIGURE 7. *Radio-frequency permeameter in use with Q meter.*

The author is indebted to William A. Edson for suggesting the solution to the problem and to the Stackpole Carbon Co., St. Marys, Pa., for their cooperation in furnishing many Carbonyl powder toroids with extremely close tolerances in characteristics that are presently used as transformer cores in NBS permeameters. Figures 1 and 7 by courtesy of the National Electronic Laboratories.

9. References

[1] V. E. Legg, Magnetic measurements at low flux density using the alternating current bridge, Bell System Tech. J. **16,** 39–62 (1936).

[2] Brockman, Dowling, and Steneck, Dimensional effects resulting from a high dielectric constant found in a ferromagnetic ferrite, Phys. Rev. **77** (January 1950).

[3] G. A. Kelsall, Permeameter for alternating current measurements at small magnetizing forces, J. Opt. Soc. Am. and Rev. Sci. Instr. **8** (February 1924).

[4] G. A. Kelsall, Permeameter for alternating current measurements at small magnetizing forces, J. Opt. Soc. Am. and Rev. Sci. Instr. **8,** 334 (February 1924).

[5] G. A. Kelsall, Furnace permeameter for alternating current measurements at small magnetizing forces, J. Opt. Soc. Am. and Rev. Sci. Instr. **8** (May 1924).

10. Appendix 1. Experimental Proof of the Validity of Equation 4

Measurements were made on a particular model to show that the conditions for which eq (4) holds true can be met without difficulty.

These conditions are most difficult to satisfy at the lowest frequencies. The data given below were taken at 100 kc/s on a high-precision bridge.

From eq (2) and (10)

$$R_2+j\omega L_2=\frac{\left(\frac{\omega L_1}{N}\right)^2(R_0-R_1)}{(R_0-R_1)^2+\omega^2(L_0-L_1)^2}+j\omega\frac{\left(\frac{\omega L_1}{N}\right)^2(L_1-L_0)}{(R_0-R_1^2)+\omega^2(L_0-L_1)^2}$$

in which $N=100$ turns; $f=100$ kilocycles; $R_0=2.54$ ohms; $R_1=1.46$ ohm; $L_0=50.59\times10^{-6}$ henry; and $L_1=81.56\times10^{-6}$ henry. Then, $R_2=2\,87\times10^{-4}$ ohm; $L_2=0.824\times10^{-6}$ henry; and $(\omega L_2/R_2)^2=325$.

11. Appendix 2. Value of Equivalent Air Inductance

The value of L_a[5] is derived in Bureau of Standards Bulletin, Vol. 5, No. 3, p. 441, as

$$L_a = \frac{4KA}{10^9 D} \text{ henry},$$

where A is the cross-sectional area in square centimeters. The mean diameter $D = b + a$, $K = 1/2p \ln (1+p)/(1-p)$, where $p = (b-a)/(b+a)$, the ratio of radial width to mean diameter, b is the outside radius, and a the inside radius.

Alternatively, an equivalent formula given in Bureau of Standards Circular 74, p. 251, eq (152), may be used:

$$L_a = 0.4606\, h \log_{10} \frac{b}{a} \times 10^{-6} \text{ henry},$$

where h is the toroidal height in meters.

[5] This is the inductance due to the space having the dimensions of the test core.

WASHINGTON, September 2, 1953.

Journal of Research of the National Bureau of Standards Vol. 51, No. 5, November 1953 Research Paper 2455

On Mildly Nonlinear Partial Difference Equations of Elliptic Type[1]

Lipman Bers[2]

The use of the finite differences method is in solving the boundary value problem of the first kind for the nonlinear elliptic equation $\Delta\phi=F(x,y,\phi,\phi_x,\phi_y)$ is justified by first showing that the problem of the corresponding difference equation has a unique solution, and then that the solution of the difference equation tends to that of the differential equation when the net unit tends to zero. Also a numerical method of the Liebmann type for the computation of the solution of the difference equation is developed, and these results are extended to more general nonlinear elliptic equations.

1. Introduction

The method of finite difference is frequently used for the numerical treatment of nonlinear partial differential equations of elliptic type. A theoretical justification of this method, however, seems to exist in the literature only for the case of linear equations. In this note such a justification is given for the simplest nonlinear elliptic equation

$$\Delta\phi=F(x,y,\phi,\phi_x,\phi_y). \tag{1}$$

We assume that the partial derivative F_ϕ, is nonnegative and the derivatives F_{ϕ_x}, F_{ϕ_y} uniformly bounded, and approximate the differential equation by the difference equation

$$\frac{\phi(x+h,y)+\phi(x,y+h)+\phi(x-h,y)+\phi(x,y-h)-4\phi(x,y)}{h^2}$$

$$=F\left\{x,y,\phi(x,y),\frac{\phi(x+h,y)-\phi(x-h,y)}{2h},\right.$$

$$\left.\frac{\phi(x,y+h)-\phi(x,y-h)}{2h}\right\}. \tag{2}$$

We shall show that the first boundary value problem for this difference equation possesses a unique solution that can be computed by a Liebmann iteration method, and we shall estimate the difference between this solution and the solution of the boundary value problem for the differential equation.

These results extend almost at once to the case when a more sophisticated difference equation is used to approximate (1), and also, due to a recent result by Motzkin and Wasow, to the elliptic equation

$$a(x,y)\phi_{xx}+2b(x,y)\phi_{xy}+c(x,y)\phi_{yy}=F(x,y,\phi,\phi_x,\phi_y).$$

Extensions to higher dimensions and to other nets are also immediate. On the other hand, our method is tied to the maximum-principle; it does not apply to such important quasi-linear equations as the equation of minimal surfaces or the equations of gas dynamics.

We state explicitly that the reasoning reproduced below involves only a straightforward application of familiar arguments. In section 3, in particular, we paraphrase well-known facts in a form suitable for our purposes.

2. Notations

We denote by Ω a fixed bounded domain in the (x,y)-plane. $\bar{\Omega}$ is the closure and Ω' the boundary of Ω. $F(x,y,z,p,q)$ denotes a fixed continuous function defined for $(x,y)\in\bar{\Omega}$ and all z, p, q. We assume that the partial derivatives F_z, F_p, F_q exist and satisfy the inequalities

$$F_z\geq 0, \tag{3}$$

$$|F_p|, |F_q|\leq A<+\infty. \tag{4}$$

Set

$$\boldsymbol{L}[\phi]=\Delta\phi-F(x,y,\phi,\phi_x,\phi_y), \tag{5}$$

where Δ is the Laplace operator ($\Delta\phi=\phi_{xx}+\phi_{yy}$). Let $v(x,y)$ be a fixed continuous function defined on $\bar{\Omega}$. *Boundary value problem* **P** consists in finding a function $\phi(x,y)$ continuous on $\bar{\Omega}$ and twice continuously differentiable in Ω such that

$$\boldsymbol{L}[\phi]=0 \text{ in } \Omega, \qquad \phi=v \text{ on } \Omega'. \tag{6}$$

It is known that this problem has at most one solution, and that a solution exists under appropriate smoothness hypotheses.

We approximate $\boldsymbol{L}$ by a difference operator $\boldsymbol{L}_h$ defined (for $h>0$) by

$$\boldsymbol{L}_h[\phi]=\Delta_h[\phi]-F\{x,y,\phi,D_{h,x}[\phi],D_{h,y}[\phi]\}, \tag{7}$$

where

$$\Delta_h[\phi(x,y)]=$$

$$\frac{\phi(x+h,y)+\phi(x,y+h)+\phi(x-h,y)+\phi(x,y-h)-4\phi(x,y)}{h^2}, \tag{8}$$

[1] The preparation of this paper was sponsored (in part) by the Office of Naval Research.

[2] Present address New York University, New York, N. Y.

$$D_{h,x}[\phi(x,y)]=\frac{\phi(x+h,y)-\phi(x-h,y)}{2h},$$

$$D_{h,x}[\phi(x,y)]=\frac{\phi(x,y+h)-\phi(x,y-h)}{2h}. \qquad (9)$$

Let P_0 be the point with the coordinates (x_0,y_0). The points (x_0+h,y_0), (x_0,y_0+h), (x_0-h,y_0), (x_0,y_0-h) will be called the h-neighbors of P_0 and will be denoted by P_{01}, . . ., P_{04}. A lattice domain Ω_h is a set of points, P_1, . . ., P_N, situated in Ω, having coordinates that are integral multiples of h, and such that all points P_ν, $i=1, \ldots, N$; $\nu=1, \ldots, 4$ belong to $\overline{\Omega}$. Neighbors of points of Ω_h that are not themselves points of Ω_h form the boundary Ω_h' of Ω_h. We denote the points of Ω_h' by $P_{N+1}, \ldots, P_M$, and the union of Ω_h and Ω_h' by $\overline{\Omega}_h$. If Ω_h is fixed, and χ is a function defined on $\overline{\Omega}_h$, we denote the value of χ at a point P_i (or at a point $P_{i\nu}$) by χ_i (or $\chi_{i\nu}$). We also set

$$L_h[\phi_i]=\Delta_h[\phi_i]-F\{x_i,y_i,\phi_i,D_{h,x}[\phi_i],D_{h,y}[\phi_i]\}, \qquad (7')$$

where

$$\Delta_h[\phi_i]=\frac{1}{h^2}\Big\{\sum_{\nu=1}^{4}\phi_{i\nu}-4\phi_i\Big\}, \qquad (8')$$

$$D_{h,x}[\phi_i]=\frac{\phi_{i1}-\phi_{i3}}{2h}, \quad D_{h,y}[\phi_i]=\frac{\phi_{i2}-\phi_{i4}}{2h}. \qquad (9')$$

The *boundary-value problem* $\boldsymbol{P_h}$ (for some fixed Ω_h) consists in determining a function ϕ defined on $\overline{\Omega}_h$ such that

$$L_h[\phi_i]=0, \qquad i=1, \ldots, N;$$

$$\phi_j=v_j, \quad j=N+1, \ldots, M. \qquad (10)$$

From now on we assume that h is so small that at least one Ω_h exists, and that

$$Ah<2\theta, \qquad 0<\theta<1, \qquad (11)$$

where θ is some fixed number.

3. An Inequality

In this section we recall some properties of the linear difference operator

$$l_h[\phi_i]=\Delta_h[\phi_i]+\alpha_i D_{h,x}[\phi_i]+\beta_i D_{h,y}[\phi_i]-\gamma_i\phi_i, \qquad (12)$$

with

$$|\alpha_i|, \ |\beta_i|\leq A, \qquad (13)$$

$$\gamma_i\geq 0. \qquad (14)$$

In particular, we want to establish the existence of a constant

$$C=C(A,\theta,d), \qquad (15)$$

depending only on A, θ and the diameter d of Ω such that *the inequality*

$$\max_{\Omega_h}|\phi|\leq C\max_{\Omega_h}|l_h[\phi]|+\max_{\Omega_h'}|\phi| \qquad (16)$$

holds for every function ϕ defined on $\overline{\Omega}_h$.

We observe first that the equation

$$l_h[\phi_i]=0, \qquad i=1, \ldots, N, \qquad (17)$$

may be written in the form

$$\phi_i=\frac{\sum_{\nu=1}^{4}\lambda^{i\nu}\phi_{i\nu}}{1+\frac{h^2}{4}\gamma_i}, \qquad i=1, \ldots, N, \qquad (18)$$

where

$$\lambda^{i1}=\frac{1}{4}\Big(1+\frac{h}{2}\alpha_i\Big), \qquad \lambda^{i2}=\frac{1}{4}\Big(1+\frac{h}{2}\beta_i\Big),$$

$$\lambda^{i3}=\frac{1}{4}\Big(1-\frac{h}{2}\alpha_i\Big), \qquad \lambda^{i4}=\frac{1}{4}\Big(1-\frac{h}{2}\beta_i\Big).$$

Since

$$\lambda^{i\nu}\geq\frac{1}{4}(1-\theta)>0, \qquad \sum_{\nu=1}^{4}\lambda^{i\nu}=1,$$

(18) implies that

$$\phi_i\begin{cases}\leq\max(\phi_{i1}, \ldots, \phi_{i4}) & \text{if} \quad \phi_i\geq 0\\ \geq\min(\phi_{i1}, \ldots, \phi_{i4}) & \text{if} \quad \phi_i\leq 0\end{cases} \qquad (19)$$

and the equality sign in (19) holds only if $\phi_{i1}=\ldots=\phi_{i4}$, $\gamma_i\phi_i=0$.

Let m and M be the minimum and maximum of a solution of (17). If $M>0$ and $\phi=M$ at a point P_i of Ω_h, then $\varphi=M$ at all neighbors of P_i, at all neighbors of neighbors, etc. Hence $\phi=M$ at a point of Ω_h'. A similar argument holds if $m<0$. Thus

$$\min(0,\min_{\Omega_h'}\phi)\leq\phi_i\leq\max(0,\max_{\Omega_h'}\varphi), \qquad i=1, \ldots, N, \qquad (20)$$

and, in particular,

$$\max_{\Omega_h}|\phi|\leq\max_{\Omega_h'}|\varphi|. \qquad (21)$$

Consider now the boundary value problem

$$l_h[\phi_i]=k_i, \quad i=1, \ldots, N;$$

$$\phi_j=v_j, \quad j=N+1, \ldots, M. \qquad (22)$$

It is equivalent to the system

$$\sum_{s=1}^{N}L^{is}\phi_s=k_i+\sum_{j=N+1}^{M}\sigma^{ij}v_j, \qquad i=1, \ldots, N,$$

where the matrices (L^{is}) and (σ^{ij}) depend only on l_h and Ω_h. In view of (21) the homogeneous system ($k\equiv 0$, $v\equiv 0$) has only the trivial solution. Hence the "Green matrix" $(G^{ij})=(L^{ij})^{-1}$ of l_h in Ω_h exists, and the unique solution of (22) is given by

$$\phi_i=\sum_{s=1}^{N}G^{is}k_s+\sum_{j=N+1}^{M}\Gamma^{ij}v_j, \qquad i=1, \ldots, N,$$

where

$$\Gamma^{ij}=\sum_{l=1}^{N}G^{il}\sigma^{lj},$$

we call (Γ^{ij}) the "Green boundary matrix" of l_h. Thus every function defined on $\bar{\Omega}_h$ satisfies the identity

$$\phi_i=\sum_{s=1}^{N}G^{is}l_h[\phi_s]+\sum_{j=N+1}^{M}\Gamma^{ij}\phi_j, \qquad i=1,\ldots,N,$$

and hence the inequality

$$\max_{\Omega_h}|\phi|\leq c_1\max_{\Omega_h}|l_h[\phi]|+c_2\max_{\Omega_h'}|\phi| \tag{23}$$

with

$$c_1=\max\sum_{s=1}^{N}|G^{is}|, \qquad c_2=\max\sum_{j=N+1}^{M}|\Gamma^{ij}|. \tag{24}$$

Let ϕ be a solution of (22) with $k_i\equiv 0$, $v_j=\delta_{jl}$ (Kronecker δ). Then $\phi_i=\Gamma^{il}$. By property (20) of solutions of (17), $0\leq\phi_i\leq 1$, $i=1,2,\ldots,N$. Thus $\Gamma^{il}\geq 0$ for all i,l. Next let ϕ be a solution of (22) with $k_i\equiv 0$, $v_{N+1}=\ldots=v_M=1$. Then

$$\phi_1=\sum_{j=N+1}^{M}\Gamma^{ij}=\sum_{j=N+1}^{M}|\Gamma^{ij}|,$$

and by property (20) of solutions of (17), $0\leq\phi_i\leq 1$. Hence,

$$c_2\leq 1. \tag{25}$$

Now let ϕ be the solution of (22) with $k_i=\delta_{il}$, $v_j\equiv 0$, so that $\phi_i=G^{il}$. Let $\dot{\Omega}_h$ denote the lattice domain obtained from Ω_h by removing P_l. Assume that $\phi_l>0$. In $\dot{\Omega}_h$ we have that $l_h[\phi]=0$, so that by (20) $0\leq\phi_i\leq\phi_l$, $i\neq l$. In particular, $0\leq\phi_{l\nu}\leq\phi_l$, $\nu=1,2,3,4$. But $l_h[\phi_l]=1$, so that

$$\frac{h^2}{4}+\left(1+\frac{h^2}{4}\gamma_l\right)\phi_l=\sum_{\nu=1}^{4}\lambda^{l\nu}\phi_{l\nu}\leq\phi_l,$$

which is absurd. Hence $\phi_l\leq 0$, and again by (20) $\phi_i\leq 0$ for $i\neq l$. Hence

$$G^{il}\leq 0. \tag{26}$$

Now set

$$\tilde{l}_h[\phi_i]=\Delta_h[\phi_i]+\alpha_i D_{h,x}[\phi_i]+\beta_i D_{h,y}[\phi_i] \tag{27}$$

and let $\tilde{G}^{il}$, $\tilde{\Gamma}^{il}$, $\tilde{c}_1$, $\tilde{c}_2$ be defined as before, with l_h replaced by $\tilde{l}_h$. Let ϕ have the same meaning as before, and let $\tilde{\phi}$ be the solution of the boundary value problem

$$\tilde{l}_h[\tilde{\phi}_i]=\delta_{il}, \quad i=1,\ldots,N;$$

$$\tilde{\phi}_j=0, \quad j=N+1,\ldots,M.$$

Then

$$\tilde{\phi}_i=\tilde{\Gamma}^{il}\leq 0,$$

and since for $i=1,\ldots,N$

$$l_h[\phi_i-\tilde{\phi}_i]=l_h[\phi_i]-\{\tilde{l}_h[\tilde{\phi}_i]-\gamma_i\tilde{\phi}_i\}=\gamma_i\tilde{\phi}_i\leq 0,$$

$$\phi_i-\tilde{\phi}_i=\sum_{s=1}^{N}G^{is}\gamma_s\tilde{\phi}_s\geq 0.$$

Thus $\tilde{G}^{il}\leq G^{il}$, or $|G^{il}|\leq|\tilde{G}^{il}|$ so that

$$c_1\leq\tilde{c}_1. \tag{28}$$

Let $\Phi(x,y)$ be a continuous positive function defined on $\bar{\Omega}$ for which $\tilde{l}_h[\Phi]>0$, and

$$\frac{\max_{\bar{\Omega}}\Phi}{\min_{\Omega_h}\tilde{l}_h[\Phi]}\leq C(A,\theta,d). \tag{29}$$

We have that

$$\Phi_i=\sum_{s=1}^{N}\tilde{G}^{is}\tilde{l}_h[\Phi_s]+\sum_{j=N+1}^{M}\tilde{\Gamma}^{ij}\Phi_j, \qquad i=1,\ldots,N,$$

and as the term on the left-hand side is positive,

$$\sum_{s=1}^{N}|\tilde{G}^{is}|\tilde{l}_h[\Phi_s]\leq\sum_{j=N+1}^{M}\tilde{\Gamma}^{ij}\Phi_j.$$

Noting that $\tilde{c}_2\leq 1$, we obtain the inequality

$$\{\min_{\Omega_h}l_h[\Phi]\}\sum_{s=1}^{N}|\tilde{G}^{is}|\leq\max_{\bar{\Omega}}\Phi,$$

which implies that

$$\tilde{c}_1\leq C. \tag{30}$$

From (23), (25), (28) and (30) the assertion (16) follows.

We conclude the proof by exhibiting a function $\Phi(x,y)$ having the desired property (without aiming at the best possible value of C). Without loss of generality we assume that Ω is located within the strip $0\leq x\leq d$.

If $Ad<2$, we set $\Phi(x,y)=[x-(d/2)]^2$. Then

$$\Delta_h[\Phi]=2, \qquad D_{h,x}[\Phi]=2x-d, \qquad D_{h,y}[\Phi]=0,$$

so that in $\bar{\Omega}$: $\tilde{l}_h[\Phi]\geq 2-Ad$, and of course $\Phi\leq d^2/4$. Hence in this case (29) holds with $C=d^2/4[2-Ad]$. If $Ad>2$, set

$$\mu=\frac{A}{\theta}\tanh^{-1}\left(\frac{3\theta-\theta^2}{2}\right), \qquad \Phi(x,y)=e^{\mu x}.$$

Then $\max_{\bar{\Omega}}\Phi\leq e^{\mu d}$ and

$$\Delta_h[\Phi]=4e^{\mu x}\left[\frac{\sinh(\mu h/2)}{h}\right]^2,$$

$$D_{h,x}[\Phi]=2e^{\mu x}\left[\frac{\sinh(\mu h/2)}{h}\right]\cosh(\mu h/2), \qquad D_{h,y}[\Phi]=0,$$

so that

$$\gamma_h \geq 2e^{\mu s}\mu \frac{\sinh(\mu h)}{\mu h}\left[\frac{\tanh(\mu h/2)}{h}-\frac{A}{2}\right].$$

Because $(\tanh \xi)/\xi$ is a decreasing function of ξ, the expression in the brackets is, for $0 \leq h \leq 2\theta/A$, not less than

$$\frac{\tanh(\mu\theta/A)}{2\theta/A}-\frac{A}{2} \leq \frac{A}{4}(1-\theta),$$

so that

$$\gamma_h[\Phi] \geq \frac{A^2(1-\theta)}{2\theta}\tanh^{-1}\left(\frac{3\theta-\theta^2}{2}\right).$$

Thus (29) holds again with

$$C=\frac{2\theta \exp\left\{\frac{Ad}{\theta}\tanh^{-1}\left(\frac{3\theta-\theta^2}{2}\right)\right\}}{A^2(1-\theta)\tanh^{-1}\left(\frac{3\theta-\theta^2}{2}\right)}.$$

4. Existence and Uniqueness of the Solution of the Difference Equation

The inequality

$$\max_{\Omega_h}|\phi^{\mathrm{I}}-\phi^{\mathrm{II}}| \leq C\max_{\Omega_h}|L_h[\phi^{\mathrm{I}}]-L_h[\phi^{\mathrm{II}}]| + \max_{\Omega_h'}|\phi^{\mathrm{I}}-\phi^{\mathrm{II}}| \quad (31)$$

holds for any two functions defined on $\overline{\Omega}_h$.

In fact, by the mean-value theorem, the function $\phi=\phi^{\mathrm{I}}-\phi^{\mathrm{II}}$ satisfies the difference equation

$$l_h[\phi]=L_h[\phi^{\mathrm{I}}]-L_h[\phi^{\mathrm{II}}],$$

where l_h is defined by (12) with

$$\alpha_i=-F_p(x_i,y_i,z_i,p_i,q_i), \qquad \beta_i=-F_q(x_i,y_i,z_i,p_i,q_i),$$

$$\gamma_i=F_z(x_i,y_i,z_i,p_i,q_i), \qquad z_i=\tau_i\varphi_i^{\mathrm{I}}+(1-\tau_i)\phi_i^{\mathrm{II}},$$

$$p_i=\frac{1}{2h}\left\{\tau_i(\phi_{i1}^{\mathrm{I}}-\phi_{i2}^{\mathrm{I}})+(1-\tau_i)(\phi_{i1}^{\mathrm{II}}-\phi_{i2}^{\mathrm{II}})\right\},$$

$$q_i=\frac{1}{2h}\left\{\tau_i(\phi_{i2}^{\mathrm{I}}-\phi_{i4}^{\mathrm{I}})+(1-\tau_i)(\phi_{i2}^{\mathrm{II}}-\phi_{i4}^{\mathrm{II}})\right\},$$

the τ_i being numbers such that $0 \leq \tau_i \leq 1$. Since conditions (13), (14) are satisfied, inequality (16) is applicable and yields (31).

It follows from (31) that *problem* P_h *has at most one solution*.

Set

$$C_2=\max_{\overline{\Omega}}|F(x,y,0,0,0)|. \quad (32)$$

Then $|L_h(0)| \leq C_2$, so that applying (31) to an arbitrary function $\phi=\phi^{\mathrm{I}}$ and to the function $\phi^{\mathrm{II}} \equiv 0$, we obtain

$$\max_{\Omega_h}|\phi| \leq CC_2+C\max_{\Omega_h}|L_h[\phi]|+\max_{\Omega_h'}|\phi| \quad (33)$$

for every function defined on $\overline{\Omega}_h$.

In particular, a *solution* ϕ *of* P_h *satisfies the inequality*

$$\max_{\Omega_h}|\phi| \leq K=CC_2+\max_{\overline{\Omega}}|v|. \quad (34)$$

Now let (G^{ij}) and (Γ^{ij}) be the Green matrix and the Green boundary matrix of the operator Δ_h for the domain Ω_h, and define the continuous transformation $\vec{\phi}^*=T_t(\vec{\phi})$ in the N-dimensional $(\phi_1, \ldots, \varphi_N)$-space by the equations

$$\phi_i^*=\phi_i-t\sum_{i=1}^{N}G^{ij}F\{x_i,y_i,\phi_i,D_{h,x}[\phi_i],D_{h,y}[\phi_i]\} - \sum_{j=N+1}^{M}\Gamma^{ij}v_j, \qquad i=1, \ldots, N, \quad (35)$$

where t is a real parameter, $0 \leq t \leq 1$. A point $\vec{\phi}=(\phi_1, \ldots, \varphi_N)$ taken by this transformation into the origin is a solution of the boundary value problem

$$\Delta_h[\phi_i]-tF\{x_i,y_i,\phi_i,D_{h,x}[\phi_i],D_{h,y}[\phi_i]\}=0, \quad i=1, \ldots, N, \quad \phi_j=v_j, \quad j=N+1, \ldots, M. \quad (36)$$

Let $\overline{S}$ denote the domain $\phi_1^2+\ldots+\phi_N^2 \leq NK^2+1$. By virtue of (34) no point of the boundary S' of $\overline{S}$ is taken into the origin by T_t. Hence the degree of the mapping T_t of $\overline{S}$ at the origin (that is the N-dimensional solid angle under which the image $T_t(S')$ is seen from the origin, divided by the measure of the N-dimensional unit sphere) is well defined. Since T_t depends continuously on t, this degree is independent of t. For $t=0$ the mapping T_0 is a translation which takes the point $\vec{\phi}^0$, with $\phi_i^0=\sum_{j=N+1}^{M}\Gamma^{ij}v_j$ of $\overline{S}$ into the origin. Hence the degree is 1. Thus for $t=1$ at least one point $\vec{\phi}$ of $\overline{S}$ satisfies $T_1(\vec{\phi})=0$, and *problem* P_h *has a solution*.

A somewhat longer but constructive existence proof will be given later.

5. Convergence of the Solution of the Difference Equation to that of the Differential Equation

We assume now that problem P has a solution $\phi(x,y)$.

Let $\omega(\eta)$ be the modulus of continuity of $\phi(x,y)$ in $\overline{\Omega}$, that is,

$$\omega(\eta)=\text{l.u.b.}|\phi(x,y)-\phi(x',y')| \quad \text{for} \quad (x,y),(x',y') \in \overline{\Omega}, \qquad (x-x')^2+(y-y')^2 \leq \eta^2.$$

By $\omega_i^{(2)}(\eta), m_i^{(2)}$ we denote the maximum of the moduli of continuity and of the absolute values, respectively, of the second derivatives of $\phi(x,y)$ in the closed subdomain of Ω consisting of all points in Ω having a distance not less than $\delta>0$ from Ω'. $m_i^{(2)}$ and (for a fixed $\eta>0$) $\omega_i^{(2)}(\eta)$ are nonincreasing functions

of Set

$$\lim_{\delta\to 0} m_\delta^{(2)} = m^{(2)}, \qquad \lim_{\delta\to 0} \omega_\delta^{(2)}(\eta) = \omega^{(2)}(\eta).$$

If the second derivatives of $\phi(x,y)$ are continuous in $\overline{\Omega}$, then $m^{(2)} < +\infty$ and $\omega_\delta^{(2)}(\eta) \to 0$ for $\eta \to 0$. If $\phi(x,y)$ possesses continuous partial derivatives of the third or fourth order, we define $m_\delta^{(3)}$, $m^{(3)}$, $m_\delta^{(4)}$, $m^{(4)}$ in a similar manner. Finally, we denote by $\omega^*(\eta)$ the modulus of continuity of $v(x,y)$ in $\overline{\Omega}$.

Let Ω_h be a lattice domain such that (i) every point of Ω_h' has a distance not exceeding ϵ from some point of Ω', (ii) $\overline{\Omega}_h$ is contained in a closed subdomain of Ω having a distance not less than $\delta > 0$ from Ω'. We denote by $\phi^{(h,\epsilon,\delta)}$ the solution of problem $\boldsymbol{P}_h$ for this domain.

Let P_j be a point of Ω_h'. By virtue of (i) there exists a point (x,y) of Ω' such that

$$|v_j - v(x,y)| \le \omega^*(\epsilon), \qquad |\phi_j - \phi(x,y)| \le \omega(\epsilon).$$

Since $\phi_j^{(h,\epsilon,\delta)} = v_j$, $\phi(x,y) = v(x,y)$, we have that

$$\max_{\Omega_h'} |\phi^{(h,\epsilon,\delta)} - \phi| \le \omega(\epsilon) + \omega^*(\epsilon). \tag{37}$$

From Taylor's formula and condition (ii) it follows easily that for every point P_i of Ω_h,

$$|D_{h,x}[\phi_i] - (\phi_x)_i|, |D_{h,y}[\phi_i] - (\phi_y)_i| \le m_\delta^{(2)} h, \tag{38}$$

so that

$$|F\{x_i, y_i, \phi_i, D_{h,x}[\phi_i], D_{h,y}[\phi_i]\} - \{F(x,y,\phi,\phi_x,\phi_y)\}_i| \le 2Am_\delta^{(2)} h.$$

Also

$$|\Delta_h[\phi_i] - (\Delta\phi)_i| \le 2\omega_\delta^{(2)}(h). \tag{39}$$

Since $\boldsymbol{L}[\phi] \equiv 0$,

$$\max_{\Omega_h} |\boldsymbol{L}_h[\phi]| \le 2Am_\delta^{(2)} h + 2\omega_\delta^{(2)}(h).$$

Inequality (31) now yields the estimate

$$\max_{\Omega_h} |\phi^{(h,\epsilon,\delta)} - \phi| \le 2C[m_\delta^{(2)} h + \omega_\delta^{(2)}(h)] + \omega(\epsilon) + \omega^*(\epsilon). \tag{40}$$

This relation shows that ϕ *can be approximated by* $\phi^{(h,\epsilon,\delta)}$ *with any desired degree of accuracy.* In fact, let $\eta > 0$ be given. We determine an $\epsilon > 0$ so that $\omega(\epsilon) + \omega^*(\epsilon) \le \eta/2$ and choose a closed subdomain $\overline{\Omega}^*$ of Ω such that every boundary point of $\overline{\Omega}^*$ has a distance not exceeding ϵ from some point of Ω'. For every $h > 0$ let Ω_h consist of all points in the interior Ω^* of $\overline{\Omega}^*$ whose coordinates are integral multiples of h and whose h-neighbors belong to $\overline{\Omega}^*$. Let δ be the (positive) distance of $\overline{\Omega}^*$ to Ω'. We choose h so small that $2C[m_\delta^{(2)} h + \omega_\delta^{(2)}(h)] \le \eta/2$. Then

$$|\phi^{(h,\epsilon,\delta)} - \phi| \le \eta.$$

If the partial derivatives of $\phi(x,y)$ of the third order exist and are continuous in Ω, we may replace (38), (39) by

$$|D_{h,x}[\phi_i] - (\phi_x)_i|, |D_{h,y}[\phi_i] - (\phi_y)_i| \le \tfrac{1}{6} m_\delta^{(3)} h^2, \tag{38'}$$

$$|\Delta_h[\phi_i] - (\Delta\phi)_i| \le \tfrac{2}{3} m_\delta^{(3)} h, \tag{39'}$$

and instead of (40) we obtain the estimate

$$\max_{\Omega_h} |\phi^{(h,\epsilon,\delta)} - \phi| \le \tfrac{1}{3} Cm_\delta^{(3)}(Ah^2 + 2h) + \omega(\epsilon) + \omega^*(\epsilon). \tag{40'}$$

If $\phi(x,y)$ possesses continuous derivatives of order four, (39′) may be replaced by

$$|\Delta_h[\phi_i] - (\Delta\phi)_i| \le \tfrac{1}{6} m_\delta^{(4)} h^2, \tag{39''}$$

so that instead of (40′) we obtain

$$\max_{\Omega_h} |\phi^{(h,\epsilon,\delta)} - \phi| \le \tfrac{1}{6} C(2m_\delta^{(3)} + m_\delta^{(4)}) h^2 + \omega(\epsilon) + \omega^*(\epsilon). \tag{40''}$$

If the derivatives of $\phi(x,y)$ (of order 2, 3, 4, respectively) are continuous in $\overline{\Omega}$, condition (ii) is superfluous. We may drop the superscript and subscript δ in (40), (40′), (40″) and obtain, for $h \to 0$, $\epsilon \to 0$, uniform convergence of $\phi^{(h,\epsilon)}$ to ϕ. In fact if all points of Ω_h' are on Ω' the terms with ϵ disappear and we have, say in the case $m^{(4)} < +\infty$, that $|\phi^{(h)} - \phi| = 0(h^2)$.

All preceding estimates involve (α), some a priori estimates for the solution of $\boldsymbol{P}$, (β) the exact solution of $\boldsymbol{P}_h$. Without some a priori information on the solution of the differential equation, however, its approximation by the solution of the difference equation can never be estimated. On the other hand, the difference between an exact and an approximate solution of the difference equation (and only approximate solutions can be obtained in practice) can be estimated at once by means of (31).

6. Solution of the Difference Equation by Iterations

In this section we describe an effective method for solving problem $\boldsymbol{P}_h$, and at the same time obtain a *constructive existence proof.*

Define (for $i = 1,2, \ldots, N$)

$$f_i(z;\zeta^1,\zeta^2,\zeta^3,\zeta^4) = z + \frac{h_2}{4} F\left(x_i, y_i, z, \frac{\zeta^1 - \zeta^3}{2h}, \frac{\zeta^2 - \zeta^4}{2h}\right). \tag{41}$$

Then

$$\frac{\partial f_i}{\partial z} = 1 + \frac{h_2}{4} F_z \tag{42}$$

is nonnegative, so that there exists functions

$$z = g_i(Z;\zeta^1, \ldots, \zeta^4) \tag{43}$$

such that

$$f_i[g_i(Z;\zeta^1,\ldots,\zeta^4);\zeta^1,\ldots,\zeta^4]\equiv Z. \tag{44}$$

Also set

$$s_i(\zeta^1,\ldots,\zeta^4)=g_i\left(\frac{1}{4}\sum_{\nu=1}^{4}\zeta^\nu;\zeta^1,\ldots,\zeta^4\right). \tag{45}$$

Let ϕ be a function defined on $\bar{\Omega}_h$ and satisfying the boundary condition $\phi_j=v_j$, $j=N+1,\ldots,M$. It satisfies the equation $\boldsymbol{L}_h[\phi_i]=0$, $i=1,\ldots,N$ and is a solution of $\boldsymbol{P}_h$ if, and only if,

$$f_i(\phi_i;\phi_{i1},\ldots,\phi_{i4})=\frac{1}{4}\sum_{\nu=1}^{4}\phi_{i\nu},\qquad i=1,\ldots,N,$$

that is, if

$$\phi_i=s_i(\phi_{i1},\ldots,\phi_{i4}),\qquad i=1,\ldots,N. \tag{46}$$

Now let $\phi^{(0)}$ by any function in $\bar{\Omega}_h$ satisfying the boundary condition and let the functions $\phi^{(1)}$, $\phi^{(2)}$, $\ldots$, be defined by either of the two following iteration schemes. (A), set

$$\phi_i^{(n+1)}=s_i(\phi_{i1}^{(n)},\ldots,\phi_{i4}^{(n)}),\qquad i=1,\ldots,N \tag{47}$$

$$\phi_j^{(n+1)}=\phi_j^{(n)}=v_j,\qquad j=N+1,\ldots,M.$$

(B), set

$$\phi_i^{(n+1)}=s_i(\tilde{\phi}_{i1}^{(n)},\ldots,\tilde{\phi}_{i4}^{(n)}),\qquad i=1,\ldots,N, \tag{48}$$

where

$$\tilde{\phi}_{i\nu}=\begin{cases}\phi_{i\nu}^{(n+1)} \text{ if } P_{i\nu}=P_j \text{ and } j<i,\\ \phi_{i\nu}^{(n)} \quad \text{otherwise,}\end{cases}$$

$$\phi_j^{(n+1)}=\phi_j^{(n)}=v_j,\qquad j=N+1,\ldots,M.$$

If the sequence $\{\phi^{(n)}\}$ converges, then the limit function is a solution of $\boldsymbol{P}_h$, for s_i is a continuous function of its arguments.

In the case of the Laplace difference equation, (A) corresponds to the difference equation of heat conduction whose solution converges to that of the Laplace equation for $n\to\infty$ (n being interpreted as time), and (B) is the well-known Liebmann method.

We assume now that (3) is replaced by the stronger condition

$$F_i\geq\eta>0 \tag{49}$$

and prove that *procedure* (B) *converges*. The proof for (A) is practically the same.

By (48)

$$\phi_i^{(n+1)}-\phi_i^{(n)}=\sum_{\nu=1}^{4}\left(\frac{\partial s_i}{\partial\zeta^\nu}\right)^{*}(\tilde{\phi}_{i\nu}^{(n)}-\tilde{\phi}_{i\nu}^{(n-1)}), \tag{50}$$

where the asterisk indicates that the partial derivatives are evaluated at a point $(\zeta^1,\ldots,\zeta^4)$,

$$\zeta^\nu=\tau_i\tilde{\phi}_{i\nu}^{(n)}+(1-\tau_i)\tilde{\phi}_{i\nu}^{(n-1)},\qquad 0\leq\tau_i\leq 1.$$

By (41), (44), (45),

$$\frac{\partial f_i}{\partial z}\frac{\partial G}{\partial Z}=1,\qquad \frac{\partial f_i}{\partial z}\frac{\partial g_i}{\partial\zeta^\nu}+\frac{\partial f_i}{\partial\zeta^\nu}=0,$$

$$\frac{\partial f_i}{\partial\zeta^1}=-\frac{\partial f_i}{\partial\zeta^3}=\frac{h}{8}F_p,\qquad \frac{\partial f_i}{\partial\zeta^2}=-\frac{\partial f_i}{\partial\zeta^4}=\frac{h}{8}F_q,$$

$$\frac{\partial s_i}{\partial\zeta^\nu}=\frac{1}{4}\frac{\partial g_i}{\partial Z}+\frac{\partial g_i}{\partial\zeta^\nu},$$

so that by (42)

$$\frac{\partial s_i}{\partial\zeta^1}=\frac{\frac{1}{4}\left(1-\frac{h}{2}F_p\right)}{1+\frac{h^2}{4}F_z},\qquad \frac{\partial s_i}{\partial\zeta^2}=\frac{\frac{1}{4}\left(1-\frac{h}{2}F_q\right)}{1+\frac{h^2}{4}F_z},$$

$$\frac{\partial s_i}{\partial\zeta^3}=\frac{\frac{1}{4}\left(1+\frac{h}{2}F_p\right)}{1+\frac{h^2}{4}F_z},\qquad \frac{\partial s_i}{\partial\zeta^4}=\frac{\frac{1}{4}\left(1+\frac{h}{2}F_q\right)}{1+\frac{h^2}{4}F_z}.$$

Hence

$$\frac{\partial s_i}{\partial\zeta^\nu}\geq 0,$$

and setting

$$\rho=\frac{1}{1+\frac{h^2\eta}{4}}<1, \tag{51}$$

it follows from (49) that

$$\sum\left|\frac{\partial s_i}{\partial\zeta^\nu}\right|=\sum\frac{\partial s_i}{\partial\zeta^\nu}\leq\rho.$$

Setting

$$m_{n+1}=\max_{\bar{\Omega}_h}|\phi^{(n+1)}-\phi^{(n)}|, \tag{52}$$

we conclude from (50) that

$$m_{n+1}\leq\rho m_n,$$

so that

$$m_n\leq\rho^{n-1}m_1,$$

and for $p>1$,

$$\max_{\bar{\Omega}_h}|\phi^{(n+p)}-\phi^{(n)}|\leq\sum_{\nu=n+1}^{n+p}m_\nu\leq\frac{m_1\rho^n}{1-\rho},$$

which implies the existence of

$$\phi=\lim_{n\to\infty}\phi^{(n)}.$$

Also, by (46), (48),

$$\phi_i^{n+1}-\phi_i=\sum\left(\frac{\partial s_i}{\partial\zeta^\nu}\right)^{**}(\tilde{\phi}_{i\nu}^{(n)}-\phi_{i\nu}),$$

where the double asterisk indicates that the partial derivatives are evaluated at a point $(\zeta^1, \ldots, \zeta^4)$,

$$\zeta^r = \tau_i \tilde{\phi}^{(\eta)}_{i\nu} + (1-\tau_i)\phi_{i\nu}, \qquad 0 \leq \tau_i \leq 1.$$

Hence, setting

$$\mu_{n+1} = \max_{\Omega_h} |\phi^{(n+1)} - \phi|, \tag{53}$$

we have that $\mu_{n+1} \leq \rho \mu_n$, so that

$$\mu_n \leq \rho^n \mu_0. \tag{54}$$

Since μ_0 can be estimated by means of (31), we can determine a priori how many steps are needed in order to obtain ϕ with a desired degree of accuracy.

Now we drop assumption (49) and set (for $\eta > 0$)

$$\boldsymbol{L}_h^{(\eta)}[\phi_i] = \boldsymbol{L}_h[\phi_i] + \eta\phi_i.$$

Let Let $\phi^{(\eta)}$ be the solution of the boundary value problem

$$L_i^{(\eta)}[\phi_i] = 0, \quad i = 1, \ldots, N;$$

$$\phi_j = v_j, \quad j = N+1, \ldots, M.$$

This solution exists by virtue of the preceding result. Applying (33) with $\boldsymbol{L}_h$ replaced by $\boldsymbol{L}_h^{(\eta)}$, we conclude that $|\phi^{(\eta)}| \leq K$, so that $|\boldsymbol{L}_h[\phi_i^{(\eta)}]| = |\eta\phi_i^{(\eta)}| \leq K\eta$. By (31)

$$\max_{\Omega_h} |\phi^{(\eta')} - \phi^{(\eta'')}| \leq 2CK(\eta' + \eta''),$$

so that

$$\phi = \lim_{\eta \to \infty} \phi^{(\eta)}$$

exists. It is clear that ϕ is a solution of $\boldsymbol{P}_h$. Also, by (31),

$$\max_{\Omega_h} |\phi^{(\eta)} - \phi| \leq CK\eta. \tag{55}$$

Since $\phi^{(\eta)}$ can be computed by procedures (A) or (B), we have an effective method of solving $\boldsymbol{P}_h$ in all cases.

7. Extension

Let $a(x,y)$, $b(x,y)$, $c(x,y)$ be continuous functions defined in Ω.

$$ac - b^2 > 0. \tag{56}$$

Set

$$\Lambda[\phi] = a\phi_{xx} + 2b\phi_{xy} + c\phi_{yy}, \tag{57}$$

$$\boldsymbol{L}[\phi] = \Lambda[\phi] - F(x,y,\phi,\phi_x,\phi_y). \tag{58}$$

With this new operator $\boldsymbol{L}$ we can state problem $\boldsymbol{P}$.

Motzkin and Wasow* showed that (t being a sufficiently large positive integer depending on Λ) Λ can be approximated by a difference operator $\Lambda_h (h > 0)$ defined by

$$\Lambda_h[\phi] = \frac{1}{h^2} \sum_{r,s=-t}^{t} \rho^{rs}(x,y)\phi(x+rh, y+sh),$$

and satisfying the following conditions:

$\Lambda_h[\phi] \equiv \Lambda[\phi]$ if $\phi(x,y)$ is a polynomial of second degree, (59)

$$\rho^{rs}(x,y) > 0 \text{ for } (r,s) \neq (0,0), \tag{60}$$

$$0 < \frac{1}{K_1} \leq \sum_{(r,s) \neq (0,0)} \rho^{rs}(x,y) \leq K_1. \tag{61}$$

Applying (59) to $\phi \equiv 1$ we have that

$$\rho^{00}(x,y) = -\sum_{(r,s) \neq (0,0)} \rho^{rs}(x,y) < 0. \tag{62}$$

If $\phi(x,y)$ has continuous derivatives of the second order whose moduli of continuity do not exceed $\omega^{(2)}(\eta)$, then

$$|\Lambda_h[\phi] - \Lambda[\phi]| \leq 2t^2 K_1 \omega^{(2)}(\sqrt{2}th), \tag{63}$$

and if $\phi(x,y)$ has partial derivatives of the third order bounded in modulus by $m^{(3)}$, then

$$|\Lambda_h[\phi] - \Lambda[\phi]| \leq \frac{4}{3} t^3 K_1 m^{(3)} h. \tag{63'}$$

Under the hypotheses that the fourth order derivatives exist and are bounded by $m^{(4)}$ in modulus this can be improved to

$$|\Lambda_h[\phi] - \Lambda[\phi]| \leq \frac{2}{3} t^4 K_1 m^{(4)} h^2, \tag{63''}$$

provided Λ_h satisfies the additional condition

$\Lambda_h[\phi] \equiv 0$ if $\phi(x,y)$ is a homogeneous polynomial of degree 3. (64)

All this follows easily from Taylor's theorem.

Once Λ_h has been chosen, it is easy to find difference operators

$$D_{h,x}[\phi] = \frac{1}{h} \sum_{r,s=-t}^{t} \sigma^{rs}(x,y)\phi(x+rh, y+sh),$$

$$D_{h,y}[\phi] = \frac{1}{h} \sum_{r,s=-t}^{t} \tau^{rs}(x,y)\phi(x+rh, y+sh),$$

satisfying the conditions

$$\sigma^{00}(x,y) \equiv \tau^{00}(x,y) \equiv 0, \tag{65}$$

$$|\sigma^{rs}(x,y)|, |\tau^{rs}(x,y)| \leq K_2 |\rho^{rs}(x,y)|, \tag{66}$$

and approximating ϕ_x, ϕ_y in the sense that

$D_{h,x}[\phi] \equiv \phi_x, D_{h,y}[\phi] \equiv \phi_y$ for every linear function $\phi(x,y)$. (67)

We have that

$$|D_{h,x}[\phi] - \phi_x|, |D_{h,y}[\phi] - \phi_y| \leq 2tK_1K_2\omega^{(1)}(\sqrt{2}th) \tag{68}$$

*J. Math. Phys. **31** (1953).

if $\phi(x,y)$ has continuous partial derivatives with moduli of continuity bounded by $\omega^{(1)}(\eta)$,

$$|D_{h,x}[\phi]-\phi_x|, |D_{h,y}[\phi]-\phi_y| \leq 2t^2K_1K_2m^{(2)}h \quad (68')$$

if the second derivatives exist and are bounded by $m^{(1)}$ in absolute value.
If

$$D_{h,x}[\phi]\equiv D_{h,y}[\phi]\equiv 0 \text{ for every homogeneous quadratic polynomial } \phi(x,y), \quad (69)$$

then, under the hypothesis of (63′),

$$|D_{h,x}[\phi]-\phi_x|, |D_{h,y}[\phi]-\phi_y| \leq \tfrac{4}{3}t^3K_1K_2m^{(3)}h^2. \quad (68'')$$

We approximate $\boldsymbol{L}$ by the difference operator

$$\boldsymbol{L}_h[\phi]=\Lambda_h[\phi]-F\{x,y,\phi,D_{h,x}[\phi],D_{h,y}[\phi]\}. \quad (70)$$

Let P_0 be the point (x_0,y_0). We order the $T=4t(t+1)$ points (x_0+rh,y_0+sh), where $r,s=0,\pm1,\ldots,\pm t$, and $(r,s)\neq(0,0)$ lexicographically with respect to (r,s) and denote them by $P_{01},\ldots,P_{0T}$. These points shall be called the h-neighbors of P_0. The new definition of neighbors leads to a new definition of the boundary Ω_h' of a lattice domain Ω_h, and having this new definition, we can state the boundary value problem $\boldsymbol{P}_h$ for the operator $\boldsymbol{L}_h$ defined by (70).

We make now two remarks concerning the linear difference operator

$$l_h[\phi_i]=\Lambda_h[\phi_i]+\alpha_iD_{h,x}[\phi_i]+\beta_iD_{h,y}[\phi_i]-\gamma_i\phi_i \quad (71)$$

subject to conditions (13), (14).

(1) Set

$$h_1=\frac{1}{2K_2}. \quad (72)$$

Then for $0<h<h_1$

$$l_h[\phi_i]=\frac{1}{h^2}\left\{\sum_{\nu=1}^{T}\lambda^{i\nu}\phi_{i\nu}-\phi_i\sum_{\nu=1}^{T}\lambda^{i\nu}\right\}-\gamma_i\phi_i \quad (73)$$

with

$$\lambda^{i\nu}\geq 0, \qquad \sum_{\nu=1}^{T}\lambda^{i\nu}>0. \quad (74)$$

In fact, applying (57) to $\phi\equiv 1$, we see that

$$\Sigma\sigma^{rs}(x,y)\equiv\Sigma\tau^{rs}(x,y)\equiv 0,$$

so that l_h can be written in the form (73) with

$$\lambda^{i\nu}=\rho^{(r,s)_\nu}(x_{i\nu},y_{i\nu})-h\sigma^{(r,s)_\nu}(x_{i\nu},y_{i\nu})-h\tau^{(r,s)_\nu}(x_{i\nu},y_{i\nu}),$$

where $P_{i\nu}=(x_i+rh,y_i+sh)$, $(r,s)=(r,s)_\nu$. By virtue of (61), (66), condition (72) implies (74).

(2) Let $\bar{l}_h$ denote the operator (71) with $\gamma_i\equiv 0$. There exists a continuous function $\Phi(x,y)$ defined in $\bar{\Omega}$ and positive constants h_2, C such that for $0<h<h_2$

$$\frac{\max_{\bar{\Omega}}\Phi(x,y)}{\min_{\bar{\Omega}}\bar{l}_h[\Phi(x,y)]}\leq C. \quad (75)$$

In fact, assume (without loss of generality) that $\bar{\Omega}$ is contained in the domain $0\leq x\leq d$, and set $\Phi\equiv e^{\mu x}$, $\mu>0$. By (63′), (68′) we have that

$$\bar{l}_h[\Phi(x,y)]\geq a(x,y)\mu^2e^{\mu x}-\tfrac{4}{3}t^3K_1\mu^3e^{\mu d}h -A\mu e^{\mu x}-2A2t^2K_1K_2\mu^2e^{\mu d}h.$$

If we first choose a fixed μ such that

$$\mu^2\min_{\bar{\Omega}}a(x,y)-\mu A>1,$$

we can determine a h_2 such that for $h<h_2$, $\bar{l}_h[\Phi(x,y)]<\frac{1}{2}$. Then (75) holds with $C=2e^{\mu d}$.

Using these two remarks and assuming that $h<\min(h_1,h_2)$, all considerations of sections 3 to 6 can be repeated with only minor and obvious modifications. Inequality (16) holds with the C determined above, and so does (31). This inequality implies the uniqueness and existence of a solution of $\boldsymbol{P}_h$. This solution can be computed effectively by the method of section 5, and its deviation from the solution of $\boldsymbol{P}$ can be estimated as in section 5, using inequalities (63), (68).

We note that the case in which eq (1) is approximated not by (2) but by a more sophisticated difference equation is included in the preceding discussion.

Los Angeles, October 9, 1952.

Journal of Research of the National Bureau of Standards Vol. 51, No. 5, November 1953 Research Paper 2456

Determination of Glucose by Means of Sodium Chlorite

Herbert F. Launer,[1] William K. Wilson, and Joseph H. Flynn

The oxidation of several aldoses with acid sodium chlorite solution was investigated in order to obtain a method for the determination of aldehyde groups in sugars and their polymers.

The kinetics of the oxidation of glucose and cellobiose were studied over the experimental ranges 3.4 to 4.4 pH, 30° to 65° C, 0.005- to 0.15-*M* sodium chlorite, and 0.00006- to 0.0016-*M* aldose, both by the determination of the change in chlorite concentration by iodometric titration and by the photometric measurement of ClO_2 formed. The rate of oxidation was found to be approximately first order with respect to aldose and chlorous acid. The measurement of the oxidation was complicated by the second-order decomposition of chlorous acid. This decomposition was corrected for by a calibration curve and an approximate formula derived from the reaction kinetics. Use of either of these corrections gave experimental values for glucose within a few percent of the theoretical value.

Melibiose, maltose, and lactose were oxidized at about the same rate as glucose and cellobiose. Nonreducing sugars and sugar acids were not appreciably oxidized under the experimental conditions used.

I. Introduction

During a study of the photochemical degradation of papers it was desired to measure small changes in functional group content, such as aldehyde and carboxyl, resulting from irradiation.

Various methods that have been proposed for the estimation of aldehyde in cellulose are the hypoiodite method [1, 2, 3, 4, 5, 6, 7],[2] the dye absorption method of Geiger and Wissler [8], the acid permanganate method of Hiller and Pacsu [9], modifications of the Kiliani reaction by Frampton et al. [10] and Yundt [11], and the mercaptalation method of Wolfrom and coworkers [12]. Isbell [13] has used the Kiliani reaction in connection with radioactive tracer techniques to determine the reducing end groups in dextrans. The hydroxylamine method of Gladding and Purves determines total carbonyl [14].

Most of the above methods use an alkaline medium or are not sensitive enough for many purposes. It has been shown that oxidized celluloses may be extensively changed in alkaline media [15, 16, 17, 18]. In the permanganate method of Hiller and Pacsu, an acidic medium is employed, but this method had been severely criticized by Meller [19] and by Husemann [20]. Attempts in the Bureau's Paper Section to obtain quantitative oxidation of several simple sugars, using the permanganate method, were not satisfactory. For example, glucose, cellobiose, galactose, and arabinose were oxidized 10, 11, 12, and 24 percent, respectively, calculated from the $KMnO_4$ reduced.

Chlorite in acid solution as a reagent for the determination of aldehyde in cellulose was suggested by the work of Jeanes and Isbell [21], who reported that the aldehyde in sugars is oxidized by acid chlorite solutions at room temperature to carboxyl with very little side reaction. Ketoses, polyhydroxy alcohols, and aldonic acids were attacked only after many days' treatment with chlorite solutions. The oxidation rates increased with a decrease in pH, thus indicating that chlorous acid was the oxidant. These workers suggested that the main reaction corresponded approximately to the equation

$$RCHO+3HClO_2 \rightarrow RCOOH+2ClO_2+HCl+H_2O. \quad (1)$$

They showed that the study of the reaction system was complicated by the spontaneous decomposition of chlorites in acid solution and that chlorine dioxide reacts slowly or not at all with aldoses.

The present paper deals with the stoichiometry and kinetics of the reaction of chlorite with glucose and, to a lesser extent, cellobiose. Some data on melibiose, maltose, and lactose are also given. This work was undertaken preliminary to a study of the determination of the aldehyde content of cellulose.

2. Chemistry and Kinetics of Decomposition of Acidic Chlorite Solutions

The chemistry of chlorite has been investigated by Holst [22], Taylor, et al. [23, 24], Jeanes and Isbell [21], and Barnett [25]. Chlorites are most useful as oxidants in acid solution, but a study of the kinetics of the reactions is complicated by the instability of chlorous acid. The decomposition of chlorous acid is a function of pH, temperature, concentration, ionic strength, and impurities that may act as catalysts.

The net equation for the decomposition (or dismutation) of chlorous acid has been shown by Barnett [25] and confirmed by Taylor et al. [23] to conform approximately to the equation

$$4HClO_2 \rightarrow 2ClO_2+HClO_3+HCl+H_2O. \quad (2)$$

Barnett [25] has shown that the decomposition is second order, and this was confirmed in the present investigation, using the differential method.

Figure 1 is a plot of decomposition versus time of a 0.005 *M* solution of sodium chlorite at a pH of 3.52

[1] Present address: Western Regional Research Laboratory, U. S. Department of Agriculture, Albany, Calif.

[2] Figures in brackets indicate the literature references at the end of this paper.

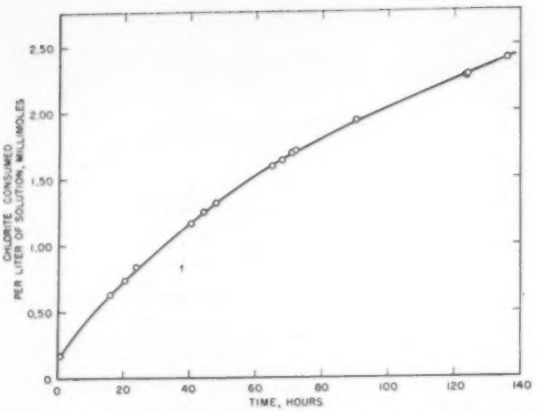

FIGURE 1. *Decomposition of chlorous acid with time.*
0.005-*M* sodium chlorite buffered to pH 3.52 at 40° C.

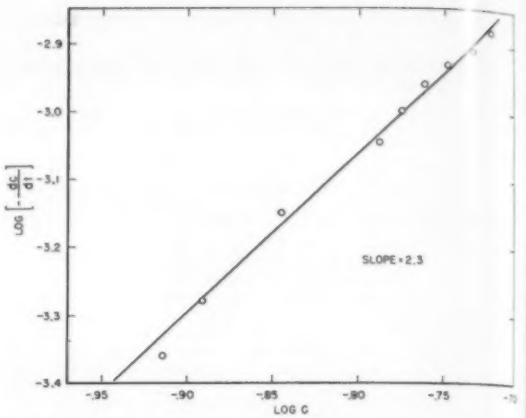

FIGURE 2. *Order of decomposition of $HClO_2$ by the differential method.*
0.005-*M* sodium chlorite buffered to pH 3.52 at 40° C.

and an ionic strength of 0.10. The chlorite concentration was determined by iodometric titration. A plot of the logarithm of the rate of decomposition against the logarithm of the chlorite concentration (fig. 2) gives a straight line with a slope of 2.3, the latter indicating the order of the decomposition with respect to chlorite.

The rate expression for the decomposition of acid chlorite solutions at constant pH may be written

$$-\frac{dC}{dt}=kC^2, \tag{3}$$

where C is the chlorite concentration at any time t. If chlorous acid is the active substance in the decomposition of acid chlorite solutions, eq (3) may be modified by expressing the concentration of chlorous acid in terms of $[H^+]$, C, and K_{HClO_2}, the dissociation constant of chlorous acid. From the equation for the dissociation of chlorous acid, $HClO_2 \rightleftharpoons ClO_2^- + H^+$, it follows that

$$[HClO_2]=\frac{[H^+]C}{[H^+]+K_{HClO_2}}=hC.$$

Then

$$-\frac{dC}{dt}=k_D h^2 C^2, \tag{4}$$

where k_D is the rate constant for the decomposition. Values of k_D were obtained by plotting $1/C$ against t in the decomposition experiments. The average of the values obtained was 0.67 ± 0.05 liter mole^{-1} sec^{-1}. These data were obtained at chlorite concentrations of 0.005 and 0.01 millimolar, a temperature of 40° C, and pH values of 3.40, 3.52, 3.70, and 4.00. The initial concentration of chlorite was obtained by extrapolating the plot of $1/C$ against t to zero. This was necessary because of an immediate reaction upon addition of chlorite to the acid reaction system, presumably with impurities in the reagents. This "initial decomposition," averaging about 1.5 percent of the total chlorite, may be reduced considerably by recrystallizing the sodium chlorite and sodium acetate, the latter a component of the buffer system.

As indicated by eq (1) and (2), acids are produced in the decomposition of chlorous acid and in oxidation of aldose by chlorous acid. Therefore, it is necessary to keep the solutions well buffered to minimize changes in acidity with time. Barnett showed, in a comparison of rates, that it is also necessary to keep the ionic strength essentially constant.

Buffer systems consisting of sodium acetate and acetic acid were prepared that effectively covered the range of hydrogen-ion concentration used in this study. Buffer data are given in table 1. The ionic strength was kept constant, and the composition of the buffers, to give the desired pH, was calculated from the Debye-Huckel form of the mass-action equation [26]. These buffers had sufficient capacity to prevent changes in acidity great enough to be measured with a pH meter.

TABLE 1. *Sodium acetate-acetic acid buffers*

Temperature	Glacial acetic acid per liter of solution [a] to obtain the following pH values [b]		
	pH=3.40	pH=3.52	pH=3.70
°C	g	g	g
40	418.6	315.4	209.6
50	453.4	------	218.2

[a] All buffers contained 55.0 g of reagent-quality sodium acetate, $NaC_2H_3O_2 \cdot 3H_2O$ per liter.
[b] The pH values apply after the buffers have been diluted 1:4 by addition to the analytical mixtures.

Ferric ion, found in traces in most reagents, catalyzes the decomposition of chlorous acid. As little as 0.005 mg of iron as ferric ion caused considerable decomposition of chlorite solutions. The addition of a small quantity of sodium oxalate to complex the iron was found to lower k_D, the rate constant for the decomposition, to 0.55 liter mole^{-1} sec^{-1} at 40° C.

dium oxalate was used in all the determinations of sugars by the iodometric titration except for the data in table 4. It was not used in the determinations in which chlorine dioxide was measured photometrically, since sodium oxalate appeared to react to a slight extent with ClO_2 under the conditions of these experiments.

3. Kinetics of the Reaction of Glucose and Cellobiose With Acid Chlorite Solutions

The quantity of aldose oxidized may be estimated photometrically from the chlorine dioxide produced or iodometrically from the chlorite reacted.

3.1. Studies Based on the Iodometric Determination of Chlorite

As the ClO_2 formed in the decomposition of chlorous acid and in the oxidation of aldose interferes with the iodometric determination of chlorite, it must be removed by aeration before titrating.

There is considerable decomposition of $HClO_2$ during the oxidation of sugars such as glucose and cellobiose. Hence it is necessary to run "controls" along with the "test solutions." The control solution is identical in compositions with a test solution, except for aldose. In a rate experiment the control curve is subtracted from the test solution curve to obtain the net curve, the latter representing the approximate amount of chlorite consumed in the oxidation of aldose.

Data for the oxidation of glucose and cellobiose are plotted in figures 3 and 4, respectively. Figure 5 is a semilog plot of percent chlorite remaining against time for an experiment with a sevenfold excess of glucose. This plot indicates a first-order reaction with respect to chlorite up to about 50-percent consumption of chlorite.

Figures 6 and 7 are semilog plots of unoxidized glucose and cellobiose (in percent) against time in the presence of excess chlorite. The data for these plots are the same as used for figures 3 and 4. The straight lines obtained indicate that the reactions were first order with respect to glucose and cellobiose.

The percentage of aldose at any time t was determined from the curves in figures 3 and 4 by assuming that the maximum of the net (test solution minus control) curves represented complete oxidation.

It is now possible to write a rate expression for the oxidation of aldose at a constant pH in terms of chlorite reacted as

$$-\frac{dC}{dt}=kAC, \tag{5}$$

where A is the concentration of aldose and C the concentration of chlorite at any time t. Assuming that chlorous acid is the oxidant, the rate expression may be written by analogy with eq (4), as

$$-\frac{dC}{dt}=k_A h AC. \tag{6}$$

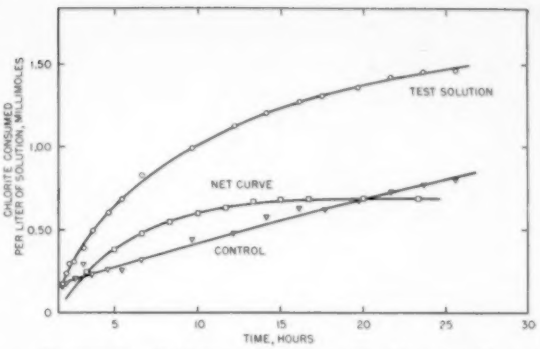

FIGURE 3. *Oxidation of glucose with chlorous acid.*
0.25 millimolar glucose in 0.005-*M* sodium chlorite buffered to pH 3.52 at 40° C.

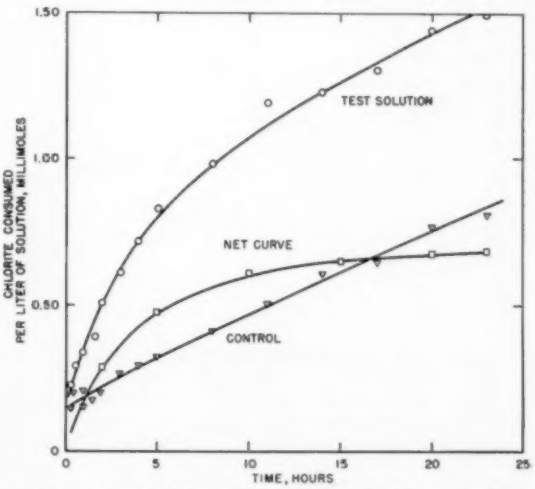

FIGURE 4. *Oxidation of cellobiose with chlorous acid.*
0.25 millimolar cellobiose in 0.005-*M* sodium chlorite buffered to pH 3.52 at 40° C.

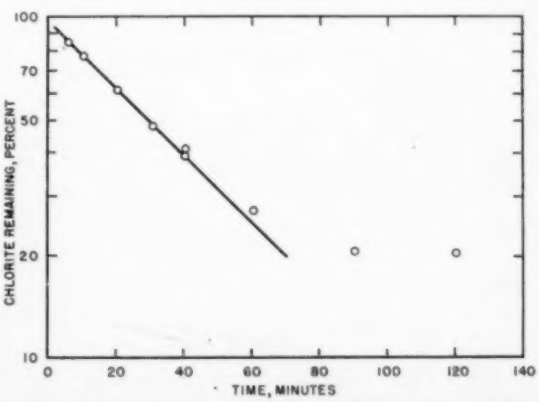

FIGURE 5. *Reaction of excess glucose with chlorous acid; determination of order with respect to chlorite by the integration method.*
0.005-*M* sodium chlorite buffered to pH 3.52 at 40° C. 0.0125-*M* glucose.

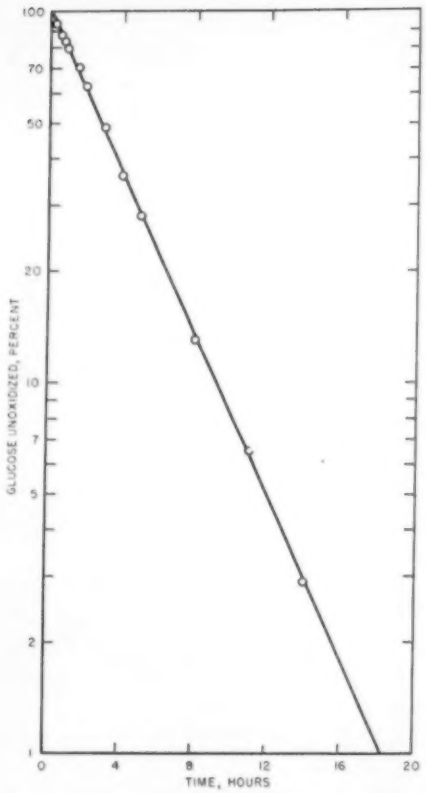

FIGURE 6. *Reaction of 0.01 millimole of glucose with excess chlorous acid; determination of order with respect to glucose by the integration method.*

0.005-*M* sodium chlorite buffered to pH 3.52 at 40° C.

The complete equation for the consumption of chlorite in a solution containing aldose may now be written

$$-\frac{dC}{dt}=k_A hAC+k_B h^2C^2. \tag{7}$$

It is possible to calculate approximate values for k_A. With a large excess of chlorite, the average value of the chlorite concentration is taken as a constant. Therefore the rate equation becomes

$$-\frac{dA}{dt}=k_A hAC, \tag{8}$$

and integrating:

$$\log A=\frac{k_A hC}{2.303}t+\text{const.} \tag{9}$$

If log A is plotted against t, then the slope m of the line is $-k_A hC/2.0303$ and

$$k_A=\frac{-2.303m}{hC}. \tag{10}$$

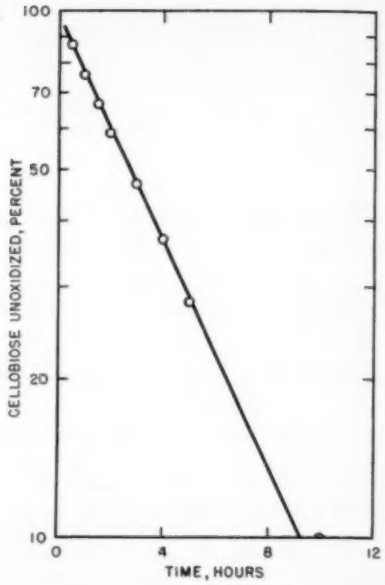

FIGURE 7. *Reaction of 0.01 millimole of cellobiose with chlorous acid; determination of order with respect to cellobiose by the integration method.*

0.005-*M* sodium chlorite buffered to pH 3.52 at 40° C.

Using values of 0.0042 *M* for C and -0.0000306 for m from figure 6, and calculating h at 40° C and a pH of 3.52 as 0.026,[3] $k_A=0.64$ liter mole^{-1} sec^{-1}.

Similarly, with a large excess of glucose, A is essentially constant, and

$$k_A=-\frac{2.303m}{hA}. \tag{11}$$

From figure 7, using values of 0.026 for h, 0.012 *M* for glucose concentration and $m=-0.000167$, $k_A=1.23$ liters mole^{-1} sec^{-1}.

It must be emphasized that this approach leaves much to be desired, and it is not surprising that the values for k_A do not show better agreement. Possible side reactions that are relatively unimportant when the chlorite is in excess may become important when the aldose is in excess, or vice versa. The combination of decomposition of chlorite and consumption of chlorite by aldose represents a decrease in chlorite concentration to about 70 percent of the initial value, and it is the average of this rather large change in chlorite concentration that is treated as a constant in eq (10).

The value of C in the control is always higher than the value of C in the test solution, as chlorite is consumed in the oxidation of aldose in the latter solution. Therefore, the decomposition of chlorite in the con-

[3] The value of K_{HClO_2} used in calculating h was calculated from the work of Barnett [25] as 0.0107 at 30° C and 0.0113 at 40° C at an ionic strength of 0.11.

trol always greater than in the test solution, and a simple subtraction of curves, as in figures 3 and 4, represents an overcorrection for decomposition.

One approach to this problem is to prepare a calibration curve for each aldose, relating millimoles of chlorite consumed by the aldose (control minus test solution) to millimoles of aldose. This procedure automatically takes into account (1) the fact that the exact stoichiometric equations for the oxidation of aldose by chlorous acid are unknown, (2) the fact that "slow" and "fast" aldoses require slightly different quantities of chlorous acid for oxidation, and (3) the difference in amount of spontaneous decomposition in the control and in the oxidation.

The data for the calibration curve for glucose, figure 8, are given in table 2. Table 3 contains data showing the accuracy with which glucose can be determined by using the calibration curve.

TABLE 2. *Data for glucose calibration curve* [a]

Glucose added	$NaClO_2$ consumed at 20 hr: control minus test solution	Glucose added	$NaClO_2$ consumed at 20 hr: control minus test solution
Millimoles/ 40 ml	*Millimoles/ 40 ml*	*Millimoles/ 40 ml*	*Millimoles/ 40 ml*
0.001	0.0028	0.020	0.0526
.002	.0055	.025	.0652
.003	.0083	.030	.0768
.004	.0109	.035	.0880
.005	.0140	.040	.0986
.005	.0144	.045	.1072
.010	.0273	.050	.1153
.015	.0402		

[a] The first five values in the table are the average of triplicate determinations at 20 hr. The other values are taken from rate curves for the specific concentration of glucose.

TABLE 3. *Determination of glucose, using a calibration curve*

Glucose added		Glucose found [a]		Error
Millimoles	*mg*	*Millimoles*	*mg*	$\frac{C_T - C_c}{C_c}$
0.0010	0.180	0.0011	0.198	+10
.0030	.540	.0031	.558	+3
.0050	.90	.0050	.90	0
.0150	2.70	.0153	2.75	+2
.0300	5.40	.0293	5.28	−2
.0450	8.10	.0444	7.99	−1

[a] Each value reported in the table represents the average of triplicates.

Another approach to the problem of difference in amount of decomposition in the control and in the oxidation is to assume that eq (1) correctly represents the stoichiometry of the reaction of chlorous acid with "slow" sugars and derive an analytical expression that one can use for calculating glucose. This involves the integration of eq (7).

Differential equations describing systems of simultaneous reactions of higher than first-order reaction kinetics are not in general integrable in a closed form [27]. Therefore, an exact analytical expression for the aldose concentration as a function of the rate constants, chlorite concentration, and time, cannot be obtained. However, an expression relating the aldose concentration to the concentrations of chlorite in the test and control solutions can be derived if certain approximations are made.

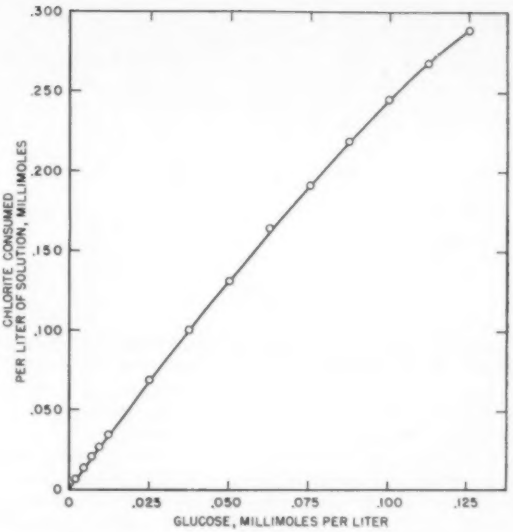

FIGURE 8. *Calibration curve for glucose.*

Assuming the stoichiometry of eq (1), the aldose concentration in the test solution (A_T) at any instant is given by

$$A_T = A_0 - \tfrac{1}{3}(C_0 - C_T - D_T), \tag{12}$$

where A_0 is the initial aldose concentration, C_0 is the initial chlorite concentration, C_T, the chlorite concentration in the test solution at time t, and D_T, the change in concentration of chlorite in the test solution due to decomposition. D_T cannot be measured directly. If C_c is the concentration of chlorite in the control solution at time t, then eq (4) may be integrated to obtain

$$C_0 - C_c = k_D h^2 C_0 C_c t. \tag{13}$$

Over any small time increment Δt, the change in concentration of chlorite in the test solution due to decomposition, ΔD_T, is approximately given from eq (4) by

$$\Delta D_T \simeq k_D h^2 \overline{C}_T^2 \Delta t, \tag{14}$$

where $\overline{C}_T$ is an average value of the chlorite concentration in the test solution over the time interval. If it is assumed that eq (14) may be applied over the time interval $\Delta t = t$, and that $\overline{C}_T^2$ may be represented by the geometric mean, then

$$D_T \simeq k_D h^2 C_0 C_T t. \tag{15}$$

Division of eq (15) by eq (13) leads to the relation

$$D_T \simeq (C_0 - C_c)\frac{C_T}{C_c}, \tag{16}$$

which expresses the decomposition in the test solution in terms of chlorite concentrations.

When the aldose oxidation is essentially complete, $A_T=0$; so substituting the expression for D_T from eq (16) into eq (12) and solving for A_0

$$A_0=\frac{C_0}{3}\left(1-\frac{C_T}{C_c}\right). \tag{17}$$

If titration volumes are substituted for concentrations,

$$\text{Millimoles of aldose}=\frac{V_0N}{12}\left(1-\frac{V_T}{V_c}\right), \tag{18}$$[4]

where V_0, V_T, and V_c are the milliliters of the thiosulfate of normality N equivalent to the chlorite in the control initially, in the test solution at the completion of the reaction, and in the control at the completion of the reaction, respectively.

Equation (18) was tested by substituting the data from rate experiments; the results are given in table 4. Considering the assumptions made in deriving the equation, the small quantities of sugar determined and the range of experimental conditions, the results are quite acceptable. Although eq (18) cannot be considered as accurate as a calibration curve, it is extremely useful in that it can be used over a wide range of experimental conditions, while a calibration curve applies only to the set of experimental conditions for which it was determined.

TABLE 4. *Analytical results for glucose and cellobiose calculated from eq (18)*

Experiment	pH	Temperature	$NaClO_2$	Glucose [a]	Time for completion	Error
		°C	*moles/liter*	*Millimoles/liter*	*hr*	
1a[b]	3.70	40	0.01	1.80	29	+1
1b	3.70	40	.01	2.40	39	+1
2a	3.70	40	.01	0.12	11	−2
2b	3.70	40	.01	.24	11	−2
2c	3.70	40	.01	.48	13	−1
3a	3.70	40	.005	.12	20	−1
3b	3.70	40	.005	.18	20	0
3c	3.70	40	.005	.24	21	−1
4	3.70	40	.005	.25	25	−2
6	3.70	40	.005	.06	18	0
7	3.70	40	.005	.06	18	−6
8	3.70	40	.005	.06	18	−7
9	3.70	40	.005	.06	(c)	−64[d]
10	3.70	40	.005	[e].06	18	−1
11	3.52	40	.005	[e].25	14	−2[f]
12	3.52	40	.005	.25	14	−1
13	3.52	40	.005	.25	14	+1[f]
14	3.40	40	.005	.25	13	−1
15a	3.40	40	.005	.06	11	−3
15b	3.40	40	.005	.12	12	−1
16	3.70	50	.005	.06	9	−2
17	3.40	50	.005	.06	4	0
18	4.00	50	.005	.06	(c)	−64[d]

[a] NBS Standard Sample. The weighed amount was large enough to permit a weighing accuracy of 0.1 percent, and aliquot portions were taken from the solutions made therefrom. The other sugars were kindly furnished by H. S. Isbell.

[b] Experiments with same numbers but different letters had same V_0 values. More than one oxidation run with one control.

[c] Incomplete.

[d] The curves for 9 and 18 were still rising rapidly, and the oxidation was obviously incomplete.

[e] Cellobiose.

[f] Curves were rising slightly at 14 hr.

[4] A similar derivation leading to this expression was given by Herbert F. Launer and Yoshio Tomimatsu in a paper presented before the Carbohydrate Division of the American Chemical Society in Chicago, September 8, 1953. This has been submitted for publication in Analytical Chemistry as a contribution from Western Regional Research Laboratory, U. S. Department of Agriculture.

3.2. Studies Based on the Photometric Determination of Chlorine Dioxide

From eq (1) it is apparent that aldoses may also be determined by measuring the concentration of the colored gas, ClO_2, photometrically when clear solutions are available. As in the iodometric method, the amount of aldose oxidized can be determined either from a calibration curve or from an analytical expression in which the quantities in eq (17) are expressed in terms of chlorine doxide.

$$2A_0=(ClO_2)_A=(ClO_2)_T-(ClO_2)_D \tag{19}$$

$$C_T=C_0-1.5(ClO_2)_A-2(ClO_2)_D \tag{20}$$

$$C_c=C_0-2(ClO_2)_c, \tag{21}$$

wherein $(ClO_2)_A$ is the chlorine-dioxide concentration arising from the oxidation of the aldose, and $(ClO_2)_D$ is that resulting from chlorous-acid decomposition. $(ClO_2)_T$ and $(ClO_2)_c$ are final concentrations in the test solution with aldose, and in the control solution without aldose, respectively, and are experimentally measurable, whereas those with subscripts A and D are not measurable and must be eliminated algebraically.

By combining eq (17), (19), (20), and (21), an expression for aldose in terms of chlorine dioxide and initial chlorite, in moles per liter, is obtained:

$$A_0=\frac{C_0}{2}\left[\frac{(ClO_2)_T-(ClO_2)_c}{C_0-1.5(ClO_2)_c}\right]. \tag{22}$$

Inasmuch as $(ClO_2)_c$ is small relative to C_0, eq (22) is insensitive to C_0 values.

The concentration of ClO_2 evolved in the test and control solutions was determined by measuring the transmission of light of 436-mμ wavelength[5] through glass-stoppered transmission cells with optically flat windows in which the reactions took place.

The simple abridged spectrophotometer previously described [28] was used in a modified form. The ranges of temperature, pH, and concentrations of chlorite and aldose used are given in table 5. Sodium-chlorite solution was added last to buffered solutions with or without aldose in volumetric flasks. A portion was then transferred by pressure through a drawn-out delivery tube to the transmission cell, and another portion was analyzed iodometrically for initial chlorite concentration, C_0. The mixing and transferring could be done with only small loss of ClO_2 by working at temperatures considerably below

[5] Obtained by use of a G. E. model H1 mercury-vapor lamp, using Corning filters 3389 and 5113 and an infrared filter.

the reaction temperatures. The filled cell was then placed in a constant-temperature water bath; it was found that the solution inside the cell attained the temperature of the bath in approximately 3 min.

TABLE 5. *Determination of glucose and cellobiose, using the photometric method*

Experiment	pH[a]	Temperature	Time for completion	Initial concentrations of reactants		ClO_2 produced		Aldose calculated from eq (22)
				$NaClO_2$	Glucose	In test solution	In control solution	
		°C	min	*Millimoles/liter*	*Millimoles/liter*	*Millimoles/liter*	*Millimoles/liter*	*Percentage of amount added*
1	3.6	30	[b] 181	73	1.56	5.33	2.62	[c] (92.0)
2	3.8	30	[b] 227	73	1.56	5.12	2.34	(93.9)
3	4.0	30	[b] 350	73	1.56	4.01	1.13	(95.2)
4	4.0	40	260	73	1.56	5.22	2.35	96.8
5	4.2	40	[b] 236	73	1.56	4.16	1.36	(92.6)
6	4.2	45	113	73	1.56	3.96	1.12	93.6
7	4.2	45	190	73	1.56	4.50	1.90	87.1
8	4.2	50	80	73	1.56	3.95	1.50	81.3
9	4.2	50	129	73	1.56	4.96	1.92	101.9
10	4.4	50	200	73	1.56	4.87	1.90	99.4
11	3.8	30	110	146	1.56	6.97	4.25	96.1
12	3.8	45	140	37	0.78	2.55	1.17	92.9
13	4.4	60	75	73	.80	3.13	1.85	82.1
14	4.2	60	70	38	.20	1.31	0.92	101.2
15	4.2	55	101	38	.40	2.03	1.27	100.0
16	4.0	55	182	25	.30	1.60	1.03	101.6
17	4.0	60	109	25	.30	1.52	0.94	102.5
18	4.0	65	109	18	.30	1.46	.87	106.2
19	4.0	65	60	40	.30	2.29	1.82	85.0
20	4.0	65	110	20	.30	1.57	1.01	101.0
21	4.0	65	205	10	.15	0.948	0.672	102.3
22	4.0	65	205	10	.075	.836	.672	122.0
23	4.0	65	180	10	.15	.930	.670	96.7
24	4.0	65	180	10	.075	.790	.670	88.7
25	4.0	65	210	10	[d] 15	.91	.69	82.0
26	4.0	65	150	20	[d] 30	1.87	1.32	101.6
Mean of values within the range 90.0 to 110.0%[e]								[f] 99.6
Mean of all values								[f] 96.5

[a] Acetate buffers were used throughout.
[b] Incomplete.
[c] The values in parentheses refer to experiments known to be incomplete and were not included in the means.
[d] Cellobiose.
[e] The correction for chlorine dioxide decomposition would raise the means by 1.0 percent (see text).

Transmittance values were converted into concentrations by the use of Beer's law:

$$(ClO_2),\ \text{moles per liter} = 0.00853 \log \frac{T_{H_2O}}{T_{\text{solution}}}. \quad (23)$$

The constant was calculated for a 10.00-mm cell thickness at a temperature of 65.0° C. At 25.0° C the constant was 0.00873, a difference of about 2 percent, allowing fairly accurate interpolation when required. Chlorine dioxide was found to follow Beer's law, with a standard deviation of individual values of 0.31 percent over the range of interest, 0.00032 to 0.0089 *M*. This was determined by measuring transmissions of fresh solutions of ClO_2 at known concentrations in buffer solution. ClO_2 was generated by adding warm 6-*N* sulfuric acid to 0.7-*M* sodium chlorite and washed by passing the gas through several portions of water. ClO_2 concentrations were determined iodometrically.

If desired, the analyst can measure the transmittance of the test cell in terms of that of the control cell by setting the transmittance scale to 100 percent when the control cell is in the beam. This gives the transmittancy of the *difference* in ClO_2 concentrations. Equations (22) and (23) may be combined to give

$$A_0 = -0.00427 \frac{C_0}{C_0 - 1.5(ClO_2)_c} \log \frac{T_T}{T_c}. \quad (24)$$

The value for $(ClO_2)_c$ must then be determined separately with eq (23), but the requirements for its accuracy are much less than for the ratio T_T/T_c.

Equation (22) was tested under experimental conditions that varied with respect to pH, temperature, and concentrations of reactants and products. The ClO_2 concentrations were taken from time-concentration curves at points indicating completion of reaction, excepting experiments 1, 2, 3, and 5 in table 5, which were discontinued before the curves had reached a maximum aldose value.

Although the aldose values calculated from eq (22), presented in table 5, show considerable variation, much more than that of aldose values determined by the volumetric technique, the mean values by the two techniques are in essential agreement and thus appear to confirm eq (1) with respect to the ratio 1 aldose:2ClO_2. The variations do not appear to be inherently greater in the photometric than in the volumetric method. They probably arise from the fact that in the photometric work, results were taken from time-concentration curves, each representing one reaction mixture, and thus, any rate discrepancy affected the entire curve. In the volumetric method, however, each point represented a separate reaction mixture and individual rate errors tended to be averaged out by the drawing of a smooth curve through the points. The same result was, of course, achieved in the photometric method by averaging the values from the individual experiments of table 5.

The aldose values of table 5 (column 9) tend to be low because of ClO_2 decomposition, shown by Bray [29] to occur in aqueous solution. This was confirmed photometrically for the present experimental conditions. Using the time-concentration curves shown in figure 9, it is possible to correct the ClO_2 values of table 5 for decomposition, raising the aldose values by an average of 1.0 percent. These corrections are maximum at high temperature and acidity and low aldose.

A factor that tends to limit the sensitivity of the photometric technique is the occurrence of the "initial immediate decomposition" of the reagent. This effect, which was discussed previously, occurs whenever the chlorite solution is added to the acidic buffer, as seen from the immediate development of yellow color. The amount of ClO_2 thus produced, before the decomposition or oxidation occurred to an appreciable extent, averaged 0.20 millimole/liter,

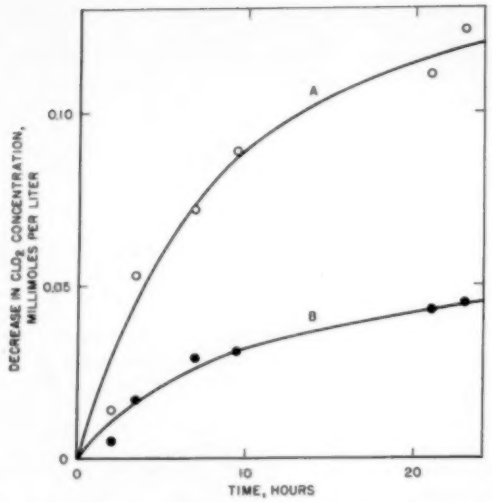

FIGURE 9. *Decomposition of ClO_2 under typical conditions.*

pH 3.7 (acetic acid-acetate buffer) 40° C, initial ClO_2 concentration for (curve A) 2.92 and for (curve B) 0.53 millimole per liter. Reaction was carried out in transmission cells and ClO_2 measured photometrically.

and appeared to be due to reaction of the reagent with impurities. Its value was taken in each experiment as the zero-time intercept of the decomposition curves and was thus accounted for in the ClO_2 values of table 5. Application of the photometric technique to very low aldose quantities would require the careful control or evaluation of this factor.

4. Determination of Melibiose, Maltose, and Lactose

Melibiose, maltose, and lactose are oxidized at about the same rate as glucose and cellobiose. Table 6 contains some analytical data on these sugars, using the iodometric method. These data are probably typical of the accuracy one could expect in the determination of small quantities of any particular sugar by this method without further standardization of conditions for it. The curves for lactose and maltose were quite smooth, but the data for melibiose were very erratic.

Results obtained with calcium lactobionate shown in table 7 suggest that lactose is hydrolyzed to a slight extent.

TABLE 6. *Determination[a] of maltose, lactose, and melibiose*

Calculated by—	Time	Error for—		
		Maltose	Lactose	Melibiose
	hr	*%*	*%*	*%*
Equation (18)	12	−1	−1	[b]
	18	−1	+7	
	24	+3	+10	
Glucose calibration curve	20	−4	+1	−10
Net curve; control minus test solution	20	−12	−6	−19

[a] Reactions were carried out in liter wash bottles and 25-ml aliquots taken at intervals. 0.25 millimole aldose per liter, 0.005-*M* $NaClO_2$, pH=3.52, t=40° C.
[b] Data too erratic to warrant calculation.

5. Action of Chlorous Acid in Nonreducing Sugars and Sugar Acids

Information on the action of chlorous acid on nonreducing sugars, sugar acids, salts, and lactones is given in table 7.

The data, in agreement with the work of Jeanes and Isbell [21], indicate that these compounds are oxidized little or not at all for the experimental conditions indicated.

TABLE 7. *Reaction of chlorous acid with lactones, salts of sugar acids, sugar acids, raffinose and sucrose*

0.005-*M* $NaClO_2$, pH=3.52, t=40°

Compound	Millimoles per liter	Extent of oxidation
		Percent
Rhamnomic lactone	0.25	Negligible
Do	1.25	Do.
Mannonic lactone	1.25	Do.
Calcium lactobionate	1.25	3
Calcium melibionate	1.25	Negligible
Gluconic acid	0.25	Do.
Raffinose	.25	Do.
Sucrose	14.6	2
Do	1.25	2

6. Recommended Procedure for Volumetric Method

The procedure recommended below is specific. As indicated by the range of conditions in table 4, one may use many different combinations of values for the pH, time, dilution, concentrations of aldose and chlorous acid, temperature, etc., to satisfy particular requirements.

This procedure was not applied to the photometric method. Higher chlorite concentrations may be used in that method to decrease the time for completion of the reaction as it does not depend upon the measurement of the change in chlorite concentration. The shorter reaction time is preferable in the photometric determination as it minimizes error introduced by the decomposition of chlorine dioxide.

Experimental conditions:	
Temperature	40° ±0.1 deg C
pH	3.52
Chlorite concentration	5.0 millimolar
Aldose	Not more than 0.50 millimolar
Sodium oxalate	125 mg/liter
Total volume	40 ml
Composition of test solution:	
Buffer [b]	10 ml
Sodium chlorite, 0.04 *M*	5 ml
Water and aldose solution to make a total volume of	40 ml
Composition of control:	
Buffer [b]	10 ml
Sodium chlorite, 0.04 *M*	10 ml
Water	5 ml
	25 ml

Glass-stoppered flasks of 250-ml capacity are recommended. The sodium chlorite solution is added last, and immediately thereafter the flask is placed in the constant-temperature bath. At the proper time the flask is removed from the bath.

[b] The buffer composition is given in table 1. The sodium oxalate is added to the buffer solution.

and ...ed with a short piece of tubing with a standard taper joint. Twenty-five to 50 ml of water is added and one or two bubblers, made by drawing about 8-mm tubing to about 1 mm at the end, are inserted. After bubbling the solution for 10 min with CO_2, N_2, or air, 50 ml of 10 percent KI and 5 ml of 6-*N* HCl are added and the liberated iodine titrated with 0.025 *N* thiosulfate. Under these conditions, 0.01 millimole of glucose is oxidized in about 20 hours.

Rate data may be obtained in the above manner, or aliquots may be taken from larger batches of solution, mixed in the same proportions as above. In the latter case, it is preferable to use wash bottles and blow out some solution into a graduated cylinder from which an aliquot may be pipetted. It must be remembered that ClO_2 is poisonous, and a water aspirator should be used when pipetting solutions containing ClO_2. The ClO_2 should be bubbled out of the above solutions under a hood.

The aldose may be estimated by eq (18), or by referring to a calibration curve.

7. References

[1] G. Romijn, Anal. Chem. **36,** 349 (1897).
[2] R. Willstatter and G. Schudel, Ber. deut. chem. Ges. **51,** 780 (1918).
[3] F. A. Cajori, J. Biol. Chem. **54,** 617 (1922).
[4] M. Bergmann and H. Machemer, Ber. deut. chem. Ges. **63,** 316, 2304 (1930).
[5] G. M. Kline and S. F. Acree, J. Research NBS **5,** 1063 (1930) RP247.
[6] A. R. Martin, L. Smith, R. L. Whistler, and M. Harris, J. Research NBS **27,** 449 (1941) RP1432.
[7] H. A. Rutherford, F. W. Minor, A. R. Martin, and M. Harris, J. Research NBS **29,** 131 (1942) RP1491.
[8] Ernst Geiger and Alfred Wissler, Helv. Chim. Acta **28,** 7, 1368 (1945).
[9] L. A. Hiller and Eugene Pacsu, Textile Research J. **16,** 318 (1946).
[10] V. L. Frampton, L. P. Foley, L. L. Smith and J. G. Malone, Anal. Chem. **23,** 1244 (1951).
[11] A. P. Yundt, Tappi **34,** 95 (1951).
[12] M. L. Wolfrom and L. W. Georges, J. Am. Chem. Soc. **59,** 282 (1937), and M. L. Wolfrom, L. W. Georges and J. C. Sowden, J. Am. Chem. Soc. **60,** 1026 (1938).
[13] H. S. Isbell, Science **113,** 532 (1951).
[14] E. K. Gladding and C. B. Purves, Paper Trade J. **116,** 150 (1943).
[15] G. F. Davidson, J. Textile Inst. **29,** T195 (1938); **31,** T81 (1940).
[16] G. F. Davidson and T. P. Nevell, J. Text. Inst. **39,** T102 (1948).
[17] C. Birtwell, D. A. Clibbens and B. P. Ridge, J. Textile Inst. **16,** T13 (1923); **17,** T145 (1926); **18,** T135 (1927).
[18] A. Meller, Tappi **34,** 171 (1951); **35,** 72 (1952).
[19] A. Meller, Tappi **33,** 11 (1950).
[20] E. Husemann and U. Consbruch, Makromol. Chem. **5,** No. 2, 179, Nov. (1950).
[21] A. Jeanes and H. S. Isbell, J. Research NBS **27,** 125 (1941) RP1408.
[22] Gustaf Holst, Ind. Eng. Chem. **42,** 2359 (1950).
[23] M. C. Taylor, J. F. White, G. P. Vincent, G. L. Cunningham, Ind. Eng. Chem. **32,** 899 (1940).
[24] M. C. Taylor, J. F. White, G. P. Vincent, Ind. Eng. Chem. **34,** 782 (1942).
[25] B. Barnett, The reactions of chlorous acid with iodide ion and with iodine: The ionization constant of chlorous acid, Ph. D. dissertation, University of Calif. (1935).
[26] W. M. Clark, The determination of hydrogen ions, p. 506 (The Williams & Wilkins Co., Baltimore, Md., 1928).
[27] A. Scrabal, Homogenkinetik, p. 140 (Edwards Bros., Inc., Ann Arbor, Mich., 1945).
[28] Herbert F. Launer, J. Research NBS **27,** 129 (1941) RP1430.
[29] William Bray, Z. physik. Chem. **54,** 569 (1906).

WASHINGTON, June 20, 1953.

UNIVERSITY OF MICHIGAN LIBRARIES

Journal of Research of the National Bureau of Standards Vol. 51, No. 5, November 1953 Research Paper 2457

Description and Analysis of the First Spectrum of Chromium, Cr I

Carl C. Kiess

Wavelengths and estimated intensities are presented for about 4,400 lines of Cr I recorded photographically between 11610 A in the infrared and 1880 A in the ultraviolet. Zeeman patterns, measured in magnetic fields of 35000 and 85000 oersteds for approximately 10 percent of the lines, are presented also. Analysis of the spectrum with these observational data has yielded classifications for about 80 percent of the Cr I lines, as combinations among the terms that arise from the various configurations assumed by the valence electrons of the atom in its excited and unexcited states. Of these terms 53 have been found due to the even electron configurations $3d^5\,ns$, $3d^4\,ns^2$, $3d^6$, and $3d^5\,nd$; and 115 due to the odd configurations $3d^5\,np$ and $3d^4\,4s\,np$. Among both even and odd terms several series of two or more members have been found converging to the ground state $a\,{}^6S$ and to the metastable state $a\,{}^4D$ of Cr II.

The ^7S, ^5S, and $^7P^\circ$ series, of three or more members, that converge to $a\,{}^6S$ are in remarkable accord in fixing the separation of the ground states of the neutral and singly ionized Cr atoms as 54570 cm^{-1}. This corresponds to an ionization potential of 6.764 electron volts.

1. Introduction

The description and analysis of the first spectrum of chromium presented in this paper represent results accumulated at the National Bureau of Standards over a period of more than 35 years. The work was begun in the summer of 1917 when, in the Spectroscopy Laboratory of this Bureau, a program was initiated of making prolonged exposures to the red and infrared spectra of several elements in order to test the photosensitizing properties of various dyes, notably dicyanin and dicyanin A. Among the elements studied was chromium, for which K. W. Meissner [1],[1] using photographic procedures, had reported some infrared lines. The new observations, as reported by Kiess and Meggers [2], not only verified the results of Meissner and of Stüting [3] but also extended our knowledge of the emission spectrum of chromium out to 9734 A and confirmed the radiometric measurements of Randall and Barker [4] in the region common to the two investigations.

The first series regularities in the chromium spectrum were pointed out by Richter [5], who showed that pairs of lines observed by him and by Miller [6] to have similar Zeeman patterns, are members of the two prominent triplets in the blue and violet. Kiess and Meggers [2] stated that the two intense triplets in the red and infrared, one with wide and the other with narrow separations, are mirror images of similar triplets in the blue and green. These first findings served to stimulate several investigators to search for additional regularities in the spectrum, and in 1922, announcements of new results were made independently and almost simultaneously from three laboratories. In his work describing the multiplet structure of the manganese spectra, Catalán [7] stated that similar structures had been discovered in the spectrum of chromium, and he gave some examples. These and other complex groups of chromium lines, together with their Zeeman patterns, were described at the same time by Frl. Gieseler [8], who sought to interpret the chromium regularities found by Paschen, but among which he could not detect series relationships. Such relationships were first published by C. C. and H. K. Kiess [9] in their note describing the first members of the principal, sharp, and diffuse series of wide and narrow triplets.

With the key to the structure of spectra in hand, various investigators soon worked out the classification of the outstanding lines of chromium. Following his preliminary announcement Catalán [10], in two brief notes, gave some additional multiplets and series from which he derived an ionization potential of 6.7 v for the neutral atom. These and other results, including a list of all known classified lines with term designations, he published in a more extended paper [11]. In the following year, Frl. Gieseler [12] published an analysis of the spectrum with her interpretations of it as derived from Zeeman patterns measured at Tübingen. In the meantime, similar investigations, made at the National Bureau of Standards for the purpose of testing the spectroscopic displacement and alternation laws of Kossel and Sommerfeld, led to the discovery and announcement by Meggers, Kiess, and Walters [13], of the first multiplets in the spectrum of singly ionized chromium. Contributing factors to the success of these investigations were temperature classifications by King [14]; Zeeman effects by Purvis [15], Miller [16], Hartman [17], Babcock [18], and Richter [19]; absorption observations by King [20], Gieseler and Grotrian [21], and Zumstein [22]; and under-water spark observations by Hulburt [23], and by Smith and Muskat [24].

The results that had been obtained up to 1925 for Cr I and Cr II showed that their prominent classified lines result from transitions among septet and quintet terms and sextet and quartet terms, respectively.

[1] Figures in brackets indicate literature references at the end of this paper.

However, the quantum theory of atomic spectra also required triplets and singlets for Cr I and doublets for Cr II. Continued work at the National Bureau of Standards brought some of these expected terms to light. They were presented, by the writer [25], in lists of all known terms, intended primarily for the use of astrophysicists interested in the spectra of the sun and stars. In 1931 Catalán and Sancho [26] published a revised list of more than 700 classified lines originating in transitions among all known levels of the septet, quintet, and triplet systems. In deriving a new value of 6.74 v for the ionization potential of neutral chromium, they made use of all terms having as a common limit the ground state $a\ ^6S$ of Cr II. When new types of plates sentitive to infrared rays became available, a new survey was made, at the National Bureau of Standards, of the chromium arc spectrum out to the limit accessible to photography. The result was an extended list of lines that brought to light new terms, especially of the triplet system. These were published in 1935 [27].

The difficulty of extracting new terms from the available wavelength data emphasized the need for a more homogeneous description of the spectra emitted by arcs and sparks between chromium electrodes. Accordingly, a new set of spectrograms of both Cr I and Cr II was secured at the NBS Spectroscopy Laboratory. From them were derived new wavelengths and intensity estimates, which, with similar data from observations made elsewhere, form the basis for the analysis of Cr I presented in this paper. The same observations served for the description and analysis of Cr II published recently [28].

2. Experimental Procedure

It is not necessary to repeat here the details of the experimental work done for this investigation. These are recorded in the two papers just cited, [27, 28]. Mention should be made, however, that some spectrograms of the arc operating in an atmosphere of nitrogen were obtained. For this purpose a stream of commercial nitrogen was kept flowing, at pressures between 600 and 700 mm Hg, through the chamber of the enclosed arc in order to suppress the CrO bands that appear as outstanding features of the yellow, red, and near-infrared regions of the spectrum. These bands mask almost completely all but the strongest lines of the atomic spectrum in this region. With their disappearance from the spectrograms, many new lines were revealed that have greatly extended the analysis of Cr I. The effectiveness of the above procedure in eliminating the bands from the spectrum is illustrated by figure 1. In measuring the spectrograms settings were made also on the band-heads given in table 6 to determine their wavelengths accurately for the use of molecular spectroscopists and astrophysicists.

3. Results

3.1. Wavelengths and intensities

The new observational data presented in this paper are the wavelengths and estimated intensities in the first two columns of table 1, the Zeeman patterns in tables 2 and 3, and the band-heads in table 6. The wavelengths are mean values from measurements on 2 to 8 spectrograms made at the National Bureau of Standards, at the Mt. Wilson Observatory, and at Princeton University, as described in the previous paper. All lines measured on only one plate have been omitted from the table unless their reality has been established by term combinations. For most of the lines the wavelengths are given to only 2 decimal places; but for some lines, measured more than 4 times, the individual measurements were highly accordant, so that it seemed desirable to retain the third decimal place in the mean. All the wavelengths longer than 1988 A are air values; those less than this wavelength are vacuum values derived from the Princeton spectrograms.

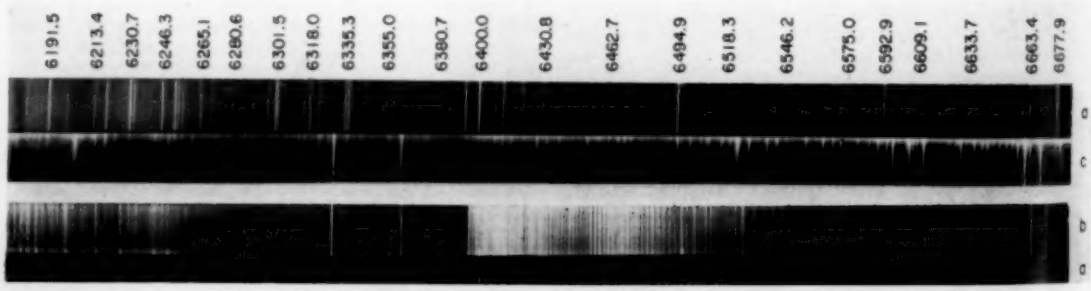

FIGURE 1. *Suppression of* CrO *bands.*
(a), Fe arc; (b), Cr arc in air; (c), Cr arc in nitrogen.

The strength and character of the lines are indicated by the numbers and letters in the second column of table 1. Absence of a letter means that the line appears sharp and symmetrical. Deviations from these characteristics, such as doubling, blending, and dissymmetries of shading, are indicated by the letter symbols adopted for this purpose by the International Astronomical Union [29]. The letter *Z* means that a Zeeman pattern, derived from NBS or MIT spectrograms, is recorded for the line in table 2.

The intensity estimates for the Cr I lines were made in the same manner as those for Cr II, and the statements made in the earier paper are pertinent here. Available for comparison are the intensity estimates derived by A. S. King [30] from two series of spectrograms of the chromium arc-in-air. The earlier series, published in 1915, extends from 6978 to 3550 A, whereas the series made nearly 10 years later covers the ultraviolet region from 3575 to 2362 A. Except for diffuse lines marked "*n*" or "*N*" in his lists, all of King's intensity numbers are smaller than those given in table 1. The factors by which King's intensities are to be multiplied to equal those of table 1 are approximately as follows:

King's intensities	Factors for—		King's intensities	Factors for—	
	1915 series	1924 series		1915 series	1924 series
1	25	5	9	5. 5	2. 5
2	15	4	10	5	2. 5
3	11	3. 5	15	4. 5	2. 0
4	9	3	20	4. 0	2. 0
5	7. 5	3	25	3. 5	1. 5
6	6. 5	2. 5	50	2. 5	1. 5
7	6	2. 5	75	2. 0	1. 5
8	6	2. 5			

Comparison of the estimated intensities with those determined photometrically is not satisfactory nor is it strictly legitimate. Both Frerichs [31] and Allen and Hesthal [32] have published photometric measurements of Cr I multiplets that show that the relative intensities of the lines are in close accord with those calculated theoretically for *LS*-coupling. In both investigations the measurements were made on lines emitted by an arc in an enclosure in which the air pressure was greatly reduced to minimize the effect of self-reversal. All the multiplets studied in these investigations contain lines that show self-reversal in the arc-in-air. More recently Hill and King [33] have published *gf*-values for 430 absorption lines of Cr I in multiplets that are of astrophysical importance. Their results also show satisfactory agreement with theoretical relative intensities. For the strongest lines of the spectrum, the estimated intensities are in only qualitative agreement with the photometric values. For the less intense lines, however, in which self-reversal is small or nonexistent, the quantitative relation, first pointed out by Russell [34], is found to hold, namely, that the estimated intensities are proportional to the square roots of the theoretical value. This finding is an illustration of the working of Fechner's law of photometry with the eye.

3.2 Zeeman Effects

The Zeeman patterns recorded for Cr I lines in table 2 were derived from NBS and MIT spectrograms, as described in the previous paper. The scheme of segregating these data in a separate table was adopted when it became evident that magnetic patterns were measured for about 10 percent of the lines. To include them with the classified lines is desirable, but to do so in this case would increase unduly the bulk of the tabulated data. As in the paper on Cr II, a dagger (†) indicates that the pattern was measured only on NBS plates; the letters *A*, *B*, *C*, and *D* indicate the type of shading displayed by unresolved patterns, Thus: *A*=/|\; *B*=|\/|; *C*=/\; *D*=⊓.

The *g*-values derived from the Zeeman patterns for energy levels of Cr I are recorded in tables 4 and 5. Those given to two decimal places were derived from the NBS plates, whereas the three-place figures were derived from the MIT plates. For many of the lines, it was not possible to measure the magnetic patterns and derive the *g*'s of the combining levels. These lines originate in terms of the $3d^5\,4s$ electron-configuration that have level separations smaller than the splitting due to the magnetic field. The Zeeman patterns of such lines are badly distorted, because of Paschen-Back interaction, and in many cases they are overlaid by similar patterns of adjacent lines so that the task of untangling them seems almost hopeless. Lines of Cr I with distorted patterns that offer a prospect of future interpretation are marked in table 2 with the symbol P–B.

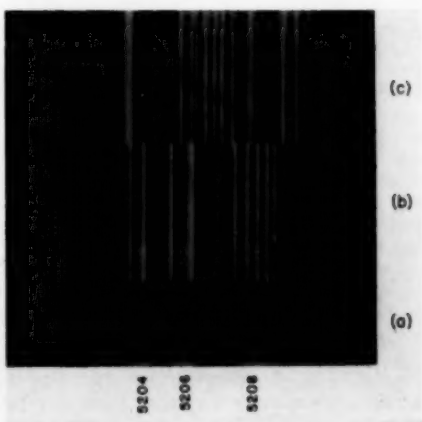

FIGURE 2. *Zeeman pattern of* $a^5S - z^5P^\circ$ *multiplet of* Cr I.
(a), No field; (b), paallel components; (c), normal components.

About twenty-five years ago Sommerfeld [35] pointed out the intense, green triplet of Cr I as an outstanding example of Paschen-Back interaction. The appearance of the pattern as produced in a field of 85,000 oersteds is illustrated by figure 2. The no-field lines are due to the transition $a\ ^5S - z\ ^5P^\circ$, which is a term combination of the same type as that producing the O I triplet at 7771 to 7775 A, namely, $3s\ ^5S^\circ - 3p\ ^5P$. A detailed analysis of the O I Zeeman patterns and the procedure for deriving the g-values of the terms have been reported by Kiess and Shortley [36]. A similar analysis, applied to the Cr I triplet, has yielded the g-values given in table 4 for the terms $a\ ^5S$ and $z\ ^5P^\circ$. Measurements of this pattern, at moderate field strengths, have been reported by Frl. Gieseler [37]. The structure of the pattern and its analysis, as derived from measurements of the MIT spectrograms, are given in table 3.

3.3 Term Structure of Cr I

The spectrum Cr I, emitted by neutral chromium atoms, results from transitions among even terms of the configurations $3d^5\ ns$, $3d^5\ ns^2$, $3d^6$ and $3d^5\ nd$ and odd terms of the configurations $3d^5\ 4s\ np$ and $3d^5\ np$ as given in tables 4 and 5. The assignment of terms to their proper electron configurations is quite obvious for many of them, but for others it is a matter of conjecture. The prominent, low, even terms with small and partially inverted level separations show a close parallelism with corresponding terms of Cr II and are, accordingly, assigned to the $d^5\ s$ configuration. On the other hand the low, even terms of the $d^4\ s^2$ configuration have wide separations; and by their positions in the energy diagram reveal their relationship to the corresponding terms of the $d^4\ s$ configuration of Cr II and the d^4 configuration of Cr III. The terms of the d^6 configuration should be similar in type to those of $d^4\ s^2$ but with inverted levels. Only one term, $c\ ^5D$, of this configuration has been found, the others lying too high to give observable combinations.

The terms of the odd configurations $3d^5\ 4p$ and $3d^4\ 4s\ 4p$ also exhibit characteristics that relate them to corresponding terms of Cr II and thus determine their configuration assignment.

3.4 Series and Ionization Potential

Among the Cr I terms are several that form Rydberg sequences of two or more members. The outstanding series are those derived by adding ns, np, and nd electrons to the ground term $3d^5(a\ ^6S)$ of Cr II, as given in table 7. The lower members of these series were among the prominent features of the spectrum pointed out by the early investigators, particularly by Frl. Gieseler [38], who recognized three ^7S series members and four ^5S members. All these series are remarkably regular and can be accurately represented by the Ritz formula $\nu = L - R/\{m+\alpha+\beta/m^2\}^2$, in which L is the limit of the series, α and β are constants peculiar to the series, and $m = 1,2,3, \ldots$ is the order number of the variable term. The values of α and β appropriate for each series are listed at the bottom of each column of table 7. From each series values of the limits may be calculated. The limit from the $^7P^\circ$ series was found to be in close agreement with those from the ^7S and ^5S series and was included with them in deriving a mean value of 54570 ± 2 cm^{-1} for the separation $a\ ^7S - a\ ^6S$ between the ground states of the neutral and singly ionized chromium atoms. This corresponds to an ionization potential of 6.764 v. This value is essentially the same as that given by Miss Moore [39] in Atomic Energy Levels, which was calculated by Professor H. N. Russell from the ^7S series alone with the method described by Shenstone [40]. With the term value 31071 thus found for $z\ ^7P^\circ$ as limit, a representation of the two members of the ^7D series shows that their Rydberg denominators are very nearly integral, and, therefore, that this series is approximately similar to those of hydrogen.

Series of $^5P^\circ$, $^5D^\circ$, and $^5F^\circ$ terms, each with three members, have been found from their combinations with $a\ ^5D$. These series arise from addition of np electrons to the $a\ ^6D$ state of Cr II, and may be satisfactorily represented with a Ritz formula. However, they give for the separation of $a\ ^5D$ from $a\ ^6D$ somewhat larger values than that calculable from the above separation of the ground states $a\ ^7S$ and $a\ ^6S$. It is well known, from analyses of other spectra, that such series are erratic and are not satisfactory for the fixing of limits; therefore, they have not been included in the determination of the ionization potential.

3.5. Chromium Oxide Band-heads

Most of the earlier investigators of the chromium arc spectrum have described the prominent band-structure that appears in the yellow and orange regions; and some of them have reported approximate wavelengths for the band-heads. A few of the most intense of these bands have been identified by Miss Davis [41] among the other bands that occur in the absorption spectrum of the giant star β Pegasi. On the National Bureau of Standards spectrograms the bands make their first appearance faintly near 4850 A in the blue, and can be traced to 11550 A in the infrared. Most of them lack the distinctive feature that can be designated with certainty as a band-head.

The first attempt to arrange the strongest bands in a vibrational array is due to Mecke and Guillery [42]. A few years later their analysis was extended by Ferguson [43] on the basis of new observations made by him at the National Bureau of Standards with a prism spectrograph. Subsequently Ghosh [44] reported a further analysis based on identifications of fainter band-heads in the region shortward of 5500 A.

Measurement of the National Bureau of Standards spectrograms included not only all the easily recognized band-heads but also some of the stronger band features that have somewhat the appearance of heads overlaid by rotational lines of preceding bands. The

prominent bands at 6051 and 6394 A appear to be accompanied by at least three and possibly more subheads, as stated by Ghosh. However, an attempt to verify the fainter band-heads reported by him in the green and blue regions was not successful. Underlying the stronger bands on our plates, there appears a fainter structure of closely spaced lines that seem to emerge from heads masked by the stronger bands. One such head is that at 6119.98 A. Wavelengths, estimated intensities, and wave numbers of the observed CrO band features are presented in table 6.

3.6. Interpretation of Some Infrared Cr I Lines

Among Randall and Barker's infrared Cr I lines that lie beyond the photographic limit reached in table 1 there are five that can be classified as combinations between terms in tables 4 and 5. They are listed in table 8, in which the calculated and observed wavelengths are listed in adjacent columns for comparison. In the last column of the table are entered the corresponding solar wavelengths as observed by Goldberg, Mohler, and McMath [45]. No satisfactory interpretation has been found for Randall and Barker's group of 11 Cr lines between 25459 and 26232 A.

4. Discussion

The atomic number of Cr is 24, which means that the neutral atom has 24 extra-nuclear electrons. Eighteen of these are bound in closed shells, leaving six to serve as valence electrons, which can form different configurations, depending on the state of excitation of the atom. According to present theories, the spectrum, Cr I, results from transitions among even and odd terms of the singlet, triplet, quintet, and septet systems that are characteristic of the various electron configurations. The terms to be expected theoretically from these configurations are set forth in table 9, which is abridged from a more extended table on pages xii and xiii of the Introduction to Volume II of Atomic Energy Levels [39]. The terms actually found in this investigation are printed in table 9 in bold-face type. Of these there are 53 even terms, as listed in table 4, and 115 odd terms, as listed in table 5.

The total number of Cr I lines given in table 1 is approximately 4,425. More than 80 percent of them have been classified with the terms of tables 4 and 5. About 10 percent of the classified lines have two or more designations, indicating that they have an unresolved structure due to blending of two or more components, even when observed with powerful gratings.

The presence in Cr I of several series of three or more members is unique in complex spectra. The series are very regular and can be represented accurately by a simple formula of the Ritz type, so that the value of the ground state can be fixed with an error not exceeding 1 part in 10,000. It is possible, therefore, to calculate for the neutral Cr atom an ionization potential of the same order of accuracy.

The occurrence of molecular bands in the spectra of arcs and of low-energy sparks in air is always annoying to the atomic spectroscopist. Nevertheless, their importance in the physical and chemical analysis of flames, and in the analysis of stellar spectra, is recognized. Inspection of the CrO bands on the high-dispersion spectrograms of the NBS reveals features that differ in several respects from the published descriptions derived from low-dispersion spectra. This suggests that the published vibrational analyses are only approximately correct, and that further investigation of them is required in sources more favorable to their excitation than the conventional arcs-in-air.

The wavelengths of numerous Cr I lines, beyond the reach of photographic registration in the infrared, may be calculated with the terms of tables 4 and 5. With modern radiometric detectors it should be possible to record not only these predicted lines, of which many have $3d^6\,{}^5D$ as their low state, but also other lines that arise from states as yet unknown, notably the ^3P and ^3H states of the $3d^6$ configuration. Similarly, there are predictable lines in the extreme ultraviolet, shortward of 2000 A, that should be observable with vacuum spectrographs. The chromium arc-in-air should be a satisfactory source for radiometric investigations because, if the electrodes are about 1 cm in thickness, the arc burns steadily for several minutes, and if the arc is in an enclosure with the air-pressure reduced to about ½ atm, it will burn without flicker for 20 minutes or more.

The description and analysis of Cr I, presented in this paper would not have reached their present status without observational material and data from various individuals. A. S. King of the Mount Wilson Observatory loaned some of his high-dispersion spectrograms of chromium and also made available, in advance of publication, his furnace observations of the ultraviolet spectrum. Similarly, H. D. Babcock, of the same Observatory, supplied his unpublished Zeeman effect observations. A. G. Shenstone of Princeton University made spectrograms of the extreme ultraviolet region with his vacuum spectrograph; and finally, both G. R. Harrison and W. F. Meggers made sets of Zeeman effect observations with the magnet and spectrographs of the Massachusetts Institute of Technology. It is a pleasure to express to each of them appreciation for his contribution to this work.

TABLE 1. *Wavelengths and term combinations of* Cr I

d, Double; *h*, hazy; *H*, very hazy; *l*, shaded longward; *s*, shaded shortward; *r*, reversed; *R*, strongly reversed; *w*, wide; *W*, very wide; *Z*, Zeeman pattern in table 2.

Wavelength λ_{air}	Intensity	Wave No.	Term combination	Wavelength λ_{air}	Intensity	Wave No.	Term combination
11610. 48	15	8610. 55	$z\ ^5P_3^0 - e\ ^5D_4$	9409. 78	3	10624. 33	$f\ ^5S_2 - v\ ^5P_2^0$
11484. 50	15	8705. 01	$z\ ^5P_2^0 - e\ ^5D_3$	9398. 13	1	10637. 50	$d\ ^3F_3 - x\ ^5G_4^0$
11472. 93	10	8713. 79	$z\ ^5P_3^0 - e\ ^5D_3$	9362. 06	10	10678. 48	$a\ ^3P_1 - z\ ^3P_2^0$
11397. 96	12	8771. 10	$z\ ^5P_1^0 - e\ ^5D_2$	9313. 55	8	10734. 10	$a\ ^3P_0 - z\ ^3P_1^0$
11390. 63	15	8776. 74	$z\ ^5P_2^0 - e\ ^5D_2$	9302. 75	2*w*	10746. 56	
11379. 26	5	8785. 52	$z\ ^5P_3^0 - e\ ^5D_2$	9294. 30	15	10756. 33	$a\ ^5G_5 - z\ ^5F_5^0$
11339. 16	15	8816. 58	$z\ ^5P_1^0 - e\ ^5D_1$	9294. 15	10	10756. 51	$a\ ^5G_6 - z\ ^5F_5^0$
11331. 88	10	8822. 25	$z\ ^5P_2^0 - e\ ^5D_1$	9290. 44	50	10760. 80	$a\ ^5G_6 - z\ ^5F_4^0$
11310. 69	12	8838. 78	$z\ ^5P_1^0 - e\ ^5D_0$	9278. 06	2	10775. 16	
11157. 03	25	8960. 51	$y\ ^7P_4^0 - e\ ^7S_3$	9263. 98	20	10791. 54	$a\ ^3F_3 - z\ ^3F_3^0$
11044. 64	5	9051. 69	$b\ ^5D_1 - z\ ^5D_0^0$	9220. 55	1	10842. 37	$c\ ^3F_4 - w\ ^5F_5^0$
11015. 63	30	9075. 53	$y\ ^7P_3^0 - e\ ^7S_3$	9208. 29	30	10856. 80	$a\ ^3F_4 - z\ ^3F_4^0$
10957. 19	12	9123. 93	$b\ ^5D_2 - z\ ^5D_1^0$	9148. 45	7	10927. 82	$a\ ^3F_3 - z\ ^3F_3^0$
10929. 90	10	9146. 71	$b\ ^5D_0 - z\ ^5D_1^0$	9142. 59	8	10934. 82	$y\ ^3G_3^0 - e\ ^3G_3$
10905. 83	25	9166. 90	$y\ ^7P_2^0 - e\ ^7S_3$	9141. 18	7	10936. 51	$y\ ^3G_3^0 - e\ ^3G_3$
10902. 90	2	9169. 37		9140. 53	8	10937. 28	$y\ ^3G_4^0 - e\ ^3G_4$
10821. 62	12	9238. 23	$b\ ^5D_2 - z\ ^5D_2^0$	9128. 12	2	10952. 15	$z\ ^3D_3^0 - e\ ^3F_4$
10816. 91	8	9242. 26	$b\ ^5D_2 - z\ ^5D_3^0$	9124. 01	1	10957. 09	$a\ ^3F_2 - z\ ^3F_2^0$
10801. 37	12	9255. 55	$b\ ^5D_1 - z\ ^5D_2^0$	9113. 08	2	10970. 23	$c\ ^5D_4 - w\ ^5D_4^0$
10672. 17	18	9367. 60	$b\ ^5D_3 - z\ ^5D_3^0$	9098. 95	1	10987. 26	$z\ ^3D_2^0 - e\ ^3F_3$
10667. 53	15	9371. 68	$b\ ^5D_2 - z\ ^5D_4^0$	9097. 39	1	10989. 15	$z\ ^3D_1^0 - e\ ^3F_2$
10647. 66	12	9389. 17	$b\ ^5D_4 - z\ ^5D_4^0$	9068. 28	2	11024. 43	$c\ ^5D_4 - w\ ^5D_4^0$
10631. 42	2	9403. 50	$b\ ^5G_4 - x\ ^5G_4^0$ $u\ ^5F_5^0 - e\ ^5G_6$	9065. 11	2	11028. 28	
10550. 12	3	9475. 97	$b\ ^5D_1 - z\ ^3P_2^0$	9059. 75	5	11034. 81	$a\ ^3F_4 - z\ ^3F_4^0$
10509. 96	10	9512. 18	$b\ ^5D_3 - z\ ^3D_3^0$	9035. 86	40	11063. 98	$a\ ^3G_3 - z\ ^3F_2^0$
10486. 24	20	9533. 70	$b\ ^5D_4 - z\ ^3D_3^0$	9027. 22	1	11074. 57	$a\ ^5F_3 - x\ ^5D_2^0$
10416. 75	2	9597. 30	$b\ ^5D_3 - z\ ^3P_2^0$	9021. 69	75	11081. 36	$z\ ^5P_1^0 - e\ ^5S_2$
10392. 10	1	9620. 08	$b\ ^5D_0 - z\ ^3P_1^0$	9017. 10	100	11087. 00	$z\ ^5P_2^0 - e\ ^5S_2$
10217. 06	1	9784. 87	$c\ ^5D_2 - x\ ^5F_3^0$	9009. 95	150	11095. 80	$z\ ^5P_3^0 - e\ ^5S_2$
10197. 05	3	9804. 07	$a\ ^3P_2 - z\ ^3P_1^0$	8989. 14	3	11121. 49	$b\ ^3H_6 - y\ ^3G_5^0$
10111. 90	1	9886. 63	$b\ ^5D_3 - z\ ^3P_2^0$	8976. 88	40	11136. 67	$a\ ^3G_4 - z\ ^3F_3^0$
10089. 61	2	9908. 48	$c\ ^5D_4 - x\ ^5F_5^0$	8959. 16	3	11158. 70	
10083. 17	5	9914. 80	$a\ ^3D_2 - z\ ^3D_1^0$	8957. 96	2	11160. 20	$a\ ^3F_2 - z\ ^3G_3^0$
10080. 32	15	9917. 60	$a\ ^3D_1 - z\ ^3D_1^0$	8955. 73	8	11162. 97	$a\ ^5F_1 - z\ ^5G_2^0$
9949. 06	20	10048. 45	$a\ ^3D_2 - z\ ^3D_2^0$	8949. 55	3	11170. 67	$b\ ^3H_5 - y\ ^3G_4^0$
9946. 30	7	10051. 24	$a\ ^3D_1 - z\ ^3D_2^0$	8947. 19	50	11173. 63	$a\ ^3G_5 - z\ ^3F_4^0$
9934. 52	2	10063. 16	$y\ ^7P_3^0 - e\ ^5S_2$	8943. 70	3	11178. 00	$b\ ^3H_4 - y\ ^3G_3^0$
9904. 47	8	10093. 69	$a\ ^3D_3 - z\ ^3D_2^0$	8939. 17	10	11183. 65	$a\ ^3F_2 - z\ ^3G_2^0$
9900. 87	15	10097. 36	$a\ ^3P_2 - z\ ^3P_2^0$	8936. 47	4*w*	11187. 03	$a\ ^5F_4 - z\ ^5G_4^0$
9845. 19	1	10154. 46	$y\ ^7P_2^0 - e\ ^5S_2$	8935. 23	2	11188. 58	
9773. 30	10	10229. 15	$a\ ^3D_2 - z\ ^3D_3^0$	8929. 41	2	11195. 88	$a\ ^5F_3 - z\ ^5G_3^0$
9758. 71	2	10244. 45	$c\ ^5F_5 - y\ ^5F_4^0$	8925. 76	35	11200. 47	$a\ ^3G_3 - z\ ^3F_3^0$ $a\ ^5F_3 - z\ ^5G_3^0$
9752. 84	4	10250. 62	$a\ ^3P_1 - z\ ^3P_0^0$	8917. 10	18	11211. 33	$a\ ^5F_4 - z\ ^5G_3^0$
9734. 52	50	10269. 91	$a\ ^5G_2 - z\ ^5F_1^0$	8916. 19	25	11212. 48	$a\ ^5F_5 - z\ ^5G_4^0$
9730. 32	25	10274. 34	$a\ ^3D_3 - z\ ^3D_3^0$	8898. 60	1	11234. 64	$c\ ^3F_3 - y\ ^3G_3^0$
9670. 48	50	10337. 91	$a\ ^5G_2 - z\ ^5F_2^0$				
9667. 20	25	10341. 42	$a\ ^5G_3 - z\ ^5F_3^0$	8870. 33	5	11270. 45	$a\ ^5F_4 - x\ ^5D_3^0$
9626. 30	4	10385. 36	$a\ ^3P_1 - z\ ^3P_1^0$	8859. 59	1	11284. 11	$a\ ^5F_3 - x\ ^5D_2^0$
9574. 25	50	10441. 82	$a\ ^5G_4 - z\ ^5F_3^0$	8835. 62	25	11314. 72	$a\ ^3G_4 - z\ ^3F_4^0$
9571. 76	25	10444. 54	$a\ ^5G_3 - z\ ^5F_3^0$	8808. 80	3	11349. 19	$c\ ^5D_1 - u\ ^5P_2^0$
9568. 58	4	10448. 01	$a\ ^5G_2 - z\ ^5F_2^0$	8796. 16	4	11365. 48	
9520. 13	4	10501. 18	$z\ ^7D_3^0 - e\ ^5S_2$	8789. 53	2	11374. 05	$b\ ^3P_2 - z\ ^3D_1^0$
9447. 01	25	10582. 46	$a\ ^5G_3 - z\ ^5F_4^0$	8788. 28	1	11375. 67	
9446. 89	20	10582. 60	$a\ ^5G_4 - z\ ^5F_4^0$ $z\ ^7D_1^0 - e\ ^5S_2$	8786. 95	10	11377. 39	$c\ ^5D_2 - u\ ^5P_3^0$
9444. 33	5	10585. 46	$a\ ^5G_3 - z\ ^5F_4^0$	8784. 11	3*w*	11381. 07	$c\ ^5D_0 - u\ ^5P_1^0$
				8773. 56	10*w*	11394. 76	$c\ ^5D_2 - u\ ^5P_2^0$

TABLE 1. *Wavelengths and term combinations of* Cr I—Continued

d, Diffuse; *h*, hazy; *H*, very hazy; *l*, shaded longward; *s*, shaded shortward; *r*, reversed; *R*, strongly reversed; *w*, wide; *W*, very wide; *Z*, Zeeman pattern in table 2.

Wavelength λ_{air}	Intensity	Wave No.	Term combination
8767. 10	10	11403. 15	$c\ ^5D_1 - u\ ^5P^\circ_1$
8753. 50	15	11420. 87	$b\ ^3P_1 - z\ ^3D^\circ_1$
8746. 40	2	11430. 14	$c\ ^3G_3 - 1^\circ_3$
8745. 44	1	11431. 39	
8743. 48	8	11434. 09	$b\ ^3P_0 - z\ ^3D^\circ_1$
8732. 14	7	11448. 81	$c\ ^5D_2 - u\ ^5P^\circ_1$
8718. 68	35	11466. 48	$c\ ^5D_2 - u\ ^5P^\circ_2$
8716. 08	2*w*	11469. 90	$c\ ^5D_1 - z\ ^3S^\circ_1$ $f\ ^7D_2 - r\ ^5D^\circ_1$
8707. 93	40	11480. 63	$c\ ^5D_4 - u\ ^5P^\circ_3$
8707. 40	25	11481. 33	$a\ ^5P_1 - z\ ^5D^\circ_0$
8687. 42	15	11507. 74	$b\ ^3P_2 - z\ ^3D^\circ_2$
8686. 38	1*w*	11509. 12	$f\ ^7D_4 - r\ ^5D^\circ_4$
8685. 23	1	11510. 64	$f\ ^7D_3 - r\ ^5D^\circ_3$
8681. 88	5	11515. 09	$a\ ^5F_5 - x\ ^5D^\circ_4$
8675. 84	2*w*	11523. 10	
8653. 56	2*w*	11552. 77	$c\ ^5D_2 - x\ ^5G^\circ_3$
8652. 22	6	11554. 56	$b\ ^3P_1 - z\ ^3D^\circ_2$
8643. 00	35	11566. 88	$a\ ^5P_1 - z\ ^5D^\circ_1$
8636. 22	35	11575. 97	$a\ ^5P_2 - z\ ^5D^\circ_1$
8609. 20	7*w*	11612. 29	
8607. 16	4	11615. 05	$f\ ^7D_1 - r\ ^5D^\circ_2$
8582. 98	30*w*	11647. 77	$y\ ^5H^\circ_5 - e\ ^5G_6$
8563. 48	7*w*	11674. 30	$d\ ^3F_4 - t\ ^5F^\circ_3$
8562. 55	25	11675. 56	$y\ ^5H^\circ_6 - e\ ^5G_5$
8555. 50	30	11685. 18	$a\ ^5P_1 - z\ ^5D^\circ_2$
8553. 17	15	11688. 37	$c\ ^5D_2 - x\ ^5G^\circ_4$ $b\ ^3P_2 - z\ ^3D^\circ_3$
8548. 83	50	11694. 30	$a\ ^5P_2 - z\ ^5D^\circ_2$
8543. 70	30	11701. 32	$a\ ^5P_3 - z\ ^5D^\circ_3$
8537. 78	30*w*	11709. 44	$y\ ^5H^\circ_5 - e\ ^5G_4$
8530. 41	4*h*	11719. 55	$y\ ^5H^\circ_5 - e\ ^5G_5$
8529. 96	4*h*	11720. 17	
8510. 99	20	11746. 29	$y\ ^5H^\circ_4 - e\ ^5G_3$
8506. 90	4*w*	11751. 94	$x\ ^5D^\circ_4 - e\ ^5F_5$ $b\ ^5D_4 - z\ ^3F^\circ_3$
8502. 60	4*w*	11757. 88	$y\ ^5H^\circ_4 - e\ ^5G_4$
8496. 74	4*w*	11765. 99	
8483. 34	15*w*	11784. 58	$y\ ^5H^\circ_3 - e\ ^5G_2$
8475. 66	4*w*	11795. 25	$y\ ^5H^\circ_3 - e\ ^5G_3$
8458. 11	10	11819. 73	
8455. 24	40	11823. 74	$a\ ^5P_2 - z\ ^5D^\circ_3$
8450. 25	50	11830. 72	$a\ ^5P_2 - z\ ^5D^\circ_2$ $c\ ^5D_4 - x\ ^5G^\circ_3$
8449. 32	3*w*	11832. 03	
8449. 10	4*w*	11832. 33	
8444. 56	5*w*	11838. 69	
8442. 97	4	11840. 92	
8418. 34	3*w*	11875. 57	$y\ ^3D^\circ_2 - e\ ^3G_3$
8416. 52	4*w*	11878. 14	
8397. 08	15	11905. 61	$a\ ^5P_1 - z\ ^3P^\circ_0$
8380. 53	3	11929. 15	$e\ ^5S_2 - t\ ^5P^\circ_3$
8380. 15	4*w*	11929. 69	$b\ ^5D_4 - z\ ^3F^\circ_4$
8378. 51	40	11932. 02	$y\ ^3F^\circ_4 - e\ ^3G_5$
8348. 27	75	11975. 24	$a\ ^5P_2 - z\ ^5D^\circ_4$
8339. 20	4	11988. 27	
8338. 84	20*w*	11988. 79	$c\ ^5D_0 - v\ ^5F^\circ_1$
8336. 82	25*w*	11991. 70	$y\ ^5F^\circ_5 - e\ ^5G_4$
8328. 45	7	12003. 74	$c\ ^3F_4 - v\ ^5D^\circ_4$ $x\ ^5D^\circ_1 - e\ ^5F_1$
8323. 41	5	12011. 01	$c\ ^5D_1 - v\ ^5F^\circ_1$
8323. 32	10	12011. 14	
8322. 98	8	12011. 63	$z\ ^7P^\circ_3 - c\ ^5D_4$
8322. 05	100	12012. 97	$c\ ^5D_1 - v\ ^5F^\circ_2$
8318. 25	30	12018. 46	$y\ ^3F^\circ_2 - e\ ^3G_3$
8307. 37	3*w*	12034. 20	
8303. 16	20	12040. 30	$a\ ^5P_1 - z\ ^3P^\circ_1$
8297. 57	7	12048. 41	
8296. 90	8	12049. 39	$a\ ^5P_2 - z\ ^3P^\circ_1$
8295. 30	2*w*	12051. 71	$b\ ^3H_6 - u\ ^5F^\circ_5$
8290. 64	75*w*	12058. 49	$c\ ^5D_2 - v\ ^5F^\circ_2$ $d\ ^3F_4 - 1^\circ_3$
8287. 40	150	12063. 20	$c\ ^5D_2 - v\ ^5F^\circ_3$
8286. 40	5	12064. 65	$c\ ^5D_2 - y\ ^3F^\circ_3$
8285. 69	5	12065. 69	$c\ ^5D_3 - y\ ^3F^\circ_3$
8283. 92	4*w*	12068. 26	
8278. 38	4*w*	12076. 34	$x\ ^5F^\circ_5 - e\ ^5G_5$
8273. 84	7*w*	12082. 97	$x\ ^5F^\circ_5 - e\ ^5G_6$
8273. 20	8	12083. 90	$d\ ^3F_3 - 1^\circ_3$
8271. 57	1	12086. 29	$x\ ^5F^\circ_4 - e\ ^5G_4$
8268. 61	4*w*	12090. 61	$x\ ^5D^\circ_1 - e\ ^5F_2$
8264. 28	5*w*	12096. 95	$x\ ^5F^\circ_6 - e\ ^5G_5$
8261. 96	15	12100. 35	$a\ ^3H_4 - z\ ^3F^\circ_3$
8250. 38	3*w*	12117. 33	$x\ ^5F^\circ_3 - e\ ^5G_4$
8246. 23	6	12123. 42	$c\ ^3D_3 - y\ ^3F^\circ_4$
8240. 65	8*l*	12131. 63	$c\ ^5D_0 - v\ ^5D^\circ_1$
8238. 29	50*w*	12135. 11	$c\ ^5D_2 - v\ ^5F^\circ_3$
8235. 89	100	12138. 65	$c\ ^5D_3 - v\ ^5F^\circ_4$
8225. 64	6	12153. 78	$c\ ^5D_1 - v\ ^5D^\circ_1$
8224. 08	50	12156. 08	$a\ ^3H_5 - z\ ^3F^\circ_4$
8218. 15	7*s*	12164. 85	$c\ ^3G_3 - w^3G^\circ_3$
8216. 28	20	12167. 62	$c\ ^5D_1 - v\ ^5D^\circ_2$
8214. 67	4	12170. 00	$c\ ^5D_1 - v\ ^5D^\circ_0$ $c\ ^3D_1 - y\ ^3D^\circ_1$
8213. 09	7	12172. 34	$b\ ^3H_4 - t\ ^3F^\circ_4$
8212. 23	5	12173. 62	$c\ ^3D_2 - y\ ^3D^\circ_2$
8210. 20	5*w*	12176. 63	
8197. 02	3	12196. 21	$z\ ^7P^\circ_2 - c\ ^5D_3$
8194. 87	4	12199. 40	$c\ ^5D_2 - v\ ^5D^\circ_1$
8192. 42	1*w*	12203. 06	$c\ ^3D_1 - y\ ^3D^\circ_2$
8188. 76	8	12208. 51	$d\ ^3F_4 - x\ ^3G^\circ_4$
8187. 84	5	12209. 88	$c\ ^3G_4 - w^3G^\circ_4$
8185. 68	15	12213. 10	$c\ ^5D_2 - v\ ^5D^\circ_2$
8180. 10	3	12221. 43	
8169. 79	15*w*	12236. 86	$c\ ^5D_0 - u\ ^5F^\circ_1$
8167. 92	15	12239. 65	$c\ ^3D_3 - y\ ^3D^\circ_3$
8166. 66	25	12241. 55	$c\ ^5D_2 - v\ ^5D^\circ_3$
8166. 41	20	12241. 92	$c\ ^5D_4 - v\ ^5F^\circ_4$
8166. 30	30	12242. 10	$b\ ^1G_4 - z\ ^1H^\circ_5$
8163. 22	150	12246. 70	$c\ ^5D_4 - v\ ^5F^\circ_5$
8155. 00	22	12259. 05	$c\ ^5D_1 - u\ ^5F^\circ_1$
8140. 16	5	12281. 40	$d\ ^3F_2 - x\ ^3D^\circ_1$
8128. 27	25	12299. 36	$c\ ^5D_1 - u\ ^5F^\circ_2$
8124. 82	7	12304. 58	$c\ ^5D_2 - u\ ^5F^\circ_1$ $c\ ^3G_5 - w^3G^\circ_5$
8119. 14	12	12313. 20	$c\ ^5D_3 - v\ ^5D^\circ_3$
8105. 70	8	12333. 60	$a\ ^5P_1 - z\ ^3P^\circ_2$
8099. 75	4	12342. 67	$a\ ^5P_2 - z\ ^3P^\circ_2$

TABLE 1. *Wavelengths and term combinations of* Cr I—Continued

d, Double; *h*, hazy; *H*, very hazy; *l*, shaded longward; *s*, shaded shortward; *r*, reversed; *R*, strongly reversed; *w*, wide; *W*, very wide; *Z*, Zeeman pattern in table 2

Wavelength λ_{air}	Intensity	Wave No.	Term combination
8098. 24	20	12344. 97	$c\ ^5D_2 - u\ ^5F^0_3$
8086. 35	5*l*	12363. 12	$c\ ^5D_3 - w^5D^0_4$
8084. 97	30	12365. 23	$c\ ^5D_1 - v\ ^5D^0_0$
8067. 65	8	12391. 78	$c\ ^5D_1 - w^5D^0_1$
8065. 04	7	12395. 79	$c\ ^5D_4 - x\ ^5H^0_5$
8061. 26	35	12401. 60	$c\ ^5D_2 - u\ ^5F^0_3$
8053. 30	6	12413. 86	$c\ ^5D_2 - w^5D^0_2$
8050. 67	7	12417. 92	$b\ ^3H_4 - y\ ^3H^0_4$
8045. 36	18	12426. 11	$b\ ^3H_5 - y\ ^3H^0_5$
8040. 56	6	12433. 53	$c\ ^3D_3 - w^5D^0_3$
8034. 42	5*w*	12443. 05	$c\ ^3D_1 - w^5D^0_2$
8018. 02	10	12468. 48	$c\ ^5D_4 - v\ ^5D^0_4$
8014. 90	15*w*	12473. 44	$c\ ^5D_3 - u\ ^5F^0_3$
8007. 92	10*W*	12484. 21	
8006. 27	5	12486. 78	
8005. 29	4	12488. 31	$c\ ^3D_3 - w^5D^0_4$
7990. 52	20	12511. 38	$b\ ^3H_6 - y\ ^3H^0_5$
7989. 37	25	12513. 34	$c\ ^5D_3 - u\ ^5F^0_4$
7976. 10	5*w*	12534. 01	
7971. 32	10	12541. 53	$c\ ^5D_2 - t\ ^5F^0_2$
7942. 05	40	12587. 75	$c\ ^5D_4 - u\ ^5F^0_5$
7939. 88	6*w*	12591. 19	
7934. 69	1	12599. 42	$c\ ^5D_1 - t\ ^5F^0_2$
7926. 86	2	12611. 87	
7924. 01	8	12616. 41	$c\ ^5D_4 - u\ ^5F^0_4$
7917. 84	25	12626. 24	$z\ ^3H^0_4 - e\ ^3G_3$
7913. 24	1	12633. 58	$z\ ^3H^0_4 - e\ ^3G_4$
7911. 60	1*w*	12636. 20	$z\ ^3H^0_5 - e\ ^3G_5$
7910. 49	25	12637. 97	$z\ ^3H^0_5 - e\ ^3G_4$
7908. 27	35	12641. 62	$z\ ^3H^0_6 - e\ ^3G_5$
7907. 33	1	12643. 02	$y\ ^5G^0_6 - e\ ^5G_6$
7906. 21	2	12644. 81	$b\ ^3H_4 - x\ ^3G^0_3$ $c\ ^5D_4 - t\ ^5F^0_4$
7901. 97	4	12651. 60	
7894. 80	3	12663. 09	
7884. 92	4	12678. 96	$c\ ^5D_2 - t\ ^3F^0_2$
7882. 07	2	12683. 54	$x\ ^5F^0_5 - e\ ^3G_5$
7877. 11	2	12691. 54	$b\ ^3H_4 - x\ ^3G^0_4$
7870. 58	8	12702. 06	$t\ ^5P^0_3 - e\ ^7S_3$
7851. 32	4	12733. 22	$d\ ^3F_4 - x\ ^3D^0_3$
7848. 25	4	12738. 19	
7816. 13	5*w*	12790. 54	$y\ ^5D^0_4 - e\ ^5F_4$
7815. 49	5*w*	12791. 59	$y\ ^5G^0_5 - e\ ^5G_5$
7809. 20	5*w*	12801. 89	
7802. 90	5	12812. 23	$d\ ^3F_2 - w^3G^0_3$
7800. 67	4	12815. 89	
7785. 92	4*wl*	12840. 17	$c\ ^5D_1 - x\ ^3P^0_2$
7782. 19	2	12846. 32	
7778. 73	4*w*	12852. 04	$b\ ^3H_6 - x\ ^3G^0_5$
7771. 69	22	12863. 67	$a\ ^1H_5 - z\ ^1H^0_5$
7763. 01	25	12878. 06	$y\ ^5D^0_4 - e\ ^5F_5$
7762. 46	2	12878. 97	
7749. 15	6*w*	12901. 10	$y\ ^5D^0_3 - e\ ^5F_3$
7748. 77	2	12901. 73	$d\ ^3F_3 - w^3G^0_4$ $b\ ^3H_5 - x\ ^3G^0_5$
7734. 00	12	12926. 37	$b\ ^3F_2 - y\ ^3F^0_2$
7726. 00	12	12939. 75	$b\ ^3F_3 - y\ ^3F^0_3$
7722. 90	20	12944. 94	$a\ ^5F_2 - y\ ^3G^0_3$ $b\ ^3F_4 - y\ ^3F^0_4$
7705. 40	5*w*	12974. 35	$y\ ^5D^0_2 - e\ ^5F_2$
7697. 35	2	12987. 91	$y\ ^5G^0_3 - e\ ^5G_3$
7691. 50	7*w*	12997. 79	$b\ ^3F_3 - y\ ^3F^0_3$ $y\ ^5D^0_3 - e\ ^5F_4$
7684. 82	3	13009. 09	$a\ ^5F_3 - y\ ^5G^0_3$
7623. 45	5	13113. 82	$c\ ^3D_2 - y\ ^3G^0_3$
7574. 70	4	13198. 22	$a\ ^5F_5 - y\ ^3G^0_5$
7570. 79	4*w*	13205. 03	$y\ ^5D^0_4 - g\ ^5D_3$
7568. 70	5	13208. 68	
7558. 16	6	13227. 10	
7549. 16	6*W*	13242. 87	$y\ ^5D^0_3 - g\ ^5D_2$
7535. 55	18	13266. 78	$y\ ^5F^0_3 - e\ ^5F_3$
7526. 44	5	13282. 84	
7502. 12	5*w*	13325. 90	$y\ ^5F^0_2 - e\ ^5F_1$
7489. 32	7*w*	13348. 68	$y\ ^5F^0_4 - e\ ^5F_4$
7486. 75	6*w*	13353. 26	$a\ ^5F_5 - y\ ^3G^0_4$
7484. 69	5	13356. 93	$y\ ^5D^0_1 - g\ ^5D_0$
7462. 35	250	13396. 60	$z\ ^7P^0_4 - e\ ^7S_3$
7454. 05	2*w*	13411. 83	$y\ ^5D^0_3 - g\ ^5D_3$ $y\ ^5F^0_3 - e\ ^5F_2$
7445. 68	25	13426. 60	$y\ ^5D^0_4 - g\ ^5D_4$
7429. 42	8	13456. 30	
7405. 26	10	13500. 20	$b\ ^3H_4 - w\ ^3G^0_4$
7400. 22	200	13509. 40	$z\ ^7P^0_3 - e\ ^7S_3$
7389. 26	7*w*	13529. 43	$x\ ^5P^0_3 - e\ ^5F_4$ $y\ ^5D^0_1 - g\ ^5D_2$
7379. 61	3	13547. 13	$d\ ^3F_2 - w^3D^0_1$
7367. 37	10	13569. 63	$b\ ^3H_5 - w^3G^0_4$
7355. 93	150	13590. 73	$z\ ^7P^0_3 - e\ ^7S_3$
7348. 68	20	13604. 14	$b\ ^3H_6 - w^3G^0_5$
7332. 55	5*w*	13634. 07	$y\ ^5D^0_3 - g\ ^5D_4$
7323. 28	10	13651. 33	$z\ ^3F^0_4 - e\ ^3F_4$
7311. 56	6	13673. 21	$a\ ^5G_2 - x\ ^3P^0_2$
7306. 01	8	13683. 60	$z\ ^3F^0_3 - e\ ^3F_2$
7305. 69	12	13684. 20	$c\ ^3G_3 - w^3F^0_3$
7304. 32	4	13686. 76	$d\ ^3F_4 - w^3D^0_3$
7303. 29	6	13688. 70	$z\ ^3F^0_2 - e\ ^3F_2$
7297. 14	1	13700. 23	$y\ ^5F^0_2 - g\ ^5D_1$
7293. 90	8	13706. 32	$c\ ^3G_4 - w^3F^0_4$
7280. 27	20	13731. 98	$y\ ^5F^0_1 - g\ ^5D_2$
7276. 22	8	13739. 62	$y\ ^5F^0_1 - g\ ^5D_0$
7264. 30	40	13762. 16	$y\ ^5F^0_4 - g\ ^5D_3$
7236. 22	50	13815. 57	$y\ ^5F^0_3 - g\ ^5D_4$ $c\ ^3G_4 - w^3F^0_4$
7230. 60	8	13826. 31	$c\ ^3G_5 - w^3F^0_5$ $b\ ^3D_1 - v\ ^5P^0_2$
7226. 89	4*w*	13833. 40	$y\ ^5F^0_2 - e\ ^3D_1$ $a\ ^3D_2 - z\ ^5G^0_3$
7221. 15	5	13844. 40	$b\ ^3F_2 - z\ ^3G^0_4$
7220. 01	7	13846. 59	$b\ ^3D_2 - v\ ^5P^0_2$ $a\ ^5F_2 - x\ ^5F^0_1$
7218. 60	9	13849. 29	$a\ ^5F_1 - x\ ^5F^0_1$
7212. 56	10	13860. 89	$a\ ^5F_3 - x\ ^5F^0_2$
7207. 85	10	13869. 94	$a\ ^5F_2 - x\ ^5F^0_2$
7206. 42	10	13872. 70	$b\ ^3F_4 - z\ ^3G^0_4$ $a\ ^5F_1 - x\ ^5F^0_2$
7205. 57	3	13874. 33	$x\ ^5P^0_1 - e\ ^3D_1$

TABLE 1. *Wavelengths and term combinations of* Cr I—Continued

d, Double; h, hazy; H, very hazy; l, shaded longward; s, shaded shortward; r, reversed; R, strongly reversed; w, wide; W, very wide; Z, Zeeman pattern in table 2.

Wavelength λ_{air}	Intensity	Wave No.	Term combination
7203. 93	10	13877. 49	$a\ ^5F_4 - x\ ^5F_5^\circ$
7200. 70	10	13883. 71	
7198. 32	7w	13888. 28	$z\ ^5D_4^\circ - g\ ^7D_4$ $x\ ^5P_3^\circ - g\ ^5D_2$ $y\ ^5F_3^\circ - e\ ^3D_2$
7196. 85	18	13891. 14	$a\ ^5F_3 - x\ ^5F_3^\circ$
7196. 04	7	13892. 71	$a\ ^5F_5 - x\ ^5F_4^\circ$
7195. 53	8	13893. 69	$z\ ^5D_4^\circ - g\ ^7D_5$
7192. 07	10w	13900. 38	$a\ ^5F_2 - x\ ^5F_3^\circ$ $y\ ^5F_3^\circ - g\ ^5D_3$
7188. 06	18	13908. 13	$a\ ^5F_4 - x\ ^5F_4^\circ$
7185. 50	20	13913. 08	$a\ ^5F_5 - x\ ^5F_5^\circ$
7181. 00	10	13921. 81	$a\ ^5F_3 - x\ ^5F_4^\circ$
7177. 53	10	13928. 54	$a\ ^5F_4 - x\ ^5F_5^\circ$
7170. 56	15	13942. 08	$b\ ^3F_4 - y\ ^3G_5^\circ$
7151. 10	8w	13980. 01	$y\ ^5F_4^\circ - e\ ^3D_3$ $c\ ^3D_1 - t\ ^3P_2^\circ$ $d\ ^3F_4 - u\ ^5D_4^\circ$
7148. 92	5w	13984. 28	$y\ ^5F_4^\circ - g\ ^5D_4$
7145. 11	7w	13991. 73	$x\ ^3P_2^\circ - e\ ^3D_2$
7143. 84	12	13994. 23	$b\ ^3F_2 - y\ ^3G_4^\circ$
7138. 31	2	14005. 06	
7136. 56	12	14008. 50	$b\ ^3F_2 - y\ ^3G_3^\circ$
7133. 81	3	14015. 29	
7128. 17	6	14024. 99	$c\ ^5D_2 - t\ ^3P_2^\circ$
7118. 33	3w	14044. 38	$x\ ^5P_1^\circ - e\ ^3D_2$
7108. 06	8	14064. 67	
7088. 05	1	14104. 37	$b\ ^3D_3 - v\ ^5P_3^\circ$
7080. 95	3w	14118. 51	$y\ ^5F_3^\circ - e\ ^3D_3$
7057. 34	3w	14165. 75	$x\ ^5P_3^\circ - g\ ^5D_4$
7056. 28	1	14167. 87	$c\ ^3G_5 - z\ ^1H_5^\circ$
7049. 05	5	14182. 40	$a\ ^1H_5 - \quad 2_4^\circ$
6990. 73	3	14300. 72	$a\ ^3I_7 - z\ ^3H_6^\circ$
6988. 66	2	14304. 96	$a\ ^3I_6 - z\ ^3H_5^\circ$
6987. 54	4	14307. 25	
6980. 91	50	14320. 84	$y\ ^7P_4^\circ - e\ ^7D_3$
6979. 81	150	14323. 09	$y\ ^7P_4^\circ - e\ ^7D_4$
6978. 46	300	14325. 86	$y\ ^7P_4^\circ - e\ ^7D_5$
6935. 57	3w	14412. 38	
6934. 04	3w	14417. 64	
6930. 13	3	14425. 77	$a\ ^1H_5 - x\ ^3H_4^\circ$
6926. 02	100	14434. 33	$y\ ^7P_3^\circ - e\ ^7D_2$
6925. 22	150	14436. 00	$y\ ^7P_3^\circ - e\ ^7D_3$
6924. 20	200	14438. 12	$y\ ^7P_3^\circ - e\ ^7D_4$
6913. 47	5w	14460. 53	
6910. 92	4w	14465. 87	
6903. 20	4w	14482. 05	$d\ ^3F_4 - w^3F_4^\circ$
6901. 09	15ws	14486. 48	
6896. 04	6	14497. 08	$z\ ^7P_3^\circ - e\ ^5S_2$
6894. 70	7	14499. 90	
6883. 05	150	14524. 44	$z\ ^7P_2^\circ - e\ ^7D_1$
6882. 40	75	14525. 81	$z\ ^7P_3^\circ - e\ ^7D_2$
6881. 62	100	14527. 46	$z\ ^7P_2^\circ - e\ ^7D_3$
6866. 28	15ws	14559. 92	
6860. 32	5	14572. 57	
6845. 00	10ws	14605. 18	
6841. 26	5w	14613. 17	
6829. 86	8	14637. 56	$a\ ^3P_2 - z\ ^3D_3^\circ$
6829. 45	10ws	14638. 44	
6818. 82	4w	14661. 25	$z\ ^3P_1^\circ - f\ ^5D_2$
6814. 52	10	14670. 51	$b\ ^3D_1 - y\ ^3P_1^\circ$
6812. 99	10	14673. 80	$b\ ^3D_1 - y\ ^3P_0^\circ$
6805. 77	12w	14689. 37	
6805. 00	15	14691. 03	$b\ ^3D_2 - y\ ^3P_1^\circ$
6798. 04	12	14706. 07	$b\ ^3D_2 - y\ ^3P_2^\circ$
6796. 52	25w	14709. 36	$c\ ^5D_3 - s\ ^5F_4^\circ$
6789. 15	18	14725. 33	$b\ ^3D_3 - y\ ^3P_2^\circ$
6784. 91	8w	14734. 53	$d\ ^3F_3 - w^3P_2^\circ$
6780. 09	8	14745. 00	$a\ ^5F_3 - y\ ^3D_2^\circ$ $z\ ^3P_0^\circ - f\ ^5D_1$
6777. 50	15wl	14750. 64	
6765. 71	4	14776. 34	
6765. 30	8	14777. 24	$z\ ^5G_2^\circ - e\ ^5G_3$
6762. 41	40	14783. 55	$z\ ^5G_6^\circ - e\ ^5G_6$ $z\ ^5G_5^\circ - e\ ^5G_4$
6757. 76	25	14793. 73	$z\ ^5G_3^\circ - e\ ^5G_3$
6756. 49	15	14796. 51	$a\ ^5F_4 - y\ ^3D_3^\circ$ $z\ ^5G_4^\circ - e\ ^5G_3$
6754. 86	5w	14800. 08	$z\ ^5G_5^\circ - e\ ^5G_6$
6751. 33	40	14807. 82	$z\ ^5G_4^\circ - e\ ^5G_4$
6750. 20	2	14810. 30	$a\ ^5F_3 - y\ ^3D_3^\circ$
6749. 43	7w	14811. 98	$z\ ^5G_3^\circ - e\ ^5G_2$
6749. 07	6w	14812. 78	$c\ ^5D_4 - s\ ^5F_4^\circ$
6746. 61	10	14818. 18	$z\ ^5G_4^\circ - e\ ^5G_5$ $a\ ^3P_2 - z\ ^3D_3^\circ$
6744. 64	15	14822. 50	$z\ ^5G_3^\circ - e\ ^5G_3$
6739. 41	6	14834. 01	$z\ ^5G_2^\circ - e\ ^5G_4$
6738. 81	18	14835. 33	$z\ ^5G_2^\circ - e\ ^5G_2$
6735. 72	8w	14842. 13	$e\ ^7D_2 - p\ ^5F_1^\circ$
6734. 16	30	14845. 57	$z\ ^5D_4^\circ - f\ ^5D_3$ $z\ ^5G_3^\circ - e\ ^5G_2$
6729. 72	40	14855. 37	$c\ ^5D_4 - s\ ^5F_5^\circ$
6726. 23	5	14863. 07	
6715. 38	35	14887. 09	$z\ ^5D_3^\circ - f\ ^5D_2$
6701. 64	10	14917. 61	$b\ ^3D_1 - y\ ^3F_2^\circ$
6692. 48	1	14938. 03	$b\ ^3D_2 - y\ ^3F_3^\circ$
6688. 96	2	14945. 89	$a\ ^5F_1 - w^5D_1^\circ$
6683. 80	2	14957. 43	$b\ ^3D_3 - y\ ^3F_3^\circ$
6680. 21	25w	14965. 46	$z\ ^5D_2^\circ - f\ ^5D_1$
6677. 24	10	14972. 12	$b\ ^3D_2 - y\ ^3F_3^\circ$
6669. 27	40, Z	14990. 01	$z\ ^5D_3^\circ - f\ ^5D_3$
6668. 67	5	14991. 36	$b\ ^3D_3 - y\ ^3F_3^\circ$
6667. 78	5	14993. 36	
6667. 40	1	14994. 22	$a\ ^5F_2 - w^5D_2^\circ$
6665. 11	2	14999. 37	$w\ ^5F_3^\circ - e\ ^5P_2$
6663. 93	18	15002. 02	$z\ ^5H_7^\circ - e\ ^5G_6$
6662. 25	2	15005. 80	
6661. 10	50, Z	15008. 40	$z\ ^5D_4^\circ - f\ ^5D_4$
6657. 40	20w	15016. 42	$z\ ^5D_3^\circ - f\ ^5D_3^\circ$
6655. 02	5	15022. 11	$c\ ^5D_0 - u\ ^5D_1^\circ$ $v\ ^5F_4^\circ - f\ ^5G_3$
6654. 45	4	15023. 40	$b\ ^1I_6 - x\ ^3G_5^\circ$
6652. 35	3	15028. 14	$b\ ^3D_1 - y\ ^3D_1^\circ$
6651. 92	10	15029. 11	$v\ ^5F_5^\circ - f\ ^5G_6$ $a\ ^5F_5 - w^5D_4^\circ$
6648. 76	7	15036. 25	$c\ ^5D_1 - u\ ^5D_2^\circ$
6645. 93	5	15042. 66	$c\ ^5D_1 - u\ ^5D_0^\circ$

TABLE 1. *Wavelengths and term combinations of* Cr I—Continued

d, Double; *h*, hazy; *H*, very hazy; *l*, shaded longward; *s*, shaded shortward; *r*, reversed; *R*, strongly reversed; *w*, wide; *W*, very wide; *Z*, Zeeman pattern in table 2

Wavelength λ_{air}	Intensity	Wave No.	Term combination
6645.12	6	15044.49	$a\ ^5F_4 - w\ ^5D^0_4$
			$c\ ^5D_1 - u\ ^5D^0_1$
6643.02	20	15049.24	$b\ ^3D_2 - y\ ^3F^0_3$
6642.27	10	15050.95	$b\ ^3G_3 - x\ ^5D^0_2$
			$v\ ^5F^0_4 - f\ ^5G_5$
6640.42	8	15055.14	$c\ ^5D_2 - u\ ^5D^0_2$
6639.91	8	15056.29	$c\ ^5D_3 - u\ ^5D^0_3$
6639.06	5	15058.22	$a\ ^5F_3 - w\ ^5D^0_4$
6638.07	1	15060.47	$b\ ^3D_1 - y\ ^3D^0_2$
6636.31	10*w*	15064.46	$z\ ^5D^0_1 - f\ ^5D_0$
6635.39	2	15066.55	$e\ ^7D_5 - p\ ^5F^0_5$
6632.43	2*w*	15073.27	
6630.00	30	15078.80	$a\ ^5D_4 - z\ ^7P^0_4$
6629.08	2	15080.89	$b\ ^3D_2 - y\ ^3D^0_2$
6628.69	6	15081.78	$c\ ^5D_2 - u\ ^5D^0_2$
6627.83	3*w*	15083.74	$z\ ^5D^0_1 - f\ ^5D_1$
6627.28	6	15084.99	$a\ ^3P_1 - z\ ^3D^0_1$
6625.18	10	15089.77	$c\ ^5D_2 - u\ ^5D^0_1$
6623.92	3	15092.64	
6620.54	2	15100.34	$b\ ^3D_3 - y\ ^3D^0_2$
6612.17	40	15119.46	$z\ ^5D^0_2 - f\ ^5D_2$
6608.90	15	15126.94	$c\ ^5D_3 - u\ ^5D^0_3$
6607.23	15	15130.76	$z\ ^5H^0_3 - e\ ^5G_5$
6605.50	35	15134.73	$z\ ^5D^0_1 - f\ ^5D_2$
6604.46	12	15137.11	$z\ ^5H^0_3 - e\ ^5G_6$
6603.77	2	15138.69	$b\ ^3F_4 - t\ ^3F^0_3$
6600.54	7	15146.10	$b\ ^3D_2 - y\ ^3D^0_3$
6597.56	40	15152.94	$z\ ^5D^0_3 - f\ ^5D_4$
6597.42	5	15153.26	$c\ ^5D_2 - u\ ^5D^0_2$
6594.69	20	15159.54	$c\ ^5D_4 - u\ ^5D^0_4$
6592.15	7	15165.38	$b\ ^3D_3 - y\ ^3D^0_3$
6590.46	10*w*	15169.27	$z\ ^5D^0_0 - f\ ^5D_1$
6586.16	12	15179.17	
6580.95	8	15191.19	$a\ ^5D_4 - z\ ^7P^0_4$
6572.90	25	15209.79	$a\ ^5D_3 - z\ ^7P^0_3$
6569.01	15	15218.80	$a\ ^3P_1 - z\ ^3D^0_2$
			$z\ ^5H^0_4 - e\ ^5G_4$
6564.57	8	15229.09	$z\ ^5H^0_4 - e\ ^5G_5$
6564.15	7	15230.07	$c\ ^5D_4 - u\ ^5D^0_3$
6556.38	15	15248.11	
6555.82	4	15249.42	$b\ ^3D_1 - w\ ^5D^0_1$
6547.02	3	15269.91	$b\ ^3D_2 - w\ ^5D^0_1$
6542.84	12	15279.67	
6542.09	10	15281.42	$z\ ^5H^0_4 - e\ ^5G_3$
6537.93	25	15291.15	$a\ ^5D_2 - z\ ^7P^0_3$
6537.15	5	15292.97	$z\ ^5H^0_4 - e\ ^5G_4$
6533.94	2	15300.48	$b\ ^3D_1 - w\ ^5D^0_2$
6529.74	5	15310.32	$a\ ^5F_4 - w\ ^5F^0_5$
6529.20	20	15311.59	$a\ ^5F_5 - w\ ^5F^0_4$
6528.66	6	15312.85	$a\ ^5F_3 - w\ ^5F^0_3$
6525.16	2	15321.07	$b\ ^3D_2 - w\ ^5D^0_2$
6524.76	15	15322.01	$a\ ^5F_3 - w\ ^5F^0_2$
6524.27	4	15323.15	$a\ ^5F_2 - w\ ^5F^0_1$
6523.95	8	15323.91	$a\ ^5F_3 - w\ ^5F^0_3$
6523.62	8	15324.69	$a\ ^5F_1 - w\ ^5F^0_2$
6523.51	5	15324.94	$z\ ^5H^0_3 - e\ ^5G_2$
6523.08	8	15325.96	$a\ ^5F_1 - w\ ^5F^0_1$
6522.64	12	15326.99	$a\ ^5F_4 - w\ ^5F^0_4$
			$a\ ^5F_5 - w\ ^5F^0_4$
6520.06	10	15333.05	$a\ ^5F_2 - w\ ^5F^0_1$
6518.98	3	15335.60	$z\ ^5H^0_4 - e\ ^5G_3$
6517.12	3	15339.97	$b\ ^3D_2 - w\ ^5D^0_1$
6516.95	4	15340.37	$b\ ^3D_3 - w\ ^5D^0_2$
6516.00	20	15342.61	$a\ ^5F_4 - w\ ^5F^0_4$
6510.24	12	15356.18	$a\ ^5F_3 - w\ ^5F^0_4$
6509.37	3	15358.24	$c\ ^3G_5 - y\ ^3I^0_6$
6508.94	4	15359.25	$b\ ^3D_3 - w\ ^5D^0_3$
6506.13	5	15365.88	
6501.21	20	15377.51	$a\ ^5D_2 - z\ ^7P^0_2$
6496.94	5	15387.62	
6495.37	10	15391.34	
6490.23	4	15403.53	$a\ ^5D_3 - z\ ^7P^0_4$
6477.53	8	15433.73	$a\ ^3P_0 - z\ ^3D^0_1$
6470.05	6	15451.57	$x\ ^5G^0_6 - f\ ^5G_6$
6467.02	8	15458.81	$a\ ^5D_2 - z\ ^7P^0_3$
6452.26	15	15494.17	$a\ ^5D_1 - z\ ^7P^0_2$
6438.57	8	15527.12	$a\ ^5F_4 - z\ ^3G^0_4$
6436.24	15	15532.74	$a\ ^1I_6 - z\ ^1I^0_6$
6434.45	4	15537.06	
6432.78	8	15541.09	$c\ ^3D_2 - y\ ^3S^0_1$
6428.14	25	15552.31	$c\ ^5D_4 - w\ ^5F^0_5$
6415.69	8	15582.49	
6411.57	10	15592.50	$a\ ^5F_5 - z\ ^3G^0_5$
6391.63	8	15641.15	$c\ ^3G_4 - x\ ^3H^0_5$
6383.14	2	15661.95	$c\ ^5D_4 - w\ ^3F^0_4$
6378.69	3	15672.88	$b\ ^3F_4 - x\ ^3G^0_4$
6377.16	1	15676.63	$z\ ^5F^0_4 - f\ ^7D_4$
6376.35	3*w*	15678.63	$z\ ^5F^0_3 - f\ ^7D_5$
6375.19	7	15681.48	$c\ ^3G_5 - x\ ^3H^0_5$
6374.60	3*w*	15682.93	$a\ ^5F_3 - x\ ^5G^0_3$
6373.45	4	15685.76	$c\ ^3D_3 - x\ ^3F^0_4$
6370.78	5	15692.34	$a\ ^5F_2 - x\ ^5G^0_2$
6369.69	1	15695.02	$a\ ^5F_1 - x\ ^5G^0_2$
6369.23	3	15696.15	
6362.87	35, *Z*	15711.84	$a\ ^5S_2 - z\ ^7P^0_3$
6361.82	2	15714.44	$c\ ^3D_2 - x\ ^3F^0_3$
6357.37	7	15725.44	
6356.50	4	15727.59	
6353.00	2	15736.25	$a\ ^5F_1 - z\ ^3S^0_1$
6349.01	3	15746.14	$c\ ^3D_1 - x\ ^3F^0_2$
6348.40	2	15747.66	$a\ ^5F_4 - x\ ^5G^0_5$
6344.42	4	15757.53	$e\ ^5S_2 - s\ ^5D^0_2$
			$c\ ^5G_3 - x\ ^3H^0_4$
6342.87	7	15761.38	$a\ ^5F_2 - x\ ^5G^0_3$
6336.44	4	15777.38	
6330.13	45, *Z*	15793.11	$a\ ^5S_2 - z\ ^7P^0_4$
6328.84	2*w*	15796.32	$a\ ^5F_5 - x\ ^5G^0_6$
6327.45	12	15799.80	$b\ ^3F_2 - x\ ^3D^0_1$
6323.78	5	15808.96	
6322.57	10	15811.99	$a\ ^5F_4 - x\ ^5G^0_4$
6317.10	1	15825.68	$a\ ^5F_3 - x\ ^5G^0_3$
6315.82	10	15828.89	$a\ ^5F_5 - x\ ^5G^0_6$
6313.21	12	15835.43	$a\ ^5F_5 - x\ ^5G^0_5$
6307.07	4	15850.85	$a\ ^5F_4 - x\ ^5G^0_5$
6296.50	2	15877.46	$c\ ^3D_3 - t\ ^3P^0_2$

TABLE 1. *Wavelengths and term combinations of* Cr I—Continued

d, double; *h*, hazy; *H*, very hazy; *l*, shaded longward; *s*, shaded shortward; *r*, reversed; *R*, strongly reversed; *w*, wide; *W*, very wide; *Z*, Zeeman pattern in table 2.

Wavelength λ_{air}	Intensity	Wave No.	Term combination
6292. 83	2	15886. 71	$c\,^3D_2 - y\,^5S^\circ_2$
6286. 87	4	15901. 78	$b\,^3P_2 - z\,^5S^\circ_2$
6261. 30	15	15966. 72	$b\,^5F_3 - x\,^3D^\circ_2$
6253. 24	5	15987. 30	$b\,^3F_2 - x\,^3D^\circ_2$
6249. 92	8	15995. 79	$y\,^5F^\circ_5 - e\,^5G_6$
6243. 13	5	16013. 18	
6224. 91	1	16060. 05	$b\,^3D_2 - z\,^3S^\circ_1$
6223. 71	7	16063. 15	$z\,^3D^\circ_3 - e\,^3D_2$
6219. 52	4	16073. 97	$z\,^3D^\circ_2 - e\,^3D_1$
6205. 20	10	16111. 07	
6204. 19	10*w*	16113. 69	
6190. 84	4	16148. 44	$y\,^5F^\circ_4 - e\,^5G_4$
6187. 14	7	16158. 10	$y\,^5F^\circ_3 - e\,^5G_3$
6176. 72	10	16185. 35	
6172. 05	15	16197. 60	$b\,^3F_4 - x\,^3D^\circ_3$
6171. 56	7	16198. 89	$c\,^3D_1 - w\,^3D^\circ_1$
6168. 21	10*w*	16207. 68	$z\,^3D^\circ_1 - e\,^3D_1$; $a\,^5F_4 - z\,^3I^\circ_5$
6159. 49	10	16230. 63	$y\,^7P^\circ_3 - e\,^5D_4$
6154. 43	25	16243. 97	$z\,^3D^\circ_3 - e\,^3D_2$
6152. 71	10	16248. 51	$y\,^7P^\circ_3 - e\,^5D_3$; $c\,^3D_2 - w\,^3D^\circ_2$
6152. 14	6	16250. 02	$b\,^3F_3 - x\,^3D^\circ_3$
6146. 83	3	16264. 06	
6141. 71	15	16277. 61	$c\,^3D_1 - w\,^3D^\circ_2$
6138. 24	4	16286. 82	$y\,^5F^\circ_5 - e\,^5G_4$
6135. 76	25	16293. 40	$z\,^3D^\circ_3 - e\,^3D_3$
6125. 06	4	16321. 83	
6122. 49	5	16328. 71	$c\,^3D_2 - w\,^3D^\circ_3$
6122. 17	7	16329. 57	$b\,^3F_2 - w\,^3G^\circ_4$; $c\,^3D_3 - w\,^3D_3$
6104. 20	5	16377. 64	$z\,^3D^\circ_1 - e\,^3D_2$
6102. 70	30, *Z*	16381. 66	
6099. 54	5	16390. 15	$y\,^5F^\circ_2 - e\,^5G_3$
6098. 39	3	16393. 24	$b\,^3F_2 - w\,^3G^\circ_4$
6087. 74	5	16421. 92	
6068. 47	10	16474. 01	$z\,^3D^\circ_2 - e\,^3D_3$
6062. 75	50	16489. 61	$z\,^7F^\circ_6 - e\,^7D_5$
6055. 09	25	16510. 47	
6054. 41	25	16512. 32	
6053. 12	30	16515. 84	
6047. 68	18	16530. 67	$a\,^3I_5 - z\,^3I^\circ_5$
6045. 41	12	16536. 91	$a\,^3I_6 - z\,^3I^\circ_5$; $b\,^3F_4 - x\,^3F^\circ_3$
6040. 44	6*w*	16550. 51	$z\,^7D^\circ_3 - e\,^5D_4$
6039. 74	8*w*	16552. 43	
6039. 27	8	16553. 72	$a\,^5F_3 - u\,^5F^\circ_2$
6037. 00	8	16559. 94	$b\,^3F_3 - x\,^3F^\circ_4$
6029. 30	18	16581. 09	$a\,^3I_6 - z\,^3I^\circ_6$
6028. 53	1	16583. 21	$a\,^1H_5 - u\,^3F^\circ_4$
6027. 75	1	16585. 35	$e\,^5D_0 - s\,^3D^\circ_1$
6025. 27	10	16592. 18	$a\,^5F_5 - u\,^5F^\circ_5$; $b\,^3F_3 - x\,^3F^\circ_3$
6023. 68	10	16596. 56	$a\,^5F_4 - u\,^5F^\circ_3$
6022. 85	2	16598. 85	$e\,^3G_3 - v\,^3G^\circ_3$
6019. 58	10	16607. 87	$a\,^5F_4 - u\,^3F^\circ_3$
6014. 79	10	16621. 09	$a\,^5F_5 - u\,^5F^\circ_4$
6011. 37	1	16630. 55	$b\,^5D_2 - x\,^5P^\circ_1$
6006. 61	1	16643. 73	$b\,^5D_1 - x\,^5P^\circ_1$
6006. 30	20	16644. 59	$a\,^3I_7 - z\,^3I_7$
6004. 57	10	16649. 38	$a\,^5F_5 - t\,^5F^\circ_4$; $a\,^1G_4 - 1^\circ_5$
5999. 97	7	16662. 14	
5998. 91	1	16665. 09	$a\,^5F_4 - t\,^5F^\circ_4$
5998. 09	15	16667. 37	
5997. 14	12	16670. 01	$a\,^1H_5 - v\,^3F^\circ_4$
5992. 31	15	16683. 45	$b\,^5D_2 - x\,^5P^\circ_2$; $c\,^3G_4 - v\,^3G^\circ_4$
5991. 20	10	16686. 54	$z\,^7D^\circ_2 - e\,^5D_3$
5983. 22	20	16708. 79	
5982. 85	40	16709. 82	$z\,^7F^\circ_5 - e\,^7D_4$
5981. 96	25	16712. 31	$z\,^7F^\circ_3 - e\,^7D_3$
5978. 73	18	16721. 34	$b\,^3H_4 - y\,^3I^\circ_5$
5978. 69	4	16721. 45	$c\,^3G_3 - v\,^3G^\circ_4$; $a\,^3D_3 - z\,^3H^\circ_4$
5977. 76	15	16724. 05	
5974. 39	10	16733. 48	
5972. 30	10	16739. 34	$b\,^5D_3 - x\,^5P^\circ_3$
5970. 69	18	16743. 85	$b\,^5D_2 - x\,^5P^\circ_3$; $b\,^3H_6 - y\,^3I^\circ_7$
5965. 23	4	16759. 18	
5964. 60	18	16760. 95	$b\,^5D_4 - x\,^5P^\circ_3$
5959. 17	18	16776. 22	$b\,^3H_5 - y\,^3I^\circ_6$
5957. 56	7	16780. 76	$z\,^7D^\circ_4 - e\,^5D_2$
5955. 56	7	16786. 39	$b\,^1G_4 - y\,^1H^\circ_5$
5954. 75	8	16788. 68	$z\,^7D^\circ_1 - e\,^5D_1$
5950. 70	10	16800. 10	$x\,^5H^\circ_3 - e\,^5H_7$
5938. 74	15	16833. 94	$c\,^3G_4 - v\,^3G^\circ_5$
5935. 37	12	16843. 49	
5935. 02	15	16844. 49	$c\,^3G_5 - v\,^3G^\circ_5$
5933. 25	15	16849. 51	$b\,^3H_4 - 2^\circ_4$
5930. 35	12	16857. 75	$a\,^5F_1 - t\,^5F^\circ_1$
5928. 61	7	16862. 70	$a\,^5F_2 - t\,^5F^\circ_2$
5925. 63	10	16871. 18	
5922. 18	20	16881. 01	
5921. 30	35	16883. 52	
5919. 90	15	16887. 51	$a\,^5F_3 - t\,^5F^\circ_3$; $a\,^3I_5 - x\,^5H^\circ_6$
5919. 31	25	16889. 19	
5917. 97	15	16893. 02	$a\,^3I_6 - x\,^5H^\circ_6$
5917. 39	20	16894. 67	$a\,^3I_7 - x\,^5H^\circ_6$
5916. 73	30	16896. 55	$z\,^7F^\circ_4 - e\,^7D_3$
5915. 94	25	16898. 81	$a\,^5D_4 - z\,^7F^\circ_3$; $z\,^7F^\circ_4 - e\,^7D_4$
5904. 21	40*s*	16932. 39	$y\,^5H^\circ_5 - f\,^5G_6$; $a\,^5F_4 - y\,^3H^\circ_5$
5903. 21	8	16935. 25	
5902. 17	25	16938. 24	$b\,^5D_1 - y\,^5D^\circ_0$
5894. 87	3	16959. 21	$a\,^3I_5 - u\,^5F^\circ_4$
5894. 16	3	16961. 25	
5892. 33	35*s*	16966. 52	$y\,^5H^\circ_5 - f\,^5G_6$
5888. 02	25	16978. 97	$a\,^1H_5 - y\,^1I^\circ_6$
5886. 44	10	16983. 50	$y\,^5H^\circ_6 - f\,^5G_5$; $c\,^3D_1 - w\,^3F^\circ_2$
5885. 07	20	16987. 46	$a\,^3I_5 - t\,^3F^\circ_3$
5884. 45	30	16989. 24	$b\,^5D_2 - y\,^5D^\circ_1$
5881. 43	15	16997. 97	$x\,^5H^\circ_5 - e\,^5H_7$
5879. 81	20	17002. 65	$b\,^5D_1 - y\,^5D^\circ_1$

TABLE 1. *Wavelengths and term combinations of* Cr I—Continued

d Double; *h*, hazy; *H*, very hazy; *l*, shaded longward; *s*, shaded shortward; *r*, reversed; *R*, strongly reversed; *w*, wide; *W*, very wide; *Z*, Zeeman pattern in Table 2.

Wavelength λ_{air}	Intensity	Wave No.	Term combination
5878.04	50*s*	17007.77	$y\ ^5H_3^\circ - f\ ^5G_4$ $x\ ^5H_2^\circ - e\ ^5H_3$
5876.57	25	17012.03	$b\ ^5D_0 - y\ ^5D_1^\circ$
5875.63	25	17014.74	$c\ ^3D_2 - w^3F_3^\circ$
5873.04	75*s*	17022.25	
5871.18	15	17027.64	$y\ ^5H_3^\circ - f\ ^5G_3$
5867.98	10	17036.93	$a\ ^3D_2 - y\ ^3P_1^\circ$
5867.05	50	17039.63	$a\ ^3D_1 - y\ ^3P_1^\circ$
5865.88	10	17043.03	$a\ ^3D_1 - y\ ^3P_0^\circ$
5864.44	20*w*	17047.21	$y\ ^5H_4^\circ - f\ ^5G_3$
5863.97	25	17048.58	$z\ ^7F_3^\circ - e\ ^7D_2$
5863.39	25	17050.26	$z\ ^7F_2^\circ - e\ ^7D_3$
5862.80	25	17051.98	$a\ ^3F_3 - y\ ^3H_4^\circ$ $a\ ^5D_4 - z\ ^7F_4^\circ$ $a\ ^3D_2 - y\ ^3P_2^\circ$
5858.15	12	17065.52	$b\ ^3F_2 - w^3D_1^\circ$
5856.42	10	17070.56	$a\ ^5P_3 - z\ ^3D_3^\circ$
5854.27	75	17076.83	
5852.11	15	17083.13	$a\ ^5D_2 - z\ ^7F_1^\circ$
5849.04	3	17092.09	$a\ ^3I_7 - x\ ^5H_7^\circ$
5847.77	20	17095.81	$y\ ^5H_3^\circ - f\ ^5G_2$
5844.60	40	17105.08	$b\ ^5D_3 - y\ ^5D_2^\circ$
5843.21	25	17109.15	$b\ ^5D_2 - y\ ^5D_2^\circ$
5839.58	50*s*	17119.78	
5838.68	25	17122.42	$b\ ^5D_1 - y\ ^5D_2^\circ$
5838.38	15	17123.30	$b\ ^3F_3 - w^3D_2^\circ$
5837.85	10	17124.86	$c\ ^3D_3 - w^3F_4^\circ$
5828.88	15	17151.21	$b\ ^3F_4 - w^3D_3^\circ$
5825.43	10	17161.37	$b\ ^3D_1 - t\ ^5F_1^\circ$ $a\ ^5D_2 - z\ ^7F_2^\circ$
5824.37	60*s*	17164.49	$z\ ^7F_3^\circ - e\ ^7D_1$
5824.05	15	17165.43	$z\ ^7F_2^\circ - e\ ^7D_2$
5823.40	8	17167.23	$z\ ^7F_2^\circ - e\ ^7D_3$
5822.87	7	17168.91	$b\ ^3D_3 - t\ ^5F_2^\circ$ $a\ ^3H_5 - y\ ^5F_4^\circ$
5822.36	75*s*	17170.42	
5820.13	10	17177.00	$b\ ^3D_1 - x\ ^3P_0^\circ$
5819.67	7	17178.36	
5818.49	8	17181.84	$b\ ^3D_2 - t\ ^5F_1^\circ$
5815.85	20	17189.63	$b\ ^3D_2 - t\ ^5F_2^\circ$
5809.56	40	17208.25	
5808.14	40*s*	17212.44	
5801.14	30	17233.22	$a\ ^3I_5 - y\ ^3H_4^\circ$
5798.50	25	17241.07	$a\ ^5D_4 - z\ ^7F_5^\circ$
5797.90	30*s*	17242.85	$z\ ^7F_1^\circ - e\ ^7D_1$ $b\ ^3D_3 - t\ ^5F_3^\circ$
5796.74	40, *Z*	17246.30	$d\ ^3F_2 - v\ ^3G_3^\circ$
5794.59	12	17252.70	$d\ ^3F_3 - v\ ^3G_3^\circ$
5793.15	5	17256.99	
5792.14	10	17260.00	$a\ ^3D_0 - z\ ^7F_1^\circ$
5791.75	25	17261.16	$a\ ^3I_6 - y\ ^3H_5^\circ$
5791.00	100, *Z*	17263.40	$z\ ^5P_3^\circ - e\ ^5D_4$
5790.65	10	17264.41	$a\ ^5D_3 - z\ ^7F_4^\circ$
5790.10	25	17266.08	
5788.79	15	17269.99	$c\ ^3D_1 - w^3P_2^\circ$
5788.38	25	17271.21	$b\ ^5D_3 - y\ ^5D_3^\circ$
5787.97	85	17272.44	$z\ ^5P_2^\circ - e\ ^5D_2$
5787.04	25	17275.21	$b\ ^5D_2 - y\ ^5D_1^\circ$
5785.92	10	17278.56	$a\ ^5D_2 - z\ ^7F_3^\circ$ $a\ ^5D_1 - z\ ^7F_2^\circ$
5785.77	75	17279.00	$z\ ^5P_1^\circ - e\ ^5D_2$
5785.02	75	17281.24	$z\ ^5P_3^\circ - e\ ^5D_1$
5783.89	75	17284.62	$z\ ^5P_2^\circ - e\ ^5D_3$ $a\ ^3D_2 - y\ ^3F_2^\circ$
5783.11	75	17286.95	$a\ ^3D_1 - y\ ^3F_2^\circ$ $z\ ^5P_1^\circ - e\ ^5D_1$
5781.79	50	17290.90	$z\ ^5P_1^\circ - e\ ^5D_0$ $a\ ^3H_4 - y\ ^5F_4^\circ$
5781.18	50	17292.72	$b\ ^5D_4 - y\ ^5D_3^\circ$ $z\ ^5P_2^\circ - e\ ^5D_1$
5780.94	25	17293.44	$z\ ^5P_3^\circ - e\ ^5D_2$
5777.76	25	17302.96	$b\ ^3D_2 - x\ ^3P_1^\circ$
5777.32	20	17304.28	
5774.94	40*s*	17311.41	$c\ ^3D_2 - w^3P_1^\circ$
5772.67	25	17318.22	$a\ ^3D_2 - y\ ^3F_3^\circ$
5772.03	15	17320.14	
5771.55	75*s*	17321.58	
5766.32	15	17337.29	$a\ ^3H_5 - y\ ^5F_5^\circ$ $a\ ^1H_5 - u\ ^3H_6^\circ$
5762.13	15	17349.89	$d\ ^3F_4 - v\ ^3G_4^\circ$
5761.51	10	17351.61	$c\ ^3D_2 - w^3P_2^\circ$
5759.41	4	17358.09	
5758.99	50*s*	17359.35	
5758.26	25*s*	17361.55	
5755.30	10	17370.48	$a\ ^1H_5 - u\ ^3H_6^\circ$
5754.54	40*s*	17372.78	
5753.66	25, *Z*	17375.43	$d\ ^3F_2 - v\ ^3G_3^\circ$
5751.10	15	17383.17	
5747.83	40*s*	17393.06	$a\ ^5F_5 - x\ ^3G_5^\circ$
5746.40	25	17397.38	$a\ ^3I_7 - y\ ^3H_6^\circ$ $a\ ^3D_1 - y\ ^3D_1^\circ$
5743.11	10	17407.35	$a\ ^1H_5 - y\ ^1H_5^\circ$
5742.56	8	17409.02	
5741.21	8	17413.11	
5738.53	30	17421.25	$a\ ^3D_3 - y\ ^3F_4^\circ$
5736.63	18	17427.01	$a\ ^3D_2 - y\ ^3D_2^\circ$
5735.54	8	17430.33	$b\ ^3D_2 - x\ ^3P_2^\circ$
5729.86	12	17447.61	
5729.20	20	17449.62	$b\ ^3D_2 - x\ ^3P_2^\circ$
5727.06	12	17456.14	
5724.01	12	17465.44	
5721.78	10	17472.24	$a\ ^3D_2 - y\ ^3D_3^\circ$
5719.82	40	17478.23	$b\ ^5D_2 - y\ ^5D_3^\circ$
5716.10	10	17489.60	$b\ ^3G_3 - x\ ^5F_4^\circ$
5715.20	15	17492.36	$a\ ^3D_2 - y\ ^3D_3^\circ$
5712.77	35, *Z*	17499.80	$b\ ^5D_4 - y\ ^5D_4^\circ$
5712.62	20, *Z*	17500.26	$d\ ^3F_4 - v\ ^3G_4^\circ$
5708.46	20	17513.01	
5706.31	8	17519.61	
5703.61	8	17527.90	
5702.30	60, *Z*	17531.93	$b\ ^3G_3 - z\ ^3H_4^\circ$
5700.50	40	17537.47	$b\ ^3G_3 - z\ ^3H_4^\circ$ $a\ ^3D_3 - y\ ^3D_3^\circ$
5698.32	100, *Z*	17544.17	$z\ ^5F_4^\circ - f\ ^5D_4$

TABLE 1. *Wavelengths and term combinations of* Cr I—Continued

d, double; *h*, hazy; *H*, very hazy; *l*, shaded longward; *s*, shaded shortward; *r*, reversed; *R*, strongly reversed; *w*, wide; *W*, very wide; *Z*, Zeeman pattern in table 2.

Wavelength λ_{air}	Intensity	Wave No.	Term combination
5696. 64	12	17549. 35	
5696. 20	50	17550. 70	$a\ ^3G_3 - z\ ^5G^0_3$
5695. 23	15	17553. 69	
5694. 72	75, *Z*	17555. 27	$z\ ^5F^0_4 - f\ ^5D_3$
5690. 97	20	17566. 83	$c\ ^3G_4 - v\ ^3H^0_4$; $a\ ^3G_5 - z\ ^5G^0_6$; $c\ ^3G_5 - z\ ^1I^0_6$
5689. 08	10	17572. 67	
5683. 53	50	17589. 83	
5682. 47	75	17593. 11	$z\ ^5F^0_3 - f\ ^5D_2$
5681. 22	20	17596. 98	
5681. 07	40	17597. 45	
5679. 42	8	17602. 56	$b\ ^3G_4 - x\ ^5F^0_5$
5677. 78	12	17607. 64	$x\ ^5G^0_5 - e\ ^5H_6$
5676. 32	10	17612. 17	$x\ ^5G^0_4 - e\ ^5H_5$
5675. 79	10	17613. 82	$x\ ^5G^0_3 - e\ ^5H_4$
5675. 08	15	17616. 02	$a\ ^3D_2 - w\ ^5D^0_1$
5674. 19	20	17618. 78	$a\ ^3D_1 - w\ ^5D^0_1$
5671. 99	12	17625. 62	$x\ ^5G^0_3 - e\ ^5H_4$
5669. 72	10	17632. 67	$c\ ^3G_5 - v\ ^3H^0_6$
5668. 49	15	17636. 50	
5667. 83	18	17638. 55	$b\ ^1I_6 - z\ ^1H^0_5$
5666. 99	10	17641. 17	$a\ ^3G_4 - z\ ^5G^0_3$
5664. 57	35	17648. 70	$z\ ^5F^0_3 - f\ ^5D_1$
5664. 04	45, *Z*	17650. 36	$b\ ^3G_4 - z\ ^3H^0_5$
5662. 64	15	17654. 72	$b\ ^3G_4 - z\ ^3H^0_4$
5659. 52	10	17664. 45	$x\ ^5G^0_2 - e\ ^5H_3$
5658. 62	25	17667. 26	$a\ ^3D_2 - w\ ^5D^0_2$; $a\ ^3G_4 - z\ ^5G^0_4$
5654. 10	10	17681. 39	$a\ ^3G_3 - z\ ^5G^0_3$
5649. 38	50	17696. 16	$c\ ^3G_5 - v\ ^3H^0_5$; $z\ ^5F^0_5 - f\ ^5D_3$
5648. 25	40	17699. 70	$z\ ^5F^0_2 - f\ ^5D_2$
5647. 89	40*w*	17700. 83	$z\ ^5F^0_1 - f\ ^5D_0$
5646. 39	20*w*	17705. 53	$a\ ^3G_3 - z\ ^5G^0_3$
5645. 53	25	17708. 23	$y\ ^7P^0_4 - f\ ^7S_3$
5644. 26	15	17712. 21	$a\ ^3D_3 - w\ ^5D^0_3$
5642. 40	50	17718. 05	$z\ ^5F^0_4 - f\ ^5D_4$; $x\ ^5G^0_6 - e\ ^5H_7$
5641. 73	40*w*	17720. 15	$z\ ^5F^0_1 - f\ ^5D_1$
5638. 20	20	17731. 25	$a\ ^3D_3 - w\ ^5D^0_3$; $a\ ^3G_3 - z\ ^5G^0_4$
5628. 64	50, *Z*	17761. 36	$b\ ^3G_3 - z\ ^3H^0_4$
5627. 72	8	17764. 27	
5625. 58	10	17771. 02	$z\ ^5F^0_1 - f\ ^5D_2$
5625. 03	7	17772. 76	
5623. 69	10	17777. 00	
5609. 17	35	17823. 01	$y\ ^7P^0_3 - f\ ^7S_3$
5601. 80	12	17846. 46	$b\ ^3G_3 - y\ ^5H^0_3$
5600. 68	12	17850. 03	$b\ ^3F_2 - w\ ^3F^0_2$
5597. 87	18	17858. 99	$z\ ^5F^0_3 - f\ ^5D_4$
5592. 44	10	17876. 33	
5591. 90	10	17878. 06	
5588. 23	12	17889. 80	$b\ ^3F_3 - w\ ^3F^0_3$
5588. 05	30	17890. 37	$b\ ^3G_3 - y\ ^5H^0_3$
5583. 72	7	17904. 25	
5581. 60	15	17911. 05	$b\ ^3G_4 - y\ ^5H^0_4$
5580. 48	25	17914. 64	$y\ ^7P^0_3 - f\ ^7S_3$
5579. 00	10	17919. 40	
5576. 48	8	17927. 49	$y\ ^5G^0_3 - f\ ^5G_4$
5575. 18	10	17931. 67	$b\ ^3D_1 - x\ ^5D^0_0$
5574. 40	12	17934. 18	$b\ ^3H_4 - v\ ^3G^0_3$
5572. 45	6	17940. 46	
5571. 46	25	17943. 65	
5568. 28	18	17953. 89	$a\ ^3H_6 - z\ ^5H^0_5$
5566. 55	20	17959. 47	$b\ ^3G_4 - y\ ^5H^0_5$
5565. 40	5	17963. 18	$c\ ^3G_4 - v\ ^3F^0_4$
5563. 66	15	17968. 80	$b\ ^3G_3 - y\ ^5H^0_4$
5560. 75	15	17978. 21	$b\ ^3D_1 - x\ ^3D^0_2$
5559. 17	25	17983. 31	$b\ ^1G_4 - 4^0_3$
5556. 18	10	17992. 99	$b\ ^5D_2 - x\ ^5D^0_1$
5555. 59	8	17994. 90	$a\ ^3D_2 - w\ ^5F^0_2$
5555. 26	4	17995. 98	$a\ ^3D_2 - w\ ^5F^0_1$
5554. 32	15	17999. 02	$a\ ^3D_1 - w\ ^5F^0_1$; $b\ ^3D_2 - x\ ^3D^0_2$; $b\ ^3F_3 - w\ ^3F^0_4$
5552. 87	5	18003. 72	
5549. 17	7	18015. 72	$b\ ^5D_0 - x\ ^5D^0_1$; $a\ ^5F_2 - w\ ^3G^0_3$
5548. 61	15	18017. 54	$b\ ^3G_3 - y\ ^5H^0_2$
5546. 61	7	18024. 04	$a\ ^3H_5 - z\ ^5H^0_4$; $w\ ^5F^0_3 - e\ ^5H_3$
5544. 56	20	18030. 70	$w\ ^5F^0_4 - e\ ^5H_4$
5543. 33	20	18034. 70	$w\ ^5F^0_2 - e\ ^5H_3$
5540. 70	15	18043. 26	$b\ ^3H_5 - v\ ^3G^0_4$
5539. 52	10	18048. 11	
5538. 20	6	18051. 41	$a\ ^3D_3 - w\ ^5F^0_3$
5535. 48	10	18060. 28	
5534. 63	7	18063. 05	$w\ ^5F^0_3 - e\ ^5H_4$
5529. 55	10	18079. 64	$a\ ^5G^0_2 - z\ ^3D^0_1$; $y\ ^5G^0_3 - f\ ^3G_4$
5528. 90	7	18081. 77	$w\ ^5F^0_2 - e\ ^5H_3$
5528. 37	3	18083. 50	$a\ ^3D_3 - w\ ^3F^0_4$
5527. 90	7	18085. 04	
5526. 49	7	18089. 65	$a\ ^5F_3 - w\ ^3G^0_4$
5525. 91	4	18091. 55	$a\ ^3H_4 - z\ ^5H^0_5$
5519. 62	18	18112. 17	
5519. 00	3	18114. 20	$a\ ^5F_2 - w\ ^3G^0_2$
5513. 38	5	18132. 67	
5512. 70	10	18134. 91	$b\ ^5D_3 - x\ ^5D^0_2$
5512. 05	7	18137. 04	$y\ ^5G^0_4 - f\ ^5G_4$
5511. 47	3	18138. 95	$b\ ^5D_2 - x\ ^5D^0_2$
5509. 94	15	18143. 99	$b\ ^3H_6 - v\ ^3G^0_5$
5508. 22	18	18149. 66	
5507. 45	6	18152. 19	$b\ ^5D_1 - x\ ^5D^0_2$
5505. 00	10	18160. 27	$a\ ^5F_4 - w\ ^3G^0_5$
5503. 72	4	18164. 49	$a\ ^5F_2 - w\ ^5G^0_3$
5497. 66	18	18184. 52	$d\ ^3F_3 - w\ ^3H^0_4$
5494. 16	4	18196. 10	$a\ ^3H_5 - z\ ^5H^0_6$
5492. 89	8	18200. 31	
5492. 70	10	18200. 94	
5490. 30	8	18208. 90	$a\ ^5F_3 - w\ ^5G^0_4$
5490. 17	7	18209. 33	$a\ ^5G_3 - z\ ^3D^0_2$
5489. 03	10	18213. 10	$a\ ^5G_3 - z\ ^3D^0_3$
5486. 52	10	18221. 44	$d\ ^3F_4 - w\ ^3H^0_5$
5486. 10	8	18222. 84	
5485. 72	8	18224. 10	$a\ ^5F_3 - w\ ^5G^0_3$
5485. 19	3	18225. 86	$b\ ^3F_3 - w\ ^3P^0_2$
5481. 01	7	18239. 76	$a\ ^5F_4 - w\ ^5G^0_5$
5480. 50	45, *Z*	18241 46	$a\ ^5F_5 - w\ ^5G^0_6$; $b\ ^3G_3 - y\ ^3F^0_4$
5476. 03		518256. 34	$a\ ^5F_3 - x\ ^3F^0_4$

TABLE 1. *Wavelengths and term combinations of* Cr I—Continued

d, Double; *h*, hazy; *H*, very hazy; *l*, shaded longward; *s*, shaded shortward; *r*, reversed; *R*, strongly reversed; *w*, wide; *W*, very wide; *Z*, Zeeman pattern in table 2.

Wavelength λ_{air}	Intensity	Wave No.	Term combination
5469.44	8	18278.34	
5468.17	10	18282.58	$b\ ^3D_2-x\ ^3D_3^\circ$
5464.39	10	18295.23	$a\ ^5F_2-x\ ^3F_3^\circ$
5463.93	40, *Z*	18296.77	$b\ ^3G_4-y\ ^3F_3^\circ$
5462.91	10	18300.19	$a\ ^5F_1-x\ ^3F_2^\circ$
5462.41	15	18301.86	$b\ ^3D_3-x\ ^3D_3^\circ$
5457.82	25	18317.26	
5449.27	10	18345.99	
5447.92	5	18350.54	
5447.50	7	18351.96	$d\ ^3F_4-v\ ^3H_5^\circ$
5446.79	10	18354.35	$b\ ^3G_4-y\ ^3F_4^\circ$
5445.78	12	18357.75	
5443.91	12	18364.06	
5443.34	10	18365.98	$b\ ^5D_4-x\ ^5D_3^\circ$ $a\ ^3D_2-y\ ^3G_3^\circ$
5442.40	35, *Z*	18369.15	$b\ ^3G_3-y\ ^3F_2^\circ$
5437.79	15	18384.73	$c\ ^5D_4-s\ ^5D_4^\circ$
5433.86	8	18398.03	$d\ ^3F_2-v\ ^3D_1^\circ$
5432.35	25	18403.14	$b\ ^3G_3-y\ ^3F_3^\circ$
5427.98	12	18417.95	$b\ ^3D_1-w^5G_2^\circ$ $a\ ^3D_2-y\ ^3G_4^\circ$
5422.70	4	18435.89	
5421.97	5*w*	18438.37	$b\ ^3D_2-w^5G_2^\circ$
5420.62	7	18442.96	
5417.98	10*w*	18451.95	
5414.24	3	18464.69	
5412.50	10	18470.63	$b\ ^3G_4-y\ ^3D_3^\circ$
5409.78	400, *Z*	18479.92	$a\ ^3D_4-z\ ^5P_3^\circ$
5408.78	8	18483.33	
5406.43	10	18491.37	$b\ ^3D_2-w^5G_3^\circ$
5405.79	15, *Z*	18493.55	
5405.00	35, *Z*	18496.26	$b\ ^3P_2-y\ ^3P_1^\circ$
5400.58	50, *Z*	18511.40	$b\ ^3G_3-y\ ^3D_2^\circ$ $b\ ^3P_2-y\ ^3P_2^\circ$
5398.92	5	18517.09	
5395.81	7, *Z*	18527.76	
5394.32	4	18532.88	
5393.05	7	18537.24	
5391.34	35	18543.12	$b\ ^3P_1-y\ ^3P_1^\circ$
5390.38	40, *Z*	18546.43	$b\ ^3P_1-y\ ^3P_0^\circ$
5387.57	35, *Z*	18556.10	$b\ ^3P_0-y\ ^3P_1^\circ$
5386.96	50, *Z*	18558.20	$b\ ^3P_1-y\ ^3P_2^\circ$
5385.93	5	18561.85	
5385.30	20*w*	18563.92	$b\ ^3D_2-w^5G_4^\circ$
5382.74	7	18573.68	
5382.23	4	18574.51	
5379.37	25	18584.38	
5377.73	35	18589.98	
5376.15	20	18595.51	
5375.85	10	18596.55	
5375.11	8*w*	18599.11	
5374.68	7*w*	18600.60	$d\ ^3F_3-v\ ^3D_2^\circ$
5373.71	30	18603.96	$b\ ^3D_1-x\ ^3F_2^\circ$
5371.48	50, *Z*	18611.68	$b\ ^3D_3-x\ ^3F_4^\circ$
5370.36	40, *Z*	18615.56	
5368.53	35, *Z*	18621.91	$b\ ^3D_2-x\ ^3F_3^\circ$
5367.81	10	18624.40	$b\ ^3D_3-x\ ^3F_3^\circ$
5367.22	8	18626.45	$b\ ^3D_1-x\ ^3D_1^\circ$
5365.99	20	18630.72	$c\ ^3G_4-u\ ^3H_5^\circ$
5362.99	25	18641.14	$b\ ^3D_3-x\ ^3F_3^\circ$
5361.87	10	18645.04	
5361.30	40	18647.02	
5360.45	20	18649.98	
5356.51	8	18663.69	$a\ ^5F_2-s\ ^5F_1^\circ$
5356.30	2*w*	18664.43	$b\ ^3G_4-w^5D_3^\circ$
5355.72	2	18666.45	$a\ ^5F_1-s\ ^5F_1^\circ$
5351.67	10	18680.57	
5349.72	5	18687.38	
5348.30	200, *Z*	18692.34	$a\ ^5D_3-z\ ^5P_3^\circ$
5347.25	10	18696.02	
5345.77	200, *Z*	18701.19	$a\ ^5D_3-z\ ^5P_2^\circ$
5344.77	40	18704.69	$y\ ^7P_3^\circ-f\ ^7D_2$
5344.04	10*w*	18707.24	
5343.54	8	18709.00	$e\ ^5S_2-v\ ^3P_2^\circ$
5341.88	8*w*	18714.81	
5340.46	40, *Z*	18719.79	$y\ ^7P_2^\circ-f\ ^7D_1$
5333.71	12	18743.47	$b\ ^3P_2-y\ ^3F_2^\circ$
5333.04	8	18745.83	
5329.76	50	18757.37	$z\ ^7P_4^\circ-e\ ^7D_3$
5329.17	100	18759.44	$z\ ^7P_4^\circ-e\ ^7D_4$
5328.36	200	18762.29	$z\ ^7P_4^\circ-e\ ^7D_5$
5324.35	8*w*	18776.42	
5324.06	20	18777.44	$b\ ^3P_2-y\ ^3F_3^\circ$
5318.79	40	18796.05	$y\ ^7P_2^\circ-f\ ^7D_2$
5312.88	50, *Z*	18816.96	$y\ ^7P_3^\circ-f\ ^7D_3$
5309.47	10	18829.05	$a\ ^5F_2-w^3D_2^\circ$ $b\ ^1I_6-y\ ^3I_5^\circ$
5308.70	4	18831.78	$a\ ^5F_1-w^3D_2^\circ$
5307.26	30	18836.88	$y\ ^5P_3^\circ-f\ ^5D_3$
5304.19	40	18848.15	$y\ ^7P_3^\circ-f\ ^7D_4$
5300.74	75, *Z*	18860.06	$a\ ^5D_2-z\ ^5P_3^\circ$
5298.29	100, *Z*	18868.78	$a\ ^5D_2-z\ ^5P_2^\circ$ $z\ ^7P_3^\circ-e\ ^7D_2$
5297.99	50, *Z*	18869.85	$z\ ^7P_3^\circ-e\ ^7D_3$
5297.37	75	18872.05	$z\ ^7P_3^\circ-e\ ^7D_4$
5296.69	100, *Z*	18874.48	$a\ ^5D_2-z\ ^5P_1^\circ$
5293.38	25	18886.28	$b\ ^3P_2-y\ ^3D_2^\circ$
5292.88	20	18888.06	$b\ ^3G_3-w^5F_4^\circ$
5292.57	5, *Z*	18889.17	
5289.28	15	18900.92	$b\ ^3P_1-y\ ^3D_1^\circ$
5288.11	7	18905.10	$b\ ^3P_1-w^5D_0^\circ$
5287.63	10*w*	18906.82	$z\ ^3F_2^\circ-e\ ^3D_1$
5287.19	40	18908.39	$y\ ^7P_2^\circ-f\ ^7D_3$
5285.64	20, *Z*	18913.94	$b\ ^3P_0-y\ ^3D_1^\circ$
5285.37	7	18914.91	$b\ ^1I_6-y\ ^3I_5^\circ$ $d\ ^3F_2-u\ ^3F_2^\circ$
5280.28	35	18933.13	$b\ ^3P_1-y\ ^3D_2^\circ$
5278.25	40	18940.42	$z\ ^3F_3^\circ-e\ ^3D_2$
5276.07	75*w*	18948.24	$z\ ^7P_2^\circ-e\ ^7D_1$
5275.71	65*w*	18949.54	$z\ ^7P_3^\circ-e\ ^7D_2$
5275.21	70, *Z*	18951.33	$b\ ^3P_2-y\ ^3D_1^\circ$ $z\ ^7P_2^\circ-e\ ^7D_1$
5273.46	50, *Z*	18957.62	$z\ ^7D_3^\circ-f\ ^7D_4$
5272.36	8	18961.58	
5272.01	50, *Z*	18962.83	$y\ ^7P_3^\circ-f\ ^7D_4$
5268.92	20*w*	18973.96	$y\ ^5P_2^\circ-f\ ^5D_2$
5267.10	10	18980.51	

TABLE 1. *Wavelengths and term combinations of* Cr I—Continued

d, Double; *h*, hazy; *H*, very hazy; *l*, shaded longward; *s*, shaded shortward; *r*, reversed; *R*, strongly reversed; *w*, wide; *W*, very wide; *Z*, Zeeman pattern in table 2.

Wavelength λ_{air}	Intensity	Wave No.	Term combination
5266. 08	10	18984. 19	$b\,^3G_4 - w\,^5F_5^0$
5265. 73	75	18985. 45	$a\,^5D_1 - z\,^5P_2^0$
5265. 17	50	18987. 47	$z\,^7D_4^0 - f\,^7D_3$
5264. 52	20	18984. 19	
5264. 16	100, *Z*	18991. 11	$a\,^5D_1 - z\,^5P_1^0$
5263. 76	30	18992. 56	$z\,^3F_4^0 - e\,^3D_3$
5261. 76	50, *Z*	18999. 77	$y\,^5P_3^0 - f\,^5D_4$
5257. 08	10	19016. 69	$b\,^3G_4 - w\,^5F_4^0$
5255. 12	100, *Z*	19023. 78	$y\,^7P_4^0 - f\,^7D_5$
5254. 92	90, *Z*	19024. 50	$z\,^7D_3^0 - f\,^7D_2$
5247. 92	15	19049. 88	$a\,^1H_5 - t\,^3G_4^0$ $a\,^5P_1 - y\,^5F_1^0$
5247. 58	125, *Z*	19051. 11	$a\,^5D_0 - z\,^5P_1^0$
5243. 38	75, *Z*	19066. 37	$z\,^7D_2^0 - f\,^7D_1$
5241. 47	30	19073. 32	$a\,^5P_1 - x\,^5P_1^0$
5240. 93	20	19075. 29	$b\,^3P_2 - w\,^5D_1^0$
5240. 47	50	19076. 96	$z\,^3F_2^0 - e\,^3D_2$ $y\,^5P_3^0 - f\,^5D_2$
5238. 97	60, *Z*	19082. 42	$a\,^5P_2 - x\,^5P_1^0$
5237. 36	2	19088. 29	$b\,^3G_5 - z\,^3G_4^0$
5237. 06	4	19089. 39	
5236. 63	10	19090. 95	$b\,^3G_3 - w\,^5F_3^0$
5230. 23	40	19114. 31	$a\,^5P_1 - y\,^5F_2^0$
5228. 10	50	19122. 10	$b\,^3P_1 - w\,^5D_1^0$
5227. 76	25	19123. 34	$b\,^3G_3 - w\,^5F_4^0$ $a\,^5P_2 - y\,^5F_3^0$
5227. 09	20	19125. 79	$a\,^5P_1 - x\,^5P_2^0$
5226. 92	50	19126. 42	$b\,^3P_2 - w\,^5D_2^0$
5225. 83	50	19130. 40	$a\,^5P_3 - y\,^5F_3^0$
5225. 05	75, *Z*	19133. 26	$z\,^7D_4^0 - f\,^7D_4$
5224. 97	75, *Z*	19133. 55	$z\,^7D_5^0 - f\,^7D_5$
5224. 55	40	19135. 09	$a\,^5P_2 - x\,^5P_2^0$ $b\,^3P_0 - w\,^5D_1^0$
5224. 10	30	19136. 74	$z\,^7D_3^0 - f\,^7D_3$
5223. 82	5*w*	19137. 76	$y\,^5P_1^0 - f\,^5D_2$
5222. 68	25	19141. 94	$a\,^5P_3 - x\,^5P_2^0$
5222. 39	10	19143. 01	$b\,^3G_4 - z\,^3G_3^0$
5221. 90	5	19144. 80	
5221. 76	50, *Z*	19145. 31	$b\,^3P_2 - w\,^5D_3^0$
5220. 92	40	19148. 39	$z\,^7D_1^0 - f\,^7D_1$
5220. 12	4	19151. 33	
5216. 59	10*w*, *d*?	19164. 29	$a\,^5F_5 - u\,^5D_4^0$ $a\,^1H_5 - t\,^3G_5^0$
5216. 16	12*w*	19165. 87	$z\,^5P_1^0 - f\,^5S_2$
5215. 27	20	19169. 14	$b\,^3G_5 - z\,^3G_5^0$
5214. 88	4*w*	19170. 54	$z\,^3F_3^0 - e\,^3D_3$
5214. 62	15*w*	19171. 53	$z\,^5P_2^0 - f\,^5S_2$
5214. 14	30	19173. 29	$b\,^3P_1 - w\,^5D_2^0$
5213. 66	5	19175. 06	$b\,^3D_3 - w\,^3D_2^0$
5212. 24	18*w*	19180. 28	$z\,^5P_3^0 - f\,^5S_2$
5208. 415	400*R*, *Z*	19194. 37	$a\,^5S_2 - z\,^5P_3^0$
5206. 61	3	19201. 02	$b\,^3G_4 - z\,^3G_4^0$
5206. 021	300*R*, *Z*	19203. 20	$a\,^5S_2 - z\,^5P_2^0$
5204. 505	200*R*, *Z*	19208. 79	$a\,^5S_2 - z\,^5P_1^0$
5200. 202	50, *Z*	19224. 68	$z\,^7D_1^0 - f\,^7D_2$
5196. 57	12	19238. 12	$b\,^3G_5 - y\,^3G_4^0$ $a\,^5P_2 - y\,^5F_3^0$
5196. 45	100	19238. 75	$b\,^3G_5 - y\,^3G_5^0$
5194. 60	10	19245. 42	$a\,^5P_3 - y\,^5F_3^0$
5193. 497	35, *Z*	19249. 50	$b\,^3G_3 - z\,^3G_3^0$ $e\,^3S_2 - u\,^3P_1^0$
5192. 009	100, *Z*	19255. 05	$z\,^7D_2^0 - f\,^7D_3$
5184. 579	100	19282. 62	$b\,^3G_4 - z\,^3G_3^0$ $z\,^7D_5^0 - f\,^7D_4$
5183. 414	10	19286. 95	$a\,^5D_3 - z\,^7D_2^0$
5177. 84	10	19307. 71	$b\,^3G_3 - z\,^3G_4^0$ $a\,^5F_2 - u\,^3D_1^0$
5177. 420	75, *Z*	19309. 28	$a\,^5F_1 - u\,^3D_0^0$ $z\,^7D_4^0 - f\,^7D_5$
5168. 61	8	19342. 19	$a\,^5D_4 - z\,^7D_4^0$
5167. 956	30	19344. 63	$b\,^3G_4 - y\,^3G_3^0$
5166. 221	150	19351. 13	$b\,^3G_4 - y\,^3G_4^0$ $b\,^3G_4 - y\,^3G_5^0$
5161. 782	25, *Z*	19367. 77	$a\,^5P_1 - y\,^5D_0^0$
5160. 77	5	19371. 57	
5160. 46	7	19372. 73	$a\,^5D_2 - z\,^7D_1^0$
5156. 39	5	19388. 03	
5151. 826	12	19405. 20	$a\,^5D_3 - z\,^7D_3^0$
5149. 49	7	19414. 01	$a\,^3F_4 - y\,^3G_5^0$ $a\,^1G_4 - z\,^1H_5^0$
5144. 673	50, *Z*	19432. 18	$a\,^5P_1 - y\,^3D_1^0$
5142. 268	20	19441. 27	$a\,^5P_2 - y\,^5D_1^0$
5139. 72	45	19450. 91	
5139. 60	55, *Z*	19451. 36	$b\,^3G_3 - y\,^3G_3^0$
5138. 86	10*w*	19454. 16	$b\,^3P_2 - w\,^5F_2^0$
5138. 715	10	19454. 71	$a\,^5D_2 - z\,^7D_2^0$
5137. 937	12	19457. 66	$b\,^3G_3 - y\,^3G_4^0$
5135. 92	18	19465. 30	$b\,^3P_2 - w\,^5F_3^0$
5135. 66	10	19466. 29	$a\,^3G_3 - y\,^5G_2^0$
5129. 57	8	19489. 40	$a\,^5D_1 - z\,^7D_1^0$
5126. 517	15	19501. 00	$b\,^3P_1 - w\,^5F_2^0$
5126. 168	10	19502. 33	$b\,^3P_1 - w\,^5F_1^0$
5123. 470	35	19512. 60	$a\,^5D_4 - y\,^7P_3^0$
5122. 770	18	19515. 27	$b\,^3P_0 - w\,^5F_1^0$
5122. 118	30	19517. 75	$a\,^5D_4 - z\,^7D_5^0$
5119. 46	10	19527. 89	
5115. 34	5	19543. 61	
5113. 140	45	19552. 02	$a\,^5P_1 - y\,^5D_2^0$
5112. 498	25	19554. 48	$a\,^5D_3 - z\,^7D_4^0$
5110. 76	40	19561. 13	$a\,^5P_2 - y\,^5D_2^0$
5108. 92	12	19568. 17	$a\,^5P_3 - y\,^5D_3^0$
5108. 34	12	19570. 39	
5107. 70	7	19572. 84	$a\,^5D_2 - z\,^7D_3^0$
5105. 40	7	19581. 66	
5093. 41	7	19627. 76	$a\,^5D_4 - y\,^7P_4^0$
5091. 898	30	19633. 59	$a\,^5D_3 - y\,^7P_3^0$
5086. 21	8	19655. 54	$b\,^3P_2 - u\,^5P_3^0$
5078. 713	40	19684. 56	
5072. 928	60, *Z*	19707. 00	$a\,^5S_2 - z\,^7D_1^0$
5072. 74	15	19707. 73	$a\,^3G_5 - y\,^5G_6^0$
5068. 312	35	19724. 95	$a\,^5D_4 - y\,^7P_5^0$
5067. 728	75, *Z*	19727. 22	$a\,^5P_2 - y\,^5D_3^0$

TABLE 1. *Wavelengths and term combinations of* Cr I—Continued

d, Double; *h*, hazy; *H*, very hazy; *l*, shaded longward; *s*, shaded shortward; *r*, reversed; *R*, strongly reversed; *w*, wide; *W*, very wide; *Z*, Zeeman pattern in Table 2.

Wavelength λ_{air}	Intensity	Wave No.	Term combination	Wavelength λ_{air}	Intensity	Wave No.	Term combination
5065. 925	50, *Z*	19734. 24	$a\ ^5P_2 - y\ ^5D_3^\dagger$	4962. 28	4*w*	20146. 42	$z\ ^5G_3^\dagger - f\ ^5G_3$
5063. 24	6	19744. 71	$b\ ^3P_2 - u\ ^5P_2^\dagger$	4956. 72	6	20169. 02	$b\ ^3G_3 - u\ ^5F_3^\dagger$
5059. 04	4	19761. 10		4954. 808	80, *Z*	20176. 80	$a\ ^3F_4 - z\ ^3H_5^\dagger$
5055. 13	3	19776. 39	$a\ ^3D_3 - x\ ^3P_3^\dagger$	4953. 725	22	20181. 22	$a\ ^3F_4 - z\ ^3H_4^\dagger$
5051. 902	40, *Z*	19789. 02	$a\ ^5S_2 - z\ ^7D_3^\dagger$	4952. 21	4*w*	20187. 39	
5049. 42	5	19798. 75	$b\ ^3P_2 - u\ ^5P_1^\dagger$	4949. 579	12	20198. 12	$b\ ^3D_1 - w\ ^3P_1^\dagger$
5048. 75	25	19801. 38	$a\ ^5D_2 - y\ ^7P_3^\dagger$	4944. 57	22	20218. 58	$b\ ^3D_2 - w\ ^3P_1^\dagger$
5045. 04	6	19815. 94	$b\ ^3H_4 - x\ ^3I_5^\dagger$	4942. 49	200, *Z*	20227. 09	$a\ ^5S_2 - y\ ^7P_3^\dagger$
5043. 58	6	19821. 67	$a\ ^3D_3 - x\ ^3P_4^\dagger$	4938. 354	12	20244. 03	
5042. 85	3	19824. 55	$a\ ^5F_1 - w\ ^3P_0^\dagger$	4937. 51	5	20247. 49	$a\ ^3G_5 - x\ ^5F_4^\dagger$
5042. 53	4*w*	19825. 80	$b\ ^5D_2 - w\ ^5P_1^\dagger$	4936. 34	150, *Z*	20252. 29	$a\ ^3F_3 - z\ ^3H_4^\dagger$
5039. 09	5*w*	19839. 34	$b\ ^5D_1 - w\ ^5P_1^\dagger$	4934. 877	15	20258. 29	$b\ ^3D_2 - w\ ^3P_2^\dagger$
5038. 58	15	19841. 35	$b\ ^3D_1 - w\ ^3F_2^\dagger$	4932. 62	4	20267. 56	
5034. 65	7	19856. 83	$b\ ^3H_5 - x\ ^3I_6^\dagger$	4932. 55	8	20267. 85	$a\ ^3G_5 - x\ ^5F_5^\dagger$
5033. 37	5	19861. 89	$b\ ^3D_2 - w\ ^3F_2^\dagger$	4931. 12	15	20273. 73	$z\ ^5I_8^\dagger - e\ ^5H_7$
5032. 54	12	19865. 16	$b\ ^3H_6 - x\ ^3I_7^\dagger$; $b\ ^3P_2 - z\ ^3S_1^\dagger$	4930. 515	10	20276. 22	
5031. 28	10	19870. 13	$c\ ^3D_3 - v\ ^3G_3^\dagger$	4930. 179	30, *Z*	20277. 60	$b\ ^3D_3 - w\ ^3P_2^\dagger$
5028. 06	15*w*	19882. 86	$b\ ^5D_3 - w\ ^5P_3^\dagger$	4923. 280	20	20306. 01	
5027. 005	10*w*	19887. 03	$b\ ^5D_2 - w\ ^5P_3^\dagger$	4922. 60	5	20308. 82	$b\ ^5D_4 - y\ ^5G_5^\dagger$
5025. 83	4	19891. 68	$a\ ^5F_2 - w\ ^3P_1^\dagger$	4922. 276	300, *Z*	20310. 14	$a\ ^3G_5 - z\ ^3H_6^\dagger$
5025. 545	10	19892. 81	$a\ ^5D_2 - y\ ^7P_4^\dagger$	4920. 95	50	20315. 62	$a\ ^3G_5 - z\ ^3H_5^\dagger$
5023. 63	5*w*	19900. 39	$b\ ^5D_1 - w\ ^5P_2^\dagger$	4919. 465	20	20321. 75	$z\ ^5I_8^\dagger - e\ ^5H_6$
5021. 910	25	19907. 21	$a\ ^5S_2 - z\ ^7D_2^\dagger$	4914. 27	3	20343. 23	$c\ ^3G_4 - t\ ^3G_4^\dagger$
5020. 80	3	19911. 61		4909. 878	6	20361. 43	$a\ ^5P_1 - x\ ^5D_0^\dagger$
5020. 608	15	19912. 37	$b\ ^5P_1 - z\ ^3S_1^\dagger$	4908. 56	4	20366. 90	$b\ ^5D_2 - v\ ^5P_1^\dagger$
5019. 200	20	19917. 96	$a\ ^5D_1 - y\ ^7P_2^\dagger$	4905. 37	7	20380. 15	$b\ ^5D_1 - v\ ^5P_1^\dagger$
5018. 17	18, *Z*	19922. 04	$a\ ^5F_3 - w\ ^3P_2^\dagger$; $b\ ^3D_2 - w\ ^3F_3^\dagger$	4905. 050	20	20381. 48	$c\ ^3G_3 - t\ ^3G_3^\dagger$
5017. 33	4	19925. 38	$b\ ^3P_0 - z\ ^3S_1^\dagger$	4903. 25	70, *Z*	20388. 96	$a\ ^5G_2 - y\ ^5F_1^\dagger$
5013. 314	100, *Z*	19941. 34	$b\ ^3D_3 - w\ ^3F_4^\dagger$; $a\ ^5P_3 - y\ ^5D_4^\dagger$	4902. 06	10*w*	20393. 91	$c\ ^3D_2 - q\ ^5F_3^\dagger$; $c\ ^3D_3 - q\ ^5F_3^\dagger$
5009. 78	10*w*	19955. 40	$b\ ^5D_3 - w\ ^5P_3^\dagger$	4898. 456	10	20408. 91	$z\ ^5I_8^\dagger - e\ ^5H_5$; $a\ ^3G_4 - x\ ^5F_5^\dagger$
5008. 75	5*w*	19959. 51	$b\ ^5D_2 - w\ ^5P_3^\dagger$	4897. 515	5	20412. 84	$a\ ^5G_2 - x\ ^5P_1^\dagger$
5007. 17	4*w*	19965. 81		4896. 47	4	20417. 19	$b\ ^3G_3 - u\ ^5F_4^\dagger$
5005. 08	7	19974. 17	$b\ ^3H_6 - u\ ^3H_6^\dagger$	4895. 44	3*w*	20421. 49	$a\ ^3G_3 - x\ ^5F_3^\dagger$
5004. 35	35*w*	19976. 94	$b\ ^5D_4 - w\ ^5P_3^\dagger$	4895. 00	3	20423. 32	
5000. 95	4	19990. 64	$b\ ^3H_5 - u\ ^3H_5^\dagger$	4894. 37	25	20425. 95	$z\ ^5I_7^\dagger - e\ ^5H_7$
4998. 57	4	20000. 16	$b\ ^5D_2 - y\ ^5G_2^\dagger$	4892. 731	10	20432. 79	
4991. 08	4	20030. 17		4891. 973	18	20435. 96	$a\ ^5P_1 - x\ ^5D_1^\dagger$
4988. 10	3	20042. 14		4891. 59	1	20437. 56	$a\ ^5F_4 - y\ ^5H_4^\dagger$; $z\ ^7F_3^\dagger - f\ ^7S_3$
4985. 951	5, *Z*	20050. 78	$b\ ^3D_2 - w\ ^3F_3^\dagger$	4890. 22	22	20443. 28	$z\ ^5I_8^\dagger - e\ ^5H_6$; $z\ ^5I_5^\dagger - e\ ^5H_4$
4983. 45	1	20060. 84	$b\ ^3H_5 - y\ ^3H_5^\dagger$	4889. 71	20	20445. 42	$a\ ^5P_2 - x\ ^5D_1^\dagger$
4982. 11	1	20066. 24		4889. 20	3*w*	20447. 55	
4981. 607	15*w*	20068. 26	$z\ ^5G_2^\dagger - f\ ^5G_3$	4888. 53	40	20450. 35	$a\ ^5G_3 - y\ ^5F_3^\dagger$
4977. 54	10*w*	20084. 66	$z\ ^5G_3^\dagger - f\ ^5G_4$; $z\ ^5G_4^\dagger - f\ ^5G_5$	4887. 71	22	20453. 78	$a\ ^5G_2 - y\ ^5F_2^\dagger$
4974. 00	6	20098. 95		4887. 013	150, *Z*	20456. 70	$a\ ^3G_4 - z\ ^3H_3^\dagger$
4973. 30	4*w*	20101. 78	$z\ ^5G_3^\dagger - f\ ^5G_3$; $c\ ^3G_5 - t\ ^3F_4^\dagger$	4885. 97	50	20461. 07	$a\ ^3G_4 - z\ ^3H_4^\dagger$
4972. 22	6*w*	20106. 15	$c\ ^3F_2 - u\ ^3H_3^\dagger$; $z\ ^5G_4^\dagger - f\ ^5G_4$	4885. 77	75, *Z*	20461. 90	$a\ ^5G_3 - x\ ^5P_2^\dagger$
4971. 36	7	20109. 63		4884. 95	25	20465. 34	$a\ ^5G_2 - x\ ^5P_3^\dagger$; $z\ ^5I_8^\dagger - e\ ^5H_7$
4970. 97	3*w*	20111. 20		4884. 11	4	20468. 86	$c\ ^3G_5 - t\ ^3G_5^\dagger$
4969. 13	7*w*	20118. 65		4882. 90	3*w*	20473. 93	
4968. 80	5*w*	20119. 99		4880. 04	22	20485. 93	$a\ ^3F_4 - y\ ^5H_5^\dagger$
4967. 97	5	20123. 34	$z\ ^5G_3^\dagger - f\ ^5G_3$	4878. 05	2	20494. 29	$z\ ^5I_8^\dagger - e\ ^5H_5$
4966. 80	25	20128. 09	$b\ ^3D_1 - w\ ^3P_0^\dagger$	4877. 293	7	20497. 47	
4966. 05	4*w*	20131. 13	$z\ ^5G_2^\dagger - f\ ^5G_2$	4875. 57	20	20504. 71	$z\ ^5I_8^\dagger - e\ ^5H_4$
4965. 82	3*w*	20132. 06	$z\ ^5G_3^\dagger - f\ ^5G_4$	4874. 653	20	20508. 56	$a\ ^3F_3 - y\ ^5H_4^\dagger$
4964. 92	100, *Z*	20135. 71	$a\ ^5S_2 - y\ ^7P_3^\dagger$	4872. 010	18	20519. 69	$a\ ^5G_4 - x\ ^5P_3^\dagger$

TABLE 1. *Wavelengths and term combinations of* Cr I—Continued

d, Dou[illegible]; *h*, hazy; *H*, very hazy; *l*, shaded longward; *s*, shaded shortward; *r*, reversed; *R*, strongly reversed; *w*, wide; *W*, very wide; *Z*, Zeeman pattern in table 2.

Wavelength λ_{air}	Intensity	Wave No.	Term combination
4870. 79	100, *Z*	20524. 84	$a\ ^2G_2 - z\ ^3H^0_4$
4869. 10	7*w*	20531. 96	
4868. 29	8	20535. 38	$a\ ^3H_5 - y\ ^5G^0_5$
4866. 60	10	20542. 51	
4865. 71	4*w*	20546. 26	$a\ ^3H_6 - y\ ^5G^0_6$
4865. 18	3*w*	20548. 50	
4863. 84	7	20554. 16	$z\ ^7F^0_2 - f\ ^7S_3$ $b\ ^1I_6 - z\ ^3K^0_6$
4861. 84	75, *Z*	20562. 62	$a\ ^5G_4 - y\ ^5F^0_3$
4861. 19	35	20565. 37	$a\ ^5G_3 - y\ ^5F^0_3$
4860. 37	7	20568. 83	$a\ ^5G_2 - y\ ^5F^0_3$
4859. 80	7	20571. 25	$b\ ^5D_3 - v\ ^5P^0_2$
4858. 83	4	20575. 35	$b\ ^5D_2 - v\ ^5P^0_2$
4857. 31	18	20581. 79	$a\ ^5P_1 - x\ ^5D^0_2$
4855. 150	15	20590. 95	$a\ ^5P_2 - x\ ^5D^0_2$
4851. 47	25	20606. 57	$b\ ^3G_4 - y\ ^3H^0_5$
4850. 96	7*w*	20608. 73	$d\ ^3F_4 - p\ ^5F^0_3$ $b\ ^3P_0 - v\ ^5D^0_1$
4850. 224	8	20611. 86	$b\ ^3P_1 - v\ ^5D^0_0$
4847. 197	18	20624. 74	$a\ ^3G_5 - y\ ^5H^0_5$ $a\ ^3F_2 - y\ ^5H^0_3$
4846. 44	18	20627. 96	$d\ ^3F_2 - p\ ^5F^0_3$ $a\ ^3F_3 - y\ ^3P^0_2$ $z\ ^3P^0_2 - g\ ^5D_2$
4846. 29	40	20628. 60	$b\ ^3G_5 - y\ ^3H^0_6$ $a\ ^3D_2 - x\ ^3D^0_3$
4845. 23	3	20633. 11	
4843. 073	6	20642. 30	$b\ ^1I_6 - z\ ^3K^0_5$
4841. 91	3	20647. 26	$a\ ^5F_1 - t\ ^5D^0_0$
4841. 734	12	20648. 01	$a\ ^5F_3 - t\ ^5D^0_2$ $a\ ^5F_2 - t\ ^5D^0_1$
4841. 14	4	20650. 54	$a\ ^5F_1 - t\ ^5D^0_1$
4840. 711	8	20652. 37	
4840. 37	10	20653. 83	$a\ ^5F_4 - t\ ^5D^0_3$
4839. 57	7	20657. 24	$a\ ^5F_3 - t\ ^5D^0_2$
4838. 88	6*w*	20660. 19	$d\ ^3F_4 - p\ ^5F^0_4$ $a\ ^5F_1 - t\ ^5D^0_1$ $z\ ^5D^0_4 - e\ ^5F_3$
4838. 418	15	20662. 16	$d\ ^3F_2 - t\ ^3F^0_2$
4837. 693	10	20665. 26	
4837. 19	8	20667. 41	$a\ ^5F_2 - t\ ^5D^0_2$
4836. 85	40	20668. 86	$a\ ^3G_5 - y\ ^5H^0_6$
4836. 36	10	20670. 95	$a\ ^5F_5 - t\ ^5D^0_4$
4835. 671	10	20673. 90	$a\ ^3D_3 - x\ ^3D^0_3$
4832. 75	4	20686. 35	$a\ ^5F_4 - t\ ^5D^0_4$
4831. 63	15	20691. 19	$b\ ^3G_3 - y\ ^3H^0_4$
4829. 35	100*w*	20700. 96	$a\ ^5G_5 - y\ ^5F^0_4$ $a\ ^5G_4 - y\ ^5F^0_3$
4828. 65	8	20703. 96	$a\ ^5G_3 - y\ ^5F^0_2$
4828. 21	3*w*	20705. 84	
4827. 44	2*w*	20709. 15	
4826. 84	5*w*	20711. 72	$z\ ^5D^0_3 - e\ ^5F_2$
4825. 50	10	20717. 47	$a\ ^3G_4 - y\ ^3H^0_4$
4825. 40	7	20717. 90	$d\ ^3F_2 - t\ ^3F^0_2$
4825. 02	2	20719. 53	
4823. 90	12, *Z*	20724. 34	$d\ ^3F_3 - t\ ^3F^0_3$
4822. 06	5	20732. 25	$a\ ^3G_3 - y\ ^3H^0_3$
4819. 30	4	20744. 12	$b\ ^3F_3 - v\ ^3G^0_3$
4818. 23	5*w*	20748. 73	
4817. 55	2	20751. 66	$b\ ^3P_2 - u\ ^5F^0_3$
4816. 39	10*w*	20756. 65	$z\ ^5D^0_4 - e\ ^5F_4$
4816. 13	25, *Z*	20757. 78	$d\ ^3F_4 - t\ ^3F^0_4$
4814. 25	35, *Z*	20765. 88	$a\ ^3G_4 - y\ ^3H^0_5$
4813. 96	5*w*	20767. 13	
4810. 71	35, *Z*	20781. 16	$a\ ^3G_3 - y\ ^3H^0_4$
4810. 58	3*w*, *Z*	20781. 72	
4810. 23	7	20783. 24	$d\ ^3F_3 - t\ ^3F^0_4$
4810. 01	10*w*	20784. 19	$a\ ^3D_2 - w\ ^5G^0_2$ $z\ ^3P^0_2 - e\ ^3D_2$
4809. 30	10	20787. 26	$a\ ^3D_1 - w\ ^5G^0_2$
4807. 14	3*w*	20796. 60	$z\ ^3P^0_2 - g\ ^5D_3$
4806. 25	25	20800. 45	$a\ ^5P_2 - x\ ^5D^0_3$
4805. 25	15*w*	20804. 77	$z\ ^5D^0_3 - e\ ^5F_3$
4804. 64	15	20807. 42	$a\ ^5P_3 - x\ ^5D^0_3$
4804. 23	4	20809. 19	$b\ ^5D_3 - v\ ^5P^0_3$
4803. 22	7*w*	20813. 57	$b\ ^5D_2 - v\ ^5P^0_3$
4803. 08	6	20814. 17	$b\ ^3F_4 - v\ ^3G^0_4$
4801. 02	75, *Z*	20823. 10	$a\ ^3F_4 - y\ ^3F^0_3$
4799. 19	8	20831. 04	$b\ ^5D_4 - v\ ^5P^0_3$
4798. 53	10	20833. 91	
4797. 68	15	20837. 60	$a\ ^3D_2 - w\ ^5G^0_3$
4797. 06	8	20840. 30	
4796. 84	12*w*	20841. 25	$z\ ^5D^0_2 - e\ ^5F_2$
4796. 145	40*w*	20844. 27	$z\ ^5D^0_4 - e\ ^5F_5$
4794. 42	8	20851. 77	
4792. 489	75, *Z*	20860. 18	$a\ ^3F_3 - y\ ^3F^0_2$
4791. 35	2*w*	20865. 13	
4790. 91	5	20867. 05	$b\ ^3F_3 - v\ ^3G^0_4$
4790. 32	20	20869. 62	$a\ ^5G_5 - y\ ^5F^0_5$ $a\ ^5G_4 - y\ ^5F^0_4$
4789. 324	75	20873. 96	$a\ ^5G_6 - y\ ^5F^0_5$
4787. 736	5	20880. 88	$a\ ^3F_4 - y\ ^3F^0_4$
4787. 302	3	20882. 77	$a\ ^3D_3 - w\ ^5G^0_3$
4786. 71	3*w*	20885. 36	
4783. 06	10*w*	20901. 30	$z\ ^5D^0_3 - e\ ^5F_4$
4782. 16	1	20905. 23	
4781. 65	2	20907. 46	$z\ ^3P^0_1 - e\ ^3D_1$
4779. 87	3	20915. 25	$b\ ^5D_1 - x\ ^5F^0_1$
4778. 514	2	20921. 18	$z\ ^3P^0_1 - g\ ^5D_2$ $b\ ^5D_3 - x\ ^5F^0_2$
4777. 73	4	20924. 61	$b\ ^5D_0 - x\ ^5F^0_1$
4777. 57	7	20925. 32	$b\ ^5D_2 - x\ ^5F^0_2$
4775. 99	1	20932. 23	$b\ ^3G_4 - 1^0_3$
4775. 54	10*w*	20934. 21	$c\ ^3G_5 - s\ ^3F^0_4$ $z\ ^5D^0_2 - e\ ^5F_3$
4775. 12	10	20936. 05	$a\ ^3D_3 - w\ ^5G^0_4$
4774. 55	8	20938. 55	$b\ ^5D_1 - x\ ^5F^0_2$
4772. 37	1	20948. 10	
4771. 59	10	20951. 53	$b\ ^5D_2 - x\ ^5F^0_3$
4770. 677	12	20955. 54	$b\ ^5D_2 - x\ ^5F^0_3$
4770. 34	4	20957. 03	$c\ ^3G_3 - s\ ^3F^0_2$
4769. 99	4*w*	20958. 56	$c\ ^3G_4 - s\ ^3F^0_3$ $z\ ^5D^0_0 - e\ ^5F_1$
4769. 79	4*w*	20959. 44	$z\ ^5D^0_1 - e\ ^5F_2$
4769. 67	2*w*	20959. 97	
4768. 56	4	20964. 85	$b\ ^3F_4 - v\ ^3G^0_5$ $b\ ^3G_3 - x\ ^3G^0_4$
4767. 86	30	20967. 93	$a\ ^3D_2 - x\ ^3F^0_3$
4767. 26	22	20970. 57	$a\ ^3D_3 - x\ ^3F^0_2$
4766. 63	35, *Z*	20973. 34	$a\ ^3D_1 - x\ ^3F^0_2$ $b\ ^5D_4 - x\ ^5F^0_3$
4764. 65	20	20982. 05	$b\ ^5D_3 - x\ ^5F^0_4$

TABLE 1. *Wavelengths and term combinations of* Cr I—Continued

d, Double; *h*, hazy; *H*, very hazy; *l*, shaded longward; *s*, shaded shortward; *r*, reversed; *R*, strongly reversed; *w*, wide; *W*, very wide; *Z*, Zeeman pattern in Table 2.

Wavelength λ_{air}	Intensity	Wave No.	Term combination
4764.28	50	20983.68	$a\ ^5D_0 - x\ ^5F_1^0$
4763.509	3	20987.08	$b\ ^3P_2 - t\ ^3F_1^0$
4761.73	5	20994.92	$b\ ^3P_2 - t\ ^3F_2^0$
4761.241	10	20997.07	$a\ ^3F_4 - y\ ^3D_3^0$
4759.90	10	21002.99	$a\ ^3F_3 - y\ ^3D_2^0$
4759.74	8	21003.70	$b\ ^5D_4 - x\ ^5F_4^0$
4757.58	18	21013.23	$a\ ^3D_3 - x\ ^3F_3^0$
4757.31	15	21014.42	$z\ ^3P_2^0 - e\ ^3D_3$
4756.98	1	21015.88	$a\ ^3D_2 - x\ ^3F_2^0$
4756.09	100, *Z*	21019.81	$a\ ^3G_5 - y\ ^3F_4^0$
4755.136	18	21024.03	$b\ ^5D_4 - x\ ^5F_3^0$
4754.73	20	21025.83	$a\ ^3F_2 - y\ ^3F_2^0$
4754.04	25, Mn?	21028.88	$b\ ^3P_2 - t\ ^5F_3^0$
4752.89	10	21033.97	$b\ ^3P_1 - t\ ^3F_1^0$
4752.066	50, *Z*	21037.62	$b\ ^1I_6 - z\ ^1I_6^0$
4751.04	5*w*	21042.16	$b\ ^3P_1 - t\ ^3F_2^0$; $z\ ^3P_0^0 - e\ ^3D_1$
4749.96	1*w*	21046.94	$b\ ^3P_0 - t\ ^3F_1^0$
4749.27	1*w*	21050.00	$b\ ^3P_1 - x\ ^3P_0^0$
4748.93	1	21051.51	$a\ ^5G_4 - y\ ^5D_3^0$
4747.63	3	21057.27	$c\ ^3D_2 - v\ ^3F_2^0$
4747.03	4	21059.93	$a\ ^3F_2 - y\ ^3F_1^0$
4746.63	1*w*	21061.71	
4745.31	30, *Z*	21067.56	$a\ ^5P_3 - x\ ^5D_4^0$
4745.20	12	21068.05	$a\ ^3F_3 - y\ ^5D_3^0$
4743.118	12*w*	21077.30	$z\ ^3P_1^0 - e\ ^3D_2$
4742.00	2*w*	21082.27	$b\ ^5G_4 - x\ ^5G_4^0$
4741.092	12	21086.31	$c\ ^3D_1 - v\ ^3F_2^0$
4737.33	75, *Z*	21103.06	$a\ ^5G_4 - y\ ^5F_4^0$
4736.60	2	21106.30	$a\ ^3H_6 - x\ ^5F_5^0$
4736.144	5	21108.34	$b\ ^3P_2 - x\ ^3P_1^0$
4734.596	4	21115.24	$b\ ^3H_4 - u\ ^3G_5^0$
4734.30	3	21116.56	
4732.55	2*w*	21124.37	$d\ ^3F_4 - t\ ^3G_5^0$; $b\ ^1I_6 - w^3H_5^0$
4731.19	4*w*	21130.44	$a\ ^3D_2 - t\ ^5P_1^0$
4730.69	50, *Z*	21132.67	$a\ ^3G_3 - y\ ^3F_2^0$
4729.84	8	21136.47	$a\ ^3F_2 - y\ ^3D_1^0$
4729.708	35, *Z*	21137.06	
4727.48	4*l*, *d*?	21147.03	$z\ ^5D_3^0 - g\ ^5D_2$
4727.13	40, *Z*	21148.59	$a\ ^3H_6 - z\ ^3H_6^0$
4725.94	7	21153.91	$a\ ^3H_6 - z\ ^3H_5^0$; $b\ ^3H_6 - u^3G_5^0$
4725.66	5	21155.16	$b\ ^3P_1 - x\ ^3P_1^0$
4724.40	35, *Z*	21160.81	$a\ ^5G_3 - y\ ^5F_4^0$
4723.88	1	21163.14	$b\ ^3H_4 - u\ ^3G_4^0$
4723.18	8	21166.27	$c\ ^3D_2 - v\ ^3F_2^0$
4723.06	15	21166.81	$a\ ^3G_3 - y\ ^3F_3^0$
4722.73	10	21168.29	$a\ ^3F_2 - y\ ^3D_2^0$; $b\ ^3P_0 - x\ ^3P_1^0$
4722.65	8	21168.65	$a\ ^3F_2 - y\ ^3D_2^0$
4722.14	3*w*	21170.93	$z\ ^5D_4^0 - g\ ^5D_3$
4721.14	8*w*	21175.42	$a\ ^5D_3 - t\ ^5P_3^0$
4718.79	7*w*	21185.96	$c\ ^3D_3 - u\ ^3F_4^0$
4718.43	75, *Z*	21187.58	$z\ ^7F_5^0 - f\ ^7D_5$
4717.674	10	21190.98	$a\ ^3F_4 - w^5D_4^0$
4713.99	10	21207.54	$b\ ^1I_6 - z\ ^1K_7^0$
4713.68	3	21208.93	$b\ ^1G_4 - q\ ^3F_4^0$
4710.24	6	21224.42	$a\ ^3G_3 - y\ ^3F_4^0$
4709.47	2	21227.89	
4708.02	60, *Z*	21234.43	$z\ ^7F_5^0 - f\ ^7D_4$
4707.73	15	21235.74	$b\ ^3P_2 - x\ ^3P_2^0$
4706.085	25	21243.16	$a\ ^3F_3 - w^5D_2^0$
4705.67	2	21245.03	$a\ ^3F_4 - w^5D_4^0$
4705.36	4	21246.43	
4703.28	1	21255.83	
4702.74	2	21258.27	$a\ ^5G_5 - y\ ^5D_4^0$
4701.92	5	21261,98	$a\ ^3F_3 - w^5D_3^0$; $b\ ^5D_3 - y\ ^5H_3^0$
4701.55	5	21263.65	
4700.595	40, *Z*	21267.97	$a\ ^5P_1 - z\ ^5S_2^0$
4699.585	25	21272.54	$c\ ^3D_3 - v\ ^3F_4^0$
4698.944	20	21275.44	$a\ ^3G_3 - y\ ^3D_2^0$
4698.61	50, *Z*	21276.95	$a\ ^3G_4 - y\ ^3D_3^0$; $a\ ^5P_2 - z\ ^5S_2^0$
4698.46	60, *Z*	21277.63	$z\ ^7F_4^0 - f\ ^7D_3$
4697.379	15	21282.53	$b\ ^3P_1 - x\ ^3P_2^0$
4697.038	40, *Z*	21284.08	$a\ ^5P_3 - z\ ^5S_2^0$
4695.142	30	21292.67	$a\ ^3H_5 - z\ ^3H_4^0$; $c\ ^3F_2 - p\ ^3F_2^0$
4694.733	3	21294.53	
4693.938	45, *Z*	21298.13	$a\ ^3H_5 - z\ ^3H_5^0$
4693.582	3	21299.75	
4692.967	10	21302.54	$a\ ^3H_5 - z\ ^3H_4^0$
4691.62	1	21308.65	
4690.15	6*w*	21315.34	$z\ ^5D_3^0 - g\ ^5D_3$
4689.382	65, *Z*	21318.83	$z\ ^7F_3^0 - f\ ^7D_2$
4686.20	15	21333.30	
4684.602	12	21340.58	$a\ ^3G_3 - y\ ^3D_3^0$
4680.864	35, *Z*	21357.62	$a\ ^3F_2 - w^5D_1^0$
4680.492	50	21359.32	$z\ ^7F_3^0 - f\ ^7D_3$
4677.62	4*w*	21372.52	$a\ ^3H_4 - x\ ^5F_3^0$
4676.85	2*w*	21375.95	
4676.30	8*w*	21378.46	$c\ ^3F_2 - p\ ^5F_3^0$
4675.80	2*w*	21380.75	$b\ ^5D_4 - y\ ^5H_5^0$
4675.03	4*w*	21384.27	$a\ ^3G_5 - w^5D_4^0$
4673.16	10*w*	21392.83	$z\ ^5D_4^0 - g\ ^5D_4$
4672.77	5*w*	21394.61	$z\ ^5D_1^0 - g\ ^5D_2$
4670.08	1	21406.94	$c\ ^3F_3 - t\ ^3F_2^0$
4669.67	10	21408.81	$a\ ^3F_2 - w^5D_2^0$
4669.34	50, *Z*	21410.33	$z\ ^7F_3^0 - f\ ^7D_5$
4667.894	2	21416.96	$c\ ^3D_2 - u\ ^3F_3^0$
4667.71	1	21417.81	$c\ ^3D_3 - u\ ^3F_3^0$
4667.170	30	21420.28	$a\ ^3H_4 - z\ ^3H_3^0$; $b\ ^5D_2 - y\ ^3P_1^0$; $a\ ^3D_2 - w^5D_1^0$
4666.508	55, *Z*	21423.32	$c\ ^3F_3 - p\ ^5F_4^0$; $z\ ^7F_4^0 - f\ ^7D_4$
4666.201	25, *Z*	21424.73	$a\ ^3H_4 - z\ ^3H_4^0$
4665.899	35	21426.12	$a\ ^3D_1 - w^5D_1^0$
4665.15	5*w*	21429.56	
4664.80	60	21431.16	$b\ ^5D_3 - y\ ^3P_2^0$; $z\ ^7F_5^0 - f\ ^7D_5$
4663.833	55	21435.61	$b\ ^5D_2 - y\ ^3P_2^0$; $z\ ^7F_3^0 - f\ ^7D_2$
4663.327	40	21437.94	$z\ ^7F_1^0 - f\ ^7D_1$
4662.42	2	21442.10	$b\ ^5D_0 - y\ ^3P_1^0$

TABLE 1. *Wavelengths and term combinations of* Cr I—Continued

d, Double; *h*, hazy; *H*, very hazy; *l*, shaded longward; *s*, shaded shortward; *r*, reversed; *R*, strongly reversed; *w*, wide; *W*, very wide; *Z*, Zeeman pattern in table 2

Wavelength λ_{air}	Intensity	Wave No.	Term combination
4661. 88	2*w*	21444. 59	$z\,^5D^0_2 - g\,^5D_3$
4661. 20	2	21447. 72	$b\,^5D_1 - y\,^3P^0_2$
4656. 822	10	21467. 88	$a\,^1H_5 - x\,^1H^0_5$
4656. 183	30	21470. 83	$a\,^3G_4 - w^5D^0_3$
4654. 76	35	21477. 39	$z\,^7F^0_6 - f\,^7D_1$
4654. 09	10*w*	21480. 48	
4652. 76	1	21486. 62	
4652. 155	100, *Z*	21489. 42	$a\,^5D_3 - y\,^5P^0_2$
4651. 285	75, *Z*	21493. 44	$a\,^5D_2 - y\,^5P^0_1$
4649. 446	45	21501. 94	$a\,^5G_4 - z\,^5H^0_5$ $a\,^3D_2 - w^3D^0_2$
4648. 856	35	21504. 67	$a\,^5G_3 - z\,^5H^0_4$ $a\,^3D_1 - w^3D^0_2$
4648. 33	2	21507. 10	$a\,^3H_6 - y\,^5H^0_5$
4648. 116	25	21508. 09	$a\,^5G_2 - z\,^5H^0_3$
4646. 803	20	21514. 17	$z\,^7F^0_1 - f\,^7D_2$
4646. 499	15	21515. 58	$a\,^3G_3 - w^5D^0_2$
4646. 151	100	21517. 19	$a\,^5D_4 - y\,^5P^0_3$
4643. 915	7	21527. 55	$a\,^3F_4 - w^5F^0_5$
4642. 413	3	21534. 51	$a\,^3G_3 - w^5D^0_3$
4641. 96	10	21536. 61	$a\,^3I_5 - y\,^3I^0_5$
4641. 69	4	21537. 87	$c\,^3D^2 - u\,^3F^0_2$
4641. 49	3	21538. 79	$z\,^5D^0_3 - g\,^5D_4$ $c\,^3D_2 - u\,^3F^0_2$
4640. 82	1	21541. 90	$c\,^3G_5 - t\,^3H^0_6$
4640. 68	1	21542. 55	$a\,^3I_6 - y\,^3I^0_7$
4640. 553	4	21543. 15	$a\,^3F_4 - w^5F^0_4$
4639. 695	25	21547. 13	$a\,^3D_3 - w^3D^0_2$
4639. 521	35, *Z*	21547. 94	$z\,^7F^0_3 - f\,^7D_3$
4637. 768	40	21556. 08	$a\,^5G_3 - z\,^5H^0_4$ $a\,^5G_4 - z\,^5H^0_4$
4637. 174	40	21558. 84	$a\,^5G_3 - z\,^5H^0_4$ $a\,^3H_5 - y\,^5H^0_4$
4635. 426	6	21566. 97	$c\,^3D_1 - u\,^3F^0_2$
4634. 585	5	21570. 89	$a\,^3F_3 - w^5F^0_2$
4633. 274	30	21576. 99	$z\,^7F^0_3 - f\,^7D_4$
4632. 165	35	21582. 16	$a\,^3D_2 - w^3D^0_3$ $a\,^3F_3 - w^5F^0_3$
4630. 439	5	21590. 20	$d\,^3F_4 - s\,^3F^0_4$
4628. 48	10	21599. 33	$z\,^7F^0_4 - f\,^7D_5$
4628. 24	1	21600. 46	
4627. 652	8	21603. 20	$x\,^5P^0_3 - f\,^5G_2$
4627. 351	7	21604. 61	$d\,^3F_2 - s\,^3F^0_2$
4626. 80	8	21607. 18	$a\,^3H_5 - y\,^5H^0_5$ $b\,^3G_4 - x\,^3D^0_3$
4626. 181	65, *Z*	21610. 08	$a\,^5D_1 - y\,^5P^0_1$
4625. 913	20, *Z*	21611. 32	$a\,^3I_6 - y\,^3I^0_6$
4625. 65	1	21612. 55	$a\,^3I_7 - y\,^3I^0_8$
4625. 295	3	21614. 22	$a\,^3F_3 - w^5F^0_4$
4624. 564	15, *Z*	21617. 62	
4622. 759	22	21626. 06	$a\,^3P_2 - y\,^3P^0_1$
4622. 466	35, *Z*	21627. 44	$a\,^3D_3 - w^3D^0_3$
4621. 924	45	21629. 97	$a\,^5G_5 - z\,^5H^0_5$ $a\,^5G_4 - z\,^5H^0_5$ $a\,^3I_7 - y\,^3I^0_8$
4621. 47	2	21632. 10	$a\,^3H_4 - y\,^5H^0_3$
4621. 112	4	21633. 77	
4621. 017	4	21634. 22	$a\,^5G_6 - z\,^5H^0_5$
4620. 40	2	21637. 11	$b\,^3G_5 - w^3G^0_4$
4619. 537	40, *Z*	21641. 15	$a\,^3P_2 - y\,^3P^0_2$
4617. 560	2	21650. 41	$d\,^3F_3 - s\,^3F^0_3$
4617. 37	2	21651. 30	$a\,^3H_5 - y\,^5H^0_6$
4616. 120	75, *Z*	21657. 17	$a\,^5D_2 - y\,^5P^0_2$
4614. 741	10	21663. 64	$x\,^5P^0_3 - f\,^5G_2$ $b\,^3P_1 - x\,^3D^0_1$
4614. 510	12	21664. 72	$a\,^3I_5 - 2^0_4$
4614. 148	12	21666. 42	$b\,^3G_4 - w^3G^0_3$ $a\,^3G_3 - w^5F^0_3$
4613. 36	60, *Z*	21670. 12	$a\,^5D_0 - y\,^5P^0_1$
4612. 62	1*w*	21673. 60	
4612. 20	1*w*	21675. 57	
4611. 964	15, *Z*	21676. 68	$b\,^3P_0 - x\,^3D^0_1$
4611. 056	4	21680. 95	$a\,^3H_4 - y\,^5H^0_4$
4609. 896	8	21686. 41	$b\,^3H_4 - t\,^3G^0_3$
4609. 64	2*w*	21687. 61	
4607. 50	1	21697. 68	$b\,^3F_4 - v\,^3H^0_4$
4607. 25	4	21698. 86	
4606. 92	1*w*	21700. 42	$b\,^5D_2 - y\,^3F^0_3$
4606. 364	15	21703. 04	$b\,^3H_5 - t\,^3G^0_4$
4605. 79	8*w*	21705. 74	$z\,^5P^0_1 - f\,^5D_1$
4604. 59	5*w*	21711. 40	$z\,^5P^0_2 - f\,^5D_1$
4604. 10	2	21713. 71	$b\,^3G_3 - x\,^3D^0_3$
4603. 84	2	21714. 94	$d\,^3F_4 - r\,^5D^0_4$
4603. 44	2	21716. 82	$b\,^3H_4 - t\,^3G^0_4$
4602. 867	7	21719. 53	$c\,^5D_3 - t\,^3F^0_3$
4602. 510	7	21721. 21	$b\,^3G_5 - w^3G^0_5$
4601. 14	10	21727. 68	$a\,^3F_4 - z\,^3G^0_4$
4601. 019	50	21728. 25	$a\,^5G_5 - z\,^5H^0_6$
4600. 745	75*r*, *Z*	21729. 54	$a\,^5D_3 - y\,^5P^0_3$
4600. 109	40, *Z*	21732. 55	$a\,^5G_6 - z\,^5H^0_6$
4599. 69	1*w*	21734. 53	
4599. 25	1	21736. 59	$a\,^3F_2 - w^5F^0_2$
4599. 003	8	21737. 77	$a\,^3F_2 - w^5F^0_1$
4598. 439	20	21740. 44	$a\,^3F_3 - z\,^3G^0_4$ $d\,^3F_3 - r\,^5D^0_4$
4596. 921	3	21747. 62	$a\,^3F_2 - w^5F_3$
4596. 388	6	21750. 14	$b\,^3F_3 - v\,^3H^0_4$ $b\,^3G_4 - w^3G^0_4$
4595. 599	45, *Z*	21753. 88	$b\,^1I_6 - y\,^1I^0_6$
4595. 04	5*w*	21756. 52	$x\,^5P^0_1 - f\,^5D_2$
4594. 408	8	21759. 51	
4593. 825	8*w*	21762. 28	$z\,^5P^0_2 - f\,^5D_2$
4592. 546	15	21768. 34	$b\,^3H_6 - t\,^3G^0_5$
4591. 405	60, *Z*	21773. 74	$b\,^3G_3 - w^3G^0_3$ $a\,^5D_1 - y\,^5P^0_2$
4590. 689	8	21777. 15	$b\,^5D_2 - y\,^3D^0_1$
4590. 48	4*w*	21778. 13	$z\,^3F^0_4 - e\,^3G_5$
4589. 03	5	21785. 01	
4587. 863	8	21790. 56	$b\,^5D_1 - v\,^3D^0_1$
4586. 990	8	21794. 71	$b\,^5D_1 - w^5D^0_0$
4586. 146	20, *Z*	21798. 71	$a\,^3F_3 - z\,^3G^0_3$
4585. 713	3	21800. 77	$b\,^3G_5 - w^5G^0_5$
4585. 096	18	21803. 71	$b\,^3G_5 - x\,^3F^0_4$
4584. 938	15	21804. 46	$b\,^3P_2 - x\,^3D^0_2$
4584. 76	12	21805. 31	$b\,^5D_3 - y\,^3D^0_2$
4584. 100	20	21808. 44	$a\,^3F_4 - z\,^3G^0_3$
4583. 898	15	21809. 41	$b\,^5D_2 - y\,^3D^0_2$
4583. 33	1	21812. 11	
4582. 40	6	21816. 53	$b\,^3F_4 - v\,^3H^0_5$

TABLE 1. *Wavelengths and term combinations of* Cr I—Continued

d, Double; *h*, hazy; *H*, very hazy; *l*, shaded longward; *s*, shaded shortward; *r*, reversed; *R*, strongly reversed; *w*, wide; *W*, very wide; *Z*, Zeeman pattern in Table 2.

Wavelength λ_{air}	Intensity	Wave No.	Term combination
4582. 04	2*w*	21818. 25	$b\,^3G_5 - w\,^5G_6^0$ $b\,^3H_5 - t\,^3G_5^0$
4581. 03	10	21823. 06	$a\,^3G_4 - w\,^5F_4^0$ $b\,^5D_1 - y\,^3D_2^0$
4580. 045	75, *Z*	21827. 75	$a\,^5S_2 - y\,^5P_1^0$
4579. 60	2	21829. 87	$a\,^3I_5 - x\,^3H_5^0$
4578. 326	12	21835. 95	$a\,^3I_6 - x\,^3H_5^0$
4576. 772	6	21843. 36	$a\,^3G_3 - w\,^5F_3^0$
4575. 112	25, *Z*	21851. 28	$b\,^3P_1 - x\,^3D_2^0$
4574. 456	6	21854. 42	$a\,^3G_3 - w\,^5F_3^0$
4574. 210	5*w*	21855. 64	
4573. 94	3	21856. 88	$b\,^3G_3 - w\,^3G_4^0$
4573. 38	1	21859. 56	$a\,^3I_5 - x\,^3H_6^0$
4572. 17	7*w*	21865. 34	$a\,^3I_6 - x\,^3H_6^0$ $z\,^5P_3^0 - f\,^5D_3$
4571. 83	12	21866. 97	$a\,^3I_7 - x\,^3H_6^0$ $a\,^3G_5 - z\,^3G_4^0$
4571. 673	40	21867. 72	$a\,^3G_6 - z\,^3H_5^0$
4571. 103	25	21870. 45	$b\,^5D_2 - y\,^3D_3^0$
4570. 988	20	21871. 00	$a\,^3F_4 - y\,^3G_5^0$
4570. 535	6	21873. 17	$a\,^3P_2 - y\,^3F_3^0$
4570. 34	6	21874. 10	$b\,^5D_2 - y\,^3D_3^0$ $z\,^5P_3^0 - f\,^5D_3$
4570. 23	1*w*	21874. 63	$b\,^5D_2 - y\,^3D_2^0$
4569. 63	30, *Z*	21877. 50	$a\,^3F_4 - y\,^3G_4^0$
4569. 53	20	21877. 98	$a\,^3F_4 - y\,^3G_5^0$
4567. 018	2	21890. 01	$a\,^1H_5 - v\,^3I_5^0$
4566. 598	7	21892. 02	$b\,^3D_4 - y\,^3D_3^0$
4565. 512	50, *Z*	21897. 23	$a\,^3D_2 - y\,^5P_3^0$
4564. 165	40, *Z*	21903. 69	$a\,^1H_5 - x\,^1I_6^0$
4563. 661	25	21906. 11	$a\,^3F_2 - z\,^3G_3^0$
4563. 426	7	21907. 24	$a\,^3P_2 - y\,^3F_3^0$
4563. 244	15	21908. 11	$a\,^3I_5 - x\,^3H_4^0$
4561. 51	10*w*	21916. 44	$b\,^3G_4 - x\,^3F_4^0$ $b\,^3F_2 - v\,^3D_1^0$
4561. 20	2	21917. 93	$a\,^5D_2 - x\,^5D_2^0$
4560. 51	1	21921. 25	$a\,^5G_2 - x\,^5D_2^0$
4560. 26	1	21922. 45	$b\,^3G_3 - w\,^5G_3^0$
4560. 01	1	21923. 65	$b\,^1I_6 - x\,^3I_5^0$
4558. 246	8	21932. 14	$b\,^3F_3 - v\,^3F_2^0$
4556. 179	40	21942. 09	$a\,^3F_3 - y\,^3G_3^0$
4555. 309	15	21946. 28	$b\,^3G_4 - x\,^3F_3^0$
4555. 088	15	21947. 34	$a\,^3G_5 - z\,^3G_5^0$
4554. 822	25	21948. 62	$a\,^3F_3 - y\,^3G_4^0$
4553. 95	18	21952. 83	$b\,^3F_2 - v\,^3F_2^0$
4552. 877	7	21958. 00	$z\,^3F_3^0 - e\,^3G_4$
4548. 652	3	21978. 40	$b\,^1I_6 - x\,^3I_6^0$
4548. 207	5	21980. 55	$a\,^3D_2 - u\,^5D_1^0$ $a\,^1I_6 - v\,^3G_5^0$
4547. 94	2	21981. 84	$a\,^3D_1 - u\,^5D_0^0$
4546. 53	1	21988. 65	$b\,^3F_4 - v\,^3F_3^0$ $b\,^3D_1 - r\,^5F_2^0$
4545. 946	100, *Z*	21991. 48	$a\,^5S_2 - y\,^5P_2^0$
4545. 335	25	21994. 43	$a\,^5G_2 - z\,^5G_2^0$
4544. 607	50	21997. 96	$a\,^5G_2 - z\,^5G_3^0$ $b\,^5D_2 - w\,^5D_1^0$
4543. 734	20	22002. 18	$a\,^3H_5 - y\,^3F_4^0$
4542. 64	35, *Z*	22007. 48	$a\,^3G_4 - z\,^3G_4^0$ $b\,^3F_3 - u\,^3F_3^0$
4541. 766	3	22011. 72	$b\,^5D_1 - w\,^5D_1^0$
4541. 506	25	22012. 98	$a\,^5G_3 - z\,^3G_3^0$
4541. 066	30	22015. 11	$a\,^5G_4 - z\,^5G_5^0$
4540. 84	10	22016. 21	$a\,^3P_2 - y\,^3D_3^0$ $a\,^3G_5 - y\,^3G_4^0$
4540. 715	50	22016. 81	$a\,^3G_5 - y\,^3G_5^0$
4540. 50	50	22017. 85	$a\,^5G_3 - z\,^5G_3^0$
4539. 787	30	22021. 32	$b\,^5D_0 - w\,^5D_1^0$ $a\,^5G_2 - z\,^5G_3^0$
4538. 76	3	22026. 30	
4537. 97	4	22030. 13	
4536. 542	4	22037. 06	$z\,^5P_3^0 - f\,^5D_4$
4536. 06	3*w*	22039. 41	
4535. 714	60	22041. 09	$b\,^3F_3 - v\,^3F_3^0$ $a\,^5G_3 - z\,^5G_4^0$ $a\,^5G_4 - z\,^5G_4^0$
4535. 14	35	22043. 88	$a\,^5G_3 - z\,^5G_4^0$
4534. 80	4	22045. 53	$b\,^5D_3 - w\,^5D_3^0$
4533. 24	2	22053. 12	$b\,^3G_3 - x\,^3F_3^0$
4532. 75	10	22055. 50	$b\,^3G_3 - x\,^3F_2^0$
4532. 71	2	22055. 69	$c\,^5D_2 - t\,^3G_3^0$
4531. 828	2	22059. 99	$b\,^3F_3 - u\,^3F_4^0$
4531. 62	1	22061. 00	
4531. 44	1	22061. 88	$b\,^3F_2 - v\,^3F_2^0$
4531. 236	5	22062. 87	$b\,^5D_1 - w\,^5D_2^0$
4530. 93	4	22064. 36	$b\,^5D_3 - w\,^5D_3^0$
4530. 72	100	22065. 38	$a\,^5G_5 - z\,^5G_5^0$ $a\,^5G_4 - z\,^5G_3^0$
4530. 48	4	22066. 55	$a\,^3H_4 - y\,^3F_3^0$
4529. 847	25	22069. 63	$b\,^5D_2 - w\,^5D_2^0$ $a\,^5G_6 - z\,^5G_5^0$
4529. 50	3	22071. 32	$a\,^3G_3 - z\,^3G_4^0$
4527. 452	30, *Z*	22081. 31	$a\,^3P_2 - y\,^3D_2^0$
4527. 335	40	22081. 88	$a\,^5G_5 - z\,^5G_6^0$
4526. 77	4*w*	22084. 63	
4526. 458	75, *Z*	22086. 15	$b\,^5D_4 - w\,^5D_3^0$ $a\,^5G_6 - z\,^5G_6^0$
4526. 090	40	22087. 95	$a\,^3G_4 - z\,^3G_5^0$ $b\,^3P_2 - x\,^3D_3^0$
4525. 29	2*wh*	22091. 83	$b\,^3F_3 - v\,^3D_3^0$
4524. 835	15	22094. 08	$b\,^3F_3 - v\,^3F_4^0$
4522. 019	12	22107. 84	$a\,^3F_2 - y\,^3G_3^0$
4521. 138	25, *Z*	22112. 14	$b\,^3F_2 - v\,^3D_2^0$ $b\,^1I_6 - u\,^3H_5^0$
4519. 833	7	22118. 53	$b\,^5D_2 - w\,^5D_4^0$
4519. 24	1*wh*	22121. 43	
4518. 633	6	22124. 40	$a\,^5G_4 - x\,^5D_4^0$ $a\,^3H_4 - y\,^3F_4^0$
4515. 435	25, *Z*	22140. 07	$b\,^5D_4 - w\,^5D_4^0$
4514. 53	40*wl*	22144. 51	$z\,^7P_4^0 - f\,^7S_3$
4514. 364	20	22145. 32	$b\,^1I_6 - u\,^3H_6^0$
4513. 88	3	22147. 70	$a\,^3F_2 - z\,^3S_1^0$
4513. 222	8	22150. 93	$d\,^3F_4 - t\,^3H_4^0$ $a\,^3G_4 - y\,^3G_5^0$
4513. 025	3	22151. 89	$c\,^3G_3 - r\,^3F_3^0$
4511. 90	60	22157. 42	$a\,^3G_4 - y\,^3G_4^0$ $a\,^3G_4 - y\,^3G_3^0$
4510. 015	15	22166. 68	$d\,^3F_2 - u\,^3D_1^0$

TABLE 1. *Wavelengths and term combinations of* Cr I—Continued

d. ible; *h*, hazy; *H*, very hazy; *l*, shaded longward; *s*, shaded shortward; *r*, reversed; *R*, strongly reversed; *w*, wide; *W*, very wide; *Z*, Zeeman pattern in table 2.

Wavelength λ_{air}	Intensity	Wave No.	Term combination
4508. 758	5	22172. 86	$c\ ^5G_4 - r\ ^3F_3^\circ$
4507. 94	4*w*	22176. 88	$d\ ^3F_4 - t\ ^3H_5^\circ$ $d\ ^3F_3 - t\ ^3H_4^\circ$ $a\ ^5F_2 - s\ ^5D_2^\circ$
4506. 844	30, *Z*	22182. 28	$b\ ^1I_6 - y\ ^1H_5^\circ$
4506. 08	2*wh*	22186. 03	$a\ ^5F_2 - s\ ^5D_2^\circ$
4505. 88	1*wh*	22187. 02	$z\ ^5G_4^\circ - e\ ^5H_4$
4505. 49	1	22188. 94	$a\ ^5F_1 - s\ ^5D_0^\circ$
4505. 22	1	22190. 27	$a\ ^3G_5 - x\ ^5G_5^\circ$
4504. 52	1*wh*	22193. 72	
4503. 91	2	22196. 72	$z\ ^5G_2^\circ - e\ ^5H_3$
4503. 04	12	22201. 01	$e\ ^5S_2 - x\ ^3S_1^\circ$
4502. 210	7	22205. 11	$a\ ^3P_2 - w^5D_1^\circ$
4501. 788	25	22207. 19	$a\ ^3P_1 - y\ ^3P_1^\circ$
4501. 65	10	22207. 87	$a\ ^3D_2 - w^3F_2^\circ$
4501. 10	35	22210. 58	$a\ ^3D_1 - w^3F_2^\circ$ $a\ ^3P_1 - y\ ^3P_0^\circ$
4500. 68	2*w*	22212. 66	$z\ ^5G_2^\circ - e\ ^5H_5$ $z\ ^5G_3^\circ - e\ ^5H_4$
4500. 29	40, *Z*	22214. 58	$a\ ^3G_3 - y\ ^3G_4^\circ$
4499. 256	5	22219. 69	$d\ ^3F_2 - t\ ^3D_2^\circ$ $a\ ^1I_6 - z\ ^3K_6^\circ$
4498. 727	35, *Z*	22222. 30	$a\ ^3P_1 - y\ ^3P_2^\circ$
4496. 85	100, *Z*	22231. 57	$a\ ^5S_2 - y\ ^5P_3^\circ$
4495. 685	2	22237. 34	$z\ ^5G_4^\circ - e\ ^5H_5$
4495. 282	12	22239. 33	$b\ ^3F_4 - u\ ^3F_3^\circ$
4495. 041	4	22240. 52	$a\ ^3H_4 - y\ ^3D_3^\circ$
4493. 41	2	22248. 59	
4492. 31	40, *Z*	22254. 04	$c\ ^3G_5 - r\ ^3F_4^\circ$ $b\ ^3P_2 - y\ ^3S_1^\circ$
4491. 858	35	22256. 28	$a\ ^3P_2 - w^5D_2^\circ$
4491. 687	30	22257. 13	$z\ ^7P_3^\circ - f\ ^7S_3$
4490. 55	8*wl*	22262. 76	$a\ ^5F_4 - s\ ^5D_3^\circ$
4489. 47	35	22268. 12	$a\ ^3D_2 - w^3F_3^\circ$ $a\ ^5P_1 - w^5P_1^\circ$
4488. 056	30, *Z*	22275. 14	$a\ ^3P_2 - w^5D_3^\circ$
4487. 85	2	22276. 16	$a\ ^5F_3 - s\ ^5D_3^\circ$
4487. 47	5*w*	22278. 05	$a\ ^5P_2 - w^5P_1^\circ$
4486. 38	1*w*	22283. 46	$b\ ^3H_5 - s\ ^3F_4^\circ$
4485. 68	1*w*	22286. 93	$z\ ^5F_4^\circ - e\ ^7G_5$
4484. 683	8	22291. 88	$a\ ^3G_3 - x\ ^5G_3^\circ$ $b\ ^3F_3 - u\ ^3F_3^\circ$
4484. 61	5	22292. 25	$a\ ^3G_4 - x\ ^5G_4^\circ$
4482. 88	40, *Z*	22300. 85	$b\ ^3P_1 - y\ ^3S_1^\circ$
4482. 73	1	22301. 60	$d\ ^3F_2 - u\ ^3D_2^\circ$
4481. 45	18	22307. 97	$a\ ^1I_6 - z\ ^3K_7^\circ$ $d\ ^3F_3 - u\ ^3D_3^\circ$
4480. 36	20	22313. 39	$a\ ^3D_3 - w\ ^3F_3^\circ$
4480. 27	30	22313. 84	$b\ ^3P_0 - y\ ^3S_1^\circ$
4478. 885	4	22320. 74	
4477. 99	4	22325. 20	
4477. 522	5	22327. 54	
4477. 05	35*w*	22329. 89	$a\ ^5P_1 - w\ ^5P_2^\circ$
4476. 131	7	22334. 48	$z\ ^5G_3^\circ - e\ ^5H_7$
4475. 36	50*w*	22338. 32	$a\ ^5P_2 - w\ ^5P_2^\circ$ $z\ ^7P_3^\circ - f\ ^7S_3$ $b\ ^3F_4 - v\ ^3D_3^\circ$
4473. 78	40	22346. 21	$a\ ^5P_3 - w\ ^5P_2^\circ$ $d\ ^3F_4 - t\ ^3D_3^\circ$
4470. 442	3	22362. 90	
4469. 84	3	22365. 91	$b\ ^3P_2 - t\ ^5P_1^\circ$
4469. 765	4	22366. 28	$a\ ^3H_5 - w\ ^5D_4^\circ$
4468. 65	4	22371. 86	$d\ ^3F_3 - t\ ^3D_3^\circ$
4468. 376	7	22373. 24	$b\ ^5D_3 - w\ ^5F_2^\circ$
4467. 567	30	22377. 28	$b\ ^5D_2 - w\ ^5F_2^\circ$
4467. 32	7	22378. 52	$b\ ^5D_2 - w\ ^5F_1^\circ$
4466. 17	25	22384. 28	$b\ ^5D_3 - w\ ^5F_3^\circ$ $a\ ^5G_3 - x\ ^5D_3^\circ$
4465. 367	35	22388. 31	$b\ ^5D_2 - w\ ^5F_3^\circ$
4465. 16	20	22389. 35	$a\ ^5F_3 - s\ ^5D_3^\circ$
4464. 925	25	22390. 53	$b\ ^5D_1 - w\ ^5F_2^\circ$ $b\ ^3F_3 - v\ ^3D_3^\circ$
4464. 66	25	22391. 86	$b\ ^5D_1 - w\ ^5F_1^\circ$
4462. 785	30	22401. 27	$b\ ^5D_0 - w\ ^5F_1^\circ$
4462. 09	2*w*	22404. 76	$a\ ^5F_4 - s\ ^5D_4^\circ$
4461. 315	7	22408. 65	$a\ ^3F_4 - z\ ^3I_5^\circ$
4460. 763	18	22411. 42	$a\ ^5P_1 - w\ ^5P_2^\circ$ $b\ ^3F_2 - v\ ^3D_3^\circ$
4459. 75	25	22416. 51	$b\ ^5D_3 - w\ ^5F_4^\circ$
4459. 37	18*w*	22418. 42	$a\ ^5F_3 - s\ ^5D_4^\circ$ $a\ ^5P_3 - w\ ^5P_3^\circ$
4458. 977	3	22420. 40	
4458. 537	45, *Z*	22422. 61	$a\ ^3D_3 - w\ ^3F_4^\circ$ $b\ ^3D_4 - w\ ^5F_5^\circ$
4456. 36	3	22433. 57	$b\ ^3F_2 - u\ ^3F_2^\circ$
4456. 19	3	22434. 42	$a\ ^3H_4 - w\ ^5D_3^\circ$
4455. 46	7	22438. 10	$b\ ^5D_4 - w\ ^5F_4^\circ$
4453. 93	1*wh*	22445. 80	
4453. 309	3	22448. 93	$z\ ^5H_7^\circ - e\ ^5H_6$
4451. 85	1	22456. 29	
4450. 28	4*w*	22464. 21	
4449. 995	4	22465. 65	
4449. 61	1	22467. 59	$a\ ^3F_4 - v\ ^5F_3^\circ$
4448. 07	2	22475. 37	
4447. 85	1	22476. 48	$b\ ^3P_1 - x\ ^3F_2^\circ$
4444. 00	1	22495. 96	$z\ ^7F_3^\circ - g\ ^7D_3$
4443. 719	30	22497. 38	$a\ ^3D_1 - w\ ^3P_0^\circ$
4443. 22	1*w*	22499. 92	
4442. 74	2*wh*	22502. 33	
4442. 277	30	22504. 68	$a\ ^3H_6 - w\ ^5F_5^\circ$
4441. 02	1	22511. 05	$a\ ^3F_4 - x\ ^5H_4^\circ$
4439. 34	4*wh*	22519. 57	$z\ ^5P_1^\circ - g\ ^5S_2$
4438. 23	5*wh*	22525. 20	$a\ ^5F_2 - v\ ^5F_2^\circ$ $z\ ^5P_2 - g\ ^5S_2$
4436. 96	5*wh*	22531. 65	
4436. 49	7*wh*	22534. 06	$a\ ^5F_3 - v\ ^5F_4^\circ$ $z\ ^5P_3^\circ - g\ ^5S_2$
4436. 44	7	22534. 29	$a\ ^5F_5 - v\ ^3G_4^\circ$
4434. 76	10	22542. 82	$b\ ^5D_3 - z\ ^3G_3^\circ$
4434. 474	8	22544. 28	$d\ ^3F_4 - u\ ^3D_3^\circ$ $c\ ^5D_1 - s\ ^3F_2^\circ$
4433. 969	20	22546. 85	$b\ ^5D_2 - z\ ^3G_3^\circ$
4433. 41	1	22549. 69	$z\ ^5H_6^\circ - e\ ^5H_5$ $a\ ^5F_4 - v\ ^3G_4^\circ$
4432. 772	15	22552. 93	$z\ ^5H_7^\circ - e\ ^5H_7$
4432. 16	40, *Z*	22556. 05	$a\ ^3P_0 - y\ ^3P_1^\circ$
4430. 480	30, *Z*	22564. 60	$a\ ^3D_2 - w\ ^3P_1^\circ$ $b\ ^5D_4 - z\ ^3G_5^\circ$
4430. 24	10*wh*	22565. 82	
4429. 932	20	22567. 40	$a\ ^3D_1 - w\ ^3P_1^\circ$
4429. 54	5*wh*	22569. 39	$a\ ^3P_1 - w\ ^5D_0^\circ$ $d\ ^3F_3 - u\ ^3D_3^\circ$
4428. 52	35	22574. 59	$b\ ^5D_3 - u\ ^5P_3^\circ$

TABLE 1. *Wavelengths and term combinations of* Cr I—Continued

d, Double; *h*, hazy; *H*, very hazy; *l*, shaded longward; *s*, shaded shortward; *r*, reversed; *R*, strongly reversed; *w*, wide; *W*, very wide; *Z*, Zeeman pattern in table 2

Wavelength λ_{air}	Intensity	Wave No.	Term combination
4427.709	10	22578.72	$b\ ^5D_2 - u\ ^5P^0_3$
4427.02	1	22582.24	$a\ ^3F_3 - x\ ^5H^0_4$
4426.653	8	22584.11	$a\ ^3P_2 - w\ ^5F^0_2$ $z\ ^5H^0_5 - e\ ^5H_6$
4425.61	2	22589.43	$b\ ^3P_2 - t\ ^5P^0_3$
4425.133	12	22591.87	$a\ ^3G_5 - z\ ^3I^0_6$
4424.293	40, *Z*	22596.15	$b\ ^5D_4 - u\ ^5P^0_3$
4424.099	10	22597.14	$a\ ^3P_1 - y\ ^3D^0_2$
4423.67	7*wh*	22599.33	$b\ ^3P_2 - y\ ^5S^0_2$
4423.325	12	22601.10	$b\ ^5D_3 - z\ ^3G^0_4$ $a\ ^3G_3 - v\ ^5F_4$
4422.97	8*w*	22602.91	
4422.697	10	22604.30	$a\ ^3D_2 - w\ ^3P^0_2$
4422.45	8*w*	22605.57	$a\ ^3G_5 - v\ ^5F^0_5$
4421.74	8*wh*	22609.20	
4420.963	10	22613.17	$z\ ^7F^0_2 - g\ ^7D_3$
4420.34	1	22616.36	$a\ ^3F_4 - x\ ^5H^0_5$
4420.117	2	22617.50	
4419.68	1	22619.73	
4419.107	10	22622.67	$b\ ^5D_4 - z\ ^3G^0_4$
4417.71	1	22629.83	$c\ ^5D_2 - g\ ^3F^0_3$
4417.24	1	22632.23	$z\ ^5H^0_4 - e\ ^5H_3$
4416.49	5	22636.07	
4414.47	8*w*	22646.44	$b\ ^3P_1 - y\ ^3S^0_1$ $c\ ^5D_2 - r\ ^5D^0_3$
4414.38	10*w*	22646.90	
4414.08	4	22648.43	$z\ ^5H^0_3 - e\ ^5H_3$
4413.86	40, *Z*	22649.56	$a\ ^3D_3 - w^3P^0_2$
4413.00	12	22653.98	$a\ ^1H_5 - s\ ^3H^0_4$
4412.56	2	22656.24	$c\ ^3D_2 - v\ ^3P^0_2$
4412.25	40	22657.83	$a\ ^5D_4 - z\ ^5F^0_5$
4411.105	40	22663.71	$b\ ^5D_3 - u\ ^5P^0_3$
4410.97	25, *Z*	22664.40	$a\ ^3H_5 - w^5F^0_4$
4410.306	40	22667.82	$b\ ^5D_2 - u\ ^5P^0_2$
4409.565	12	22671.62	$z\ ^5H^0_4 - e\ ^5H_4$
4407.70	40*d*	22681.22	$b\ ^5D_1 - u\ ^5P^0_2$ $a\ ^3F_2 - x\ ^5H^0_3$
4407.027	3	22684.68	$a\ ^5F_3 - v\ ^3G^0_3$
4406.67	20	22686.52	$z\ ^5H^0_3 - e\ ^5H_3$
4406.272	18	22688.57	$a\ ^3G_4 - z\ ^3I^0_5$ $z\ ^5H^0_6 - e\ ^5H_7$
4403.513	40	22702.79	$a\ ^1I_6 - z\ ^1I^0_5$
4403.377	35	22703.48	$b\ ^5D_4 - z\ ^3G^0_3$
4400.03	3*w*	22720.75	
4399.821	30	22721.83	$b\ ^5D_2 - u\ ^5P^0_1$
4399.04	2	22725.87	$z\ ^5H^0_3 - e\ ^5H_4$
4397.243	30	22735.16	$b\ ^5D_1 - u\ ^5P^0_1$
4396.16	2	22740.76	$b\ ^3G_5 - u\ ^5D^0_4$
4395.416	18	22744.61	$b\ ^5D_3 - y\ ^3G^0_3$ $b\ ^5D_0 - u\ ^5P^0_1$
4394.84	8	22747.59	$b\ ^5D_2 - x\ ^5G^0_2$
4394.67	2	22748.47	$b\ ^5D_2 - y\ ^3G^0_3$
4394.188	5	22750.96	$b\ ^5D_3 - y\ ^3G^0_4$
4393.536	12	22754.34	$a\ ^3H_4 - w^5F^0_3$
4393.369	5	22755.20	$a\ ^3G_5 - x\ ^5H^0_5$
4392.81	2*w*	22758.10	
4392.261	10	22760.94	$b\ ^5D_1 - x\ ^5G^0_2$
4391.755	40, *Z*	22763.56	$a\ ^5D_3 - z\ ^5F^0_3$
4391.43	1	22765.25	$b\ ^5D_4 - y\ ^3G^0_3$
4391.073	10	22767.10	
4390.82	1	22768.41	$a\ ^3F_3 - z\ ^5P^0_3$
4390.53	1	22769.92	$c\ ^5D_4 - s\ ^3F^0_4$
4390.07	2*d*	22772.30	$b\ ^5D_4 - y\ ^3G^0_4$ $b\ ^5D_4 - y\ ^3G^0_5$
4387.511	30, *Z*	22785.59	$a\ ^3H_6 - z\ ^3G^0_5$ $a\ ^3P_2 - u\ ^5P^0_3$
4387.38	20	22786.26	$a\ ^3P_1 - w^5D^0_1$
4386.945	5	22788.53	$b\ ^5D_2 - z\ ^3S^0_1$
4386.465	4	22791.02	$a\ ^3G_4 - x\ ^5H^0_4$
4385.30	2	22797.07	$a\ ^3F_4 - u\ ^5F^0_5$ $a\ ^3G_3 - v\ ^5F^0_3$
4384.974	75, *Z*	22798.77	$a\ ^5D_4 - z\ ^5F^0_4$
4384.373	8*d*?	22801.89	$b\ ^5D_1 - z\ ^3S^0_1$ $a\ ^3G_3 - v\ ^5F^0_4$
4383.96	2	22804.04	
4383.90	2	22804.35	$c\ ^5D_4 - s\ ^3F^0_3$
4382.86	20	22809.77	$a\ ^5P_1 - v\ ^5P^0_1$
4382.54	5, *Z*	22811.43	$b\ ^5D_0 - z\ ^3S^0_1$
4382.47	2	22811.79	$a\ ^3F_3 - u\ ^5F^0_2$
4381.113	35, *Z*	22818.86	$a\ ^5P_2 - v\ ^5P^0_1$
4380.793	4	22820.53	$b\ ^3H_6 - t\ ^3H^0_5$
4380.552	10	22821.78	$b\ ^5D_3 - x\ ^5G^0_3$
4380.05	1	22824.40	
4379.768	20	22825.87	$b\ ^5D_2 - x\ ^5G^0_3$
4378.321	10	22833.41	
4377.545	30, *Z*	22837.46	$a\ ^3P_1 - w^5D^0_2$
4376.803	25, *Z*	22841.33	$b\ ^3H_6 - t\ ^3H^0_6$
4375.338	30, *Z*	22848.98	$a\ ^3H_5 - z\ ^3G^0_4$
4374.166	40	22855.10	$a\ ^3H_6 - y\ ^3G^0_5$
4373.65	15, *Z*	22857.79	$b\ ^3H_4 - t\ ^3H^0_4$
4373.255	35, *Z*	22859.86	$a\ ^5D_2 - z\ ^5F^0_1$
4372.31	4	22864.80	$a\ ^3F_4 - t\ ^5F^0_4$ $d\ ^3F_3 - r\ ^3F^0_3$
4371.279	75	22870.19	$b\ ^3H_5 - t\ ^3H^0_5$ $a\ ^5D_3 - z\ ^5F^0_3$
4370.87	5	22872.33	$a\ ^3I_5 - v\ ^3G^0_4$
4370.76	5	22872.91	$a\ ^1I_6 - z\ ^1K^0_7$
4370.44	2	22874.58	$a\ ^3P_2 - u\ ^5P^0_2$
4369.624	1	22878.85	$b\ ^3P_2 - s\ ^3F^0_2$
4369.122	3	22881.48	$b\ ^3P_1 - s\ ^3F^0_2$
4368.903	8	22882.63	$b\ ^3P_2 - w^3D^0_1$
4368.647	2	22883.97	$b\ ^3H_4 - t\ ^3H^0_3$
4368.35	4	22885.52	
4368.254	20	22886.03	$b\ ^5D_3 - x\ ^5G^0_4$
4367.445	4	22890.27	
4367.307	2	22890.99	$b\ ^3H_3 - t\ ^3H^0_3$
4366.62	2	22894.59	$c\ ^5D_4 - r\ ^5D^0_4$
4366.327	4	22896.13	$a\ ^3G_4 - x\ ^5H^0_5$
4364.875	10	22903.74	$a\ ^3G_3 - x\ ^5H^0_4$
4364.136	10	22907.62	$b\ ^5D_4 - x\ ^5G^0_4$
4364.09	4*w*	22907.87	$a\ ^3F_3 - u\ ^5F^0_3$
4363.693	4	22909.95	$d\ ^3F_4 - r\ ^3F^0_4$
4363.132	30, *Z*	22912.90	$a\ ^3H_4 - z\ ^3G^0_3$
4362.97	7*w*	22913.75	$a\ ^3P_0 - y\ ^3D^0_1$
4362.08	3	22918.42	$b\ ^3D_3 - v\ ^3G^0_4$
4361.86	3	22919.58	
4361.45	3	22921.73	$z\ ^5P^0_2 - e\ ^5F_3$
4360.955	3	22924.33	$b\ ^3G_4 - u\ ^5D^0_3$
4359.984	20	22929.44	$a\ ^3H_5 - z\ ^3G^0_5$ $b\ ^3P_1 - w^3D^0_1$
4359.647	75, *Z*	22931.21	$a\ ^5D_4 - z\ ^5F^0_5$
4358.663	10	22936.39	$a\ ^3F_3 - t\ ^5F^0_4$
4358.57	2	22936.88	$a\ ^3F_2 - u\ ^5F^0_1$

TABLE 1. *Wavelengths and term combinations of* Cr I—Continued

ble; *h*, hazy; *H*, very hazy; *l*, shaded longward; *s*, shaded shortward; *r*, reversed; *R*, strongly reversed; *w*, wide; *W*, very wide; *Z*, Zeeman pattern in table 2.

Wavelength λ_{air}	Intensity	Wave No.	Term combination	Wavelength λ_{air}	Intensity	Wave No.	Term combination
4357. 508	15	22942. 47	$b\ ^3P_0 - w\ ^3D_1^\circ$	4312. 48	15	23182. 01	$a\ ^3F_3 - y\ ^3H_4^\circ$
4356. 766	20	22946. 38	$b\ ^5D_4 - x\ ^5G_5^\circ$	4311. 94	1	23184. 92	
4356. 56	3	22947. 46	$a\ ^3G_5 - u\ ^5F_5^\circ$	4310. 47	3	23192. 82	
4356. 285	8	22948. 91		4309. 73	8, *Z*	23196. 81	$c\ ^3D_2 - u\ ^3P_1^\circ$
4355. 28	4*w*	22954. 20	$a\ ^3P_2 - x\ ^5G_2^\circ$	4307. 67	2	23207. 90	$c\ ^3G_5 - x\ ^1I_6^\circ$
4353. 942	15	22961. 26	$b\ ^3P_2 - w\ ^3D_2^\circ$	4307. 487	10	23208. 89	$a\ ^3G_3 - t\ ^5F_4^\circ$
4353. 28	3*w*	22964. 75	$a\ ^5F_3 - q\ ^5F_3^\circ$	4305. 91	1	23217. 39	
4351. 77	100, *Z*	22972. 72	$a\ ^5D_4 - z\ ^5F_5^\circ$	4305. 468	30	23219. 79	$z\ ^7P_2^\circ - f\ ^7D_2$
4351. 055	75, *Z*	22976. 50	$a\ ^5D_1 - z\ ^5F_1^\circ$	4304. 737	3	23223. 71	$c\ ^3G_4 - s\ ^3G_5^\circ$ $b\ ^3D_2 - q\ ^5F_3^\circ$
4350. 00	1*w*	22982. 07		4304. 331	5	23225. 90	$c\ ^3D_1 - u\ ^3P_1^\circ$
4347. 491	8	22995. 33	$a\ ^3P_2 - z\ ^3S_1^\circ$	4302. 784	15	23234. 25	$c\ ^3G_5 - s\ ^3G_5^\circ$
4347. 13	1	22997. 24		4302. 12	5*w*	23237. 84	
4346. 829	30	22998. 83	$a\ ^3H_5 - y\ ^3G_5^\circ$ $a\ ^3H_5 - y\ ^3G_5^\circ$	4301. 185	25, *Z*	23242. 89	$b\ ^3G_5 - w\ ^3F_4^\circ$
4345. 808	7	23004. 24	$a\ ^3G_5 - t\ ^5F_4^\circ$	4300. 522	20, *Z*	23246. 47	$b\ ^3G_4 - w\ ^3F_3^\circ$
4345. 08	15	23008. 09	$b\ ^3P_1 - w\ ^3D_2^\circ$	4300. 28	1*w*	23247. 78	$c\ ^3D_1 - u\ ^3P_0^\circ$
4344. 51	100, *Z*	23011. 11	$a\ ^5D_3 - z\ ^5F_4^\circ$	4299. 97	12, *Z*	23249. 46	
4343. 17	18, *Z*	23018. 21	$a\ ^5P_1 - v\ ^5P_2^\circ$	4299. 92	4	23249. 73	$a\ ^3G_5 - y\ ^3H_4^\circ$
4342. 00	7	23024. 41		4299. 723	20	23250. 79	$z\ ^7P_3^\circ - f\ ^7D_3$
4341. 464	7	23027. 25	$a\ ^5P_2 - v\ ^5P_2^\circ$	4298. 048	10	23259. 86	$c\ ^3G_4 - s\ ^3G_4^\circ$
4341. 196	3	23028. 68	$a\ ^3I_6 - v\ ^3G_5^\circ$	4297. 753	30, *Z*	23261. 45	$a\ ^3I_5 - z\ ^3K_6^\circ$
4340. 14	18, *Z*	23034. 28	$a\ ^5P_3 - v\ ^5P_2^\circ$	4297. 064	20	23265. 18	$a\ ^5P_2 - v\ ^5P_3^\circ$
4339. 74	60, *Z*	23036. 40	$a\ ^5D_0 - z\ ^5F_1^\circ$	4296. 63	8	23267. 63	$a\ ^3I_6 - z\ ^3K_5^\circ$
4339. 45	75, *Z*	23037. 94	$a\ ^5D_2 - z\ ^5F_3^\circ$	4296. 296	8	23269. 34	$a\ ^3F_2 - t\ ^5F_1^\circ$
4338. 795	15	23041. 42	$b\ ^3P_2 - w\ ^3D_3^\circ$	4296. 11	2	23270. 35	$c\ ^3G_5 - s\ ^3G_4^\circ$
4338. 401	12	23043. 51		4295. 769	25, *Z*	23272. 22	$a\ ^3G_5 - y\ ^3H_5^\circ$ $a\ ^5P_3 - v\ ^5P_3^\circ$
4337. 566	75, *Z*	23047. 95	$a\ ^5D_1 - z\ ^5F_2^\circ$	4295. 43	2	23274. 03	$c\ ^3G_4 - s\ ^3G_3^\circ$
4337. 25	10*w*	23049. 63	$c\ ^3D_2 - u\ ^3G_3^\circ$	4294. 84	2	23277. 23	$a\ ^3F_2 - t\ ^5F_2^\circ$
4336. 55	1	23053. 35	$b\ ^3H_4 - t\ ^3D_3^\circ$	4294. 63	3	23278. 37	
4335. 78	1	23057. 44	$b\ ^3G_3 - u\ ^5D_2^\circ$	4293. 578	25	23284. 07	$z\ ^7P_4^\circ - f\ ^7D_4$
4335. 15	1*w*	23060. 79	$a\ ^5F_3 - r\ ^5F_4^\circ$	4293. 42	2	23284. 93	$c\ ^3D_2 - t\ ^3F_2^\circ$
4332. 574	15	23074. 51	$a\ ^3F_4 - t\ ^5F_3^\circ$	4291. 972	30, *Z*	23292. 78	$b\ ^3G_3 - w\ ^3F_2^\circ$
4332. 24	2	23076. 28	$z\ ^5P_3^\circ - e\ ^3F_4$	4289. 733	500, *Z*	23304. 94	$a\ ^7S_3 - z\ ^7P_2^\circ$
4332. 13	2	23076. 87	$a\ ^3G_4 - u\ ^5F_3^\circ$	4288. 404	6	23311. 97	$a\ ^3F_2 - t\ ^5F_1^\circ$
4330. 76	3	23084. 17	$a\ ^3G_3 - u\ ^5F_2^\circ$	4284. 909	10, *Z*	23331. 18	$b\ ^5D_2 - v\ ^5F_2^\circ$ $c\ ^5D_4 - t\ ^3H_4^\circ$
4328. 86	1	23094. 30	$b\ ^3F_3 - v\ ^5G_3^\circ$	4284. 728	25	23332. 16	$z\ ^7P_2^\circ - f\ ^7D_3$ $b\ ^5D_3 - v\ ^5F_3^\circ$
4328. 007	5	23098. 85	$c\ ^3D_3 - u\ ^3G_4^\circ$	4284. 00	3*w*	23336. 13	$b\ ^5D_3 - v\ ^5F_4^\circ$ $b\ ^5D_2 - v\ ^5F_3^\circ$
4327. 61	4*w*	23100. 97		4283. 17	1	23340. 65	$c\ ^3D_2 - t\ ^3F_3^\circ$
4325. 65	8	23111. 44	$a\ ^3F_3 - t\ ^5F_2^\circ$	4283. 004	4	23341. 55	$c\ ^3D_3 - t\ ^3F_3^\circ$
4325. 075	40, *Z*	23114. 50	$a\ ^3H_4 - y\ ^3G_4^\circ$	4282. 75	1	23342. 94	$b\ ^5D_1 - v\ ^5F_1^\circ$
4324. 642	10	23116. 82	$a\ ^3G_4 - u\ ^5F_4^\circ$	4281. 80	2	23348. 12	$a\ ^5F_5 - w\ ^3H_4^\circ$
4323. 847	3	23121. 07	$a\ ^3H_4 - y\ ^3G_4^\circ$ $a\ ^3H_4 - y\ ^3G_5^\circ$	4281. 04	3	23352. 26	$a\ ^3F_2 - x\ ^3P_2^\circ$ $b\ ^5D_0 - v\ ^5F_1^\circ$
4323. 521	30, *Z*	23122. 82		4280. 89	4*w*	23353. 05	$b\ ^3G_3 - w\ ^3F_3^\circ$
4321. 624	20	23132. 97	$a\ ^3F_4 - y\ ^3H_5^\circ$	4280. 65	3*w*	23354. 39	$a\ ^3G_4 - t\ ^5F_3^\circ$
4321. 248	20	21334. 98	$a\ ^3P_0 - w\ ^5D_1^\circ$	4280. 42	75, *Z*	23355. 64	$b\ ^5D_4 - v\ ^5F_3^\circ$ $a\ ^3I_6 - z\ ^3K_7^\circ$
4320. 608	30, *Z*	23138. 41	$z\ ^7P_4^\circ - f\ ^7D_3$ $z\ ^7P_3^\circ - f\ ^7D_2$	4280. 186	7	23356. 92	$b\ ^5D_4 - v\ ^5F_4^\circ$ $c\ ^5D_4 - t\ ^3H_5^\circ$ $a\ ^3I_7 - z\ ^3K_7^\circ$
4319. 659	40	23143. 49	$z\ ^7P_3^\circ - f\ ^7D_1$	4279. 55	2*h*	23360. 39	
4319. 308	7	23145. 37	$a\ ^3F_3 - t\ ^5F_3^\circ$ $a\ ^3G_4 - t\ ^5F_4^\circ$	4279. 17	1*h*	23362. 46	$b\ ^5D_4 - v\ ^5F_5^\circ$
4318. 615	4	23149. 08	$b\ ^3D_3 - q\ ^5F_4^\circ$ $b\ ^3F_3 - v\ ^3G_3^\circ$	4277. 80	2*h*	23369. 95	$a\ ^3I_5 - q\ ^5F_5^\circ$ $z\ ^5F_4^\circ - e\ ^5F_5$
4318. 05	3	23152. 11	$c\ ^3D_2 - u\ ^3P_2^\circ$	4275. 98	7*w*	23379. 90	$z\ ^5F_5^\circ - e\ ^5F_5$
4317. 914	15	23152 84	$c\ ^3D_3 - u\ ^3P_2^\circ$	4274. 806	750*R*	23386. 32	$a\ ^7S_3 - z\ ^7P_3^\circ$
4316. 88	1*wh*	23158. 39	$a\ ^5F_4 - r\ ^5F_5^\circ$				
4315. 62	5	23165. 15	$a\ ^3P_1 - w\ ^5F_2^\circ$				
4315. 405	5	23166. 30	$a\ ^3P_1 - w\ ^5F_1^\circ$ $b\ ^3F_4 - v\ ^5G_4^\circ$				
4313. 97	5*w*	23174. 01					
4312. 772	8	23180. 44	$a\ ^3G_3 - u\ ^5F_4^\circ$				

TABLE 1. *Wavelengths and term combinations of* Cr I—Continued

d, Double; *h*, hazy; *H*, very hazy; *l*, shaded longward; *s*, shaded shortward; *r*, reversed; *R*, strongly reversed; *w*, wide; *W*, very wide; *Z*, Zeeman pattern in table 2.

Wavelength λ_{air}	Intensity	Wave No.	Term combination
4274.01	2*w*	23390.72	$a\ ^5F_2-x\ ^5P^\circ_1$
			$a\ ^3G_4-y\ ^3H^\circ_4$
4273.64	2*w*	23392.70	
4272.93	50*w*	23396.58	$z\ ^7P^\circ_3-f\ ^7D_4$
4271.20	1*w*	23406.06	$b\ ^5D_4-x\ ^5H^\circ_4$
			$a\ ^5F_5-w^3H^\circ_5$
4271.073	30, *Z*	23406.75	$a\ ^3G_5-y\ ^3H^\circ_5$
4269.959	20	23412.86	$a\ ^3G_4-y\ ^3H^\circ_5$
4269.54	1*w*	23415.17	$b\ ^5D_3-w\ ^7P^\circ_4$
4269.02	5*h*	23418.01	$a\ ^3G_3-t\ ^5F^\circ_3$
			$z\ ^5F^\circ_3-e\ ^5F_2$
4268.794	10, *Z*	23419.25	$a\ ^1I_6-y\ ^1I^\circ_6$
4266.812	8	23430.13	$a\ ^3H_6-z\ ^3I^\circ_6$
4266.42	2*w*	23432.28	
4264.11	1*w*	23444.97	$a\ ^5P_3-x\ ^5F^\circ_4$
			$a\ ^5P_1-x\ ^5F^\circ_1$
4263.149	70, *Z*	23450.27	$a\ ^3I_7-z\ ^3K^\circ_8$
4262.372	12	23454.53	$a\ ^3G_3-y\ ^3H^\circ_4$
4262.129	22	23455.87	$a\ ^5P_1-u\ ^5P^\circ_2$
			$a\ ^3F_3-x\ ^3G^\circ_4$
4261.627	25	23458.64	$a\ ^3F_4-1^\circ_3$
4261.353	60	23460.15	$z\ ^7P^\circ_4-f\ ^7D_5$
4260.18	5*h*	23466.60	$z\ ^5F^\circ_4-e\ ^5F_4$
4259.136	10*w*	23472.36	$b\ ^5D_2-v\ ^5D^\circ_1$
4257.35	15*w*	23482.20	$b\ ^5D_2-v\ ^5D^\circ_2$
4256.63	8*w*	23486.17	$b\ ^5D_1-v\ ^5D^\circ_1$
			$b\ ^5D_2-v\ ^5D^\circ_2$
4255.501	30, *Z*	23492.41	$a\ ^3H_6-z\ ^3I^\circ_7$
4254.331	1000*R*, *Z*	23498.87	$a\ ^7S_3-z\ ^7P^\circ_4$
4252.235	20	23510.45	$b\ ^5D_3-v\ ^5D^\circ_3$
4251.50	1	23514.51	$b\ ^5D_2-v\ ^5D^\circ_3$
4251.38	3*w*	23515.18	$a\ ^3P_0-w^5F^\circ_1$
4250.17	3*h*	23521.87	
4249.68	4*w*	23524.59	$z\ ^5F^\circ_2-e\ ^5F_2$
			$a\ ^3G_5-x\ ^3G^\circ_4$
4248.73	6*w*	23529.84	$a\ ^3H_5-z\ ^3I^\circ_5$
4248.70	5*w*	23530.01	$a\ ^3F_3-1^\circ_3$
4248.34	12	23532.00	$b\ ^5D_4-v\ ^5D^\circ_3$
4245.66	2*w*	23546.86	$b\ ^3H_4-r\ ^3F^\circ_3$
4244.78	2*w*	23551.74	$b\ ^3F_2-v\ ^3P^\circ_2$
			$a\ ^5F_4-v\ ^3H^\circ_3$
4244.34	3*w*	23554.18	$c\ ^3F_4-r\ ^3F^\circ_3$
			$z\ ^5F^\circ_2-e\ ^5F_5$
4242.84	10	23562.51	$b\ ^5D_3-v\ ^5D^\circ_4$
4241.179	7	23571.74	
4240.714	50, *Z*	23574.32	$a\ ^3F_2-x\ ^3G^\circ_3$
			$a\ ^3H_5-z\ ^3I^\circ_6$
4240.33	2	23576.46	$a\ ^3P_1-z\ ^3S^\circ_1$
4238.96	40, *Z*	23584.08	$b\ ^5D_4-v\ ^5D^\circ_4$
4238.19	2	23588.36	
4237.72	15*w*	23590.97	$b\ ^5D_1-u\ ^5F^\circ_1$
4237.25	2	23593.60	$a\ ^3H_6-x\ ^5H^\circ_5$
4236.79	2*w*	23596.15	$z\ ^5F^\circ_1-e\ ^5F_2$
4235.99	25*w*	23600.61	$b\ ^5D_0-u\ ^5F^\circ_1$
4235.50	1	23603.34	$b\ ^3H_5-r\ ^3F^\circ_4$
			$c\ ^3F_3-r\ ^3F^\circ_3$
4234.78	2*w*	23607.35	$z\ ^5F^\circ_3-e\ ^5F_4$
4234.52	15	23608.80	$a\ ^3F_4-x\ ^3G^\circ_3$
4232.87	12*w*	23618.00	$b\ ^5D_2-u\ ^5F^\circ_2$
			$a\ ^3G_4-x\ ^3G^\circ_5$
4232.233	15, *Z*	23621.56	$c\ ^3D_2-t\ ^3G^\circ_3$
4231.65	3	23624.81	$c\ ^3F_4-r\ ^3F^\circ_4$
4231.515	1	23625.57	$y\ ^5F^\circ_3-e\ ^5H_3$
4231.335	18	23626.57	$c\ ^3G_4-s\ ^3H^\circ_5$
4231.03	5	23628.27	$a\ ^5F_2-w^3F^\circ_2$
4230.494	35, *Z*	23631.27	$b\ ^5D_1-u\ ^5F^\circ_2$
4230.29	5*w*	23632.41	$a\ ^3H_5-x\ ^5H^\circ_4$
4226.753	40, *Z*	23652.18	$a\ ^3H_4-z\ ^3I^\circ_5$
			$c\ ^3D_3-t\ ^3G^\circ_4$
4224.522	20, *Z*	23664.68	$a\ ^3G_4-x\ ^3G^\circ_5$
			$c\ ^3G_2-s\ ^3H^\circ_3$
4223.468	10	23670.58	$b\ ^5D_2-u\ ^5F^\circ_3$
4222.752	40*d*?	23674.60	$b\ ^5D_2-u\ ^5F^\circ_2$
4221.583	40, *Z*	23681.15	$a\ ^3I_5-w^3H^\circ_5$
			$a\ ^3G_3-x\ ^3G^\circ_3$
4220.46	8	23687.45	$a\ ^3H_4-x\ ^5H^\circ_3$
4219.61	3	23692.22	$b\ ^5D_4-u\ ^5F^\circ_3$
4219.03	1	23695.48	$a\ ^3F_2-1^\circ_2$
4217.65	50, *Z*	23703.23	$b\ ^5D_4-u\ ^5F^\circ_5$
4216.386	30	23710.33	$b\ ^5D_3-u\ ^5F^\circ_4$
4216.20	2*h*	23711.38	
4215.96	3*hs*	23712.73	
4215.62	2*w*	23714.64	
4215.31	1*w*	23716.39	$c\ ^3G_4-p\ ^3F^\circ_4$
4215.00	2*wh*	23718.14	$a\ ^5P_2-y\ ^5H^\circ_3$
4214.78	10*wh*	23719.37	
4214.19	1*w*	23722.69	$a\ ^5G_3-z\ ^5I^\circ_4$
4214.159	8	23722.86	$a\ ^5G_4-z\ ^5I^\circ_5$
4213.18	12	23728.37	$a\ ^3G_3-x\ ^3G^\circ_3$
4212.65	15*w*	23731.36	$b\ ^5D_4-u\ ^5F^\circ_4$
4211.48	22	23737.95	$a\ ^3H_5-x\ ^5H^\circ_5$
4211.34	40, *Z*	23738.74	$b\ ^5D_2-t\ ^5F^\circ_4$
			$a\ ^3G_4-1^\circ_3$
4210.76	18	23742.01	$a\ ^3H_6-x\ ^5H^\circ_4$
4210.42	3*ws*	23743.93	$a\ ^3I_5-w^3H^\circ_5$
4209.76	40, *Z*	23747.65	$a\ ^3G_5-x\ ^3G^\circ_5$
4209.37	60, *Z*	23749.85	$a\ ^3I_6-w^3H^\circ_5$
4209.21	4*w*	23750.76	$a\ ^1I_6-z\ ^1I^\circ_6$
4208.50	2	23754.77	$c\ ^3G_3-p\ ^3F^\circ_3$
			$a\ ^3H_4-x\ ^5H^\circ_4$
4208.36	40	23755.55	$a\ ^3I_5-v\ ^3H^\circ_4$
4208.10	4	23757.02	
4207.85	2*w*	23758.43	
4207.77	2*w*	23758.88	
4207.503	5	23760.39	$b\ ^5D_4-t\ ^5F^\circ_4$
4207.11	1	23762.61	
4206.909	40, *Z*	23763.75	$c\ ^3G_4-s\ ^3H^\circ_5$
4206.64	8	23765.27	
4206.22	2*w*	23768.21	
4205.68	1*w*	23770.70	
4205.04	8	23774.31	$a\ ^5P_3-y\ ^5H^\circ_4$
			$c\ ^3G_5-s\ ^3H^\circ_5$
4204.48	55, *Z*	23777.47	$a\ ^1I_6-u\ ^3H^\circ_5$
4204.20	30	23779.06	$a\ ^5G_2-y\ ^5G^\circ_2$
4203.59	50, *Z*	23782.51	$a\ ^5G_2-y\ ^5G^\circ_3$
4203.05	2*w*	23785.56	$a\ ^3H_6-u\ ^5F^\circ_5$
4200.10	35, *Z*	23802.27	$a\ ^3G_3-1^\circ_3$
4198.54	55	23811.12	$a\ ^3I_5-v\ ^3H^\circ_5$
			$a\ ^1I_6-u\ ^3H^\circ_6$
4198.02	2	23814.07	$a\ ^5F_5-w^3F^\circ_4$
4197.824	8	23815.18	
4197.45	10	23817.30	$a\ ^3I_6-v\ ^3H^\circ_6$
4197.24	50	23818.49	$a\ ^3I_7-v\ ^3H^\circ_6$
4195.59	2*w*	23827.86	

TABLE 1. *Wavelengths and term combinations of* Cr I—Continued

d, D...e; *h*, hazy; *H*, very hazy; *l*, shaded longward; *s*, shaded shortward; *r*, reversed; *R*, strongly reversed; *w*, wide; *W*, very wide; *Z*, Zeeman pattern in table 2.

Wavelength λ_{air}	Intensity	Wave No.	Term combination
4194. 96	55, *Z*	23831. 44	$a\ ^3I_5 - w\ ^3H_4^\circ$
4194. 331	25	23835. 01	
4193. 89	15	23837. 52	$a\ ^3I_6 - w\ ^3H_5^\circ$
4193. 662	60, *Z*	23838. 81	$a\ ^3I_7 - w\ ^3H_6^\circ$
4192. 558	12	23845. 09	
4192. 113	40, *Z*	23847. 56	$a\ ^1I_6 - y\ ^1H_5^\circ$
4191. 754	30	23849. 66	$a\ ^5G_4 - y\ ^5G_3^\circ$
4191. 274	50, *Z*	23852. 39	$a\ ^5G_3 - y\ ^5G_2^\circ$
4190. 664	15, *Z*	23855. 87	$a\ ^5G_2 - y\ ^5G_1^\circ$
4190. 15	40, *Z*	23858. 79	$a\ ^3P_0 - u\ ^5P_1^\circ$
4189. 965	18	23859. 85	$a\ ^3H_4 - x\ ^5H_5^\circ$
4186. 888	10	23877. 38	$a\ ^3P_1 - y\ ^3P_2^\circ$
4186. 59	7*w*	23879. 08	$c\ ^3G_4 - r\ ^3G_4^\circ$
4186. 358	45	23880. 41	$a\ ^3I_6 - v\ ^3H_5^\circ$ $z\ ^5F_4^\circ - g\ ^5D_3$
4185. 347	30	23886. 17	$a\ ^3H_5 - x\ ^5H_4^\circ$
4185. 04	12	23888. 13	
4184. 901	40	23888. 72	$a\ ^3G_4 - x\ ^3G_5^\circ$
4184. 662	20	23890. 08	$d\ ^3F_4 - s\ ^3G_5^\circ$
4183. 73	2*w*	23895. 40	
4183. 071	30	23899. 17	$a\ ^3F_2 - x\ ^3D_1^\circ$
4181. 645	10*w*	23907. 32	
4181. 54	4*h*	23907. 92	$b\ ^3D_1 - v\ ^3D_1^\circ$
4181. 34	3	23909. 06	
4180. 67	8*h*	23912. 90	
4180. 52	8*h*	23913. 75	$b\ ^5D_3 - t\ ^5F_2^\circ$
4179. 971	30	23916. 90	$c\ ^3G_4 - r\ ^3G_5^\circ$
4179. 78	2	23917. 99	$b\ ^5D_2 - t\ ^5F_2^\circ$
4179. 42	20	23920. 05	$b\ ^3F_4 - u\ ^3G_4^\circ$
4179. 27	70, *Z*	23920. 91	$a\ ^3F_3 - x\ ^3D_2^\circ$ $a\ ^3I_6 - z\ ^1K_7^\circ$
4179. 047	18	23922. 18	$a\ ^3I_7 - z\ ^1K_8^\circ$ $b\ ^3H_5 - w\ ^3I_5^\circ$
4178. 78	4*w*	23923. 71	$b\ ^5D_1 - t\ ^5F_1^\circ$
4178. 52	4*w*	23925. 20	$b\ ^3F_3 - u\ ^3G_3^\circ$ $a\ ^3P_0 - z\ ^3S_1^\circ$
4178. 36	2	23926. 12	$d\ ^3F_4 - s\ ^3G_4^\circ$
4178. 07	25*w*	23927. 78	$c\ ^3G_5 - r\ ^3G_5^\circ$ $b\ ^3D_2 - v\ ^3D_1^\circ$
4177. 84	50*h*	23928. 81	$z\ ^5F_3^\circ - g\ ^5D_4$
4177. 46	4	23931. 27	$b\ ^5D_1 - t\ ^5F_2^\circ$
4177. 166	4	23932. 96	$b\ ^5D_0 - t\ ^5F_1^\circ$
4176. 68	25	23935. 74	$b\ ^3H_4 - w\ ^3I_5^\circ$
4175. 958	40, *Z*	23939. 87	$a\ ^3H_6 - x\ ^5H_7^\circ$
4175. 235	35	23944. 02	$b\ ^3D_1 - v\ ^3F_2^\circ$
4174. 96	25	23945. 60	$b\ ^3F_2 - u\ ^3G_3^\circ$ $z\ ^5F_2^\circ - e\ ^3D_1$
4174. 808	75	23946. 47	
4174. 336	8	23949. 18	
4174. 159	7	23950. 19	$b\ ^3H_6 - w\ ^3I_6^\circ$
4173. 98	4	23951. 22	
4173. 877	7	23951. 84	$b\ ^5D_2 - t\ ^5F_3^\circ$ $d\ ^3F_3 - s\ ^3G_4^\circ$
4172. 782	50, *Z*	23958. 09	$a\ ^1G_4 - y\ ^1H_5^\circ$ $c\ ^3G_5 - s\ ^3H_6^\circ$
4172. 517	10*w*	23959. 62	$d\ ^3F_2 - s\ ^3G_3^\circ$ $z\ ^5F_3^\circ - g\ ^5D_2$
4171. 676	40	23964. 45	$b\ ^3D_2 - v\ ^3F_3^\circ$
4170. 75	4*w*	23969. 77	$b\ ^5D_4 - t\ ^5F_3^\circ$
4170. 214	50, *Z*	23972. 85	$b\ ^3F_3 - u\ ^3G_4^\circ$
4169. 841	65, *Z*	23974. 99	$b\ ^3F_4 - u\ ^3G_5^\circ$
4168. 309	8	23983. 81	$b\ ^3D_3 - v\ ^3F_3^\circ$
4168. 12	2	23984. 89	$b\ ^5D_3 - y\ ^3H_4^\circ$
4167. 811	12	23986. 67	$a\ ^3H_5 - t\ ^5F_4^\circ$
4166. 44	1*h*	23994. 56	$a\ ^5G_6 - z\ ^5I_7^\circ$
4165. 52	60, *Z*	23999. 86	$b\ ^3H_5 - w\ ^3I_6^\circ$
4163. 91	7*w*	24009. 14	$z\ ^5F_5^\circ - e\ ^3D_2$
4163. 627	75, *Z*	24010. 77	$a\ ^5G_5 - y\ ^5G_4^\circ$ $a\ ^5G_4 - y\ ^5G_3^\circ$
4163. 15	4	24013. 52	$a\ ^5G_3 - y\ ^5G_2^\circ$
4162. 48	4*h*	24017. 39	$z\ ^5F_1^\circ - e\ ^3D_1$
4161. 78	7*h*	24021. 43	$z\ ^5F_3^\circ - g\ ^5D_3$
4161. 43	55, *Z*	24023. 45	$b\ ^3P_2 - w\ ^3P_1^\circ$ $b\ ^3H_6 - w\ ^3I_7^\circ$
4160. 82	2	24026. 97	$b\ ^3F_2 - u\ ^3P_2^\circ$
4160. 61	4*w*	24028. 18	$b\ ^5D_4 - y\ ^3H_5^\circ$
4160. 03	1*w*	24031. 54	$b\ ^5D_2 - x\ ^3P_1^\circ$
4158. 89	15*w*	24038. 12	$d\ ^3F_4 - s\ ^3D_3^\circ$
4157. 25	2*w*	24047. 61	$b\ ^3F_2 - u\ ^3P_2^\circ$
4154. 99	4*w*	24061. 27	
4154. 17	2	24065. 43	$a\ ^3I_5 - u\ ^3F_4^\circ$
4153. 812	60	24067. 51	$a\ ^5G_5 - y\ ^5G_5^\circ$ $a\ ^5G_4 - y\ ^5G_5^\circ$
4153. 072	30	24071. 80	$a\ ^5G_6 - y\ ^5G_5^\circ$
4152. 779	40, *Z*	24073. 50	$b\ ^3D_2 - v\ ^3F_2^\circ$
4152. 05	5*w*	24077. 72	$d\ ^3F_3 - s\ ^3D_2^\circ$
4151. 575	15*w*	24080. 48	$a\ ^3H_4 - u\ ^5F_4^\circ$
4151. 02	6*w*	24083. 70	$b\ ^3P_0 - w\ ^3P_1^\circ$ $b\ ^3D_3 - v\ ^3F_2^\circ$
4150. 81	5*wh*	24084. 92	
4150. 48	2	24086. 83	$a\ ^3F_2 - x\ ^3D_2^\circ$
4149. 453	30	24092. 79	$b\ ^3D_3 - v\ ^3F_3^\circ$
4148. 49	8*w*	24098. 38	$z\ ^5F_4^\circ - e\ ^3D_2$
4147. 74	8*h*	24102. 74	$z\ ^5F_4^\circ - g\ ^5D_4$
4147. 55	4*h*	24103. 85	$b\ ^3D_1 - v\ ^3D_2^\circ$
4146. 695	45	24108. 82	$a\ ^3H_4 - t\ ^5F_4^\circ$
4146. 467	20	24110. 14	$b\ ^3P_1 - w\ ^3P_2^\circ$ $a\ ^3H_6 - y\ ^3H_5^\circ$
4146. 206	40	24111. 66	$b\ ^3D_3 - u\ ^3F_4^\circ$
4145. 49	5*w*	24115. 82	$z\ ^5F_2^\circ - e\ ^3D_2$
4145. 01	3	24118. 62	$a\ ^3P_2 - y\ ^3F_2^\circ$
4144. 55	5	24121. 29	$b\ ^3H_5 - x\ ^1H_5^\circ$
4142. 46	22	24133. 46	$a\ ^3F_4 - x\ ^3D_3^\circ$
4142. 192	45, *Z*	24135. 03	$b\ ^3H_4 - x\ ^1H_5^\circ$
4140. 71	5*wh*	24143. 66	$b\ ^3D_3 - v\ ^3D_2^\circ$
4139. 47	4*wh*	24150. 90	
4139. 28	8*w*	24152. 01	$a\ ^3I_5 - v\ ^3F_4^\circ$
4139. 18	7*w*	24152. 59	$a\ ^5P_2 - y\ ^3F_2^\circ$
4139. 07	7*whs*	24153. 23	
4137. 95	3*w*	24159. 77	$a\ ^5P_3 - y\ ^3F_3^\circ$
4137. 92	10, *Z*	24159. 94	$b\ ^3F_3 - t\ ^3F_2^\circ$
4137. 374	10	24163. 13	$b\ ^3F_4 - t\ ^3F_3^\circ$
4135. 84	3	24172. 09	$b\ ^5D_1 - x\ ^3P_2^\circ$
4135. 05	3*w*	24176. 71	$b\ ^3F_2 - p\ ^5F_4^\circ$
4134. 387	35, *Z*	24180. 59	$b\ ^3F_2 - t\ ^3F_2^\circ$
4132. 17	2*w*	24193. 56	$a\ ^3F_4 - w\ ^3G_5^\circ$ $a\ ^3G_3 - x\ ^3D_2^\circ$
4131. 98	3*w*	24194. 68	
4131. 36	50, *Z*	24198. 31	$b\ ^3D_2 - v\ ^3F_4^\circ$
4130. 50	3*w*	24203. 34	$z\ ^7P_4^\circ - g\ ^7D_3$

TABLE 1. *Wavelengths and term combinations of* Cr I—Continued

d, Double; *h*, hazy; *H*, very hazy; *l*, shaded longward; *s*, shaded shortward; *r*, reversed; *R*, strongly reversed; *w*, wide; *W*, very wide; *Z*, Zeeman pattern in Table 2.

Wavelength λ_{air}	Intensity	Wave No.	Term combination
4130. 10	15*w*	24205. 68	$a\ ^3F_3 - x\ ^3D_3^0$
			$z\ ^7P_4^0 - g\ ^7D_4$
4129. 90	1	24206. 86	$z\ ^7P_4^0 - g\ ^7D_5$
4129. 20	50*WH*, *Z*	24210. 96	$b\ ^5D_3 - x\ ^3G_3^0$
4128. 392	35, *Z*	24215. 71	$b\ ^3F_3 - t\ ^3F_3^0$
4128. 08	5*w*	24217. 53	$a\ ^5P_3 - y\ ^3F_4^0$
4127. 639	40	24220. 12	$a\ ^5P_1 - y\ ^3D_1^0$
4127. 297	40	24222. 13	$b\ ^3F_4 - t\ ^3F_4^0$
			$a\ ^5G_5 - y\ ^5G_6$
4126. 920	30	24224. 34	$a\ ^5P_1 - w^3D_2^0$
			$a\ ^1H_5 - r\ ^3H_4^0$
4126. 513	75, *Z*	24226. 73	$a\ ^5G_6 - y\ ^5G_6^0$
4126. 092	25	24229. 20	$a\ ^5P_2 - y\ ^3D_1^0$
4125. 56	10*w*	24232. 32	$a\ ^3H_5 - y\ ^3H_4^0$
4125. 44	15*w*, *Z*	24232. 93	$b\ ^5D_4 - x\ ^3G_3^0$
			$c\ ^3D_3 - s\ ^3F_2^0$
4124. 57	3*w*	24238. 14	$a\ ^3P_2 - x\ ^3P_1^0$
4124. 35	2*w*	24239. 44	$z\ ^5F_3^0 - e\ ^3D_3$
			$z\ ^5P_3^0 - h\ ^5S_2$
4123. 85	2*w*	24242. 37	
4123. 386	50, *Z*	24245. 10	$a\ ^3H_6 - y\ ^3H_6^0$
4122. 87	4*h*	24248. 13	$z\ ^5P_3^0 - h\ ^5S_2$
			$b\ ^3G_3 - t\ ^5D_3^0$
4122. 164	25, *Z*	24252. 28	$a\ ^5P_1 - y\ ^3D_2^0$
4121. 815	45, *Z*	24254. 34	$a\ ^3H_5 - y\ ^3H_5^0$
4121. 487	7*w*	24256. 27	$c\ ^3D_1 - s\ ^3F_2^0$
4121. 261	30, *Z*	24257. 60	
4120. 621	50	24261. 37	$a\ ^5P_2 - y\ ^3D_3^0$
4120. 11	4*w*	24264. 38	$a\ ^3F_3 - w^3G_3^0$
4119. 69	6*w*	24266. 85	$c\ ^3D_2 - s\ ^3F_3^0$
4119. 54	1	24267. 73	$c\ ^3D_3 - s\ ^3F_3^0$
4119. 42	6	24268. 44	$a\ ^5P_3 - y\ ^3D_3^0$
4118. 99	4*whl*	24270. 97	
4118. 05	4	24276. 51	$a\ ^3F_4 - w^3G_4^0$
4116. 52	2*hl*	24285. 54	
4116. 46	4*w*	24285. 89	
4115. 32	15*w*	24292. 62	$d\ ^3F_4 - s\ ^3H_4^0$
			$a\ ^1H_5 - r\ ^3H_5^0$
4111. 60	4*w*	24314. 60	$z\ ^7P_3^0 - g\ ^7D_2$
4111. 33	4*w*	24316. 19	$z\ ^7P_3^0 - g\ ^7D_3$
4110. 95	15*w*	24318. 24	$z\ ^7P_3^0 - g\ ^7D_4$
			$d\ ^3F_3 - s\ ^3H_4^0$
			$a\ ^3H_4 - t\ ^3F_3^0$
4109. 95	3*w*	24324. 36	$b\ ^3D_2 - u\ ^3F_3^0$
4109. 58	40	24326. 55	$a\ ^5P_2 - y\ ^3D_2^0$
4108. 396	25	24333. 56	$a\ ^5P_3 - y\ ^3D_3^0$
4106. 69	4	24343. 66	$b\ ^3D_3 - u\ ^3F_3^0$
4106. 033	20	24347. 54	$a\ ^3F_2 - w^3G_3^0$
4104. 864	50, *Z*	24354. 50	$a\ ^3H_6 - y\ ^3H_5^0$
			$a\ ^5G_2 - v\ ^5P_2^0$
4104. 29	4*w*	24357. 90	$c\ ^3D_2 - r\ ^5D_3^0$
			$a\ ^5G_2 - v\ ^5P_2^0$
4103. 835	30, *Z*	24360. 60	$a\ ^3F_4 - w^3G_3^0$
			$a\ ^3F_3 - w^3G_2^0$
4103. 02	4	24365. 44	$a\ ^3P_2 - x\ ^3P_2^0$
			$a\ ^1H_5 - r\ ^3H_6^0$
4102. 22	3	24370. 19	$a\ ^3F_2 - x\ ^3D_2^0$
4101. 163	35	24376. 48	$a\ ^3H_4 - y\ ^3H_4^0$
4099. 82	15*w*	24384. 46	
4099. 44	8*w*	24386. 72	
4099. 02	30	24389. 22	$a\ ^3H_5 - y\ ^3H_6^0$
4098. 02	8*w*	24395. 17	$z\ ^7P_2^0 - g\ ^7D_1$
4097. 89	20*WH*	24395. 94	$a\ ^3F_4 - w^5G_4^0$
			$z\ ^7P_2^0 - g\ ^7D_2$
4097. 69	2*w*	24397. 13	$z\ ^7P_2^0 - g\ ^7D_3$
4096. 04	2*w*	24406. 96	
4094. 963	15	24413. 38	$a\ ^3F_3 - w^3G_3^0$
			$a\ ^3G_4 - x\ ^3D_3^0$
4094. 62	3	24415. 43	$a\ ^3G_5 - w^3G_4^0$
			$b\ ^3G_3 - t\ ^5D_3^0$
4093. 31	7*h*	24423. 24	$b\ ^3D_2 - v\ ^3D_3^0$
4093. 059	18	24424. 74	$b\ ^3D_3 - u\ ^3F_3^0$
4092. 178	30, *Z*	24430. 00	$a\ ^3F_2 - w^3G_3^0$
			$d\ ^3F_4 - s\ ^3H_5^0$
4090. 47	10	24440. 20	$a\ ^3F_4 - w^5G_5^0$
4090. 35	7	24440. 91	
4090. 305	30, *Z*	24441. 18	$a\ ^5P_1 - w^5D_1^0$
4090. 07	8*hs*	24442. 59	$b\ ^3D_3 - v\ ^3D_3^0$
			$a\ ^3F_4 - x\ ^3F_4^0$
4089. 627	12	24445. 23	$c\ ^3F_2 - q\ ^3F_2^0$
			$b\ ^3D_2 - u\ ^3F_2^0$
4088. 766	12	24450. 39	$a\ ^5P_2 - w^5D_1^0$
4087. 90	1	24455. 56	$b\ ^3H_4 - q\ ^3F_3^0$
4087. 58	1	24457. 47	
4086. 941	15	24461. 30	$a\ ^3I_5 - y\ ^1I_6^0$
4086. 05	6	24466. 63	$a\ ^3F_3 - w^5G_4^0$
4085. 932	15	24467. 34	$a\ ^3I_6 - y\ ^1I_6^0$
4085. 71	6	24468. 67	$a\ ^3I_7 - y\ ^1I_6^0$
4085. 03	25	24472. 74	$a\ ^3F_4 - x\ ^3F_3^0$
4084. 30	3	24477. 11	$a\ ^3G_3 - x\ ^3D_3^0$
4083. 43	3	24482. 33	
4083. 32	10	24482. 99	$b\ ^3H_5 - q\ ^3F_4^0$
4081. 896	22	24491. 54	
4081. 738	35	24492. 48	$a\ ^5P_1 - w^5D_2^0$
4080. 564	10	24499. 53	$a\ ^3G_5 - w^3G_5^0$
4080. 229	40	24501. 54	$a\ ^5P_2 - w^5D_2^0$
4079. 70	3*w*	24504. 71	$c\ ^3F_4 - q\ ^3F_4^0$
4079. 04	3	24508. 68	$a\ ^5P_3 - w^5D_3^0$
4078. 475	4	24512. 07	$c\ ^3F_2 - q\ ^3F_3^0$
4078. 095	2	24514. 36	$a\ ^3F_3 - x\ ^3F_3^0$
			$a\ ^5F_5 - u\ ^3H_6^0$
4077. 679	60, *Z*	24516. 86	$b\ ^3F_2 - t\ ^3G_3^0$
4077. 467	10	24518. 14	$c\ ^3F_2 - q\ ^3F_2^0$
4077. 089	60, *Z*	24520. 41	$a\ ^5P_2 - w^5D_3^0$
4076. 071	60, *Z*	24526. 47	$b\ ^3F_3 - t\ ^3G_4^0$
			$a\ ^3F_2 - w^5G_3^0$
4075. 921	15	24527. 43	$a\ ^5P_3 - w^5D_3^0$
4074. 857	50, *Z*	24533. 84	$b\ ^3H_6 - s\ ^3G_5^0$
4074. 52	1	24535. 86	$a\ ^3F_2 - y\ ^3S_1^0$
4074. 35	3	24536. 89	$a\ ^3G_3 - w^3G_3^0$
4073. 32	6	24543. 09	$b\ ^3H_5 - v\ ^3I_5^0$
			$a\ ^3P_2 - 1_3^0$
4072. 767	25	24546. 43	$a\ ^3F_2 - x\ ^3F_2^0$
4072. 25	3*w*	24549. 54	
4071. 10	1	24556. 48	$a\ ^3G_4 - w^3G_4^0$
4070. 991	30	24557. 14	$b\ ^3H_4 - v\ ^3I_4^0$
4070. 065	8	24562. 72	$b\ ^5D_0 - x\ ^3D_1^0$

TABLE 1. *Wavelengths and term combinations of* Cr I—Continued

d, [illegible] *h*, hazy; *H*, very hazy; *l*, shaded longward; *s*, shaded shortward; *r*, reversed; *R*, strongly reversed; *w*, wide; *W*, very wide; *Z*, Zeeman pattern in table 2.

Wavelength λ_{air}	Intensity	Wave No.	Term combination
4069. 68	3*w*	24565. 04	$c\ ^3F_4 - v\ ^3I_5^\circ$
4069. 35	2*w*	24567. 04	
4069. 01	5*w*	24569. 09	
4068. 70	5*w*	24570. 96	$d\ ^3F_3 - r\ ^3G_4^\circ$
4068. 41	15	24572. 71	
4068. 03	3*h*	24575. 01	
4067. 829	30, *Z*	24576. 22	
4067. 63	1	24577. 42	
4067. 346	10	24579. 14	$a\ ^3G_5 - w\ ^5G_5^\circ$ $a\ ^3F_2 - w\ ^5G_3^\circ$
4066. 928	70, *Z*	24581. 67	$a\ ^5P_3 - w\ ^5D_4^\circ$ $a\ ^3G_5 - x\ ^3F_4^\circ$
4066. 610	8	24583. 59	$b\ ^3H_5 - s\ ^3G_5^\circ$ $d\ ^3F_4 - r\ ^3G_5^\circ$
4065. 714	50, *Z*	24589. 01	$b\ ^3F_4 - t\ ^3G_5^\circ$ $a\ ^3G_4 - v\ ^5P_3^\circ$
4064. 94	5	24593. 69	$b\ ^3H_6 - p\ ^3I_6^\circ$
4064. 582	30	24595. 85	$a\ ^5G_2 - p\ ^5P_2^\circ$
4063. 08	10	24604. 94	$c\ ^3F_4 - s\ ^3G_5^\circ$
4062. 84	2*w*	24606. 40	$a\ ^1H_5 - q\ ^3H_5^\circ$
4061. 74	3*w*	24613. 06	
4060. 646	45, *Z*	24619. 69	$b\ ^3H_5 - s\ ^3G_4^\circ$ $a\ ^3G_3 - w\ ^3G_4^\circ$
4059. 093	7	24629. 11	
4058. 778	70, *Z*	24631. 02	$a\ ^3I_5 - x\ ^3I_5^\circ$
4057. 83	18, *Z*	24636. 78	$a\ ^3I_6 - x\ ^3I_5^\circ$
4057. 214	15, *Z*	24640. 52	$a\ ^3G_4 - w\ ^3G_5^\circ$
4057. 126	10	24641. 05	$c\ ^3F_4 - s\ ^3G_4^\circ$
4056. 785	35, *Z*	24643. 12	$b\ ^3H_5 - v\ ^3I_6^\circ$
4056. 047	50, *Z*	24647. 61	$b\ ^3H_4 - s\ ^3G_5^\circ$
4054. 80	3	24655. 19	$c\ ^3F_4 - s\ ^3G_3^\circ$
4051. 319	50, *Z*	24676. 37	
4050. 81	5	24679. 47	
4050. 026	30	24681. 25	$a\ ^5G_2 - x\ ^5F_1^\circ$
4049. 779	40	24685. 76	$a\ ^3I_5 - x\ ^3I_6^\circ$ $a\ ^3G_3 - w\ ^5G_3^\circ$
4049. 083	15, *Z*	24690. 00	$c\ ^3F_3 - s\ ^3G_4^\circ$
4048. 784	60, *Z*	24691. 82	$a\ ^3I_6 - x\ ^3I_6^\circ$
4046. 758	35	24704. 19	$a\ ^5G_3 - x\ ^5F_2^\circ$
4046. 187	15	24707. 67	$a\ ^5G_2 - x\ ^5F_2^\circ$
4045. 75	5, Fe ?	24710. 34	$c\ ^3F_4 - s\ ^3G_3^\circ$
4045. 61	3*l*	24711. 20	
4045. 47	3	24712. 05	$a\ ^3F_2 - x\ ^3F_2^\circ$ $y\ ^5P_2^\circ - e\ ^5F_1$
4045. 12	3*w*	24714. 19	$a\ ^3P_1 - x\ ^3P_0$ $a\ ^3P_0 - u\ ^5F_1^\circ$
4044. 152	20	24720. 10	$a\ ^3G_4 - w\ ^5G_3^\circ$
4043. 684	50	24722. 97	$b\ ^3H_6 - v\ ^3I_7^\circ$ $a\ ^3G_4 - x\ ^3F_4^\circ$
4042. 92	3	24727. 64	$b\ ^5D_2 - x\ ^3D_2^\circ$
4042. 246	40	24731. 76	$a\ ^5G_4 - x\ ^5F_3^\circ$
4041. 795	22	24734. 52	$a\ ^5G_3 - x\ ^5F_3^\circ$
4041. 04	10	24739. 14	$a\ ^3G_3 - w\ ^3G_4^\circ$
4040. 753	12	24740. 90	$b\ ^5D_1 - x\ ^3D_2^\circ$
4039. 58	4	24748. 08	$y\ ^5P_3^\circ - e\ ^5F_4$
4039. 294	20	24749. 84	$a\ ^3I_6 - x\ ^3I_7^\circ$
4039. 098	60, *Z*	24751. 04	$a\ ^3I_7 - x\ ^3I_7^\circ$
4038. 832	15	24752. 66	$a\ ^3G_4 - x\ ^3F_3^\circ$ $c\ ^3F_4 - s\ ^3D_3^\circ$
4038. 63	3*s*	24753. 90	
4038. 22	2	24756. 42	
4037. 621	20	24760. 09	
4037. 293	50	24762. 10	$a\ ^5G_5 - x\ ^5F_4^\circ$ $a\ ^5G_4 - x\ ^5F_4^\circ$
4036. 81	6	24765. 06	$a\ ^5G_3 - x\ ^5F_4^\circ$
4035. 88	2	24770. 77	$c\ ^3G_3 - q\ ^3G_4^\circ$
4035. 21	10	24774. 88	$b\ ^3G_5 - y\ ^3I_5^\circ$
4035. 076	8	24775. 81	
4033. 965	10	24782. 53	$a\ ^5G_5 - x\ ^5F_5^\circ$
4033. 94	8	24782. 68	$a\ ^5G_4 - x\ ^5F_5^\circ$
4033. 267	25	24786. 82	$a\ ^5G_6 - x\ ^5F_5^\circ$ $a\ ^3G_3 - x\ ^3F_4^\circ$
4032. 63	5	24790. 73	$a\ ^5F_3 - v\ ^5G_3^\circ$
4032. 18	2*w*	24793. 50	$c\ ^3D_2 - t\ ^3H_4^\circ$ $c\ ^3G_4 - q\ ^3G_5^\circ$
4031. 125	25	24799. 99	$a\ ^5F_2 - v\ ^5G_2^\circ$
4030. 69	40	24802. 66	$a\ ^5F_1 - v\ ^5G_2^\circ$
4028. 467	10	24816. 35	$a\ ^3G_3 - x\ ^3F_3^\circ$ $c\ ^3F_3 - s\ ^3D_2^\circ$
4028. 09	10	24818. 67	$c\ ^3D_1 - u\ ^3D_1^\circ$
4028. 04	10	24818. 98	$a\ ^3G_3 - x\ ^3F_2^\circ$ $a\ ^3P_1 - x\ ^3P_1^\circ$
4027. 84	3	24820. 22	$a\ ^5P_1 - w\ ^5F_2^\circ$
4027. 61	2	24821. 63	$a\ ^5P_1 - w\ ^5F_1^\circ$
4027. 102	55	24824. 76	$a\ ^5G_5 - z\ ^3H_6^\circ$
4026. 174	60	24830. 48	$a\ ^5G_6 - z\ ^3H_5^\circ$ $a\ ^3G_4 - z\ ^3H_5^\circ$
4025. 95	6	24831. 86	$a\ ^5F_4 - v\ ^5G_3^\circ$
4025. 605	10	24833. 99	
4025. 447	25	24834. 97	$a\ ^5G_5 - z\ ^3H_4^\circ$ $a\ ^5G_4 - z\ ^3H_4^\circ$
4025. 013	50, *Z*	24837. 65	$a\ ^5G_3 - z\ ^3H_4^\circ$
4024. 564	20	24840. 42	$a\ ^5P_2 - w\ ^5F_3^\circ$
4024. 03	1	24843. 71	$b\ ^3G_5 - y\ ^3I_6^\circ$
4023. 74	40	24845. 50	$a\ ^5F_3 - v\ ^5G_3^\circ$
4023. 43	10	24847. 42	$a\ ^5P_3 - w\ ^5F_3^\circ$
4022. 57	2	24852. 73	$a\ ^3H_4 - x\ ^3G_5^\circ$
4022. 27	50, *Z*	24854. 58	$a\ ^5F_2 - v\ ^5G_2^\circ$
4021. 385	12	24860. 05	$a\ ^3I_7 - u\ ^3H_6^\circ$ $a\ ^3I_8 - u\ ^3H_7^\circ$
4019. 80	5*h*	24869. 86	$c\ ^3F_2 - s\ ^3D_1^\circ$
4018. 216	35, *Z*	24879. 66	$a\ ^5P_3 - w\ ^5F_2^\circ$
4017. 72	1*w*	24882. 73	
4017. 37	3*w*	24884. 90	
4016. 824	30	24888. 28	$b\ ^3G_4 - y\ ^3I_5^\circ$
4016. 60	3	24889. 67	$a\ ^3I_5 - y\ ^1H_5^\circ$
4016. 26	3*h*	24891. 77	$y\ ^5P_2^\circ - e\ ^5F_3$
4015. 752	4	24894. 92	
4014. 673	40	24901. 62	$a\ ^5F_4 - v\ ^5G_4^\circ$
4014. 44	5	24903. 06	$b\ ^3G_5 - 2_4^\circ$
4012. 48	50, *Z*	24915. 22	$a\ ^5F_3 - v\ ^5G_4^\circ$
4012. 00	2*ws*	24918. 20	
4010. 983	10	24924. 52	$c\ ^3D_2 - u\ ^3D_2^\circ$
4010. 836	8	24925. 44	$c\ ^3D_3 - u\ ^3D_2^\circ$
4009. 411	4	24934. 30	$a\ ^3P_2 - x\ ^3D_2^\circ$
4007. 43	1	24946. 62	$a\ ^3P_1 - x\ ^3P_2^\circ$
4004. 697	12	24963. 65	$c\ ^3D_1 - t\ ^3D_1^\circ$
4003. 916	30	24968. 52	$a\ ^5F_5 - v\ ^5G_5^\circ$ $d\ ^3F_2 - t\ ^3P_1^\circ$

TABLE 1. *Wavelengths and term combinations of* Cr I—Continued

d, Double; *h*, hazy; *H*, very hazy; *l*, shaded longward; *s*, shaded shortward; *r*, reversed; *R*, strongly reversed; *w*, wide; *W*, very wide; *Z*, Zeeman pattern in table 2.

Wavelength λ_{air}	Intensity	Wave No.	Term combination
4001.443	75, *Z*	24983.95	$a\ ^5F_4 - v\ ^5G^0_5$
4000.96	3*ws*	24986.96	$b\ ^3H_5 - s\ ^3H^0_4$
4000.60	20	24989.21	$c\ ^3D_3 - t\ ^3D^0_3$
3999.938	7	24993.35	
3999.679	40, *Z*	24994.97	
3998.861	30	25000.08	$b\ ^3H_4 - s\ ^3H^0_4$
3997.92	3	25005.96	$c\ ^3F_3 - p\ ^3F^0_3$; $a\ ^5P_3 - z\ ^3G^0_3$
3997.76	2*w*	25006.97	$b\ ^5D_2 - x\ ^3D^0_3$
3997.113	18	25011.01	$b\ ^5D_2 - x\ ^3D^0_2$
3996.84	3*w*	25012.72	$b\ ^1I_6 - t\ ^3H^0_5$
3996.277	8	25016.25	$b\ ^3G_4 - 2^0_4$
3994.317	6	25028.52	$b\ ^5D_4 - x\ ^3D^0_3$
3993.97	50	25030.70	$a\ ^5P_2 - u\ ^5P^0_3$
3992.846	100, *Z*	25037.74	$a\ ^5P_3 - u\ ^5P^0_3$
3992.104	18	25042.39	$a\ ^5G_4 - y\ ^5H^0_3$
3991.677	50	25045.08	$a\ ^5G_2 - y\ ^5H^0_3$
3991.118	25	25048.58	$a\ ^5G_2 - y\ ^5H^0_3$
3990.16	10*w*	25054.60	$b\ ^3F_4 - s\ ^3F^0_4$
3989.984	75, *Z*	25055.70	$a\ ^5F_5 - v\ ^5G^0_6$
3989.77	5*w*	25057.04	$c\ ^5D_2 - s\ ^5D^0_2$; $c\ ^3F_3 - s\ ^3H^0_4$
3988.65	6*w*	25064.08	$a\ ^5P_3 - z\ ^3G^0_4$
3988.43	5*w*	25065.46	$c\ ^5D_1 - o\ ^5F^0_1$
3985.03	1*W*	25086.85	$y\ ^5P^0_2 - g\ ^5D_1$; $a\ ^3F_4 - w^3D^0_3$
3984.65	1	25089.24	$b\ ^3F_4 - s\ ^3F^0_4$; $a\ ^7S_3 - z\ ^7F^0_2$
3984.339	75	25091.19	$a\ ^5G_5 - y\ ^5H^0_4$; $a\ ^5G_4 - y\ ^5H^0_4$
3983.901	125*r*	25093.95	$a\ ^5G_3 - y\ ^5H^0_4$
3983.236	25	25098.14	$c\ ^3F_4 - p\ ^3F^0_4$; $b\ ^3G_5 - x\ ^3H^0_6$
3982.613	7	25102.07	$b\ ^3F_2 - s\ ^3F^0_2$
3981.93	20	25106.38	
3981.242	100	25110.71	$a\ ^5P_1 - u\ ^5P^0_2$
3980.70	2*W*	25114.13	$c\ ^5D_3 - s\ ^5D^0_3$
3979.80	50, *Z*	25119.81	$a\ ^5P_2 - u\ ^5P^0_2$
3979.33	25	25122.78	$b\ ^3F_2 - s\ ^3F^0_2$; $b\ ^3G_3 - 2^0_4$
3979.22	20	25123.47	$b\ ^3H_5 - s\ ^3H^0_6$; $d\ ^3F_3 - t\ ^3P^0_2$
3978.683	75	25126.86	$a\ ^5P_3 - u\ ^5P^0_2$
3978.22	2*w*	25129.79	
3976.674	200*R*	25139.56	$a\ ^5G_5 - y\ ^5H^0_5$; $a\ ^5G_4 - y\ ^5H^0_5$
3976.308	18	25141.87	$b\ ^3F_2 - s\ ^3F^0_3$
3976.018	20	25143.70	$a\ ^5G_6 - y\ ^5H^0_5$
3975.56	2	25146.60	$b\ ^3G_5 - x\ ^3H^0_4$; $c\ ^3F_2 - p\ ^3F^0_2$
3975.03	2*w*	25149.95	$y\ ^5P^0_3 - e\ ^3D_2$; $b\ ^5D_3 - w^3G^0_4$
3974.70	3*w*	25152.04	
3973.76	2	25157.99	$a\ ^3F_2 - w^3D^0_3$
3973.08	5*h*	25162.30	$b\ ^3F_2 - s\ ^3F^0_3$; $b\ ^5D_3 - w^5G^0_2$; $c\ ^5D_1 - o\ ^5F^0_2$
3972.694	50	25164.75	$a\ ^5P_1 - u\ ^5P^0_1$
3972.35	2	25166.92	$b\ ^5D_2 - w^5G^0_3$
3971.266	75	25173.79	$a\ ^5P_2 - u\ ^5P^0_1$
3970.73	4*w*	25177.19	$b\ ^5D_2 - y\ ^3S^0_1$
3970.39	3*w*	25179.34	$b\ ^3F_4 - r\ ^5D^0_4$; $b\ ^5D_1 - w^5G^0_2$
3970.06	30	25181.44	$b\ ^3G_4 - x\ ^3H^0_4$
3969.748	150*R*	25183.42	$a\ ^5G_5 - y\ ^5H^0_4$
3969.064	60	25187.76	$a\ ^5G_6 - y\ ^5H^0_5$
3968.64	6	25190.45	$a\ ^5P_1 - x\ ^5G^0_2$; $b\ ^5D_1 - y\ ^3S^0_1$
3967.34	4*w*	25198.70	
3967.16	5	25199.85	$a\ ^5P_2 - x\ ^5G^0_2$; $b\ ^5D_0 - y\ ^3S^0_1$
3967.03	3	25200.67	$a\ ^5P_2 - y\ ^3G^0_3$
3965.94	1	25207.60	$b\ ^3H_4 - r\ ^3G^0_3$; $a\ ^5P_2 - y\ ^3G^0_3$
3965.82	1	25208.36	$c\ ^5D_2 - o\ ^5F^0_2$
3965.10	1	25212.94	
3964.91	3	25214.15	$a\ ^5P_3 - y\ ^3G^0_4$; $a\ ^5G_3 - y\ ^3P^0_2$
3964.65	3	25215.80	$b\ ^5D_3 - w^5G^0_3$
3964.352	12	25217.70	$a\ ^5G_2 - y\ ^3P^0_2$; $a\ ^5P_2 - x\ ^3D^0_2$
3963.99	3	25220.00	$b\ ^5D_2 - w^5G^0_2$; $y\ ^5P^0_2 - e\ ^3D_1$
3963.694	200*R*	25221.89	$a\ ^5G_6 - y\ ^5H^0_5$
3962.80	1*l*	25227.57	$a\ ^5F_3 - v\ ^3P^0_2$; $b\ ^3H_6 - r\ ^3G^0_5$
3962.189	12	25231.47	$a\ ^5P_1 - z\ ^3S^0_1$
3960.768	25	25240.52	$a\ ^5P_2 - z\ ^3S^0_1$
3959.14	1	25250.89	$y\ ^5P^0_1 - g\ ^5D_1$
3958.41	10	25255.55	$b\ ^5D_4 - w^3G^0_4$
3958.084	30, *Z*	25257.63	$b\ ^3H_6 - s\ ^3H^0_6$
3957.62	1*l*	25260.59	$b\ ^3G_4 - x\ ^3H^0_4$; $c\ ^3F_4 - r\ ^3G^0_4$
3956.304	30	25268.99	$b\ ^5D_3 - w^5G^0_4$
3956.075	10	25270.45	$c\ ^3F_2 - r\ ^3G^0_3$
3954.94	2*l*	25277.70	$b\ ^3H_5 - r\ ^3G^0_5$; $a\ ^5P_2 - x\ ^5G^0_2$
3954.59	3*wh*	25279.94	$c\ ^5D_2 - o\ ^5F^0_2$
3953.83	2	25284.80	$a\ ^5P_3 - x\ ^5G^0_3$
3953.17	25*w*	25289.02	$b\ ^5D_2 - t\ ^5P^0_1$
3952.398	40*w*	25293.96	$b\ ^5D_3 - t\ ^5P^0_2$
3951.767	20*w*	25298.00	$b\ ^5D_2 - t\ ^5P^0_2$; $c\ ^3F_4 - r\ ^3G^0_5$
3951.094	35*w*	25302.31	$b\ ^5D_1 - t\ ^5P^0_1$
3950.32	5	25307.27	$b\ ^3H_5 - s\ ^3H^0_5$
3949.655	20*w*	25311.53	$b\ ^5D_1 - t\ ^5P^0_2$
3949.60	25*w*	25311.88	$b\ ^5D_0 - t\ ^5P^0_1$
3948.862	35	25316.61	$b\ ^5D_3 - x\ ^3F^0_2$
3947.86	5	25323.04	
3947.12	5	25327.78	$a\ ^3P_1 - x\ ^3D^0_1$
3946.44	1*h*	25332.15	$c\ ^5D_2 - o\ ^5F^0_1$
3945.967	45	25335.19	$b\ ^5D_4 - w^5G^0_5$
3945.50	40	25338.18	$b\ ^5D_4 - x\ ^3F^0_4$; $a\ ^3H_6 - w^3G^0_5$
3944.90	2*w*	25342.04	
3944.25	20	25346.22	$b\ ^5D_3 - x\ ^3F^0_3$
3943.618	20	25350.28	$b\ ^5D_2 - x\ ^3F^0_2$
3943.221	15	25352.83	$b\ ^5D_2 - x\ ^3F^0_3$
3942.82	2*h*	25355.41	$b\ ^3G_3 - r\ ^5F^0_3$
3941.499	90*r*, *Z*	25363.90	$a\ ^5D_4 - z\ ^5D^0_3$

TABLE 1. *Wavelengths and term combinations of* Cr I—Continued

Diffuse: *h*, hazy; *H*, very hazy; *l*, shaded longward; *s*, shaded shortward; *r*, reversed; *R*, strongly reversed; *w*, wide; *W*, very wide; *Z*, Zeeman pattern in table 2

Wavelength λ_{air}	Intensity	Wave No.	Term combination
3941. 163	22	25366. 07	$b\ ^5D_1 - x\ ^3F^0_3$ $b\ ^3G_3 - x\ ^3H^0_4$
3940. 90	8	25367. 76	$a\ ^5F_2 - v\ ^3P^0_1$ $b\ ^5D_4 - x\ ^3F^0_3$
3940. 54	3	25370. 08	$b\ ^3G_4 - r\ ^5F^0_5$ $a\ ^5F_1 - v\ ^3P^0_1$
3940. 245	7*w*	25371. 98	$d\ ^3F_2 - q\ ^3G^0_3$
3940. 00	1	25373. 55	$a\ ^3P_2 - w^5G^0_3$
3939. 81	3*w*	25374. 78	$y\ ^7P^0_3 - h\ ^7D_2$
3939. 302	10*w*	25378. 05	$d\ ^3F_3 - q\ ^3G^0_3$
3938. 98	2	25380. 13	$y\ ^5P^0_3 - e\ ^3D_3$ $a\ ^3F_4 - u\ ^5D^0_4$ $y\ ^5P^0_1 - e\ ^3D_1$
3938. 352	25*w*	25384. 17	$a\ ^3P_2 - y\ ^3S^0_1$ $y\ ^5P^0_2 - g\ ^5D_4$
3937. 45	6*h*	25389. 99	$a\ ^1H_5 - p\ ^3H^0_5$ $y\ ^5P^0_2 - e\ ^3D_2$
3936. 24	7*hl*	25397. 79	$a\ ^3H_5 - w^3G^0_4$ $y\ ^5P^0_1 - g\ ^5D_2$
3936. 115	20	25398. 60	$d\ ^3F_4 - q\ ^3G^0_4$
3935. 55	8*w*	25402. 24	$y\ ^5P^0_2 - g\ ^5D_3$
3934. 03	2*h*	25412. 06	
3933. 20	4	25417. 42	$a\ ^3H_6 - w^5G^0_5$
3933. 11	4*ws*	25418. 00	
3932. 77	4	25420. 20	
3932. 48	3*w*	25422. 07	$c\ ^3D_2 - r\ ^3F^0_2$
3932. 01	1	25425. 11	$c\ ^5D_0 - r\ ^5P^0_1$
3931. 17	2*w*	25430. 54	$a\ ^3G_3 - w^3D^0_3$
3930. 27	2, *Z*	25436. 37	$a\ ^3H_4 - w^3G^0_5$
3929. 66	20*wh*	25440. 32	$b\ ^3G_3 - r\ ^5F^0_2$ $y\ ^7P^0_4 - h\ ^7D_4$
3928. 647	100*r*, *Z*	25446. 88	$a\ ^5D_3 - z\ ^5D^0_2$
3928. 16	5	25450. 03	$a\ ^5F_1 - v\ ^3P^0_0$
3927. 96	2	25451. 33	$a\ ^3F_3 - u\ ^5D^0_4$ $c\ ^3D_1 - r\ ^3F^0_2$
3926. 66	40, *Z*	25459. 75	$d\ ^3F_4 - q\ ^3G^0_5$
3926. 00	7*whl*	25464. 03	$y\ ^7P^0_3 - h\ ^7D_3$
3925. 65	5*hs*	25466. 30	$y\ ^7P^0_2 - h\ ^7D_2$
3924. 965	7	25470. 76	
3924. 90	2*w*	25471. 17	
3924. 68	1*w*	25472. 70	$z\ ^7D^0_5 - e\ ^7G_4$
3924. 04	4	25476. 75	$a\ ^5G_4 - y\ ^3F^0_3$ $b\ ^3G_3 - r\ ^5F^0_3$
3923. 66	4	25479. 22	$a\ ^5G_3 - y\ ^3F^0_3$
3923. 345	20	25481. 27	$c\ ^3D_2 - r\ ^3F^0_3$
3923. 26	3	25481. 82	$a\ ^3H_5 - w^3G^0_5$ $c\ ^3D_2 - r\ ^3F^0_2$
3922. 73	5*ws*	25485. 26	
3922. 44	2*w*	25487. 14	$y\ ^7P^0_3 - e\ ^7F_1$
3922. 14	2*h*	25489. 09	$c\ ^5D_1 - r\ ^5P^0_2$
3921. 50	2*h*	25493. 25	$c\ ^5D_2 - r\ ^5P^0_1$
3921. 031	100*r*, *Z*	25496. 30	$a\ ^5D_2 - z\ ^5D^0_1$
3920. 104	20	25502. 33	
3919. 165	200*R*, *Z*	25508. 45	$b\ ^5D_3 - t\ ^5P^0_3$ $a\ ^5D_4 - z\ ^5D^0_4$
3918. 10	10	25515. 38	$a\ ^3P_1 - x\ ^3D^0_2$
3917. 85	3*w*	25517. 00	$a\ ^3H_5 - w^5G^0_4$
3917. 608	75	25518. 58	$b\ ^5D_2 - y\ ^5S^0_2$
3917. 20	3	25521. 24	
3916. 986	35	25522. 63	$b\ ^5D_2 - y\ ^5S^0_2$
3916. 25	100, *Z*	25527. 43	$a\ ^5D_1 - z\ ^5D^0_0$
3915. 854	100, *Z*	25530. 01	$b\ ^5D_4 - t\ ^5P^0_3$
3915. 514	25	25532. 23	
3915. 203	4	25534. 26	$a\ ^5G_5 - y\ ^3F^0_4$ $a\ ^5G_4 - y\ ^3F^0_3$
3914. 948	7*w*	25535. 91	$b\ ^3D_1 - y\ ^5S^0_2$
3914. 70	1*w*	25537. 54	$a\ ^3G_3 - y\ ^3F^0_4$
3914. 35	40	25539. 82	
3913. 90	1*w*	25542. 76	$b\ ^3D_1 - v\ ^3P^0_2$
3912. 79	2*h*	25550. 00	$z\ ^7D^0_5 - h\ ^7D_4$
3912. 36	4	25552. 80	$c\ ^3D_3 - r\ ^3F^0_4$
3912. 01	7*w*, *Z*	25555. 10	$y\ ^7P^0_3 - h\ ^7D_4$ $c\ ^5D_2 - o\ ^5F_4$
3911. 83	50*wh*	25556. 27	$c\ ^3G_3 - r\ ^3H^0_4$ $y\ ^7P^0_3 - h\ ^7D_3$
3911. 04	7*w*	25561. 43	$a\ ^3H_5 - w^5G^0_5$
3910. 724	12, *Z*	25563. 50	$b\ ^3D_2 - v\ ^3P^0_2$
3910. 56	2	25564. 57	$a\ ^3H_5 - x\ ^3F^0_4$
3909. 98	2*w*	25568. 36	$z\ ^7D^0_5 - e\ ^7G_5$
3908. 762	150*r*, *Z*	25576. 33	$a\ ^5D_3 - z\ ^5D^0_3$
3907. 777	30,	25582. 77	$b\ ^5D_3 - v\ ^3P^0_2$
3907. 26	20*w*, *Z*	25586. 06	$a\ ^3H_4 - w^5G^0_5$ $c\ ^3G_4 - r\ ^3H^0_5$
3906. 94	3*w*	25588. 26	$a\ ^5G_3 - y\ ^3D^0_3$
3906. 45	3	25591. 46	$a\ ^5G_2 - y\ ^3D^0_2$
3904. 407	5	25604. 86	$a\ ^1I_6 - t\ ^3G^0_5$
3904. 006	10	25607. 49	$a\ ^5F_4 - u\ ^3G^0_4$
3903. 171	50, *Z*	25612. 96	$a\ ^5D_1 - z\ ^5D^0_1$
3902. 911	125, *Z*	25614. 67	$a\ ^5D_2 - z\ ^5D^0_2$
3902. 26	10	25618. 94	
3902. 00	75	25620. 65	
3900. 95	2*w*	25627. 55	
3899. 23	4*w*	25638. 85	
3899. 20	4*w*	25639. 05	$a\ ^3H_4 - w^3G^0_4$
3899. 012	5	25640. 29	$a\ ^5F_3 - u\ ^3G^0_4$
3898. 40	8*w*	25644. 31	
3898. 29	2*h*	25645. 03	
3897. 66	75, *Z*	25649. 18	
3897. 42	4	25650. 76	$a\ ^5G_4 - y\ ^3D^0_3$
3897. 008	5	25653. 47	$a\ ^5G_3 - y\ ^3D^0_3$
3896. 67	10	25655. 70	$a\ ^5F_4 - u\ ^3G^0_4$
3896. 48	5	25656. 94	$a\ ^5G_2 - y\ ^3D^0_2$
3894. 89	1	25667. 42	$b\ ^3F_3 - t\ ^3H^0_4$
3894. 57	8*h*	25669. 54	$a\ ^5F_3 - u\ ^3G^0_4$ $c\ ^3G_3 - r\ ^3H^0_4$
3894. 039	100, *Z*	25673. 03	$a\ ^5D_0 - z\ ^5D^0_1$
3893. 50	3	25676. 58	$a\ ^3P_0 - x\ ^3D^0_1$
3893. 25	6*w*	25678. 24	
3893. 14	5*h*	25678. 96	$z\ ^7P^0_4 - g\ ^7S_3$
3892. 87	2	25680. 74	
3891. 932	100*w*, *Z*	25686. 93	$a\ ^3H_4 - x\ ^3F^0_4$ . . .
3891. 06	7*WH*	25692. 69	$z\ ^7D^0_5 - e\ ^7G_6$ $y\ ^7P^0_4 - h\ ^7D_3$
3890. 826	20, *Z*	25694. 23	$b\ ^3D_3 - v\ ^3P^0_1$

275121—53——6

TABLE 1. *Wavelengths and term combinations of* Cr I—Continued

d, Double; *h*, hazy; *H*, very hazy; *l*, shaded longward; *s*, shaded shortward; *r*, reversed; *R*, strongly reversed; *w*, wide; *W*, very wide; *Z*, Zeeman pattern in table 2

Wavelength λ_{air}	Intensity	Wave No.	Term combination
3890. 72	8*hs*	25694. 93	$a\ ^5F_5 - u\ ^3G_5^0$ $z\ ^7D_5^0 - h\ ^7D_2$
3890. 148	10*w*	25698. 71	
3889. 10	1*h*	25705. 63	$y\ ^7P_3^0 - e\ ^7F_4$
3888. 39	1	25710. 32	$a\ ^5F_4 - u\ ^3G_4^0$
3888. 26	10	25711. 19	$b\ ^3F_3 - t\ ^3D_3^0$
3887. 08	15*hl*	25718. 99	$b\ ^5D_2 - s\ ^5F_1^0$
3886. 80	50, *Z*	25720. 84	$a\ ^5D_3 - z\ ^5D_4^0$
3886. 05	10*hs*	25725. 81	$z\ ^7D_4^0 - h\ ^7D_4$
3885. 24	100, *Z*	25731. 17	$a\ ^5D_1 - z\ ^5D_2^0$
3885. 20	75, *Z*	25731. 43	
3885. 083	100*w*	25732. 21	$b\ ^5D_1 - s\ ^5F_1^0$ $a\ ^5F_2 - u\ ^3P_2^0$
3884. 67	3*w*	25734. 97	$a\ ^5F_1 - u\ ^3P_2^0$ $z\ ^7D_4^0 - e\ ^7F_3$
3884. 45	10*w*	25736. 41	$a\ ^5F_3 - p\ ^5F_2^0$
3883. 664	100*W*	25741. 61	$b\ ^5D_0 - s\ ^5F_1^0$ $a\ ^5F_2 - p\ ^5F_1^0$
3883. 289	200*W*, *Z*	25744. 10	$a\ ^5D_2 - z\ ^5D_3^0$ $a\ ^5F_1 - p\ ^5F_1^0$ $z\ ^7D_4^0 - e\ ^7G_3$
3882. 67	4*w*	25748. 20	$a\ ^5F_1 - p\ ^5F_2^0$
3881. 862	25	25753. 56	$b\ ^3D_1 - v\ ^3P_0^0$ $b\ ^5D_2 - s\ ^5F_2^0$
3881. 23	50*W*	25757. 76	$b\ ^5D_2 - s\ ^5F_2^0$
3880. 35	10*w*	25763. 60	$c\ ^5D_4 - r\ ^5G_5^0$ $a\ ^5F_4 - 4_5^0$
3879. 231	50*W*, *Z*	25771. 03	$b\ ^5D_1 - s\ ^5F_2^0$ $y\ ^7P_4^0 - e\ ^7F_5$
3878. 945	8	25772. 93	$a\ ^3F_4 - w^3F_4^0$ $a\ ^5P_1 - v\ ^5F_1^0$
3878. 86	3	25773. 50	$a\ ^5P_2 - x\ ^5H_3^0$
3878. 72	3*w*	25774. 42	$a\ ^5P_1 - v\ ^5F_2^0$
3878. 30	10*ws*	25777. 22	$a\ ^5F_3 - 4_3^0$ $a\ ^5F_2 - u\ ^3P_1^0$
3877. 87	3	25780. 07	$a\ ^5F_1 - u\ ^3P_1^0$
3877. 79	3*w*	25780. 60	$a\ ^5P_3 - x\ ^5H_3^0$ $a\ ^5G_2 - w^5D_1^0$
3877. 39	4*h*	25783. 26	$z\ ^7D_3^0 - h\ ^7D_3$
3877. 317	12	25783. 75	$a\ ^5P_2 - v\ ^5F_2^0$ $a\ ^3F_3 - w^3F_3^0$
3877. 104	10	25785. 16	
3876. 88	5*h*	25786. 65	$a\ ^5F_2 - 4_2^0$
3876. 60	4*h*	25788. 52	$a\ ^5P_2 - v\ ^5F_3^0$ $b\ ^3P_2 - r\ ^5F_1^0$
3876. 38	4*h*	25789. 98	$a\ ^5P_3 - v\ ^5F_3^0$
3876. 20	4*h*	25791. 18	$z\ ^7P_3^0 - g\ ^7S_3$
3876. 12	4*w*	25791. 71	
3875. 54	2*w*	25795. 57	$z\ ^7D_2^0 - e\ ^7G_2$ $a\ ^5P_3 - v\ ^5F_3^0$
3875. 23	50*W*	25797. 64	$c\ ^5D_4 - o\ ^5F_5^0$
3875. 14	15*w*	25798. 24	$z\ ^7D_3^0 - e\ ^7G_4$ $a\ ^5P_3 - v\ ^5F_4^0$ $b\ ^5D_3 - s\ ^5F_3^0$
3874. 55	75*W*, *Z*	25802. 16	$a\ ^5F_1 - u\ ^3P_0^0$ $b\ ^5D_2 - s\ ^5F_3^0$ $z\ ^7D_3^0 - h\ ^7D_3$
3873. 58	7*h*	25808. 63	$c\ ^5D_4 - r\ ^5P_3^0$ $a\ ^5F_4 - p\ ^5F_3^0$
3873. 07	4*h*	25812. 02	$z\ ^7D_3^0 - h\ ^7D_2$
3872. 74	3*w*	25814. 22	$b\ ^3P_2 - r\ ^5F_2^0$
3871. 53	10*h*	25822. 29	$a\ ^5F_3 - p\ ^5F_3^0$
3870. 24	50*WH*	25830. 90	$a\ ^5S_2 - z\ ^5D_2^0$ $a\ ^5F_2 - p\ ^5F_2^0$
3869. 21	4	25837. 77	
3868. 56	2	25842. 12	
3868. 27	25	25844. 05	$a\ ^5F_5 - p\ ^5F_4^0$ $a\ ^3F_3 - w^3F_3^0$
3868. 21	7	25844. 45	$a\ ^5G_4 - w^5D_4^0$
3867. 75	4*w*	25847. 53	$a\ ^5G_3 - w^5D_3^0$ $z\ ^7D_1^0 - e\ ^7G_1$
3866. 98	5*wh*	25852. 67	
3865. 96	20*wh*	25859. 49	$a\ ^5F_4 - p\ ^5F_4^0$
3865. 03	4*wh*	25865. 72	$a\ ^5F_2 - t\ ^3F_2^0$
3863. 96	5*h*	25872. 88	$a\ ^5F_3 - p\ ^5F_4^0$ $z\ ^7P_3^0 - g\ ^7S_3$
3863. 68	15*wh*	25871. 75	$z\ ^7D_3^0 - h\ ^7D_4$
3863. 50	10*wh*	25875. 96	$z\ ^7D_3^0 - e\ ^7F_4$
3862. 54	30, *Z*	25882. 38	$a\ ^3F_4 - w^3F_4^0$
3862. 26	3*h*	25884. 27	$b\ ^5D_2 - w^3D_3^0$ $z\ ^7D_3^0 - e\ ^7F_3$
3861. 86	2*h*	25886. 95	
3860. 47	1	25896. 27	$z\ ^7D_2^0 - e\ ^7F_2$
3860. 12	18	25898. 62	$a\ ^5G_3 - w^5D_3^0$ $a\ ^5G_4 - w^5D_4^0$
3858. 89	50*W*	25906. 87	$b\ ^5D_3 - s\ ^5F_2^0$
3857. 63	100*w*, *Z*	25915. 33	$z\ ^7D_1^0 - e\ ^7F_1$ $a\ ^5P_1 - v\ ^5D_1^0$
3856. 75	3*w*	25921. 24	$a\ ^5F_2 - t\ ^3F_2^0$
3856. 283	60	25924. 38	$a\ ^5P_2 - v\ ^5D_1^0$
3855. 58	100	25929. 11	$a\ ^5P_1 - v\ ^5D_2^0$ $b\ ^5D_4 - s\ ^5F_3^0$
3855. 296	50, *Z*	25931. 02	$a\ ^5P_1 - v\ ^5D_0^0$
3854. 80	50*w*	25934. 36	$a\ ^5F_3 - p\ ^5F_3^0$
3854. 229	100, *Z*	25938. 20	$a\ ^5P_2 - v\ ^5D_2^0$
3853. 188	50, *Z*	25945. 21	$a\ ^5P_2 - v\ ^5D_2^0$
3852. 63	8*w*	25948. 96	$a\ ^5S_2 - z\ ^5D_2^0$
3852. 56	15	25949. 44	$a\ ^3F_2 - w^3F_2^0$ $c\ ^3G_3 - q\ ^3H_3^0$ $a\ ^5F_4 - p\ ^5F_3^0$
3852. 221	60, *Z*	25951. 72	$a\ ^5D_1 - z\ ^3P_0^0$
3851. 96	10	25953. 48	$a\ ^3F_2 - w^3F_3^0$
3851. 29	5*w*	25957. 99	
3850. 90	3*h*	25960. 62	$b\ ^5D_3 - w^3D_2^0$
3850. 54	3*h*	25963. 05	
3850. 26	5	25964. 94	$a\ ^3P_1 - y\ ^3S_1^0$ $b\ ^5D_2 - w^3D_2^0$
3850. 029	200*W*	25966. 50	$a\ ^5P_2 - v\ ^5D_3^0$
3849. 541	100*W*, *Z*	25969. 79	$a\ ^5D_2 - z\ ^3P_1^0$
3849. 35	175*W*, *Z*	25971. 07	$b\ ^5D_4 - s\ ^5F_4^0$ $a\ ^5F_3 - t\ ^3F_3^0$
3848. 983	150*W*	25973. 55	$a\ ^5P_3 - v\ ^5D_3^0$
3847. 77	4*w*	25981. 74	$b\ ^5D_4 - w^3D_3^0$
3847. 38	10*WH*	25984. 37	
3846. 41	1*w*	25990. 92	
3846. 18	1*w*	25992. 48	
3845. 47	1*w*	25997. 28	

TABLE 1. *Wavelengths and term combinations of* Cr I—Continued

d, D...le; h, hazy; *H*, very hazy; *l*, shaded longward; *s*, shaded shortward; *r*, reversed; *R*, strongly reversed; *w*, wide; *W*, very wide; *Z*, Zeeman pattern in table 2.

Wavelength λ_{air}	Intensity	Wave No.	Term combination
3843. 78	4	26008. 71	$b\ ^3F_4 - u\ ^5D^0_3$
3843. 63	10	26009. 72	$a\ ^3F_3 - w\ ^3F^0_3$
3842. 024	20*W*	26020. 60	$a\ ^5P_1 - u\ ^5F^0_1$ $a\ ^3G_3 - w\ ^3F^0_4$
3841. 56	1*H*	26023. 74	
3841. 28	200*W*, *Z*	26025. 64	$a\ ^5P_3 - v\ ^5D^0_4$ $z\ ^7D^0_5 - e\ ^7F_4$
3840. 69	8*w*	26029. 63	$a\ ^5P_2 - u\ ^5F^0_1$
3838. 02	3*h*	26047. 74	$b\ ^3D_1 - p\ ^5F^0_1$
3837. 88	5*h*	26048. 69	
3837. 76	2*h*	26049. 51	
3837. 42	2*h*	26051. 81	$b\ ^3D_1 - p\ ^5F^0_2$
3836. 73	7*WH*	26056. 50	$a\ ^3G_3 - w^3F^0_2$ $z\ ^7D^0_4 - e\ ^7F_5$
3836. 08	60	26060. 91	$a\ ^5P_1 - u\ ^5F^0_2$
3834. 742	75	26070. 01	$a\ ^5P_2 - u\ ^5F^0_2$
3833. 708	10*w*	26077. 04	$a\ ^5P_3 - u\ ^5F^0_3$
3833. 487	20*w*	26078. 55	$a\ ^5S_2 - z\ ^5D^0_3$ $b\ ^3D_3 - u\ ^3P^0_2$
3833. 16	8*WH*	26080. 77	
3832. 73	10*wh*	26083. 69	$b\ ^3D_1 - u\ ^3P^0_1$
3832. 318	20	26086. 50	$a\ ^3D_1 - z\ ^3P^0_1$
3832. 10	4*wh*	26087. 98	
3831. 56	7*w*	26091. 66	$b\ ^3D_2 - p\ ^5F^0_2$ $b\ ^3H_5 - q\ ^3G^0_4$
3831. 032	35, *Z*	26095. 25	$a\ ^5D_2 - z\ ^3P^0_2$
3830. 03	150*H*	26102. 08	$z\ ^7D^0_5 - e\ ^7F_6$
3829. 714	8*w*	26104. 23	$b\ ^3D_2 - u\ ^3P^0_1$ $b\ ^3H_6 - q\ ^3G^0_5$
3829. 50	8	26105. 69	$b\ ^3D_1 - u\ ^3P^0_0$ $b\ ^3H_4 - q\ ^3G^0_4$
3828. 48	15*wh*	26112. 64	
3827. 88	3	26116. 74	$a\ ^3G_3 - w^3F^0_3$
3826. 427	125	26126. 66	$a\ ^5P_2 - u\ ^5F^0_3$
3825. 398	75	26133. 68	$a\ ^5P_3 - u\ ^5F^0_4$
3823. 519	35, *Z*	26146. 53	$a\ ^5D_0 - z\ ^3P^0_1$
3822. 84	3*w*	26151. 17	
3822. 096	15	26156. 26	$a\ ^5G_3 - w^5F^0_2$
3821. 586	25	26159. 75	$a\ ^5G_2 - w^5F^0_2$
3821. 39	4*w*	26161. 09	$a\ ^5G_2 - w^5F^0_1$
3821. 21	10	26162. 32	$a\ ^3G_4 - w^3F^0_4$
3820. 872	30	26164. 64	$a\ ^5G_4 - w^5F^0_3$
3820. 60	5*w*	26166. 50	
3820. 46	20, *Z*	26167. 46	$a\ ^5G_3 - w^5F^0_3$
3819. 97	35	26170. 82	$a\ ^5G_2 - w^5F^0_3$
3819. 88	3*w*	26171. 43	$a\ ^3P_2 - w^3D^0_3$
3819. 57	100, *Z*	26173. 57	$a\ ^5P_3 - u\ ^5F^0_4$
3819. 41	2	26174. 65	$c\ ^3F_4 - q\ ^3G^0_3$
3818. 92	4*h*	26178. 01	
3818. 474	60	26181. 07	$a\ ^5G_5 - w^5F^0_5$ $a\ ^5G_4 - w^5F^0_3$
3818. 25	3*w*	26182. 61	
3817. 846	40, *Z*	26185. 37	$a\ ^5G_6 - w^5F^0_5$
3817. 65	2*w*	26186. 72	
3816. 189	60	26196. 75	$a\ ^5G_5 - w^5F^0_4$ $a\ ^5G_4 - w^5F^0_4$
3815. 438	75	26201. 90	$a\ ^5P_3 - t\ ^5F^0_4$
3814. 626	50, *Z*	26207. 58	$b\ ^3G_3 - v\ ^3G^0_3$
3813. 50	3*w*	26215. 22	$a\ ^3G_4 - z\ ^3F^0_3$
3812. 76	5*w*	26220. 31	
3812. 259	65, *Z*	26223. 76	$b\ ^3G_4 - v\ ^3G^0_4$ $a\ ^3F_4 - z\ ^1H^0_5$
3811. 94	5	26225. 95	$a\ ^3G_3 - w^3F^0_4$
3810. 26	8*wh*	26237. 51	
3809. 487	25	26242. 83	$b\ ^1I_6 - x\ ^1H^0_5$
3807. 924	60, *Z*	26253. 60	$b\ ^5D_3 - u\ ^5D^0_4$
3806. 83	50, *Z*	26261. 15	$b\ ^3G_5 - v\ ^3G^0_5$
3806. 558	18	26262. 82	$a\ ^5D_2 - z\ ^3P^0_2$
3805. 91	2*w*	26267. 50	$b\ ^3D_3 - t\ ^3F^0_3$
3804. 801	150, *Z*	26275. 15	$b\ ^5D_4 - u\ ^5D^0_4$
3803. 02	8*hl*	26287. 46	
3802. 22	7*h*	26292. 99	
3801. 38	3*h*	26298. 80	
3801. 19	10*hl*, *Z*	26300. 11	
3800. 65	10*hl*	26303. 85	$b\ ^3F_4 - r\ ^3F^0_3$ $a\ ^5S_2 - z\ ^3P^0_1$
3799. 22	15*w*	26313. 75	$a\ ^3P_0 - y\ ^3S^0_1$ $a\ ^5D_1 - v\ ^3F^0_2$
3797. 714	100, *Z*	26324. 19	$b\ ^5D_3 - u\ ^5D^0_3$
3797. 386	5	26326. 46	$b\ ^3D_3 - t\ ^3F^0_4$ $a\ ^5G_3 - z\ ^3G^0_3$
3797. 138	75	26328. 18	$b\ ^5D_2 - u\ ^5D^0_3$
3796. 977	12	26329. 29	$a\ ^5G_2 - z\ ^3G^0_3$
3796. 833	8	26330. 29	$b\ ^3G_2 - v\ ^3G^0_4$
3795. 79	4*w*	26337. 52	
3794. 613	50	26345. 70	$b\ ^5D_4 - u\ ^5D^0_3$
3793. 872	65	26350. 84	$b\ ^5D_3 - u\ ^5D^0_2$
3793. 545	7	26353. 11	$a\ ^5P_1 - t\ ^5F^0_1$
3793. 288	65	26354. 90	$b\ ^5D_2 - u\ ^5D^0_2$ $a\ ^5G_4 - u\ ^5P^0_3$
3792. 86	2*w*	26357. 87	$a\ ^5G_3 - u\ ^5P^0_3$
3792. 42	10*w*	26360. 93	$a\ ^5G_3 - u\ ^5P^0_3$ $a\ ^5P_1 - t\ ^5F^0_2$
3792. 142	70	26362. 86	$b\ ^5D_2 - u\ ^5D^0_1$
3791. 384	70	26368. 14	$b\ ^5D_1 - u\ ^5D^0_2$
3791. 12	7*w*	26369. 97	$a\ ^5P_1 - x\ ^3P^0_0$ $a\ ^5P_2 - t\ ^5F^0_3$ $b\ ^3F_4 - r\ ^3F^0_4$
3790. 461	60	26374. 55	$b\ ^5D_1 - u\ ^5D^0_0$ $b\ ^3G_4 - v\ ^3G^0_3$
3790. 225	35	26376. 20	$b\ ^5D_1 - u\ ^5D^0_1$
3789. 719	40	26379. 72	$a\ ^5D_1 - z\ ^3P^0_2$
3789. 50	5*w*	26381. 24	$a\ ^5G_5 - z\ ^3G^0_4$ $a\ ^5G_4 - z\ ^3G^0_4$
3789. 08	10	26384. 16	$a\ ^5G_3 - z\ ^3G^0_4$
3788. 858	50	26385. 71	$b\ ^5D_0 - u\ ^5D^0_1$
3788. 06	8*w*	26391. 27	$c\ ^3D_2 - q\ ^3F^0_3$ $c\ ^3D_3 - q\ ^3F^0_3$
3786. 217	40	26404. 12	$a\ ^5P_2 - t\ ^5F^0_2$
3783. 98	3	26419. 72	$a\ ^3D_2 - v\ ^3F^0_2$
3783. 702	8*w*	26421. 67	
3782. 96	1	26426. 85	$b\ ^3F_3 - r\ ^3F^0_4$
3780. 99	6*h*	26440. 62	
3780. 737	15*w*	26442. 39	
3780. 12	8*h*	26446. 71	$a\ ^5G_2 - u\ ^5P^0_2$
3779. 994	8	26447. 58	$a\ ^5P_3 - y\ ^3H^0_4$
3777. 92	8	26462. 10	$a\ ^5G_5 - z\ ^3G^0_5$
3777. 90	3	26462. 24	$a\ ^5G_4 - z\ ^3G^0_5$
7737. 508	3	26464. 99	$a\ ^3D_3 - v\ ^3F^0_3$
3777. 316	25	26466. 33	$a\ ^5G_6 - z\ ^3G^0_5$

TABLE 1. *Wavelengths and term combinations of* Cr I—Continued

d, Double; *h*, hazy; *H*, very hazy; *l*, shaded longward; *s*, shaded shortward; *r*, reversed; *R*, strongly reversed; *w*, wide; *W*, very wide; *Z*, Zeeman pattern in table 2

Wavelength λ_{air}	Intensity	Wave No.	Term combination
3776. 76	4*h*	26470. 23	$a\ ^3D_2 - v\ ^3D_2^0$
3776. 17	8*wl*	26474. 37	$a\ ^5P_1 - x\ ^3P_1^0$
3774. 65	4*ws*	26485. 03	
3772. 01	2	26503. 54	$a\ ^3G_4 - z\ ^1H_5^0$
3768. 994	25	26524. 77	$a\ ^5G_4 - y\ ^3G_5^0$
3768. 733	50	26526. 61	$a\ ^5G_3 - x\ ^5G_3^0$
3768. 60	20	26527. 54	$a\ ^5G_3 - y\ ^3G_3^0$
3768. 237	100	26530. 10	$a\ ^5G_2 - x\ ^5G_2^0$
3768. 08	50*w*	26531. 20	$s\ ^5G_5 - y\ ^3G_4^0$ $a\ ^5G_5 - y\ ^3G_5^0$ $a\ ^5G_4 - y\ ^3G_5^0$ $a\ ^5G_4 - y\ ^3G_4^0$ $a\ ^5G_2 - y\ ^3G_3^0$
3767. 433	45	26535. 76	$a\ ^5G_6 - y\ ^3G_5^0$
3766. 99	2	26538. 88	$d\ ^3F_4 - q\ ^3H_4^0$
3766. 56	5	26541. 91	
3766. 38	5	26543. 18	
3765. 82	2	26547. 13	
3765. 69	2	26548. 04	$b\ ^3D_3 - t\ ^3G_3^0$
3764. 605	10*w*	26555. 69	
3763. 28	2	26565. 04	$d\ ^3F_3 - q\ ^3H_4^0$
3762. 51	3*w*	26570. 48	$a\ ^3D_3 - v\ ^3F_4^0$
3761. 39	10	26578. 39	$b\ ^3D_3 - t\ ^3G_4^0$
3760. 28	3	26586. 24	$b\ ^5D_3 - w\ ^3F_2^0$
3759. 49	3*w*	26591. 82	
3759. 24	6*w*	26593. 59	$a\ ^3P_1 - w\ ^3D_1^0$
3758. 713	6	26597. 32	$a\ ^5S_2 - z\ ^3P_2^0$
3758. 60	3	26598. 12	
3758. 043	50	26602. 06	$a\ ^5G_4 - x\ ^5G_3^0$
3757. 659	100	26604. 78	$a\ ^5G_3 - x\ ^5G_3^0$
3757. 49	3	26605. 98	$a\ ^5F_1 - r\ ^5D_0^0$
3757. 168	40	26608. 26	$a\ ^5G_2 - x\ ^5G_3^0$
3756. 81	2	26610. 79	$a\ ^5P_2 - x\ ^3P_2^0$
3756. 50	4*w*	26612. 99	
3755. 816	15	26617. 83	$a\ ^5P_3 - x\ ^3P_2^0$
3754. 90	2	26624. 33	
3753. 89	3	26631. 49	
3752. 84	1*w*	26638. 94	
3752. 72	5*w*	26639. 80	$a\ ^5F_2 - r\ ^5D_1^0$
3752. 33	4*ws*	26642. 56	$a\ ^5F_1 - r\ ^5D_1^0$
3751. 778	4	26646. 48	$b\ ^5D_2 - w\ ^3F_3^0$
3751. 205	10	26650. 55	$b\ ^5D_2 - w\ ^3F_2^0$
3750. 79	1	26653. 50	
3750. 14	1	26658. 12	
3749. 73	2*w*	26661. 04	
3749. 00	100	26666. 23	$a\ ^5G_5 - x\ ^5G_4^0$ $a\ ^5G_4 - x\ ^5G_4^0$
3748. 61	35	26669. 00	$a\ ^5G_3 - x\ ^5G_4^0$
3748. 17	2	26672. 13	$a\ ^3P_1 - w\ ^3D_2^0$
3747. 84	1	26674. 48	$a\ ^5P_3 - x\ ^3G_3^0$
3747. 25	15, *Z*	26678. 68	$b\ ^1I_6 - x\ ^1I_6$
3746. 92	1	26681. 03	$c\ ^3D_3 - s\ ^3D_3^0$
3746. 37	4	26684. 95	
3745. 08	3	26694. 14	$c\ ^3D_2 - s\ ^3D_2^0$
3744. 95	5	26695. 07	$c\ ^3D_2 - s\ ^3D_3^0$
3744. 83	1	26695. 92	
3744. 492	30	26698. 33	$a\ ^5G_5 - x\ ^5G_5^0$
3744. 33	2*w*	26699. 49	$a\ ^5F_3 - r\ ^5D_2^0$
3743. 887	125	26702. 65	$a\ ^5G_6 - x\ ^5G_5^0$
3743. 57	100	26704. 91	$a\ ^5G_5 - x\ ^5G_5^0$ $a\ ^5G_4 - x\ ^5G_5^0$
3742. 97	30, *Z*	26709. 18	$a\ ^5G_6 - x\ ^5G_5^0$
3742. 43	2	26713. 04	
3742. 05	7	26715. 75	$a\ ^3D_3 - u\ ^3F_3^0$
3741. 99	4	26716. 18	
3740. 13	3	26729. 46	
3739. 81	3	26731. 76	$b\ ^3G_3 - q\ ^3F_3^0$
3738. 95	3	26737. 90	
3736. 444	10	26755. 83	$b\ ^5D_2 - w\ ^3F_2^0$
3735. 23	2*w*	26764. 53	$c\ ^3G_5 - p\ ^3H_4^0$
3735. 11	2*w*	26765. 39	$b\ ^1I_6 - v\ ^3I_5^0$
3734. 52	4	26769. 62	$a\ ^5F_4 - r\ ^5D_3^0$
3734. 254	3	26771. 52	$c\ ^3D_1 - s\ ^3D_1^0$
3733. 85	10	26774. 42	$a\ ^5F_5 - s\ ^3F_4^0$
3733. 439	10	26777. 37	$b\ ^5D_4 - w\ ^3F_4^0$
3732. 98	1*w*	26780. 67	
3732. 63	3*w*	26783. 18	$a\ ^5F_3 - r\ ^5D_2^0$
3732. 03	50	26787. 48	$a\ ^7S_3 - z\ ^5P_3^0$
3731. 64	3*w*	26790. 28	$a\ ^5F_4 - s\ ^3F_4^0$
3730. 805	50	26796. 27	$a\ ^7S_3 - z\ ^5P_2^0$
3729. 86	2*w*	26803. 06	$a\ ^5F_3 - s\ ^3F_3^0$
3729. 26	2*w*	26807. 37	$a\ ^5F_2 - s\ ^3F_2^0$
3728. 86	3	27810. 25	$a\ ^5F_1 - s\ ^3F_2^0$
3728. 289	2	26814. 35	$a\ ^5D_3 - v\ ^3D_3^0$
3726. 845	6	26824. 75	$a\ ^5F_4 - s\ ^3F_3^0$
3725. 934	6*w*	26831. 31	
3724. 93	3*w*	26838. 54	$a\ ^5F_3 - s\ ^3F_3^0$
3723. 69	3*w*	26847. 47	$a\ ^5F_2 - s\ ^3F_2^0$
3723. 496	8*w*	26848. 87	
3722. 818	10	26853. 76	
3721. 825	2	26860. 93	
3719. 45	3*w*	26878. 08	$b\ ^3H_5 - r\ ^3H_4^0$
3718. 57	5	26884. 44	$c\ ^3D_2 - p\ ^3F_2^0$
3718. 01	1*w*	26888. 49	
3717. 76	6	26890. 30	$b\ ^5D_1 - w\ ^3P_0^0$
3717. 63	3	26891. 23	
3717. 58	7	26891. 60	$b\ ^3H_4 - r\ ^3H_4^0$
3716. 52	20*w*	26899. 27	$c\ ^3F_4 - r\ ^3H_4^0$ $a\ ^5F_5 - r\ ^5D_4^0$
3714. 39	7*w*	26914. 69	$a\ ^5F_4 - r\ ^5D_4^0$
3712. 52	2	26928. 25	$a\ ^5F_3 - r\ ^5D_3^0$
3711. 61	4	26934. 85	
3711. 55	2	26935. 29	$b\ ^1G_4 - p\ ^3G_4^0$
3710. 59	10	26942. 25	$a\ ^3P_0 - w\ ^3D_1^0$
3710. 15	6	26945. 45	
3710. 08	10	26945. 96	$b\ ^3H_5 - r\ ^3H_5^0$
3709. 94	5	26946. 97	$b\ ^5D_2 - w\ ^3P_1^0$
3708. 05	2	26960. 71	$b\ ^3D_1 - w\ ^3P_1^0$
3707. 85	2	26962. 16	
3706. 908	10	26969. 02	$b\ ^3H_6 - r\ ^3H_5^0$
3706. 82	4	26969. 65	$b\ ^5D_0 - w\ ^3P_1^0$
3705. 94	4*w*	26976. 06	
3705. 75	2	26977. 44	
3705. 075	5	26982. 36	$b\ ^3G_3 - w\ ^3H_3^0$ $b\ ^5D_3 - w\ ^3P_2^0$
3704. 91	5	26983. 56	$b\ ^3G_5 - z\ ^1I_6^0$
3704. 64	4	26985. 52	
3702. 664	2	26999. 93	$b\ ^5D_1 - w\ ^3P_2^0$

TABLE 1. *Wavelengths and term combinations of* Cr I—Continued

d, D[illegible]; *h*, hazy; *H*, very hazy; *l*, shaded longward; *s*, shaded shortward; *r*, reversed; *R*, strongly reversed; *w*, wide; *W*, very wide; *Z*, Zeeman pattern in table 2.

Wavelength λ_{air}	Intensity	Wave No.	Term combination
3702.158	2	27003.62	$a\ ^3H_5 - w\ ^3F_4^\circ$
3701.33	1*h*	27009.66	
3700.395	2	27016.48	$a\ ^3H_4 - w\ ^3F_3^\circ$
3700.088	1	27018.73	$b\ ^3H_5 - r\ ^3H_5^\circ$
3699.12	1*hl*	27025.79	$c\ ^3D_3 - p\ ^3F_4^\circ$; $a\ ^3G_5 - t\ ^5D_4^\circ$
3698.18	4	27032.59	$b\ ^3G_4 - w\ ^3H_4^\circ$
3697.45	2*wl*	27038.00	
3697.15	1*w*	27040.19	
3696.70	3*w*	27043.48	
3695.86	10	27049.63	$b\ ^3G_5 - v\ ^3H_6^\circ$
3694.65	1	27058.49	
3694.124	10	27062.34	$a\ ^5G_5 - z\ ^3I_5^\circ$; $a\ ^5G_4 - z\ ^3I_5^\circ$
3693.57	2	27066.40	$a\ ^5G_6 - z\ ^3I_6^\circ$
3693.09	15	27069.92	$b\ ^3G_5 - w\ ^3H_6^\circ$
3692.72	1*wh*	27072.63	$z\ ^7D_5^\circ - e\ ^5F_4$
3689.65	15, *Z*	27095.15	$b\ ^3G_4 - w\ ^3H_5^\circ$
3689.315	18	27097.62	$a\ ^5G_4 - x\ ^5H_5^\circ$
3688.98	1	27100.07	$a\ ^5G_3 - x\ ^5H_4^\circ$
3688.47	25	27103.82	$a\ ^5G_2 - x\ ^5H_3^\circ$
3688.12	12	27106.40	$a\ ^5G_3 - z\ ^3I_6^\circ$
3687.58	20	27110.36	$a\ ^5G_3 - v\ ^5F_2^\circ$
3687.32	20	27112.28	$a\ ^5G_2 - v\ ^5F_1^\circ$
3687.25	25	27112.79	$a\ ^5G_4 - v\ ^5F_3^\circ$
3687.07	7	27114.11	$b\ ^3D_1 - s\ ^3F_2^\circ$; $a\ ^5G_2 - v\ ^5F_2^\circ$; $a\ ^5G_3 - v\ ^5F_3^\circ$
3686.82	60*w*	27115.95	$a\ ^5G_5 - v\ ^5F_4^\circ$; $a\ ^5G_4 - v\ ^5F_4^\circ$
3686.41	2*w*	27118.97	$a\ ^5G_2 - v\ ^5F_3^\circ$; $a\ ^5G_3 - v\ ^5F_4^\circ$
3686.16	10*w*	27120.81	$a\ ^5G_5 - v\ ^5F_5^\circ$; $a\ ^5G_4 - v\ ^5F_5^\circ$
3685.57	70*w*	27125.15	$a\ ^5G_6 - v\ ^5F_5^\circ$
3685.25	5*w*	27127.50	
3684.98	8*w*	27129.49	
3684.31	2	27134.43	$b\ ^3D_2 - s\ ^3F_2^\circ$; $a\ ^3G_4 - t\ ^5D_3^\circ$
3683.66	10	27139.21	$b\ ^3G_3 - w\ ^3H_4^\circ$
3683.17	2	27142.82	$c\ ^3D_2 - r\ ^3G_3^\circ$; $a\ ^3P_1 - u\ ^5D_2^\circ$
3682.30	2	27149.24	$a\ ^3P_1 - u\ ^5D_0^\circ$
3681.69	22, *Z*	27153.74	$a\ ^3P_2 - w\ ^3P_1^\circ$
3680.99	10	27158.90	$b\ ^3D_3 - s\ ^3F_4^\circ$
3680.19	12	27164.80	$a\ ^5G_5 - x\ ^5H_4^\circ$; $a\ ^5G_4 - x\ ^5H_4^\circ$
3679.81	18	27167.61	$a\ ^5G_2 - x\ ^5H_4^\circ$
3679.074	20	27173.04	$a\ ^5G_6 - z\ ^3I_7^\circ$
3678.88	6	27174.48	$b\ ^3D_2 - s\ ^3F_3^\circ$
3677.24	1	27186.60	$a\ ^5P_3 - x\ ^3D_3^\circ$
3677.00	2	27188.37	$c\ ^3D_3 - r\ ^3G_4^\circ$
3676.321	25, *Z*	27193.39	$a\ ^3P_2 - w\ ^3P_2^\circ$; $b\ ^3D_2 - s\ ^3F_3^\circ$
3676.14	5*w*	27194.73	
3673.732	2	27212.56	$b\ ^3F_4 - q\ ^3F_3^\circ$
3673.68	2	27212.94	$b\ ^3F_2 - q\ ^3F_2^\circ$
3673.58	6	27213.68	$b\ ^3G_2 - v\ ^3H_4^\circ$
3671.93	4	27225.91	$b\ ^3G_4 - v\ ^3H_5^\circ$
3670.66	5	27235.33	
3669.19	2	27246.24	$b\ ^3H_4 - q\ ^3H_4^\circ$
3668.13	1	27254.12	$b\ ^3F_4 - q\ ^3F_4^\circ$
3668.03	20	27254.86	$a\ ^5G_2 - v\ ^5D_1^\circ$
3667.36	2	27259.83	$b\ ^3H_5 - q\ ^3H_5^\circ$
3666.63	50	27265.26	$a\ ^5G_3 - v\ ^5D_2^\circ$; $b\ ^3F_3 - q\ ^3F_3^\circ$
3666.18	20	27268.60	$a\ ^5G_2 - v\ ^5D_2^\circ$
3665.981	30	27270.02	$a\ ^5G_5 - x\ ^5H_5^\circ$; $a\ ^5G_4 - x\ ^5H_5^\circ$
3665.426	10	27274.22	$a\ ^5G_6 - x\ ^5H_5^\circ$; $b\ ^3H_4 - q\ ^3H_5^\circ$
3664.163	2	27283.62	$b\ ^3D_3 - r\ ^5D_4^\circ$
3663.206	40	27290.75	$a\ ^5G_4 - v\ ^5D_3^\circ$
3662.836	25	27293.50	$a\ ^5G_3 - v\ ^5D_3^\circ$
3662.376	5	27296.93	$a\ ^5G_2 - v\ ^5D_2^\circ$
3661.43	6	27303.98	$b\ ^3G_5 - u\ ^3F_4^\circ$
3661.227	7	27305.50	
3659.976	3	27314.83	
3659.91	1	27315.32	
3656.97	4	27337.28	$z\ ^7D_4^\circ - g\ ^5D_3$
3656.26	100	27342.59	$a\ ^5G_5 - v\ ^5D_4^\circ$; $a\ ^5G_4 - v\ ^5D_4^\circ$
3655.858	5	27345.82	$a\ ^5G_3 - v\ ^5D_4^\circ$
3653.916	100, *Z*	27360.13	$a\ ^5G_2 - u\ ^5F_1^\circ$
3652.61	2*w*	27369.91	$a\ ^5F_2 - u\ ^3D_1^\circ$
3652.04	2	27374.19	
3651.36	2	27379.28	
3650.83	1*w*	27383.26	
3650.76	1*w*	27383.78	$z\ ^7D_5^\circ - g\ ^5D_4$
3650.47	3	27385.96	
3649.863	20	27390.51	$b\ ^3G_5 - v\ ^3F_4^\circ$
3648.993	75	27397.04	$a\ ^5G_3 - u\ ^5F_2^\circ$
3648.534	40	27400.49	$a\ ^5G_2 - u\ ^5F_2^\circ$
3647.15	3*w*	27410.89	
3646.68	2	27414.42	$a\ ^3F_4 - y\ ^3I_5^\circ$
3646.158	30	27418.35	$a\ ^5G_5 - x\ ^5H_6^\circ$
3645.581	12	27422.69	$a\ ^5G_6 - x\ ^5H_6^\circ$
3641.84	85	27450.85	$a\ ^5G_4 - u\ ^5F_4^\circ$
3641.466	30	27453.67	$a\ ^5G_3 - u\ ^5F_3^\circ$
3641.011	6	27457.10	$a\ ^5G_2 - u\ ^5F_2^\circ$
3640.384	30	27461.83	$a\ ^5G_5 - u\ ^5F_5^\circ$; $a\ ^5G_4 - u\ ^5F_5^\circ$
3639.80	200*R*	27466.24	$a\ ^5G_6 - u\ ^5F_5^\circ$
3638.38	2*h*	27476.96	
3637.96	3*w*	27480.13	
3637.82	2*w*	27481.19	$c\ ^3D_1 - t\ ^3P_0^\circ$
3637.61	2*w*	27482.77	
3636.87	5	27488.37	
3636.588	100	27490.50	$a\ ^5G_5 - u\ ^5F_4^\circ$; $a\ ^5G_4 - u\ ^5F_4^\circ$
3636.193	5	27493.49	$a\ ^5G_3 - u\ ^5F_4^\circ$
3635.281	30	27500.39	$a\ ^7S_3 - z\ ^7D_3^\circ$
3634.996	20	27502.53	$b\ ^3F_4 - s\ ^3D_3^\circ$
3633.976	3	27510.25	
3633.314	4	27515.27	
3632.832	75	27518.92	$a\ ^5G_5 - t\ ^5F_4^\circ$; $a\ ^5G_4 - t\ ^5F_4^\circ$
3632.444	4	27521.86	$a\ ^5G_3 - t\ ^5F_4^\circ$
3629.389	6	27545.02	
3628.299	3	27553.30	$a\ ^3G_5 - y\ ^3I_5^\circ$
3628.054	7	27555.16	$b\ ^3F_2 - s\ ^3D_3^\circ$
3626.335	10	27568.22	
3626.208	12	27569.19	$b\ ^3F_3 - s\ ^3D_2^\circ$

TABLE 1. *Wavelengths and term combinations of* Cr I—Continued

d, Double; *h*, hazy; *H*, very hazy; *l*, shaded longward; *s*, shaded shortward; *r*, reversed; *R*, strongly reversed; *w*, wide; *W*, very wide; *Z*, Zeeman pattern in table 2.

Wavelength λ_{air}	Intensity	Wave No.	Term combination
3625.57	1*w*	27574.04	
3623.49	5	27589.86	$b\ ^3F_2 - s\ ^3D_3^1$
3623.25	2	27591.69	$c\ ^3D_2 - t\ ^3P_1^1$
3620.00	6	27616.46	
3619.46	30	27620.58	$a\ ^3G_5 - x\ ^5H_5^0$ $c\ ^3D_1 - t\ ^3P_1^1$
3618.332	8	27629.20	$a\ ^5P_2 - y\ ^3S_1^1$
3617.947	2	27632.14	
3617.37	2*wh*	27636.54	
3617.159	4	27638.16	$b\ ^3F_2 - s\ ^3D_1^1$
3615.646	40, *Z*	27649.72	$a\ ^7S_3 - z\ ^7D_4^1$
3615.075	3*wh*	27654.09	
3614.506	4	27658.03	
3613.66	20	27664.91	$a\ ^3P_1 - w^3P_0^1$
3612.606	35, *Z*	27672.98	$a\ ^3I_5 - t\ ^3H_4^1$
3611.48	2	27681.61	$a\ ^3G_3 - 2_3^1$
3610.043	35	27692.63	$a\ ^5G_2 - t\ ^5F_1^1$
3609.483	40	27696.92	$a\ ^5G_3 - t\ ^5F_2^1$
3609.10	1	27699.87	$b\ ^3G_3 - y\ ^1I_5^1$
3609.025	10	27700.44	$a\ ^5G_2 - t\ ^5F_3^1$
3608.407	30, *Z*	27705.19	$a\ ^3I_4 - t\ ^3H_5^1$
3608.05	2	27707.93	$a\ ^3F_4 - x\ ^3H_4^1$
3605.320	1000*R*, *Z*	27728.91	$a\ ^7S_3 - y\ ^7P_2^1$
3604.92	8	27731.98	$b\ ^5D_2 - t\ ^5D_3^1$ $a\ ^5P_1 - t\ ^5P_1^1$
3604.536	7	27734.94	$a\ ^5G_2 - t\ ^5F_2^1$ $a\ ^3P_1 - w^3P_1^1$
3603.74	20	27741.06	$a\ ^5P_2 - t\ ^5P_1^1$ $a\ ^5P_1 - t\ ^5P_2^1$
3602.571	22	27750.06	$a\ ^5P_2 - t\ ^5P_2^1$
3601.655	75, *Z*	27757.12	$a\ ^5P_3 - t\ ^5P_3^1$
3601.22	2	27760.48	$b\ ^5D_3 - t\ ^5D_4^1$
3600.88	1	27763.10	$b\ ^5D_3 - t\ ^5D_2^1$
3600.67	2	27764.72	$a\ ^5G_4 - y\ ^3H_4^1$
3599.396	30, *Z*	27774.54	$a\ ^3P_1 - w^3P_2^1$
3598.668	4	27780.16	$a\ ^5P_3 - x\ ^3F_4^1$
3598.57	3	27780.92	
3598.04	1	27785.01	
3595.755	4	27802.67	$a\ ^5P_2 - x\ ^3F_3^1$ $a\ ^5D_3 - z\ ^3F_3^1$
3594.31	8	27813.84	
3593.481	2000*R*, *Z*	27820.26	$a\ ^7S_3 - y\ ^7P_3^1$
3590.33	7*wh*	27844.68	$z\ ^5P_1^1 - g\ ^5D_0$ $z\ ^7F_3^1 - e\ ^7G_3$
3588.726	3	27857.12	$a\ ^3F_3 - x\ ^3H_4^1$
3587.01	1*w*	27870.45	$z\ ^5P_1^1 - g\ ^5D_1$
3586.23	8	27876.51	$a\ ^3G_5 - x\ ^3H_5^0$ $b\ ^3G_3 - u\ ^3F_3^1$
3584.337	15*WH*	27891.24	$z\ ^7F_5^1 - e\ ^7G_7$
3583.74	3*wh*	27895.88	$b\ ^3D_3 - t\ ^3D_3^1$
3582.613	25, *Z*	27904.65	$a\ ^5D_4 - z\ ^5F_4^1$
3582.15	4	27908.26	$a\ ^1I_6 - x\ ^1H_5^1$
3581.42	2	27913.95	
3578.682	3000*R*, *Z*	27935.30	$a\ ^7S_3 - y\ ^7P_4^1$
3574.947	25	27964.49	$a\ ^5P_2 - t\ ^5P_3^1$
3574.796	30, *Z*	27965.67	$a\ ^5P_1 - y\ ^5S_2^1$
3574.66	7*H*	27966.73	
3574.38	10*H*	27968.93	$z\ ^7F_5^1 - e\ ^7G_6$
3574.042	35	27971.57	$b\ ^3H_4 - p\ ^3H_4^1$ $a\ ^5P_3 - t\ ^5P_3^1$
3573.636	40	27974.75	$a\ ^5P_2 - y\ ^5S_2^1$
3573.00	2	27978.00	$z\ ^7F_3^1 - e\ ^7F_4$
3572.74	30	27981.76	$a\ ^5P_2 - y\ ^5S_2^1$
3571.97	6	27987.80	$a\ ^3G_4 - x\ ^3H_3^1$
3571.65	1*h*	27990.30	
3571.13	2	27994.38	$c\ ^3D_2 - q\ ^3G_3^1$ $a\ ^5G_2 - x\ ^3G_3^1$
3570.99	1	27995.47	$c\ ^3D_2 - q\ ^3G_3^1$
3570.24	6	28001.36	
3569.37	1*w*	28008.18	$a\ ^3H_5 - t\ ^5D_4^1$
3569.143	10	28009.96	$b\ ^3F_4 - r\ ^3G_4^1$
3568.37	5*w*	28016.03	$z\ ^5D_3^1 - e\ ^5P_2$ $z\ ^5D_2^1 - e\ ^5P_1$
3568.29	2*w*	28016.66	$z\ ^5P_1^1 - g\ ^5D_2$ $z\ ^7F_5^1 - h\ ^7D_4$
3567.57	3*wh*	28022.31	$z\ ^5P_3^1 - g\ ^5D_2$ $z\ ^7F_3^1 - e\ ^7G_3$
3566.11	20*WH*	28033.78	$z\ ^7F_4^1 - e\ ^7G_3$ $z\ ^5D_4^1 - e\ ^5P_3$
3565.547	5	28038.21	$a\ ^5G_5 - x\ ^3G_4^1$ $a\ ^5G_4 - x\ ^3G_3^1$ $b\ ^3F_2 - r\ ^3G_3^1$
3565.153	10	28041.31	$a\ ^5G_2 - x\ ^3G_4^1$
3565.08	2	28041.88	$c\ ^3D_3 - q\ ^3G_4^1$
3564.942	10	28042.97	$b\ ^3H_5 - p\ ^3H_5^1$
3564.708	18	28044.81	
3564.286	15	28048.14	$b\ ^3F_4 - r\ ^3G_5^1$
3563.18	1*w*	28056.83	$b\ ^3H_4 - p\ ^3H_4^1$
3562.87	5*w*	28059.28	$z\ ^7F_2^1 - e\ ^7G_1$
3562.465	8	28062.47	$b\ ^3F_3 - r\ ^3G_4^1$
3562.281	8, *Z*	28063.91	$b\ ^3H_6 - p\ ^3H_6^1$
3561.766	2*w*	28067.97	
3560.94	3*wh*	28074.49	$z\ ^7F_3^1 - e\ ^7F_2$
3560.43	3*wh*	28078.50	$z\ ^7F_3^1 - h\ ^7D_2$ $z\ ^7F_3^1 - h\ ^7D_3$
3560.31	5	28079.45	
3559.777	20, *Z*	28083.65	$a\ ^3P_0 - w\ ^3P_1^1$
3559.19	2*H*	28089.08	$z\ ^7F_2^1 - e\ ^7G_2$
3558.80	1	28091.36	$b\ ^3G_5 - u\ ^3H_6^1$
3558.57	10*WH*	28093.19	$z\ ^7F_3^1 - e\ ^7G_4$
3558.30	3*H*	28095.31	
3556.93	3*w*	28106.13	$z\ ^7F_2^1 - h\ ^7D_1$
3556.73	3	28107.71	
3556.131	9	28112.45	$a\ ^5G_4 - 1_3^1$
3556.00	1*w*	28113.48	$b\ ^3D_2 - u\ ^3D_3^1$ $b\ ^3H_5 - p\ ^3H_6^1$
3555.783	10	28115.20	$a\ ^5G_3 - 1_3^1$
3555.597	8	28116.67	$a\ ^5D_2 - z\ ^3F_3^1$
3555.34	5	28118.70	$a\ ^5G_2 - 1_2^1$
3554.78	3	28123.13	$a\ ^3D_1 - v\ ^3P_0^1$
3554.39	1*h*	28126.22	$z\ ^7F_2^1 - e\ ^7F_1$
3553.955	10	28129.66	$a\ ^3G_3 - x\ ^3H_4^1$ $b\ ^3P_2 - u\ ^3F_3^1$
3552.95	7*w*	28137.62	$z\ ^7F_1^1 - e\ ^7G_1$
3552.72	5*WH*	28139.44	$z\ ^7F_2^1 - e\ ^7G_2$
3552.177	2	28143.74	
3551.46	2	28149.42	
3550.63	20*w*, *Z*	28156.00	$z\ ^7F_5^1 - e\ ^7F_6$

TABLE 1. *Wavelengths and term combinations of* Cr I—Continued

d, [illegible]; *h*, hazy; *H*, very hazy; *l*, shaded longward; *s*, shaded shortward; *r*, reversed; *R*, strongly reversed; *w*, wide; *W*, very wide; *Z*, Zeeman pattern in table 2.

Wavelength λ_{air}	Intensity	Wave No.	Term combination
3550. 50	4*w*	28157. 03	$z\ ^7F^0_5 - e\ ^7F_5$
3549. 25	4*wh*	28166. 95	$z\ ^7F^0_1 - e\ ^7G_2$ $z\ ^7F^0_2 - e\ ^7F_4$
3548. 89	4*wh*	28169. 80	$z\ ^7F^0_3 - h\ ^7D_4$
3548. 718	4	28171. 17	$b\ ^3G_4 - u\ ^3H^0_5$
3547. 97	6*wh*	28177. 11	$z\ ^7F^0_5 - e\ ^7G_1$
3547. 79	3	28178. 54	$z\ ^5D^0_3 - e\ ^5P_3$
3547. 76	3*wh*	28178. 78	$z\ ^7F^0_3 - e\ ^7F_3$
3547. 04	2*w*	28184. 50	$z\ ^7F^0_1 - h\ ^7D_2$
3546. 28	2*wh*	28190. 54	$z\ ^7F^0_2 - e\ ^7F_2$ $z\ ^5P^0_3 - g\ ^5D_3$
3545. 71	2*wh*	28195. 07	$z\ ^7F^0_2 - h\ ^7D_3$
3545. 19	1*w*	28199. 20	$z\ ^5P^0_3 - g\ ^5D_3$
3544. 94	1*w*	28201. 20	
3544. 51	1*w*	28204. 62	$z\ ^7F^0_1 - e\ ^7F_1$
3544. 46	2	28205. 02	
3543. 70	1*w*	28211. 06	
3543. 525	3	28212. 46	
3542. 127	2	28223. 59	
3541. 499	2*w*	28228. 66	$b\ ^3P_2 - v\ ^3D^0_3$
3540. 684	2	28235. 10	
3539. 913	6	28241. 24	$b\ ^3G_4 - y\ ^1H^0_5$
3539. 44	1	28245. 02	
3539. 223	2	28246. 75	
3538. 736	4	28250. 64	$b\ ^3P_2 - u\ ^3F^0_3$
3537. 56	1	28260. 03	
3537. 253	12*l*	28262. 48	$a\ ^5G_3 - x\ ^3G^0_3$ $a\ ^5G_4 - x\ ^3G^0_5$
3536. 894	5	28265. 35	
3536. 77	4	28266. 33	$a\ ^5G_6 - x\ ^3G^0_5$
3536. 50	5*wh*	28268. 50	$z\ ^7F^0_4 - h\ ^7D_5$ $z\ ^7F^0_1 - e\ ^7F_2$
3534. 05	1	28288. 10	
3532. 89	12, *Z*	28297. 38	$b\ ^3P_1 - u\ ^3F^0_2$
3532. 63	2*wh*	28299. 46	
3531. 442	12	28308. 98	$b\ ^3D_1 - r\ ^3F^0_2$
3531. 09	10	28311. 80	
3529. 17	1	28327. 21	$a\ ^5P_1 - w\ ^3D^0_2$
3528. 87	1	28329. 61	$b\ ^3D_2 - r\ ^3F^0_2$
3528. 56	2	28332. 10	
3528. 055	5	28336. 16	$a\ ^5P_2 - w\ ^3D^0_3$
3527. 18	1*h*	28343. 19	$a\ ^5P_3 - w\ ^3D^0_3$
3527. 09	10*wh*	28343. 91	$a\ ^1I_6 - x\ ^1I^0_6$
3527. 04	4*wh*	28344. 31	
3525. 47	5*wh*	28356. 94	
3524. 51	6	28364. 66	
3523. 582	7	28372. 12	
3522. 958	7	28377. 15	
3522. 83	2*wh*	28378. 18	$z\ ^7F^0_3 - e\ ^7F_4$
3521. 523	3	28388. 72	$b\ ^3D_2 - r\ ^3F^0_3$
3519. 70	2*h*	28403. 42	
3519. 445	2	28405. 48	$a\ ^3D_2 - u\ ^3P^0_2$
3519. 10	1*w*	28408. 26	$a\ ^3D_1 - u\ ^3P^0_2$ $b\ ^3D_2 - r\ ^3F^0_2$
3518. 40	3, *Z*	28413. 91	$a\ ^3D_2 - p\ ^5F^0_1$
3518. 08	1	28416. 50	$a\ ^5P_2 - w\ ^3D^0_3$ $a\ ^3D_1 - p\ ^5F^0_1$
3517. 82	1	28418. 60	$a\ ^3D_2 - p\ ^5F^0_2$
3517. 46	2	28421. 51	$a\ ^3D_1 - p\ ^5F^0_2$ $z\ ^5P^0_3 - g\ ^5D_4$
3517. 21	3	28423. 53	$a\ ^5P_3 - w\ ^3D^0_3$
3515. 645	2	28436. 18	
3513. 88	2*w*	28450. 46	$a\ ^3D_2 - u\ ^3P^0_2$ $a\ ^3D_2 - u\ ^3P^0_1$
3513. 52	2*h*	28453. 38	$a\ ^3D_1 - u\ ^3P^0_1$
3512. 70	2*w*	28460. 02	$a\ ^3D_3 - 4^0_3$
3512. 66	3	28460. 34	$a\ ^3H_6 - y\ ^3I^0_6$
3510. 534	30, *Z*	28477. 58	$a\ ^3H_6 - y\ ^3I^0_7$
3510. 425	3	28478. 46	$b\ ^3D_3 - r\ ^3F^0_4$
3510. 34	2*wh*	28479. 15	
3508. 83	7*w*	28491. 41	
3508. 09	10, *Z*	28497. 42	
3507. 223	4*w*	28504. 46	$a\ ^3D_2 - p\ ^3F^0_3$
3507. 06	1*h*	28505. 78	$a\ ^3D_3 - 4^0_3$
3506. 54	2	28510. 01	
3503. 87	1*wh*	28531. 73	
3503. 37	1	28536. 08	$a\ ^3H_5 - y\ ^3I^0_5$
3503. 053	2	28538. 39	$a\ ^3D_2 - t\ ^3F^0_2$
3502. 695	2*w*	28541. 31	$a\ ^3D_1 - t\ ^3F^0_2$
3502. 304	12	28544. 50	
3501. 68	3	28549. 58	$a\ ^3D_3 - p\ ^5F^0_3$
3501. 54	2	28551. 05	
3501. 42	3	28551. 70	
3496. 215	2	28594. 21	$a\ ^3D_2 - t\ ^3F^0_3$
3496. 02	7	28595. 80	
3494. 957	30, *Z*	28604. 50	$a\ ^3H_5 - y\ ^3I^0_4$
3493. 65	2*w*	28615. 20	$b\ ^3F_3 - t\ ^3P^0_2$
3492. 14	1	28627. 57	$a\ ^3F_4 - v\ ^3G^0_3$
3491. 15	1*w*	28635. 69	$b\ ^3F_2 - t\ ^3P^0_2$
3488. 445	18, *Z*	28657. 90	$a\ ^3H_4 - y\ ^3I^0_3$
3486. 472	12	28674. 11	
3485. 14	3	28685. 07	$a\ ^3H_6 - x\ ^3H^0_5$
3483. 901	4	28695. 27	
3483. 512	8	28698. 48	$a\ ^3D_3 - t\ ^3F^0_4$ $a\ ^3F_3 - v\ ^3G^0_3$
3481. 87	2	28712. 01	$b\ ^5D_2 - r\ ^5F^0_1$
3481. 541	22, *Z*	28714. 72	$a\ ^3H_6 - x\ ^3H^0_6$
3481. 301	25	28716. 70	$a\ ^5P_3 - u\ ^5D^0_4$
3480. 272	10	28725. 18	$b\ ^5D_1 - r\ ^5F^0_1$
3479. 335	2	28732. 93	
3479. 251	3	28733. 62	$b\ ^5D_3 - r\ ^5F^0_2$
3479. 122	12	28734. 69	$b\ ^5D_0 - r\ ^5F^0_1$
3478. 763	15	28737. 65	$b\ ^5D_2 - r\ ^5F^0_3$
3477. 243	8	28750. 21	$a\ ^3F_4 - v\ ^3G^0_4$
3477. 156	15	28750. 93	$a\ ^3I_5 - w\ ^3I^0_5$ $b\ ^5D_1 - r\ ^5F^0_2$
3476. 166	4, *Z*	28759. 12	
3474. 865	10	28769. 89	$b\ ^5D_2 - r\ ^5F^0_3$
3474. 373	12	28773. 96	
3473. 611	18	28780. 27	$a\ ^5P_2 - u\ ^5D^0_3$
3472. 902	15	28786. 15	$a\ ^3H_4 - 2$
3472. 764	18, *Z*	28787. 30	$a\ ^5P_3 - u\ ^5D^0_2$ $b\ ^5D_4 - r\ ^5F^0_5$
3471. 492	10	28797. 84	$a\ ^5P_1 - u\ ^5D^0_2$
3470. 865	4	28803. 04	$c\ ^3G_5 - p\ ^3G^0_5$
3470. 716	8	28804. 28	$a\ ^5P_1 - u\ ^5D^0_0$
3470. 528	12	28805. 84	$a\ ^5P_1 - u\ ^5D^0_1$
3470. 395	15	28806. 95	$a\ ^5P_2 - u\ ^5D^0_2$
3469. 588	20	28813. 64	$b\ ^5D_3 - r\ ^5F^0_4$ $a\ ^5P_3 - u\ ^5D^0_3$
3469. 434	8	28814. 92	$a\ ^5P_2 - u\ ^5D^0_1$
3469. 17	1	28817. 12	$b\ ^3F_4 - q\ ^3G^0_5$

TABLE 1. *Wavelengths and term combinations of* Cr I—Continued

d. Double; *h*, hazy; *H*, very hazy; *l*, shaded longward; *s*, shaded shortward; *r*, reversed; *R*, strongly reversed; *w*, wide; *W*, very wide; *Z*, Zeeman pattern in table 2

Wavelength λ_{air}	Intensity	Wave No.	Term combination	Wavelength λ_{air}	Intensity	Wave No.	Term combination
3468. 742	12, *Z*	28820. 67		3431. 993	15	29129. 27	$a\ ^5G_3-x\ ^3F_3^\circ$
3467. 713	22, *Z*	28829. 22	$a\ ^3H_5-x\ ^3H_5^\circ$	3431. 86	3	29130. 40	$a\ ^5F_2-q\ ^5D_1^\circ$
3467. 012	20	28835. 05	$b\ ^5D_4-r\ ^5F_4^\circ$ $a\ ^3I_6-w^3H_5^\circ$	3431. 694	10	29131. 81	$a\ ^5G_3-x\ ^3F_2^\circ$
3465. 571	12	28847. 05	$a\ ^5G_4-w^3G_4^\circ$	3431. 582	5	29132. 75	$a\ ^5G_2-x\ ^3F_1^\circ$
3465. 248	25	28849. 81	$a\ ^5G_3-w^3G_3^\circ$ $c\ ^3G_4-p\ ^3G_4^\circ$	3431. 278	20	29135. 34	$a\ ^5G_2-x\ ^3F_2^\circ$
				3430. 15	1	29144. 92	
3465. 06	3	28851. 30		3429. 06	2	29154. 18	
3464. 825	10	28853. 25	$a\ ^5G_2-w^3G_3^\circ$	3427. 65	5	29166. 17	
3463. 616	7	28863. 33	$b\ ^3F_4-q\ ^3G_4^\circ$	3427. 62	5	29166. 43	
3463. 511	5	28864. 20	$a\ ^3F_2-v\ ^3G_3^\circ$				
3462. 894	5	28869. 34	$b\ ^3F_3-q\ ^3G_3^\circ$	3425. 97	12	29180. 48	$a\ ^3G_4-v\ ^3G_3^\circ$
				3424. 46	1*w*	29193. 34	
3462. 237	2	28874. 82	$z\ ^5D_1^\circ-f\ ^5G_2$ $a\ ^5D_2-t\ ^3G_3^\circ$	3423. 178	7	29204. 28	$b\ ^3D_1-q\ ^3F_2^\circ$
				3423. 047	7	29205. 40	
3460. 426	35	28889. 93	$b\ ^3F_2-q\ ^3G_3^\circ$ $b\ ^5D_4-r\ ^5F_5^\circ$	3421. 71	5	29216. 80	$b\ ^3G_5-u\ ^3G_4^\circ$
3459. 14	3	28900. 67	$a\ ^3F_4-v\ ^3G_4^\circ$				
3458. 34	4	28907. 35	$a\ ^3H_5-x\ ^3H_4^\circ$	3421. 67	3	29217. 15	
3458. 085	18	28909. 48	$a\ ^3I_7-w^3I_7^\circ$	3421. 45	3	29219. 03	$a\ ^5P_2-w\ ^3F_3^\circ$
				3421. 02	2	29222. 78	$a\ ^3F_3-q\ ^5F_3^\circ$
3456. 31	1	28924. 41	$b\ ^3F_4-q\ ^3G_3^\circ$	3419. 89	3*w*	29232. 35	
3455. 607	50	28930. 22	$a\ ^5G_5-w^3G_4^\circ$ $a\ ^5G_4-w^3G_3^\circ$	3419. 66	2*w*	29234. 32	$a\ ^5F_5-q\ ^5D_4^\circ$
3455. 273	20	28933. 01	$a\ ^5G_3-w^3G_4^\circ$	3418. 81	1*w*	29241. 59	$b\ ^5D_2-s\ ^5D_2^\circ$
3453. 737	20	28945. 88	$a\ ^5G_2-w^3G_3^\circ$	3418. 667	1	29242. 81	
3453. 328	40	28949. 31	$a\ ^5G_2-w^3G_2^\circ$	3417. 98	2	29248. 67	
				3415. 58	1*w*	29269. 24	
3453. 217	10	28950. 24	$a\ ^3D_3-t\ ^3G_4^\circ$ $a\ ^3I_5-x\ ^1H_5^\circ$	3415. 311	7, *Z*	29271. 55	$b\ ^3G_5-u\ ^3G_5^\circ$
3452. 60	1	28955. 41	$a\ ^3F_4-s\ ^5P_3^\circ$				
3452. 48	1	28956. 42	$a\ ^3I_6-x\ ^1H_5^\circ$	3414. 35	1*w*	29279. 79	
3450. 811	10, *Z*	28970. 42		3414. 089	2	29282. 02	$b\ ^3G_4-u\ ^3G_3^\circ$
3449. 10	1	28984. 80		3412. 264	8, *Z*	29297. 69	$b\ ^3D_2-q\ ^3F_3^\circ$
				3411. 02	10*w*	29308. 37	
3448. 188	8	28992. 46		3410. 03	1	29316. 88	$b\ ^3D_3-q\ ^3F_3^\circ$
3447. 762	35	28996. 04	$a\ ^5G_4-w^5G_3^\circ$				
3447. 426	40	28998. 87	$a\ ^5G_3-w^5G_3^\circ$	3409. 76	1	29319. 20	$a\ ^5P_1-w^3P_0^\circ$
3447. 012	25	29002. 35	$a\ ^5G_2-w^5G_2^\circ$	3409. 37	6*w*	29322. 55	
3446. 03	1	29010. 62	$a\ ^5F_3-q\ ^5D_3^\circ$	3408. 94	7	29326. 25	
				3408. 66	2	29328. 66	$a\ ^5F_2-o\ ^5F_1^\circ$
3445. 604	50	29014. 20	$a\ ^5G_3-w^3G_3^\circ$ $a\ ^5G_4-w^3G_4^\circ$	3408. 56	2	29329. 52	$b\ ^3G_4-u\ ^3G_4^\circ$
3445. 097	15	29018. 48	$a\ ^5G_3-w^3G_3^\circ$				
3443. 779	20, *Z*	29029. 58	$a\ ^3H_4-x\ ^3H_4^\circ$	3408. 37	2	29331. 15	$a\ ^5F_1-o\ ^5F_1^\circ$
3442. 592	3	29039. 59	$a\ ^3G_5-v\ ^3G_5^\circ$	3408. 01	6*w*	29334. 25	
3441. 449	50	29049. 24	$a\ ^5G_5-w^5G_4^\circ$ $a\ ^5G_4-w^5G_4^\circ$	3407. 23	8*w*	29340. 97	$b\ ^5D_2-s\ ^5D_3^\circ$
				3406. 87	2*w*	29344. 07	
3441. 109	25	29052. 10	$a\ ^5G_3-w^5G_4^\circ$	3405. 217	10	29358. 31	$b\ ^3D_3-q\ ^3F_4^\circ$
3439. 358	8	29066. 90		3403. 983	5	29368. 96	$b\ ^3P_2-v\ ^3P_2^\circ$
3436. 190	50	29093. 70	$a\ ^5G_5-w^5G_5^\circ$ $a\ ^5G_4-w^5G_5^\circ$	3403. 588	18	29372. 36	$a\ ^3I_5-v\ ^3I_5^\circ$
				3402. 91	1	29378. 21	$a\ ^3I_6-v\ ^3I_5^\circ$
3435. 818	15	29096. 84	$a\ ^5G_5-x\ ^3F_4^\circ$ $a\ ^5G_4-x\ ^3F_4^\circ$	3401. 72	5	29388. 49	$b\ ^5G_3-u\ ^3G_3^\circ$
3435. 676	18	29098. 05	$a\ ^5G_6-w^5G_5^\circ$	3401. 14	2	29393. 50	$a\ ^3I_7-x\ ^1I_6^\circ$
3435. 479	10	29099. 91	$a\ ^5G_3-x\ ^3F_4^\circ$	3396. 02	4*w*, *Z*	29437. 82	$b\ ^3G_4-4_5^\circ$
3435. 26	1	29101. 57		3392. 06	2	29472. 18	$a\ ^3I_5-v\ ^3I_4^\circ$
3435. 14	1	29102. 58	$a\ ^5P_2-w^3F_3^\circ$	3391. 36	18	29478. 27	$a\ ^3I_6-v\ ^3I_4^\circ$
3434. 47	1*w*	29108. 26		3391. 08	5	29480. 70	$a\ ^3D_2-s\ ^3F_2^\circ$
3434. 30	1*w*	29109. 70	$a\ ^5P_3-w^3F_4^\circ$	3390. 766	18	29483. 43	$a\ ^3D_1-s\ ^3F_2^\circ$
3434. 106	25	29111. 34	$a\ ^5G_3-w^5G_4^\circ$	3389. 44	2	29494. 97	$b\ ^3D_2-s\ ^3G_3^\circ$
3433. 68	3	29114. 96	$a\ ^5F_4-q\ ^5D_3^\circ$	3388. 894	3	29499. 72	$b\ ^3P_2-v\ ^3P_1^\circ$
3433. 589	40	29115. 73	$a\ ^5G_5-w^5G_4^\circ$	3388. 705	20	29501. 36	$a\ ^5G_2-s\ ^5F_1^\circ$
3432. 840	8	29122. 08		3386. 717	3	29518. 68	$b\ ^3G_5-t\ ^3F_4^\circ$
3432. 311	12	29126. 57	$a\ ^5G_4-x\ ^3F_3^\circ$	3386. 513	12*s*	29520. 45	$a\ ^3D_2-s\ ^3F_3^\circ$

TABLE 1. *Wavelengths and term combinations of* Cr I—Continued

d, [illegible]; *h*, hazy; *H*, very hazy; *l*, shaded longward; *s*, shaded shortward; *r*, reversed; *R*, strongly reversed; *w*, wide; *W*, very wide; *Z*, Zeeman pattern in table 2.

Wavelength λ_{air}	Intensity	Wave No.	Term combination
3385. 313	15	29530. 91	$a\ ^3D_3 - s\ ^3F_4^\dagger$
3384. 649	18*w*	29536. 71	$a\ ^5G_3 - s\ ^5F_2^\dagger$
3384. 242	10*w*	29540. 26	$a\ ^5G_2 - s\ ^5F_2^\dagger$ $a\ ^5F_3 - o\ ^5F_3^\dagger$
3383. 628	3	29545. 62	
3383. 54	1	29546. 39	$b\ ^3P_1 - v\ ^3P_1^\dagger$
3382. 068	7	29559. 25	$a\ ^3F_4 - w\ ^3H_4^\dagger$ $b\ ^3P_0 - v\ ^3P_1^\dagger$
3381. 33	2	29565. 70	$a\ ^3D_2 - s\ ^3F_3^\dagger$
3380. 55	4*w*	29572. 53	$b\ ^3G_4 - t\ ^5F_3^\dagger$
3379. 85	7	29578. 65	$a\ ^5G_4 - s\ ^5F_5^\dagger$
3379. 56	4*w*	29581. 19	$a\ ^5G_3 - s\ ^5F_3^\dagger$ $b\ ^3D_1 - s\ ^3D_2^\dagger$
3379. 168	30	29584. 62	$a\ ^7S_3 - y\ ^5P_2^\dagger$
3377. 24	1	29601. 51	$b\ ^3D_2 - s\ ^3D_2^\dagger$
3377. 08	2	29602. 91	$d\ ^3F_4 - p\ ^3G_5^\dagger$
3376. 628	3	29606. 87	$a\ I_6 - v\ ^3I_7^\dagger$ $b\ ^3D_3 - s\ ^3D_3^\dagger$
3376. 397	20	29608. 90	$a\ ^3I_7 - v\ ^3I_7^\dagger$
3376. 13	4*wh*	29611. 24	
3375. 593	5	29615. 95	
3375. 32	1*wh*	29618. 34	
3375. 08	2	29620. 45	$b\ ^3D_3 - s\ ^3D_2^\dagger$
3374. 927	10	29621. 80	$a\ ^3F_4 - w\ ^3H_5^\dagger$
3374. 74	3	29623. 43	$b\ ^5D_3 - v\ ^3G_4^\dagger$ $b\ ^3G_3 - t\ ^3F_2^\dagger$
3374. 58	12	29624. 84	
3374. 406	4	29626. 37	$b\ ^3P_1 - v\ ^3P_0^\dagger$
3374. 13	1*w*	29628. 79	
3373. 958	6	29630. 30	$a\ ^3F_3 - w\ ^3H_4^\dagger$
3372. 31	2*w*	29644. 78	$b\ ^5D_4 - v\ ^3G_4^\dagger$
3371. 34	3	29653. 31	
3371. 07	6	29655. 68	$a\ ^3D_3 - r\ ^5D_4^\dagger$
3370. 98	4	29656. 48	
3370. 22	8*w*	29663. 16	$a\ ^5F_5 - o\ ^5F_4^\dagger$ $b\ ^5D_2 - s\ ^5P_1^\dagger$
3368. 45	2	29678. 75	$a\ ^5F_4 - o\ ^5F_4^\dagger$ $b\ ^3G_3 - t\ ^3F_3^\dagger$
3367. 54	10*w*	29686. 77	$a\ ^5G_5 - s\ ^5F_4^\dagger$ $a\ ^5G_4 - s\ ^5F_4^\dagger$
3366. 28	1	29697. 89	$a\ ^3G_5 - w\ ^3H_4^\dagger$
3365. 52	10, *Z*	29704. 59	$a\ ^3F_3 - v\ ^3H_4^\dagger$
3365. 03	1	29708. 91	
3362. 70	10*w*	29729. 50	$b\ ^5D_3 - s\ ^5P_2^\dagger$ $a\ ^5G_5 - s\ ^5F_5^\dagger$ $a\ ^5G_4 - s\ ^5F_5^\dagger$
3362. 216	25*w*	29733. 78	$b\ ^5D_2 - s\ ^5P_2^\dagger$ $a\ ^5G_6 - s\ ^5F_5^\dagger$
3360. 145	6	29752. 10	$a\ ^3F_4 - v\ ^3H_5^\dagger$
3359. 176	6	29760. 69	$a\ ^3G_5 - w\ ^3H_5^\dagger$
3357. 86	2	29772. 35	$a\ ^3G_3 - v\ ^3H_4^\dagger$
3356. 76	1*wh*	29782. 11	
3356. 38	3*wh*	29785. 47	$z\ ^7P_4^\dagger - h\ ^7D_5$
3354. 65	1*w*	29800. 80	
3353. 626	7*w*	29809. 94	
3353. 022	15	29815. 30	$a\ ^3I_5 - s\ ^3H_4^\dagger$
3352. 70	1*w*	29818. 17	$a\ ^5F_4 - o\ ^5F_3^\dagger$
3351. 966	40, *Z*	29824. 70	$a\ ^7S_3 - y\ ^5P_3^\dagger$
3351. 591	25	29828. 04	$a\ ^5G_5 - v\ ^3H_5^\dagger$
3351. 49	3*w*	29828. 93	$b\ ^5D_2 - s\ ^5P_3^\dagger$
3350. 72	1*w*	29835. 79	
3350. 30	4	29839. 53	$a\ ^3G_4 - w\ ^3H_4^\dagger$
3349. 322	20	29848. 24	$a\ ^3G_5 - w\ ^3H_5^\dagger$
3349. 067	20*w*	29850. 51	$b\ ^5D_4 - s\ ^3P_3^\dagger$
3347. 467	7	29864. 78	$b\ ^3P_2 - u\ ^3P_2^\dagger$
3346. 79	10, *Z*	29870. 82	$a\ ^3H_4 - v\ ^3G_3^\dagger$
3346. 72	30, *Z*	29871. 44	$a\ ^3H_5 - v\ ^3G_4^\dagger$
3346. 15	7*w*	29876. 53	$z\ ^7P_4^\dagger - h\ ^7D_4$
3346. 008	40	29877. 80	$a\ ^3H_6 - v\ ^3G_5^\dagger$
3345. 36	8	29883. 59	$b\ ^3G_4 - t\ ^3G_4^\dagger$
3345. 144	9	29885. 52	$b\ ^3G_5 - t\ ^3G_5^\dagger$
3344. 507	10	29891. 21	$a\ ^3G_3 - v\ ^3H_3^\dagger$
3343. 75	5*wh*	29897. 98	$z\ ^7P_3^\dagger - h\ ^7D_3$
3343. 344	20, *Z*	29901. 61	$a\ ^3G_4 - w\ ^3H_5^\dagger$
3343. 221	12	29902. 71	$a\ ^3G_3 - w\ ^3H_4^\dagger$
3342. 457	5	29909. 54	$b\ ^3P_2 - u\ ^3P_1^\dagger$
3342. 233	12	29911. 54	$b\ ^3P_1 - u\ ^3P_2^\dagger$
3342. 025	5	29913. 41	$a\ ^3G_4 - v\ ^3H_4^\dagger$
3341. 454	7*w*	29918. 52	$b\ ^3P_2 - 4_2^\dagger$
3340. 641	10	29925. 80	
3338. 677	7	29943. 40	$a\ ^3F_4 - u\ ^3F_4^\dagger$
3337. 85	1	29950. 82	
3337. 219	5	29956. 48	$b\ ^3P_1 - u\ ^3P_1^\dagger$
3336. 98	18	29958. 63	$a\ ^3I_6 - s\ ^3H_5^\dagger$
3336. 855	5	29959. 75	$b\ ^3G_3 - t\ ^3G_3^\dagger$
3336. 72	1*w*	29960. 96	
3335. 771	6	29969. 49	$b\ ^3P_0 - u\ ^3P_1^\dagger$
3334. 922	12	29977. 12	$a\ ^3G_3 - v\ ^3H_4^\dagger$
3334. 78	5	29978. 40	$b\ ^3P_1 - u\ ^3P_0^\dagger$
3334. 68	10*w*	29979. 29	$z\ ^7P_3^\dagger - h\ ^7D_3$
3333. 61	12*w*	29988. 92	$z\ ^7P_3^\dagger - h\ ^7D_4$
3333. 50	4*w*	29989. 90	$b\ ^3G_3 - t\ ^3G_4^\dagger$
3332. 88	25, *Z*	29995. 48	$a\ ^3F_3 - v\ ^3F_3^\dagger$
3332. 54	3	29998. 54	$b\ ^3G_4 - t\ ^3G_5^\dagger$
3331. 19	1	30010. 70	
3330. 596	7*w*, *Z*	30016. 05	$a\ ^3F_2 - v\ ^3D_1^\dagger$
3329. 058	40, *Z*	30029. 92	$a\ ^3F_4 - v\ ^3F_4^\dagger$
3328. 807	15	30032. 18	$a\ ^3G_4 - v\ ^3H_5^\dagger$
3328. 64	2	30033. 69	$a\ ^5G_3 - u\ ^5D_4^\dagger$
3327. 26	3*w*	30046. 15	$a\ ^3D_1 - u\ ^3D_1^\dagger$
3327. 23	3*w*	30046. 42	$a\ ^3F_3 - v\ ^3D_2^\dagger$ $b\ ^5D_4 - q\ ^5F_5^\dagger$
3327. 10	2	30047. 59	
3326. 588	30, *Z*	30052. 21	$a\ ^3F_2 - v\ ^3F_2^\dagger$
3325. 664	4	30060. 56	
3324. 86	1	30067. 83	$a\ ^3I_5 - r\ ^3G_4^\dagger$
3324. 06	20	30075. 09	
3323. 27	7*s*	30082. 22	$a\ ^3G_5 - u\ ^3F_4^\dagger$
3321. 188	8	30101. 07	$a\ ^3F_3 - v\ ^3F_4^\dagger$
3320. 57	1*WH*	30106. 68	$a\ ^3I_5 - r\ ^3G_5^\dagger$
3319. 95	3	30112. 30	$a\ ^3I_6 - r\ ^3G_5^\dagger$
3318. 96	1	30121. 28	$b\ ^5D_2 - q\ ^5F_4^\dagger$
3318. 73	2	30123. 37	
3318. 10	5*WH*	30129. 09	$z\ ^7P_4^\dagger - h\ ^7D_5$
3317. 06	2	30138. 53	$b\ ^3H_4 - p\ ^3G_5^\dagger$
3316. 60	3	30142. 72	$b\ ^5D_4 - q\ ^5F_4^\dagger$ $a\ ^5P_1 - t\ ^5D_0^\dagger$
3316. 496	25	30143. 66	$a\ ^3I_7 - s\ ^3H_4^\dagger$

TABLE 1. *Wavelengths and term combinations of* Cr I—Continued

d, Double; *h*, hazy; *H*, very hazy; *l*, shaded longward; *s*, shaded shortward; *r*, reversed; *R*, strongly reversed; *w*, wide; *W*, very wide; *Z*, Zeeman pattern in table 2.

Wavelength λ_{air}	Intensity	Wave No.	Term combination
3316.229	5	30146.09	$a\,^5P_1 - t\,^5D_1^\circ$
3315.20	4	30155.44	$a\,^5P_2 - t\,^5D_2^\circ$
			$a\,^5P_1 - t\,^5D_2^\circ$
3314.804	10	30159.05	$a\,^3G_2 - v\,^3F_2^\circ$
3314.32	2*wh*	30163.45	
3314.19	8	30164.63	$a\,^5P_2 - t\,^5D_2^\circ$
3313.728	12	30168.84	$a\,^3G_5 - v\,^5F_4^\circ$
3313.023	7	30175.26	$a\,^3F_4 - u\,^3F_3^\circ$
3312.707	3	30178.14	$a\,^3D_2 - u\,^3D_2^\circ$
3312.074	10	30183.90	$a\,^5P_2 - t\,^5D_3^\circ$
3311.30	4	30190.96	$a\,^3D_1 - t\,^3D_1^\circ$
			$a\,^5P_3 - t\,^5D_3^\circ$
3309.83	15	30204.36	$a\,^3G_4 - v\,^3F_3^\circ$
			$a\,^3H_6 - z\,^3K_7^\circ$
3309.238	1	30209.77	$b\,^3H_5 - p\,^3G_4^\circ$
3307.754	30	30223.32	$a\,^5P_3 - t\,^5D_4^\circ$
			$a\,^3G_4 - u\,^3F_4^\circ$
3305.232	5	30246.38	$b\,^3H_6 - p\,^3G_5^\circ$
			$a\,^3F_3 - u\,^3F_3^\circ$
3304.39	1*wh*	30254.09	$b\,^5D_4 - q\,^5F_5^\circ$
3303.32	1*wh*	30263.89	
3302.874	18	30267.98	$a\,^3G_3 - v\,^3F_3^\circ$
3302.19	5*wh*	30274.25	$a\,^3F_4 - v\,^3D_3^\circ$
3300.79	4	30287.09	$a\,^3G_3 - u\,^3F_4^\circ$
			$a\,^3D_3 - t\,^3D_3^\circ$
3298.39	1	30309.12	
3298.313	20	30309.83	$a\,^3G_4 - v\,^3F_4^\circ$
3297.33	2*wh*	30318.87	$a\,^3G_3 - v\,^3D_3^\circ$
3296.837	3	30323.40	$a\,^5F_1 - t\,^3P_2^\circ$
3293.91	1*h*	30350.35	
3293.83	10	30351.08	$b\,^3G_5 - s\,^3F_4^\circ$
3292.07	2	30367.31	$a\,^3F_3 - u\,^3F_2^\circ$
3291.39	2	30373.58	$a\,^3G_3 - v\,^3F_4^\circ$
3290.95	1*h*	30377.64	
3287.72	2*H*	30407.48	
3286.355	15	30420.12	
3284.84	2*w*	30434.14	
3282.56	2	30455.28	$a\,^3G_4 - u\,^3F_3^\circ$
3280.36	2	30475.71	$b\,^3G_5 - r\,^5D_4^\circ$
3280.11	2	30478.03	$a\,^3G_5 - y\,^1I_6^\circ$
3279.95	1	30479.51	
3279.344	2	30485.14	$a\,^3D_2 - u\,^3D_3^\circ$
3277.873	8	30498.82	$b\,^3G_4 - s\,^3F_3^\circ$
3275.817	3	30517.97	
3275.73	2	30518.78	$a\,^3G_3 - u\,^3F_3^\circ$
3271.93	4*wh*	30554.22	$a\,^3G_4 - v\,^3D_3^\circ$
3270.708	8	30565.64	$b\,^3G_3 - s\,^3F_2^\circ$
3267.038	3	30599.97	$a\,^3H_6 - z\,^1I_6^\circ$
3266.631	15	30603.79	$a\,^5D_4 - z\,^3D_3^\circ$
3265.93	1*w*	30610.35	
3265.34	1*w*	30615.88	
3262.77	1	30640.00	$a\,^3G_3 - u\,^3F_2^\circ$
3259.976	25, *Z*	30666.26	$a\,^3H_6 - v\,^3H_6^\circ$
3259.61	2	30669.70	$a\,^5D_2 - z\,^3D_1^\circ$
3257.826	40, *Z*	30686.50	$a\,^3H_6 - w\,^3H_6^\circ$
3254.94	2*wh*	30713.71	
3253.262	10, *Z*	30729.54	$a\,^3H_6 - v\,^3H_5^\circ$
			$a\,^5G_2 - w\,^3P_1^\circ$
3251.831	40, *Z*	30743.07	$a\,^3H_5 - w\,^3H_5^\circ$
3251.582	18, *Z*	30745.42	
3251.063	3	30750.33	
3250.58	10	30754.90	$a\,^3H_5 - v\,^3H_4^\circ$
3249.223	10	30767.74	$a\,^3F_4 - y\,^1H_5^\circ$
3248.98	2	30770.04	$a\,^5H_6 - z\,^1K_7^\circ$
3248.90	1	30770.80	$z\,^5F_1^\circ - e\,^5P_1$
3247.278	15, *Z*	30786.17	$a\,^5D_1 - z\,^3D_1^\circ$
3245.543	25, *Z*	30802.63	$a\,^3H_4 - w\,^3H_5^\circ$
3245.50	12	30803.04	$a\,^5D_2 - z\,^3D_2^\circ$
3244.713	4	30810.51	$a\,^3H_5 - v\,^3H_6^\circ$
3244.121	20, *Z*	30816.13	$a\,^5D_2 - z\,^3D_3^\circ$
3242.58	2	30830.78	$a\,^3H_5 - w\,^3H_6^\circ$
3240.95	18	30846.28	$a\,^5D_0 - z\,^3D_1^\circ$
3239.18	4	30863.14	$a\,^3P_2 - v\,^3D_1^\circ$
3238.953	6	30865.30	$a\,^3H_4 - w\,^3H_5^\circ$
3238.504	10	30869.58	$a\,^3G_5 - u\,^3H_6^\circ$
3238.088	20	30873.55	$a\,^5H_5 - v\,^3H_5^\circ$
3237.727	30, *Z*	30876.98	$a\,^3H_4 - v\,^3H_4$
			$a\,^5G_5 - z\,^1H_5^\circ$
3237.27	6	30881.34	$a\,^5G_6 - z\,^1H_5^\circ$
3226.25	3*w*	30891.07	
3235.34	1	30899.76	$a\,^3P_2 - v\,^3F_3^\circ$
3235.13	6	30901.77	$b\,^3D_2 - q\,^3G_3^\circ$
3234.556	8	30907.25	
3233.24	18, *Z*	30919.83	$a\,^5D_1 - z\,^3D_2^\circ$
3231.38	2	30937.63	$b\,^3G_5 - t\,^3H_5^\circ$
3229.206	25, *Z*	30958.46	$b\,^5G_5 - t\,^3H_6^\circ$
3227.232	7	30977.39	$a\,^3G_4 - u\,^3H_5^\circ$
3226.555	15	30983.89	$a\,^5D_2 - z\,^3D_2^\circ$
3222.33	2	31024.51	$b\,^3G_4 - t\,^3H_5^\circ$
3219.97	2	31047.25	$a\,^3G_4 - y\,^1H_5^\circ$
3219.62	20, *Z*	31050.63	$b\,^3G_4 - t\,^3H_5^\circ$
3218.70	7*wh*	31059.50	$a\,^3P_2 - v\,^3D_2^\circ$
3218.17	2	31064.62	$a\,^3H_5 - u\,^3F_4^\circ$
3216.37	2	31082.00	$a\,^3G_3 - u\,^3H_4^\circ$
3211.316	20, *Z*	31130.92	$b\,^3G_3 - t\,^3H_4^\circ$
3210.633	7	31137.54	$a\,^3S_2 - z\,^3D_2^\circ$
3207.51	1	31167.86	$a\,^3H_4 - v\,^3F_3^\circ$
3207.17	1*w*	31171.16	$z\,^7P_2^\circ - e\,^5F_2$
3205.81	1	31184.38	$a\,^3F_4 - v\,^3G_5^\circ$
3198.116	20, *Z*	31259.40	$a\,^3P_2 - u\,^3F_3^\circ$
3196.83	3	31271.98	
3196.67	1	31273.54	$a\,^3H_4 - v\,^3F_4^\circ$
3192.287	5	31316.48	$a\,^3H_6 - y\,^1I_6^\circ$
3192.118	15, *Z*	31318.13	$a\,^5S_2 - z\,^3D_3^\circ$
3188.02	15*wh*	31358.45	$a\,^3P_2 - v\,^3D_3^\circ$
3184.02	2	31397.79	$a\,^5F_2 - r\,^3H_3^\circ$
3179.283	10*w*	31444.56	$a\,^3P_1 - v\,^3D_1^\circ$
3177.659	3	31460.63	$a\,^3H_5 - y\,^1I_6^\circ$
3175.598	4	31481.05	$a\,^3P_1 - v\,^3F_2^\circ$
3175.03	2	31486.68	$a\,^3H_6 - x\,^3I_5^\circ$
3169.578	8	31540.84	$a\,^5G_5 - t\,^5D_4^\circ$
			$a\,^5G_4 - t\,^5D_4^\circ$
			$a\,^3H_6 - x\,^3I_6^\circ$
3168.745	5	31549.13	$b\,^3P_1 - u\,^3D_1^\circ$
			$b\,^3P_2 - t\,^3D_3^\circ$
3167.44	5, *Z*	31562.13	$b\,^3P_0 - u\,^3D_1^\circ$
3167.156	2	31564.96	
3164.492	4	31591.53	
3164.055	3	31595.90	$b\,^3P_1 - t\,^3D_2^\circ$
3163.764	25, *Z*	31598.80	$a\,^3H_6 - x\,^3I_7^\circ$
3160.617	8	31630.27	$a\,^3H_5 - x\,^3I_6^\circ$

TABLE 1. *Wavelengths and term combinations of* Cr I—Continued

d, double; *h*, hazy; *H*, very hazy; *l*, shaded longward; *s*, shaded shortward; *r*, reversed; *R*, strongly reversed; *w*, wide; *W*, very wide; *Z*, Zeeman pattern in table 2.

Wavelength λ_{air}	Intensity	Wave No.	Term combination	Wavelength λ_{air}	Intensity	Wave No.	Term combination
3159.909	3	31637.35	$b\,^3P_2-u\,^3D_3^\circ$	3109.34	20, *Z*	32151.87	$a\,^3G_3-u\,^3G_3^\circ$
3159.58	20*wh*, *Z*	31640.65	$a\,^3P_1-v\,^3D_2^\circ$	3105.84	1	32188.10	
3158.814	4	31648.32		3105.574	5	32190.85	$a\,^3G_4-u\,^3G_5^\circ$
3156.094	2	31675.59		3104.706	7, *Z*	32199.86	$a\,^3G_3-u\,^3G_4^\circ$
3155.25	3	31684.06	$b\,^3P_1-u\,^3D_2^\circ$ $a\,^5P_1-s\,^5D_2^\circ$	3100.46	1	32243.95	$a\,^3G_4-4_4^\circ$
				3099.497	4	32253.97	$a\,^3G_3-u\,^3P_2^\circ$
3155.161	20, *Z*	31684.96	$a\,^3H_5-x\,^3I_6^\circ$	3098.26	1	32266.85	$y\,^5P_1^\circ-e\,^5P_2$ $a\,^3G_3-p\,^5F_2^\circ$
3154.62	1*H*	31690.31					
3153.547	10, *Z*	31701.17	$b\,^3P_2-t\,^3D_3^\circ$	3096.704	10	32283.06	
3153.02	4	31706.47		3096.516	10*w*	32285.02	$a\,^3P_2-s\,^5P_3^\circ$
3152.99	10	31706.78	$a\,^3I_3-r\,^3H_4^\circ$ $b\,^3P_0-t\,^3D_1^\circ$	3095.85	15*w*	32291.96	$a\,^3P_2-s\,^5P_3^\circ$
				3095.385	15, *Z*	32296.82	$a\,^3G_5-t\,^3F_4^\circ$
3152.888	12, *Z*	31707.80	$a\,^3H_6-u\,^3H_6^\circ$	3094.283	1*w*	32308.32	$a\,^3G_3-4_3^\circ$
3151.703	3	31719.45		3092.833	20	32323.46	$a\,^3D_3-p\,^3F_4^\circ$
3150.65	4	31730.32	$a\,^3D_3-q\,^3F_3^\circ$	3092.708	50 Al?	32324.78	
3149.21	1	31744.83	$a\,^3H_5-y\,^1H_5^\circ$	3087.534	10, *Z*	32378.93	$a\,^3G_4-t\,^3F_3^\circ$
3148.44	20, *Z*	31752.60	$a\,^3H_4-x\,^3I_5^\circ$				
				3086.785	8	32386.79	$a\,^3G_3-t\,^3F_2^\circ$
3145.62	10	31781.06	$a\,^3I_6-r\,^3H_5^\circ$	3084.579	6	32409.95	$a\,^3F_4-t\,^3G_4^\circ$
3144.39	12*w*, *Z*	31793.49	$a\,^3P_2-s\,^5D_3^\circ$ $a\,^3P_0-v\,^3D_1^\circ$	3084.05	2	32415.51	
				3082.157	40*s* Al?	32435.42	
3143.74	2*w*	31800.07	$a\,^5P_3-s\,^5D_3^\circ$	3081.92	1	32437.91	$a\,^3G_4-t\,^3F_4^\circ$
3141.885	12, *Z*	31818.84	$a\,^3H_5-u\,^3H_5^\circ$				
3140.36	5	31834.29	$z\,^7F_5^\circ-e\,^5G_6$	3080.712	6, *Z*	32450.63	$a\,^3F_3-t\,^3G_3^\circ$
				3077.835	30, *Z*	32480.96	$a\,^3F_3-t\,^3G_4^\circ$
3138.31	8	31855.08	$a\,^3I_7-r\,^3H_6^\circ$	3076.57	6	32494.32	$a\,^5G_2-r\,^5F_1^\circ$
3138.20	15	31856.20	$a\,^3F_4-u\,^3G_4^\circ$	3076.151	6	32498.74	$a\,^3P_2-v\,^3P_2^\circ$
3137.62	3	31862.09		3074.465	7	32516.56	$a\,^5G_2-r\,^5F_2^\circ$
3135.917	7	31879.39	$a\,^3F_2-u\,^3G_3^\circ$				
3135.18	1*w*	31886.88		3074.13	2	32520.11	$a\,^5G_2-r\,^5F_3^\circ$
				3073.68	25, *Z*	32524.87	$a\,^3F_4-t\,^3G_5^\circ$
3134.97	8	31889.02	$a\,^3H_5-y\,^1H_5^\circ$	3071.41	2	32548.91	$a\,^3G_5-t\,^3G_4^\circ$ $a\,^5G_2-r\,^5F_2^\circ$
3133.969	5	31899.20	$b\,^3P_2-u\,^5D_3^\circ$				
3132.816	18	31910.95	$a\,^3F_4-u\,^3G_5^\circ$	3071.297	10, *Z*	32550.10	$a\,^5G_4-r\,^5F_3^\circ$
3131.213	20	31927.28	$a\,^3F_3-u\,^3G_4^\circ$	3071.03	3	32552.94	
3129.76	2	31942.10	$a\,^5P_2-s\,^5D_1^\circ$				
				3067.20	10	32593.58	$a\,^5G_3-r\,^5F_4^\circ$ $a\,^5G_4-r\,^5F_4^\circ$
3127.589	5*w*	31964.28	$a\,^3F_4-4_3^\circ$ $a\,^5P_2-v\,^3G_3^\circ$	3065.065	25, *Z*	32616.29	$a\,^3F_2-t\,^3G_3^\circ$
3125.911	8	31981.43	$a\,^5H_4-u\,^3H_4^\circ$ $a\,^3F_2-u\,^3P_2^\circ$	3063.83	2	32629.43	$a\,^3P_2-v\,^3P_1^\circ$
				3063.64	1	32631.46	
3122.998	4	32011.26	$a\,^3H_4-y\,^1H_5^\circ$	3062.05	2	32648.40	$a\,^5G_5-r\,^5F_5^\circ$ $a\,^5G_4-r\,^5F_5^\circ$
3121.60	3*wkhs*	32025.60	$y\,^5P_3^\circ-e\,^5P_3$				
3120.63	10	32035.55	$a\,^5F_2-4_3^\circ$				
				3061.814	10, *Z*	32650.91	$b\,^3G_5-s\,^3G_5^\circ$
3119.704	20, *Z*	32044.69	$a\,^3F_2-u\,^3G_3^\circ$	3061.64	15, *Z*	32652.77	$a\,^5G_6-r\,^5F_5^\circ$
3119.252	20, *Z*	32049.70	$a\,^3G_5-u\,^3G_5^\circ$	3061.01	2	32659.49	$a\,^3G_4-t\,^3G_3^\circ$
3119.18	3	32050.44		3060.624	2	32663.61	$a\,^3G_5-t\,^3G_5^\circ$
3118.80	4	32054.35		3058.164	6, *Z*	32689.88	$a\,^3G_4-t\,^3G_4^\circ$
3118.13	3	32061.23	$a\,^3I_5-q\,^3H_4^\circ$				
				3056.435	3	32708.37	$a\,^3D_1-t_1^\circ\,^3P_0^\circ$
3115.505	5	32088.25	$a\,^3G_4-u\,^3G_4^\circ$	3055.055	5	32723.15	$a\,^3G_3-t\,^3G_3^\circ$
3114.835	10	32095.15	$a\,^3I_6-q\,^3H_5^\circ$	3054.94	3	32724.38	
3114.455	6	32099.07	$a\,^3F_4-t\,^3F_3^\circ$	3053.87	100*r*, *Z*	32735.85	$a\,^5D_4-x\,^5P_3^\circ$
3114.10	1*w*	32102.72	$b\,^3G_4-w\,^3I_5^\circ$ $y\,^5P_2^\circ-e\,^5P_2$	3052.218	18, *Z*	32753.56	$a\,^3G_3-t\,^3G_4^\circ$
3112.962	5	32114.46	$a\,^3F_2-t\,^3F_2^\circ$				
				3049.878	8	32778.70	$a\,^5D_4-y\,^5F_5^\circ$
3111.312	2	32131.49		3047.88	6	32800.18	$b\,^3G_4-s\,^3G_4^\circ$
3110.986	8	32134.86	$a\,^3I_7-q\,^3H_6^\circ$				$b\,^5D_2-p\,^5F_2^\circ$
3110.866	15, *Z*	32136.10	$a\,^3G_4-u\,^3G_4^\circ$	3047.445	15	32804.86	$a\,^3G_4-t\,^3G_5^\circ$
3110.75	5	32137.30	$y\,^5P_1^\circ-e\,^5P_1$ $a\,^3D_2-p\,^5F_3^\circ$	3046.57	3	32814.29	$b\,^3G_4-s\,^3G_5^\circ$ $b\,^5D_1-p\,^5F_2^\circ$
3109.81	1	32147.01	$a\,^3F_2-u\,^3P_2^\circ$	3046.10	2	32819.34	$b\,^3D_0-p\,^5F_1^\circ$

TABLE 1. *Wavelengths and term combinations of* Cr I—Continued

d, Double; *h*, hazy; *H*, very hazy; *l*, shaded longward; *s*, shaded shortward; *r*, reversed; *R*, strongly reversed; *w*, wide; *W*, very wide; *Z*, Zeeman pattern in table 2.

Wavelength λ_{air}	Intensity	Wave No.	Term combination
3045. 324	2	32827. 71	
3044. 04	1	32841. 56	$b\ ^5D_2-4^5_4$
3043. 714	3	32845. 07	$a\ ^3D_2-t\ ^3P^1_1$
3043. 46	2	32847. 82	$a\ ^3D_1-t\ ^3P^1_1$
3042. 24	1	32860. 99	$b\ ^3P_2-x\ ^3S^1_1$
3040. 837	100*r*	32876. 15	$a\ ^5D_3-y\ ^5F^3_3$
3039. 77	25, *Z*	32887. 69	$a\ ^5D_3-x\ ^5P^3_2$
3039. 73	15, *Z*	32888. 12	$a\ ^3H_6-u\ ^3G^5_5$
3037. 049	75*r*, *Z*	32917. 15	$a\ ^5D_4-y\ ^5F^4_4$
3036. 707	6	32920. 86	$b\ ^3P_0-x\ ^3S^1_1$ $b\ ^3G_3-s\ ^3G^4_4$
3035. 55	2	32933. 40	$b\ ^5D_3-p\ ^5F^4_4$
3034. 191	50, *Z*	32948. 16	$a\ ^5D_3-x\ ^5P^3_3$
3031. 498	20, *Z*	32977. 42	$a\ ^3H_5-u\ ^3G^4_4$
3031. 346	50, *Z*	32979. 08	$a\ ^5D_2-y\ ^5F^1_1$
3030. 25	100*r*, *Z*	32991. 00	$a\ ^5D_2-y\ ^5F^3_3$
3029. 165	50, *Z*	33002. 83	$a\ ^5D_2-x\ ^5P^1_1$
3025. 87	3	33038. 75	$a\ ^3D_3-t\ ^3P^2_2$
3024. 689	12	33051. 66	$a\ ^3H_4-u\ ^3G^3_3$
3024. 359	125*r*, *Z*	33055. 26	$a\ ^5D_2-x\ ^5P^2_2$
3023. 78	1	33061. 59	$a\ ^3F_2-s\ ^3F^4_4$
3021. 576	200*r*, *Z*	33085. 71	$a\ ^5D_4-y\ ^5F^5_5$
3020. 671	50*r*, *Z*	33095. 62	$a\ ^5D_1-y\ ^5F^1_1$
3019. 39	3	33109. 65	
3018. 827	40*r*, *Z*	33115. 83	$b\ ^3G_4-p\ ^3F^3_3$ $a\ ^5D_2-x\ ^5P^3_3$
3018. 492	50*r*, *Z*	33119. 50	$a\ ^5D_1-x\ ^5P^1_1$
3017. 591	100*r*, *Z*	33129. 39	$a\ ^5D_3-y\ ^5F^4_4$
3016. 29	3	33143. 68	$b\ ^3G_3-p\ ^3F^4_4$
3015. 197	50*r*, *Z*	33155. 70	$a\ ^5D_0-y\ ^5F^1_1$
3014. 932	75*r*, *Z*	33158. 61	$a\ ^5D_2-y\ ^5F^3_3$
3014. 756	50*r*, *Z*	33160. 55	$a\ ^5D_1-y\ ^5F^2_2$
3013. 72	40*r*, *Z*	33171. 95	$a\ ^5D_1-x\ ^5P^2_2$
3013. 033	20, *Z*	33179. 51	$a\ ^5D_0-x\ ^5P^1_1$
3011. 109	7, *Z*	33200. 71	
3010. 22	2	33210. 51	$a\ ^3P_1-v\ ^3P^1_1$
3009. 16	2	33222. 21	$b\ ^3G_3-p\ ^3F^3_3$ $a\ ^3F_2-s\ ^3F^2_2$
3007. 945	2	33235. 63	
3006. 86	1	33247. 62	$a\ ^3D_2-q\ ^3G^3_3$
3005. 06	40*r*, *Z*	33267. 54	$a\ ^5D_4-y\ ^5D^4_4$
3003. 79	7, *Z*	33281. 60	
3002. 99	2	33290. 47	$a\ ^3P_1-v\ ^3P^0_1$
3002. 757	2	33293. 05	$a\ ^3D_3-q\ ^3G^4_4$
3002. 44	1	33296. 56	
3001. 76	1	33304. 11	$b\ ^3G_4-s\ ^3H^5_5$
3001. 55	1	33306. 44	$b\ ^3G_3-r\ ^3G^4_4$
3000. 88	50*r*, *Z*	33313. 87	$a\ ^5S_2-y\ ^5F^1_1$ $a\ ^5D_3-y\ ^5D^2_2$
2998. 783	40, *Z*	33337. 17	$a\ ^5S_2-x\ ^5P^1_1$
2998. 118	8, *Z*	33344. 57	$b\ ^5G_5-r\ ^3G^5_5$
2996. 571	40*r*, *Z*	33361. 78	$a\ ^5D_2-y\ ^5D^1_1$
2995. 42	2	33374. 60	$b\ ^3G_4-r\ ^3G^3_3$ $b\ ^3G_5-s\ ^3H^4_4$
2995. 094	30*r*, *Z*	33378. 22	$a\ ^5S_2-y\ ^5F^2_2$
2994. 06	25, *Z*	33389. 75	$a\ ^5S_2-x\ ^5P^2_2$
2991. 877	30*r*, *Z*	33414. 12	$a\ ^5D_1-y\ ^5D^0_0$
2991. 403	6, *Z*	33419. 41	$b\ ^3G_4-r\ ^3G^4_4$
2988. 638	40*r*, *Z*	33450. 33	$a\ ^5S_2-x\ ^5P^3_3$
2986. 466	50*r*, *Z*	33474. 66	$a\ ^5D_4-y\ ^5D^4_4$
2986. 13	15, *Z*	33478. 42	$a\ ^5D_1-y\ ^5D^2_2$
2986. 01	25*r*, *Z*	33479. 77	$a\ ^5D_3-y\ ^5D^3_3$
2985. 849	20, *Z*	33481. 57	$a\ ^5D_2-y\ ^5D^2_2$
2984. 82	3, *Z*	33493. 11	$a\ ^5S_2-y\ ^5F^2_2$
2984. 014	7, *Z*	33502. 12	$a\ ^3H_6-t\ ^3G^5_5$
2981. 42	4, *Z*	33531. 31	$a\ ^3H_5-t\ ^3G^4_4$
2980. 784	25*r*, *Z*	33538. 47	$a\ ^5D_0-y\ ^5D^1_1$
2978. 98	1	33558. 77	$a\ ^5G_6-v\ ^5G^5_5$
2975. 478	30*r*, *Z*	33598. 27	$a\ ^5D_1-y\ ^5D^2_2$
2973. 51	1	33620. 50	$a\ ^3P_1-u\ ^3P^1_1$
2973. 26	1	33623. 33	$a\ ^3H_4-t\ ^3G^3_3$
2971. 102	25*r*, *Z*	33647. 75	$a\ ^5D_2-y\ ^5D^2_2$
2969. 53	1	33665. 56	$a\ ^3F_3-t\ ^3D^3_3$
2968. 98	2*w*	33671. 80	$b\ ^5D_1-r\ ^5D^2_2$ $a\ ^7S_3-z\ ^5D^3_3$
2968. 20	2, *w*	33680. 64	$a\ ^5G_2-r\ ^5F^1_1$
2967. 64	15, *Z*	33687. 00	$a\ ^5D_3-y\ ^5D^4_4$
2966. 85	7	33695. 97	$a\ ^5S_2-y\ ^5D^2_2$
2963. 74	4*wh*	33731. 33	$a\ ^5G_3-r\ ^5F^2_2$
2963. 26	2	33736. 80	$a\ ^3G_5-t\ ^3H^5_5$
2962. 40	6	33746. 58	$a\ ^3F_4-t\ ^3D^3_3$
2961. 77	4	33753. 76	$a\ ^3F_3-u\ ^3D^3_3$
2961. 18	4	33760. 49	$b\ ^5D_3-r\ ^5D^3_3$
2959. 07	7	33784. 56	$a\ ^3F_2-u\ ^3D^2_2$
2957. 28	2*wh*	33805. 01	$a\ ^5G_4-r\ ^5F^3_3$
2956. 328	15	33815. 90	$a\ ^5S_2-y\ ^5D^3_3$ $a\ ^7S_3-z\ ^5D^4_4$
2956. 13	1	33818. 16	$a\ ^3F_2-t\ ^3D^2_2$
2952. 15	1	33863. 64	$b\ ^5D_2-s\ ^3F^3_3$ $b\ ^5D_3-s\ ^3F^4_4$
2948. 87	6*h*	33901. 41	$a\ ^5G_5-r\ ^5F^4_4$
2945. 104	3	33944. 76	$a\ ^3F_4-u\ ^3D^4_4$
2943. 12	1	33967. 64	$a\ ^5D_4-x\ ^7P^4_4$
2941. 874	10	33982. 03	$a\ ^5S_2-y\ ^5D^1_1$
2941. 643	2	33984. 70	$a\ ^5D_2-z\ ^5H^3_3$
2941. 03	3	33991. 78	
2930. 31	8*h*	34000. 10	
2939. 44	5, *Z*	34010. 16	$b\ ^5D_4-r\ ^5D^4_4$
2938. 83	7*h*	34017. 23	$a\ ^5G_6-r\ ^5F^5_5$
2938. 59	2	34020. 00	
2938. 03	8	34026. 49	$a\ ^3G_4-t\ ^3D^3_3$
2935. 534	10, *Z*	34055. 42	
2934. 45	8*h*	34068. 00	
2933. 47	6*h*	34079. 38	
2932. 57	3*h*	34089. 83	$a\ ^3G_3-t\ ^3D^3_3$
2932. 35	2*h*	34092. 39	
2931. 85	1	34098. 20	$a\ ^5D_2-z\ ^5H^3_3$
2931. 30	1	34104. 61	
2930. 53	1	34113. 57	
2929. 48	4*h*	34125. 79	
2927. 77	1*w*	34145. 72	
2925. 55	5*h*	34171. 63	
2925. 03	4	34177. 71	
2922. 12	4	34211. 74	$b\ ^3P_1-t\ ^3P^2_2$
2921. 35	8	34220. 76	$b\ ^3G_5-q\ ^3G^5_5$
2921. 05	1	34224. 28	$a\ ^3G_4-u\ ^3D^4_4$
2919. 74	1	34239. 63	$a\ ^3F_4-r\ ^3F^3_3$
2919. 39	2*h*	34243. 73	

TABLE 1. *Wavelengths and term combinations of* Cr I—Continued

d, double; *h*, hazy; *H*, very hazy; *l*, shaded longward; *s*, shaded shortward; *r*, reversed; *R*, strongly reversed; *w*, wide; *W*, very wide; *Z*, Zeeman pattern in table 2.

Wavelength λ_{air}	Intensity	Wave No.	Term combination
2918.72	1	34251.59	$a\ ^5F_2 - r\ ^3F_2^0$
2918.24	4	34257.23	$a\ ^5D_4 - z\ ^5G_4^0$
2917.50	3*h*	34265.92	
2917.07	4*h*	34270.97	
2916.70	2	34275.31	$a\ ^5G_4 - w\ ^3H_5^0$
2916.16	12	34281.66	$a\ ^5D_4 - z\ ^5G_5^0$
2914.224	3	34304.43	$b\ ^3P_2 - t\ ^3P_1^0$
2913.716	20*d*, *Z*	34310.41	$a\ ^3F_4 - r\ ^3F_4^0$ $a\ ^3F_3 - r\ ^3F_3^0$ $a\ ^5D_2 - x\ ^7P_3^0$
2911.148	22	34340.68	$a\ ^5D_4 - x\ ^5D_3^0$
2910.892	25, *Z*	34343.82	$a\ ^5D_3 - x\ ^5D_3^0$
2910.252	3	34351.25	$b\ ^3P_1 - t\ ^3P_1^0$
2909.049	30, *Z*	34365.46	$a\ ^5D_2 - x\ ^5D_1^0$
2907.704	4	34381.35	$a\ ^3F_3 - r\ ^3F_4^0$
2907.111	5	34388.37	
2905.477	25, *Z*	34407.71	$a\ ^5D_1 - x\ ^5D_0^0$
2904.674	12, *Z*	34417.22	$a\ ^3F_2 - r\ ^3F_2^0$
2903.36	4*w*	34432.79	
2902.44	4	34443.70	$a\ ^5D_3 - z\ ^5G_3^0$
2901.98	4	34449.16	$a\ ^3G_3 - r\ ^3F_4^0$
2901.65	5*w*	34453.08	$b\ ^3P_2 - t\ ^3P_2^0$
2900.25	12	34469.71	$a\ ^5D_2 - z\ ^5G_3^0$
2899.68	10	34476.49	$a\ ^3F_2 - r\ ^3F_3^0$
2899.203	22	34482.16	$a\ ^5D_1 - x\ ^5D_1^0$
2898.24	4	34493.61	
2897.14	2*w*	34506.71	
2896.756	25, *Z*	34511.29	$a\ ^5D_2 - x\ ^5D_2^0$
2896.064	6	34519.53	$a\ ^5G_4 - r\ ^3F_3^0$
2895.675	7	34524.17	$a\ ^3G_3 - r\ ^3F_2^0$
2895.50	2*w*	34526.26	
2894.168	20, *Z*	34542.15	$a\ ^5D_0 - x\ ^5D_1^0$
2893.254	30, *Z*	34553.03	$a\ ^5D_3 - x\ ^5D_3^0$
2891.42	15, *Z*	34574.97	$a\ ^3H_5 - t\ ^3H_4^0$
2890.738	10	34583.13	$a\ ^3G_3 - r\ ^3F_3^0$
2890.35	1	34587.77	$a\ ^5D_2 - z\ ^5G_2^0$
2890.16	12	34590.05	$a\ ^3G_4 - r\ ^3F_4^0$
2889.294	25, *Z*	34600.41	
2889.219	10, *Z*	34601.31	$a\ ^5D_4 - x\ ^5D_4^0$
2888.38	7	34611.36	$a\ ^5D_2 - z\ ^5G_2^0$
2886.995	25, *Z*	34627.96	$a\ ^5D_1 - x\ ^5D_2^0$
2886.65	2	34632.10	$a\ ^3P_2 - u\ ^3D_1^0$
2884.83	4	34653.95	$a\ ^3G_3 - r\ ^3F_3^0$
2883.30	2	34672.34	$a\ ^3H_5 - t\ ^3H_4^0$
2882.76	3	34678.83	$a\ ^3P_2 - t\ ^3D_2^0$
2881.14	12, *Z*	34698.33	$a\ ^3H_5 - t\ ^3H_5^0$
2880.62	2	34704.59	$a\ ^5D_1 - z\ ^5G_2^0$
2880.42	2	34707.00	$b\ ^3P_2 - q\ ^3G_3^0$
2879.27	22, *Z*	34720.87	$a\ ^5D_3 - x\ ^5D_4^0$
2875.44	5	34767.11	$a\ ^3P_2 - u\ ^3D_3^0$
2873.181	12	34794.44	$a\ ^3H_4 - t\ ^3H_4^0$
2872.28	2	34805.36	
2871.628	22, *Z*	34813.26	$a\ ^5D_3 - x\ ^5D_4^0$
2871.023	3	34820.60	$a\ ^3H_4 - t\ ^3H_5^0$
2870.175	10	34830.88	$a\ ^3P_2 - t\ ^3D_3^0$
2870.01	10*w*	34832.88	$z\ ^7D_3^0 - f\ ^7F_4$
2863.484	4*w*	34912.27	
2855.22	4	35013.31	$b\ ^3G_5 - r\ ^3H_5^0$
2853.94	8	35029.01	$a\ ^3P_2 - u\ ^3D_2^0$
2853.89	8	35029.62	$a\ ^5D_2 - z\ ^5S_2^0$
2851.56	3	35058.25	$b\ ^3G_4 - r\ ^3H_4^0$ $b\ ^3D_2 - r\ ^3F_2^0$
2850.46	2*w*	35071.78	$b\ ^3D_1 - r\ ^3F_2^0$
2849.30	8, *Z*	35086.05	$b\ ^3G_5 - r\ ^3H_6^0$
2846.49	4	35120.69	
2846.024	12	35126.44	$b\ ^3G_4 - r\ ^3H_5^0$
2845.03	2	35138.71	
2844.65	2*w*	35143.41	$a\ ^3F_2 - x\ ^3S_1^0$
2844.38	1	35146.74	$a\ ^3F_3 - q\ ^3F_3^0$
2842.918	10	35164.81	$b\ ^3G_3 - r\ ^3H_4^0$
2840.891	15, *Z*	35190.02	$a\ ^3F_4 - q\ ^3F_4^0$
2840.292	7	35197.32	$a\ ^5D_2 - z\ ^5S_2^0$
2839.013	8	35213.18	$a\ ^3P_1 - u\ ^3D_1^0$
2838.491	10	35219.66	$a\ ^3F_3 - q\ ^3F_3^0$
2835.242	7	35260.01	$a\ ^3P_1 - t\ ^3D_2^0$
2835.16	2	35261.03	$a\ ^3F_2 - q\ ^3F_3^0$
2834.043	3	35274.93	
2832.794	8	35290.48	$a\ ^3F_4 - s\ ^3G_5^0$
2831.039	12, *Z*	35312.36	$a\ ^3F_2 - q\ ^3F_2^0$
2830.90	2	35314.09	$a\ ^5D_1 - z\ ^5S_2^0$
2829.903	5	35326.53	$a\ ^3F_4 - s\ ^3G_4^0$
2829.725	5	35328.75	$a\ ^3G_5 - q\ ^3F_4^0$
2828.167	12	35348.21	$a\ ^3P_1 - u\ ^3D_2^0$
2826.734	20, *Z*	35366.13	$b\ ^3G_5 - q\ ^3H_6^0$
2825.196	8	35385.38	$a\ ^3F_2 - q\ ^3F_2^0$
2824.87	1	35389.46	$a\ ^3G_5 - v\ ^3I_5^0$
2824.60	2	35392.85	
2824.224	10	35397.56	$a\ ^3F_3 - s\ ^3G_4^0$
2823.80	1	35402.88	$a\ ^3G_5 - x\ ^1I_6^0$
2823.08	1*d*?	35411.91	$a\ ^3F_2 - s\ ^3G_3^0$
2822.51	2	35419.06	$a\ ^3G_3 - q\ ^3F_2^0$
2821.76	6	35428.47	$a\ ^3G_4 - q\ ^3F_3^0$
2821.69	3	35429.35	$a\ ^3G_5 - s\ ^3G_5^0$
2820.97	2	35438.39	$a\ ^3F_4 - s\ ^3D_3^0$
2820.81	15	35440.40	$b\ ^3G_4 - q\ ^3H_5^0$
2818.47	12	35469.82	$a\ ^3G_4 - q\ ^3F_4^0$
2816.95	7	35488.96	$a\ ^3G_5 - v\ ^3I_6^0$
2816.684	12	35492.30	$a\ ^3G_3 - q\ ^3F_3^0$
2816.36	1	35496.39	
2815.317	2	35509.54	$a\ ^3F_2 - s\ ^3D_3^0$
2814.52	10*w*	35519.60	$b\ ^3G_2 - q\ ^3H_3^0$
2813.685	4	35530.13	$a\ ^3G_4 - v\ ^3I_5^0$
2813.552	4	35531.82	$a\ ^5S_2 - z\ ^5S_2^0$
2813.41	1	35533.61	$a\ ^3G_3 - q\ ^3F_4^0$
2811.169	12	35561.94	$a\ ^3P_0 - u\ ^3D_1^0$
2810.503	5	35570.37	$a\ ^3G_4 - s\ ^3G_5^0$
2809.932	10	35577.59	$a\ ^3F_2 - s\ ^3G_3^0$
2807.43	1	35609.30	
2805.456	1	35634.35	$a\ ^5G_2 - v\ ^5G_2^0$
2805.19	2	35637.73	
2802.65	8	35670.02	$a\ ^3G_3 - s\ ^3G_4^0$
2802.40	2	35673.21	
2802.00	6	35678.30	

TABLE 1. *Wavelengths and term combinations of* Cr I—Continued

d, Double; *h*, hazy; *H*, very hazy; *l*, shaded longward; *s*, shaded shortward; *r*, reversed; *R*, strongly reversed; *w*, wide; *W*, very wide; *Z*, Zeeman pattern in table 2

Wavelength λ_{air}	Intensity	Wave No.	Term combination
2801. 553	3	35683. 99	$a\ ^3H_6-w\ ^3I_7^0$
			$a\ ^3G_3-s\ ^3G_4^0$
2801. 385	1	35686. 13	$a\ ^5G_4-v\ ^5G_5^0$
2801. 13	15	35689. 38	$a\ ^3F_2-s\ ^3D_3^0$
2799. 743	3	35707. 06	$a\ ^3P_0-t\ ^3D_1^0$
2799. 21	1	35713. 86	
2796. 965	1*w*	35742. 53	
2795. 818	12, *Z*	35757. 19	$a\ ^3H_4-w^3I_5^0$
2795. 263	5	35764. 29	$a\ ^3F_3-s\ ^3H_4^0$
2794. 945	7	35768. 36	
2793. 87	2	35782. 12	$a\ ^3G_3-s\ ^3D_3^0$
2793. 78	3	35783. 27	$a\ ^3F_4-p\ ^3F_4^0$
2791. 83	4	35808. 27	
2790. 28	12, *Z*	35828. 15	$a\ ^3H_5-w\ ^3I_6^0$
2790. 092	8	35830. 57	$a\ ^3F_4-s\ ^3H_5^0$
2789. 52	2	35837. 91	$a\ ^5G_3-v\ ^5G_3^0$
2788. 09	3	35856. 30	
2787. 843	15, *Z*	35859. 47	
2786. 814	1	35872. 71	$a\ ^3H_4-w^3I_5^0$
2786. 597	4	35875. 51	
2784. 63	4	35900. 84	$a\ ^3F_4-r\ ^3G_5^0$
2783. 45	5	35916. 06	
2782. 988	3	35922. 03	$a\ ^3G_5-p\ ^3F_4^0$
			$a\ ^3G_4-p\ ^3F_3^0$
2782. 73	1	35925. 36	$a\ ^5G_5-v\ ^5G_6^0$
2781. 15	10	35945. 77	$a\ ^3F_4-r\ ^3G_4^0$
2780. 695	60*r*, *Z*	35951. 65	$a\ ^5D_4-w^5P_3^0$
2779. 33	1	35969. 30	$a\ ^3G_5-s\ ^3H_5^0$
2779. 134	12	35971. 84	$a\ ^3F_2-r\ ^3G_3^0$
2778. 213	12	35983. 76	$a\ ^3F_4-r\ ^3G_5^0$
2777. 664	10*w*	35990. 88	$a\ ^3P_2-x\ ^3S_1^0$
2776. 603	2	36004. 63	$b\ ^5D_1-q\ ^5D_1^0$
2775. 89	2	36013. 87	$b\ ^5D_0-q\ ^5D_1^0$
2775. 668	12, *Z*	36016. 76	$a\ ^3F_3-r\ ^3G_4^0$
2774. 84	1	36027. 50	
2774. 13	2	36036. 72	$a\ ^3G_3-s\ ^3H_4^0$
2773. 67	1*wh*	36042. 70	
2773. 00	5	36051. 40	
2772. 37	2*wh*	36059. 60	
2771. 449	10, *Z*	36071. 58	$a\ ^3H_4-x\ ^1H_5^0$
2770. 44	3	36084. 72	$a\ ^3G_3-r\ ^3G_4^0$
2769. 902	50*r*, *Z*	36091. 72	$a\ ^5D_3-w\ ^5P_3^0$
2768. 46	2	36110. 52	$a\ ^3G_4-s\ ^3H_5^0$
			$b\ ^3G_5-p\ ^3H_5^0$
2767. 53	7, *Z*	36122. 66	$a\ ^3G_5-r\ ^3G_5^0$
2767. 21	1	36126. 83	$a\ ^3G_3-p\ ^3F_4^0$
2766. 39	10	36137. 54	$b\ ^3G_4-p\ ^3H_4^0$
			$a\ ^3F_2-r\ ^3G_3^0$
2765. 21	5	36152. 96	$a\ ^3G_5-s\ ^3H_5^0$
2765. 03	1	36155. 32	
2764. 355	35*r*	36164. 15	$a\ ^5D_2-w\ ^5P_3^0$
2763. 40	2	36176. 64	
2763. 09	15	36180. 70	$b\ ^3G_5-p\ ^3H_6^0$
			$a\ ^3G_4-r\ ^3G_5^0$
2762. 38	1	36189. 99	$b\ ^5D_3-q\ ^5D_3^0$
2761. 735	40*r*	36198. 45	$a\ ^5D_2-w\ ^5P_2^0$
2759. 84	12	36223. 30	$b\ ^3G_4-p\ ^3H_5^0$
2759. 67	8	36225. 53	$a\ ^3G_4-r\ ^3G_4^0$
2758. 48	3	36241. 16	$a\ ^3H_6-x\ ^1I_6^0$
2758. 236	10	36244. 37	$b\ ^3G_3-p\ ^3H_4^0$
			$a\ ^3G_3-r\ ^3G_3^0$
2757. 086	40*r*	36259. 49	$a\ ^5D_2-w\ ^5P_2^0$
2756. 77	10	36263. 64	$a\ ^3G_4-r\ ^3G_5^0$
2755. 29	10	36283. 12	
2755. 24	8	36283. 78	$a\ ^5D_4-y\ ^5G_5^0$
2754. 821	15	36289. 30	$a\ ^3G_3-r\ ^3G_4^0$
2752. 851	50*r*	36315. 27	$a\ ^5D_1-w^5P_1^0$
2752. 21	1	36323. 72	$b\ ^5D_3-q\ ^5D_4^0$
2751. 58	18	36332. 03	$a\ ^5D_2-w^5P_1^0$
2750. 51	2	36346. 17	$b\ ^5D_4-q\ ^5D_4^0$
2748. 58	3	36371. 69	$a\ ^3H_5-v\ ^3I_6^0$
2748. 275	50*r*	36375. 74	$a\ ^5D_1-w^5P_2^0$
			$a\ ^5D_0-w^5P_1^0$
2745. 534	1	36412. 04	$a\ ^3H_5-s\ ^3G_5^0$
2742. 98	3	36445. 94	$a\ ^5D_2-y\ ^5G_3^0$
2742. 165	20, *Z*	36456. 78	$a\ ^3H_6-v\ ^3I_7^0$
2741. 078	22, *Z*	36471. 23	$a\ ^3H_5-v\ ^3I_6^0$
2739. 395	20, *Z*	36493. 63	$a\ ^3H_4-v\ ^3I_5^0$
2738. 17	1	36509. 97	$a\ ^5G_5-u\ ^3G_4^0$
2737. 222	8	36522. 60	$a\ ^3P_2-s\ ^3D_3^0$
2736. 463	50*r*, *Z*	36532. 71	$a\ ^5S_2-w\ ^5P_1^0$
2733. 76	2	36568. 85	$a\ ^5G_6-u\ ^3G_5^0$
2733. 51	8	36572. 20	$a\ ^3P_1-x\ ^3S_1^0$
2733. 00	1*h*	36579. 02	$a\ ^5G_2-p\ ^5F_1^0$
2732. 95	2	36579. 69	$a\ ^5G_2-p\ ^5F_2^0$
2731. 895	65*r*, *Z*	36593. 81	$a\ ^5S_2-w^5P_2^0$
2730. 07	3	36618. 27	$a\ ^5G_4-4_5^0$
2729. 85	3*w*	36621. 23	$a\ ^5G_3-4_4^0$
2729. 58	2*h*	36624. 85	$a\ ^5G_2-4_3^0$
2728. 44	3*h*	36640. 16	$z\ ^7F_5^0-f\ ^7F_4$
2726. 496	75*r*, *Z*	36666. 27	$a\ ^5S_2-w^5P_3^0$
2725. 86	4*w*	36674. 83	$z\ ^7F_4^0-f\ ^7F_3$
2725. 35	1*h*	36681. 69	$a\ ^3H_4-s\ ^3D_3^0$
2723. 90	2*h*	36701. 21	$z\ ^7F_3^0-f\ ^7F_3$
2722. 98	2*w*	36713. 60	$a\ ^5G_5-p\ ^5F_5^0$
			$a\ ^5G_4-p\ ^5F_4^0$
2722. 085	10	36725. 69	$b\ ^5D_4-s\ ^3H_5^0$
2721. 38	2*h*	36735. 20	$a\ ^3F_2-t\ ^3P_2^0$
2719. 10	4	36766. 00	$b\ ^5D_2-r\ ^5P_1^0$
2718. 07	7	36779. 93	$a\ ^5D_3-v\ ^5P_3^0$
2716. 643	10	36799. 25	$a\ ^3F_4-q\ ^3G_5^0$
2716. 177	20, *Z*	36805. 57	$a\ ^5D_4-v\ ^5P_3^0$
2715. 98	4*w*	36808. 23	$a\ ^3H_6-s\ ^3H_5^0$
			$a\ ^3G_6-p\ ^3F_4^0$
2715. 51	2	36814. 60	$a\ ^3H_5-s\ ^3H_4^0$
			$a\ ^3G_3-t\ ^3F_4^0$
2714. 834	8	36823. 77	$a\ ^3F_2-q\ ^3G_3^0$
2714. 48	4*h*	36828. 57	$z\ ^7F_3^0-f\ ^7F_2$
			$z\ ^7F_4^0-f\ ^7F_4$
2713. 93	3	36836. 04	
2713. 36	6	36843. 78	
2711. 40	6*wl*	36870. 40	$a\ ^3F_3-q\ ^3G_4^0$
2710. 19	25*w*	36886. 86	$z\ ^7F_5^0-f\ ^7F_5$
2708. 24	3	36913. 43	$b\ ^5D_4-o\ ^5F_5^0$
2708. 14	2	36914. 79	
2707. 69	7*w*	36920. 92	$a\ ^3P_0-x\ ^3S_1^0$
2707. 46	2*h*	36924. 06	$z\ ^7F_5^0-f\ ^7F_5$
			$a\ ^3P_2-t\ ^3D_2^0$
2706. 531	20, *Z*	36936. 73	$a\ ^3H_4-s\ ^3H_4^0$
2705. 92	2	36945. 07	$z\ ^7F_2^0-f\ ^7F_2$
2705. 724	10	36947. 75	$a\ ^5D_4-x\ ^5F_5^0$
			$a\ ^5D_2-v\ ^5P_2^0$
2705. 414	12, *Z*	36951. 98	$a\ ^3H_5-s\ ^3H_5^0$

TABLE 1. *Wavelengths and term combinations of* Cr I—Continued

d, double; *h*, hazy; *H*, very hazy; *l*, shaded longward; *s*, shaded shortward; *r*, reversed; *R*, strongly reversed; *w*, wide; *W*, very wide; *Z*, Zeeman pattern in table 2.

Wavelength λ_{air}	Intensity	Wave No.	Term combination
2704. 89	15*w*	36959. 14	
2704. 744	12, *Z*	36961. 13	$a\ ^3H_6 - r\ ^3G_5^0$
2703. 48	12	36978. 41	$a\ ^5D_4 - x\ ^5F_4^0$
2703. 11	2*h*	36983. 47	$z\ ^7F_5^0 - f\ ^7F_4$
2702. 68	2	36989. 35	$a\ ^3F_2 - q\ ^3G_3^0$
2702. 519	15, *Z*	36991. 56	$a\ ^3H_6 - s\ ^3H_6^0$
2701. 990	30, *Z*	36998. 80	$a\ ^5D_4 - x\ ^5F_5^0$; $a\ ^3G_5 - q\ ^3G_5^0$
2700. 590	20	37017. 98	$a\ ^5D_3 - v\ ^5P_3^0$
2700. 29	3	37022. 09	$a\ ^5P_2 - t\ ^3D_1^0$
2698. 19	2	37050. 91	$a\ ^5D_4 - z\ ^3H_4^0$
2698. 094	4	37052. 23	
2697. 200	8	37064. 50	$a\ ^5D_1 - v\ ^5P_2^0$
2697. 01	15	37067. 11	$a\ ^3H_5 - r\ ^3G_4^0$
2696. 534	20	37073. 66	$a\ ^5S_2 - v\ ^5P_1^0$
2696. 135	10	37079. 15	$a\ ^3G_4 - q\ ^3G_4^0$
2694. 887	10	37096. 31	$a\ ^3G_3 - q\ ^3G_3^0$
2694. 24	2	37105. 22	$a\ ^3H_5 - r\ ^3G_3^0$
2693. 90	5*w*	37109. 90	$z\ ^7F_5^0 - f\ ^7F_6$
2693. 62	4*w*	37113. 76	$z\ ^7F_4^0 - f\ ^7F_5$
2693. 315	8	37117. 97	$a\ ^3P_1 - s\ ^3D_2^0$
2692. 441	10	37130. 01	$a\ ^5D_3 - x\ ^5F_3^0$
2691. 712	4	37140. 07	$a\ ^3G_4 - q\ ^3G_5^0$
2691. 404	12	37144. 32	$a\ ^3H_4 - r\ ^3G_3^0$
2690. 82	2	37152. 38	$z\ ^7D_3^0 - e\ ^5H_5$
2690. 251	20	37160. 24	$a\ ^5D_2 - x\ ^5F_2^0$
2689. 82	2	37166. 19	$a\ ^3P_1 - s\ ^3D_1^0$
2688. 035	22, *Z*	37190. 87	$a\ ^5D_3 - x\ ^5F_4^0$
2687. 85	2	37193. 43	
2687. 57	2	37197. 30	
2686. 608	2	37210. 62	
2686. 52	2	37211. 84	$z\ ^7D_3^0 - e\ ^5H_3$
2685. 40	4*h*	37227. 36	$a\ ^3H_4 - r\ ^3G_3^0$
2683. 16	4	37258. 44	$a\ ^5D_4 - y\ ^5H_5^0$
2682. 01	10	37274. 41	$a\ ^5D_2 - x\ ^5F_1^0$
2681. 46	18	37282. 06	$a\ ^5S_2 - v\ ^5P_2^0$
2680. 64	2*w*	37293. 46	
2680. 33	3*w*	37297. 78	$a\ ^5D_2 - x\ ^5F_2^0$
2679. 82	4	37304. 87	
2679. 28	4*w*	37312. 39	
2678. 15	12	37328. 13	$a\ ^5D_2 - x\ ^5F_3^0$
2677. 43	3	37338. 17	
2675. 955	3*w*	37358. 76	
2673. 644	12	37391. 04	$a\ ^5D_1 - x\ ^5F_1^0$
2671. 980	10	37414. 32	$a\ ^5D_1 - x\ ^5F_2^0$
2671. 17	2	37425. 67	
2670. 562	10	37434. 20	$a\ ^3P_2 - t\ ^3P_1^0$
2669. 359	12	37451. 06	$a\ ^5D_0 - x\ ^5F_1^0$
2668. 328	1	37465. 53	
2665. 10	5	37510. 90	
2664. 818	3	37514. 88	$a\ ^3P_0 - s\ ^3D_1^0$
2664. 44	7	37520. 14	$a\ ^5S_2 - v\ ^5P_3^0$
2662. 29	2	37550. 49	
2660. 006	8*w*	37582. 73	$a\ ^3P_2 - t\ ^3P_2^0$
2657. 23	1	37621. 99	
2656. 02	4	37638. 99	$a\ ^5D_3 - y\ ^3P_2^0$
2655. 05	4	37652. 88	$a\ ^3F_4 - r\ ^3H_5^0$
2654. 844	5	37655. 80	$a\ ^3F_3 - r\ ^3H_4^0$
2654. 412	10, *Z*	37661. 93	
2652. 44	4	37689. 93	
2651. 303	7	37706. 09	
2648. 17	2	37750. 70	$a\ ^5D_4 - y\ ^3F_4^0$
2646. 82	1*wh*	37769. 95	
2645. 30	2	37791. 65	$a\ ^3G_5 - r\ ^3H_5^0$; $a\ ^5D_2 - y\ ^3P_1^0$
2644. 63	1	37801. 23	
2644. 23	7	37806. 95	$a\ ^5D_2 - y\ ^3P_2^0$
2644. 12	5	37808. 52	
2642. 118	20, *Z*	37837. 17	$a\ ^3H_6 - q\ ^3G_5^0$
2640. 221	5	37864. 35	$a\ ^3G_5 - r\ ^3H_6^0$; $a\ ^3G_4 - r\ ^3H_4^0$
2640. 056	7	37866. 72	$a\ ^5D_4 - y\ ^3D_3^0$
2639. 54	5	37874. 12	
2639. 42	7	37875. 84	$a\ ^3P_1 - t\ ^1P_0^0$
2638. 892	15	37883. 42	
2637. 168	4	37908. 20	$a\ ^5D_1 - y\ ^3P_1^0$
2636. 89	4	37912. 18	$a\ ^5D_1 - y\ ^3P_0^0$
2636. 094	5	37923. 62	$a\ ^5D_1 - y\ ^3P_2^0$
2635. 777	8	37928. 19	$a\ ^3G_3 - r\ ^3H_4^0$
2635. 44	7	37933. 04	$a\ ^3G_4 - r\ ^3H_5^0$
2634. 23	4	37950. 46	
2633. 38	2	37962. 70	$a\ ^5D_3 - y\ ^3F_4^0$
2633. 19	1	37965. 44	
2633. 09	2	37966. 89	$a\ ^3F_4 - q\ ^3H_5^0$
2632. 987	4	37968. 39	$a\ ^5D_0 - y\ ^3P_1^0$
2632. 06	5	37981. 74	$a\ ^3H_5 - q\ ^3G_5^0$
2629. 815	12	38014. 17	$a\ ^5D_3 - y\ ^3D_2^0$
2627. 847	4	38042. 78	$a\ ^3H_4 - q\ ^3G_4^0$
2626. 601	15, *Z*	38060. 68	$a\ ^5D_4 - w\ ^5D_3^0$
2625. 318	15	38079. 28	$a\ ^5D_3 - y\ ^3D_3^0$
2622. 867	18, *Z*	38114. 87	$a\ ^5D_4 - w\ ^5D_4^0$
2622. 10	1	38126. 01	$a\ ^5S_2 - y\ ^3P_1^0$
2621. 06	1	38141. 14	$a\ ^5S_2 - y\ ^3P_2^0$
2620. 841	7	38144. 32	$a\ ^3G_5 - q\ ^3H_6^0$
2620. 480	12, *Z*	38149. 57	$a\ ^5D_2 - y\ ^3D_1^0$
2619. 978	12	38156. 87	
2619. 87	2	38158. 46	
2619. 504	8	38163. 79	$a\ ^3P_1 - t\ ^3P_1^0$
2618. 273	15	38181. 72	$a\ ^5D_2 - y\ ^3D_2^0$
2617. 44	1	38193. 88	
2616. 46	3*w*	38208. 18	
2614. 18	2	38241. 51	
2613. 82	8	38246. 77	$a\ ^3G_4 - q\ ^3H_5^0$; $a\ ^5D_2 - y\ ^3D_3^0$
2613. 305	10	38254. 31	$a\ ^5D_3 - w\ ^5D_3^0$
2612. 490	7	38266. 24	$a\ ^5D_1 - y\ ^3D_1^0$
2612. 202	8	38270. 46	$a\ ^5D_1 - w\ ^5D_0^0$
2612. 009	7	38273. 29	$a\ ^5D_2 - w\ ^5D_2^0$
2611. 75	1	38277. 08	$b\ ^3G_5 - p\ ^3G_4^0$
2611. 342	3	38283. 06	$a\ ^3G_3 - q\ ^3H_4^0$
2610. 29	8	38298. 49	$a\ ^5D_1 - y\ ^3D_2^0$
2609. 84	1	38305. 10	$b\ ^3G_4 - p\ ^3G_3^0$
2608. 385	10	38326. 46	$a\ ^5D_0 - y\ ^3D_1^0$
2605. 82	6	38364. 19	$a\ ^3P_0 - t\ ^3P_1^0$; $b\ ^3G_5 - p\ ^3G_5^0$

TABLE 1. *Wavelengths and term combinations of* Cr I—Continued

d, Double; *h*, hazy; *H*, very hazy; *l*, shaded longward; *s*, shaded shortward; *r*, reversed; *R*, strongly reversed; *w*, wide; *W*, very wide; *Z*, Zeeman pattern in Table 2.

Wavelength λ_{air}	Intensity	Wave No.	Term combination
2605. 36	7	38370. 96	$a\ ^5D_2 - w\ ^5D^\circ_1$
2604. 71	3	38380. 53	$a\ ^5D_4 - w\ ^5F^\circ_5$
2604. 08	2*w*	38389. 82	$b\ ^3G_4 - p\ ^3G^\circ_4$
2603. 56	10	38397. 49	$a\ ^5D_4 - w\ ^5F^\circ_4$
2602. 62	1	38411. 35	$b\ ^3G_3 - p\ ^3G^\circ_3$
2602. 50	6	38413. 12	$a\ ^5D_4 - w\ ^5F^\circ_4$
2602. 19	3	38417. 70	
2601. 88	4	38422. 28	$a\ ^5D_2 - w\ ^5D^\circ_3$
2600. 61	8	38441. 04	$a\ ^5D_2 - w\ ^5D^\circ_2$
2595. 75	1	38513. 01	
2594. 02	8	38538. 69	$a\ ^5D_1 - w\ ^5D^\circ_2$
2593. 41	8	38547. 75	$a\ ^5D_0 - w\ ^5D^\circ_1$
2591. 84	50*r*, *Z*	38571. 11	$a\ ^5D_4 - u\ ^5P^\circ_3$
2591. 16	2	38581. 23	$a\ ^5S_2 - y\ ^5D^\circ_3$
2590. 95	1	38584. 35	
2590. 83	1	38586. 14	
2590. 37	2	38593. 00	$a\ ^5D_3 - w\ ^5F^\circ_3$
2590. 07	5	38597. 46	$a\ ^5D_4 - z\ ^5G^\circ_4$
2588. 19	12	38625. 49	$a\ ^5D_3 - w\ ^5F^\circ_4$
2587. 88	2	38630. 12	$a\ ^3H_6 - r\ ^3H^\circ_5$
2587. 50	3	38635. 79	
2584. 67	10	38678. 10	$a\ ^5D_4 - z\ ^5G^\circ_3$
2583. 02	8*w*	38702. 80	$a\ ^3H_6 - r\ ^3H^\circ_6$
2580. 48	2	38740. 89	$a\ ^5D_4 - y\ ^5G^\circ_5$
2580. 04	7	38747. 50	$a\ ^5D_4 - y\ ^5G^\circ_5$ $a\ ^5D_4 - y\ ^5G^\circ_4$
2579. 90	4	38749. 60	$a\ ^5D_2 - w\ ^5F^\circ_2$
2579. 77	4	38751. 55	$a\ ^5D_2 - w\ ^5F^\circ_1$ $a\ ^5D_3 - z\ ^3G^\circ_3$
2579. 14	12, *Z*	38761. 02	$a\ ^5D_2 - w\ ^5F^\circ_3$
2578. 27	10, *Z*	38774. 10	$a\ ^3H_5 - r\ ^3H^\circ_5$
2577. 66	20*r*, *Z*	38783. 28	$a\ ^5D_2 - u\ ^5P^\circ_2$
2576. 99	2	38793. 35	
2575. 89	8	38809. 92	$a\ ^5D_3 - z\ ^3G^\circ_4$
2575. 60	2	38814. 29	
2575. 11	2 Al?	38821. 67	
2574. 68	10	38828. 16	$a\ ^3H_4 - r\ ^3H^\circ_4$
2572. 15	12, *Z*	38866. 35	$a\ ^5D_1 - w\ ^5F^\circ_2$
2572. 07	5	38867. 56	$a\ ^5D_1 - w\ ^5F^\circ_1$
2571. 74	30*r*, *Z*	38872. 54	$a\ ^5D_3 - u\ ^5P^\circ_3$
2571. 10	4	38882. 22	$a\ ^5D_4 - x\ ^5G^\circ_4$
2570. 17	1	38896. 29	$a\ ^3H_4 - r\ ^3H^\circ_3$
2569. 89	2	38900. 52	
2568. 66	5	38919. 15	$a\ ^5D_2 - z\ ^5G^\circ_3$
2568. 52	8	38921. 27	$a\ ^5D_4 - x\ ^5G^\circ_5$
2568. 29	3	38924. 76	
2568. 098	12	38927. 65	$a\ ^5D_0 - w\ ^5F^\circ_1$
2566. 55	12, *Z*	38951. 14	$a\ ^5D_2 - u\ ^5P^\circ_2$
2566. 41	1	38953. 27	$a\ ^5D_3 - y\ ^3G^\circ_3$
2566. 00	10	38959. 49	$a\ ^5D_3 - y\ ^3G^\circ_4$ $a\ ^3G_5 - p\ ^3H^\circ_4$
2565. 51	5*w*	38966. 93	
2565. 21	3	38971. 49	$a\ ^3P_2 - p\ ^3F^\circ_3$
2564. 65	6	38979. 99	
2564. 47	7	38982. 74	$a\ ^3H_6 - q\ ^3H^\circ_4$
2563. 67	2	38995. 00	
2561. 38	4	39029. 76	$a\ ^3G_4 - p\ ^3H^\circ_5$
2561. 33	5	39030. 42	$a\ ^5D_3 - x\ ^5G^\circ_3$
2560. 86	2	39037. 68	
2560. 695	30, *Z*	39040. 18	$a\ ^5D_2 - u\ ^5P^\circ_1$
2560. 28	4	39046. 53	
2559. 01	1	39065. 90	
2557. 82	1	39084. 08	$a\ ^5S_2 - w\ ^5F^\circ_2$
2557. 56	4	39088. 05	$a\ ^3H_5 - q\ ^3H^\circ_5$
2557. 144	25, *Z*	39094. 40	$a\ ^5D_2 - u\ ^5P^\circ_1$ $a\ ^5D_3 - x\ ^5G^\circ_4$
2556. 40	2	39105. 79	
2555. 50	10	39119. 56	$a\ ^5D_2 - x\ ^5G^\circ_3$ $a\ ^5P_3 - p\ ^3F^\circ_4$
2555. 42	6*w*	39120. 78	$a\ ^5D_2 - y\ ^3G^\circ_3$
2553. 82	1	39145. 29	
2553. 064	15	39156. 88	$a\ ^5D_1 - u\ ^5P^\circ_2$
2552. 79	10	39161. 08	$a\ ^5D_2 - z\ ^3S^\circ_1$
2552. 05	2*w*	39172. 44	$z\ ^7P^\circ_4 - f\ ^5G_4$
2551. 36	2	39183. 03	$a\ ^3H_4 - q\ ^3H^\circ_4$
2550. 364	8	39198. 33	$a\ ^5D_2 - x\ ^5G^\circ_3$
2549. 548	40, *Z*	39210. 88	$a\ ^5D_1 - u\ ^5P^\circ_1$
2547. 868	8	39236. 73	$a\ ^5D_1 - x\ ^5G^\circ_2$
2547. 206	5*w*	39246. 93	
2546. 353	5*w*	39260. 07	$a\ ^5P_2 - r\ ^5P^\circ_2$ $z\ ^7P^\circ_3 - f\ ^5G_2$
2545. 645	12, *Z*	39270. 99	$a\ ^5D_0 - u\ ^5P^\circ_1$
2545. 21	10	39277. 70	$a\ ^5D_1 - z\ ^3S^\circ_1$
2544. 702	15	39285. 54	$a\ ^5S_2 - u\ ^5P^\circ_3$
2543. 11	6*w*	39310. 13	
2542. 872	3	39313. 81	$a\ ^5D_4 - x\ ^5H^\circ_5$
2541. 91	3	39328. 69	$a\ ^5D_4 - v\ ^5F^\circ_5$
2541. 68	8	39332. 25	$a\ ^5D_4 - v\ ^5F^\circ_4$
2541. 359	20*r*	39337. 22	$a\ ^5D_4 - v\ ^5F^\circ_3$ $a\ ^5D_0 - z\ ^3S^\circ_1$
2540. 48	2*w*	39350. 83	$a\ ^5P_2 - r\ ^5P^\circ_3$
2540. 03	2*w*	39357. 80	$a\ ^5P_3 - r\ ^5P^\circ_3$
2538. 95	12	39374. 54	$a\ ^5S_2 - u\ ^5P^\circ_2$
2538. 53	2	39381. 05	$a\ ^5D_4 - x\ ^5H^\circ_4$
2537. 61	1	39395. 33	
2536. 50	2	39412. 57	
2536. 21	3*w*	39417. 07	
2535. 96	6	39420. 96	
2535. 47	10	39428. 57	$a\ ^5S_2 - u\ ^5P^\circ_1$
2533. 35	3*w*	39461. 57	
2532. 17	2	39479. 96	
2531. 82	3	39485. 41	
2531. 76	5	39486. 35	$a\ ^5D_4 - x\ ^5H^\circ_3$
2530. 44	15	39506. 95	$a\ ^5D_4 - v\ ^5D^\circ_3$
2529. 20	5	39526. 32	$a\ ^5D_3 - x\ ^5H^\circ_3$
2528. 96	5	39530. 06	
2528. 56	8	39536. 32	$a\ ^5D_2 - v\ ^5F^\circ_3$
2528. 25	10	39541. 17	$a\ ^5D_3 - v\ ^5F^\circ_4$
2528. 02	15	39544. 76	$a\ ^5D_3 - v\ ^5F^\circ_3$
2527. 57	1	39551. 80	
2527. 11	20*r*, *Z*	39559. 00	$a\ ^5D_4 - v\ ^5D^\circ_4$
2526. 55	2*w*	39567. 77	
2523. 44	2	39616. 53	
2522. 23	2*w*	39635. 54	
2520. 23	6	39666. 99	$a\ ^5D_4 - u\ ^5F^\circ_5$
2519. 51	50*r*, *Z*	39678. 32	$a\ ^5D_4 - u\ ^5F^\circ_4$
2518. 71	12	39690. 92	$a\ ^5D_3 - v\ ^5D^\circ_3$

TABLE 1. *Wavelengths and term combinations of* Cr I—Continued

d, double; *h*, hazy; *H*, very hazy; *l*, shaded longward; *s*, shaded shortward; *r*, reversed; *R*, strongly reversed; *w*, wide; *W*, very wide; *Z*, Zeeman pattern in table 2.

Wavelength λ_{air}	Intensity	Wave No.	Term combination	Wavelength λ_{air}	Intensity	Wave No.	Term combination
2518.52	4	39693.92	$a\ ^5D_2-x\ ^5H^0_3$	2485.04	1*w*	40228.66	
2517.99	2	39702.27	$a\ ^5D_2-v\ ^5F^0_1$	2484.86	4	40231.57	
2517.87	6	39704.16	$a\ ^5D_2-v\ ^5F^0_2$	2482.62	1*w*	40267.87	
2517.57	10	39708.89	$a\ ^5D_2-v\ ^5F^0_3$	2482.25	3*w*	40273.87	
2516.92	20*r*, *Z*	39719.15	$a\ ^5D_2-v\ ^5D^0_3$	2482.03	3*w*	40277.84	
2516.42	1	39727.04	$a\ ^3H_6-p\ ^3H^0_5$	2481.65	2*w*	40283.61	$a\ ^5D_2-t\ ^5F^0_1$
2515.90	7	39735.25	$a\ ^5D_4-t\ ^5F^0_4$	2481.23	10	40290.42	$a\ ^5D_2-t\ ^5F^0_2$
2514.73	2	39753.74		2480.10	2	40308.78	
2513.62	15	39771.29	$a\ ^5D_3-v\ ^5D^0_4$	2479.94	1	40311.38	
2511.96	15	39797.57	$a\ ^3H_6-p\ ^3H^0_6$	2479.14	15	40324.39	$a\ ^5D_2-t\ ^5F^0_3$
2511.01	3	39812.63		2476.07	1	40374.38	
2510.63	6	39818.65	$a\ ^5D_1-v\ ^5F^0_1$	2474.55	8	40399.18	$a\ ^5D_1-t\ ^5F^0_1$
2510.49	8	39820.86	$a\ ^5D_1-v\ ^5F^0_2$	2474.27	4	40403.75	$a\ ^5D_2-x\ ^3P^0_1$
2510.37	2	39822.77	$a\ ^5D_2-u\ ^5F^0_2$	2474.08	15	40406.85	$a\ ^5D_1-t\ ^5F^0_2$
2508.97	15, *Z*	39844.99	$a\ ^5D_2-v\ ^5D^0_1$	2473.53	1*w*	40415.84	$a\ ^5D_1-x\ ^3P^0_0$
2508.11	18, *Z*	39858.65	$a\ ^5D_2-v\ ^5D^0_2$	2470.88	12	40459.18	$a\ ^5D_0-t\ ^5F^0_1$
2507.32	12	39871.21	$a\ ^3H_5-p\ ^3H^0_5$	2470.27	1	40469.17	
2506.82	25, *Z*	39879.16	$a\ ^5D_0-v\ ^5F^0_1$ $a\ ^5D_3-u\ ^5F^0_3$	2470.06	1*w*	40472.61	
2506.45	2	39885.05		2469.70	4	40478.51	$a\ ^5D_4-x\ ^3G^0_3$
2506.33	4	39886.96	$a\ ^5D_2-v\ ^5D^0_3$	2469.35	2*w*	40484.25	$a\ ^5G_5-s\ ^3H^0_5$ $a\ ^5G_4-s\ ^3H^0_5$
2505.99	1*w*	39892.37		2468.33	10*w*	40500.97	
2505.37	4*w*	39902.24		2467.14	8	40520.52	$a\ ^5D_1-x\ ^3P^0_1$
2505.00	10	39908.14	$a\ ^3H_4-p\ ^3H^0_4$	2466.49	7	40531.18	$a\ ^5D_2-x\ ^3P^0_2$
2504.31	40*r*, *Z*	39919.13	$a\ ^5D_3-u\ ^5F^0_4$	2466.34	1	40533.65	
2502.89	3	39941.78	$a\ ^3H_5-p\ ^3H^0_6$	2465.90	2	40540.88	$a\ ^5D_3-1^0_3$
2502.72	2	39944.49	$a\ ^5D_4-t\ ^5F^0_3$	2465.74	4*w*	40543.51	
2502.55	25*r*, *Z*	39947.20	$a\ ^5D_3-t\ ^5F^0_4$	2465.50	5*w*	40547.46	
2502.27	1*w*	39951.68		2465.30	3*w*	40550.75	
2501.91	4*w*	39957.42		2464.00	1*w*	40572.14	
2501.65	10	39961.57	$a\ ^5D_1-v\ ^5D^0_1$	2463.49	5	40580.54	$a\ ^5D_0-x\ ^3P^0_1$
2500.79	4	39975.32	$a\ ^5D_1-v\ ^5D^0_2$	2463.37	2*w*	40582.51	
2500.66	12	39977.39	$a\ ^5D_1-v\ ^5D^0_0$	2460.96	2*w*	40622.26	
2500.44	2	39980.91	$a\ ^5D_4-y\ ^3H^0_4$	2460.20	3	40634.80	
2499.84	15	39990.50	$a\ ^5D_2-u\ ^5F^0_2$	2458.74	2	40658.93	$a\ ^5S_2-t\ ^5F^0_3$
2499.66	2	39993.39	$a\ ^3H_4-p\ ^3H^0_5$	2458.43	3*w*	40664.06	
2499.56	4	39994.99		2457.86	4*w*	40673.49	
2499.34	4	39998.50		2457.08	4*w*	40686.40	
2497.91	10	40021.40	$a\ ^5D_0-v\ ^5D^0_1$	2456.54	1	40695.34	
2497.15	5*w*	40033.58		2456.28	8	40699.65	
2496.30	35*r*, *Z*	40047.21	$a\ ^5D_2-u\ ^5F^0_3$	2455.71	2	40709.09	$a\ ^5D_2-1^0_2$
2495.68	3*w*	40057.16					
2495.08	20	40066.79	$a\ ^5D_1-u\ ^5F^0_1$	2455.67	1	40709.76	
2493.89	4	40085.91		2453.14	2	40751.74	
2493.75	2	40088.16		2453.08	1	40752.74	
2493.60	8	40090.57		2452.11	2	40768.85	
				2451.51	3	40778.83	
2492.57	30, *Z*	40107.30	$a\ ^5D_1-u\ ^5F^0_2$				
2491.35	20, *Z*	40126.78	$a\ ^5D_0-u\ ^5F^0_1$	2451.36	3	40781.33	
2489.48	8	40156.91	$a\ ^5D_3-t\ ^5F^0_3$	2449.81	3*wh*	40807.13	
2488.96	2*w*	40165.30		2449.25	2*w*	40816.46	
2488.81	2*w*	40167.72		2447.90	1	40838.97	
				2447.11	2	40852.15	
2488.62	1*w*	40170.79					
2487.24	2	40193.08	$a\ ^5D_2-y\ ^3H^0_4$ $a\ ^5S_2-v\ ^5D^0_2$	2446.29	2	40865.84	$a\ ^5S_2-x\ ^3P^0_2$
2486.97	2*w*	40197.44		2445.76	1	40874.70	
2485.83	4	40215.87		2443.25	2	40916.69	$a\ ^3F_4-p\ ^3G^0_4$
2485.48	2	40221.53	$a\ ^5S_2-v\ D^0_2$	2442.31	2	40932.43	$a\ ^5D_3-x\ ^3D^0_2$
				2441.30	3*wh*	40949.36	

TABLE 1. *Wavelengths and term combinations of* Cr I—Continued

d, Double; *h*, hazy; *H*, very hazy; *l*, shaded longward; *s*, shaded shortward; *r*, reversed; *R*, strongly reversed; *w*, wide; *W*, very wide; *Z*, Zeeman pattern in table 2.

Wavelength λ_{air}	Intensity	Wave No.	Term combination
2439.02	7	40987.64	$a\ ^3F_3 - p\ ^3G^0_4$
2438.76	2	40992.01	
2438.22	2*w*	41001.09	
2438.10	3*w*	41003.10	$a\ ^3F_4 - p\ ^3G^0_5$; $a\ ^5D_4 - x\ ^5D^0_3$
2435.69	1	41043.67	$a\ ^7S_3 - x\ ^5P^0_3$
2435.59	1*w*	41045.36	
2434.98	1	41055.64	$a\ ^3G_5 - p\ ^3G^0_4$
2434.36	2*wh*	41066.09	
2434.22	4	41068.46	$a\ ^3F_2 - p\ ^3G^0_3$
2432.99	3	41089.21	$a\ ^5D_0 - x\ ^5D^0_1$
2431.67	3	41111.52	$a\ ^3G_6 - p\ ^3G^0_5$
2429.89	6*w*	41141.63	$a\ ^3G_5 - p\ ^3G^0_4$
2428.89	4*w*	41158.57	$a\ ^5G_2 - t\ ^3P^0_2$
2427.92	8	41175.02	$a\ ^3G_3 - p\ ^3G^0_3$
2426.66	7	41196.40	$a\ ^3G_4 - p\ ^3G^0_4$
2425.52	2	41215.75	$a\ ^5D_3 - x\ ^3D^0_3$
2425.46	1	41216.77	$a\ ^5D_1 - x\ ^3D^0_2$
2424.65	3	41230.54	$a\ ^5D_4 - w\ ^3G^0_5$
2423.24	10*w*	41254.53	
2422.57	12	41265.94	$a\ ^5D_4 - w\ ^5G^0_4$
2421.71	10	41280.59	
2421.31	1	41287.41	
2421.16	1*w*	41289.97	
2419.98	8	41310.10	$a\ ^5D_4 - w\ ^5G^0_5$
2419.82	2	41312.73	$a\ ^5D_4 - x\ ^3F^0_4$
2419.30	1	41321.71	
2418.56	1*wh*	41334.35	
2415.41	2	41388.25	
2415.09	2*w*	41393.73	
2412.33	1*w*	41441.09	
2410.18	2	41478.05	$a\ ^5D_2 - w\ ^5G^0_3$
2408.72	35*r*	41503.19	$a\ ^5D_2 - t\ ^5P^0_3$
2408.60	50*r*	41505.26	$a\ ^5D_4 - t\ ^5P^0_3$
2407.41	8	41525.78	$a\ ^5D_3 - x\ ^3F^0_4$
2406.03	5	41549.59	$a\ ^5D_2 - y\ ^3S^0_1$
2405.70	2	41555.29	$a\ ^5D_3 - x\ ^3F^0_3$
2403.92	1	41586.06	
2401.81	1	41622.59	
2399.56	20	41661.61	$a\ ^5D_2 - t\ ^5P^0_1$
2399.29	3	41666.30	$a\ ^5D_1 - y\ ^3S^0_1$
2399.02	20*r*	41670.99	$a\ ^5D_2 - t\ ^5P^0_2$
2397.19	1	41702.80	
2396.36	30*r*	41717.25	$a\ ^5D_3 - t\ ^5P^0_3$
2396.04	7	41722.81	$a\ ^5D_2 - x\ ^3F^0_3$
2395.89	2	41725.82	$a\ ^5D_2 - x\ ^3F^0_2$
2395.84	2	41726.29	$a\ ^5D_0 - y\ ^3S^0_1$
2395.77	8	41727.51	$a\ ^5D_3 - y\ ^3S^0_2$
2392.86	25*r*	41778.25	$a\ ^5D_1 - t\ ^5P^0_1$
2392.34	10*w*	41787.33	$a\ ^5D_1 - t\ ^5P^0_2$
2391.95	3*w*	41794.15	$a\ ^5D_4 - s\ ^5F^0_5$
2390.09	4*wh*	41826.67	
2389.43	10*w*	41838.22	$a\ ^5D_0 - t\ ^5P^0_1$
2389.21	3*w*	41842.07	$a\ ^5D_1 - x\ ^3F^0_2$
2387.46	2*wh*	41872.74	$a\ ^5S_2 - w\ ^5G^0_3$
2386.77	7*w*	41884.84	$a\ ^5D_3 - t\ ^5P^0_3$
2386.18	10	41895.20	$a\ ^5D_2 - y\ ^5S^0_2$
2385.72	7*wh*	41903.28	$a\ ^5D_4 - s\ ^5F^0_4$
2384.28	1*wh*	41926.83	$a\ ^5S_2 - w\ ^5G^0_2$
2383.303	40*r*	41945.77	$a\ ^5D_4 - s\ ^5F^0_3$
2382.67	1	41956.91	$a\ ^5D_4 - w\ ^3D^0_3$
2382.36	7*w*	41962.37	$a\ ^5D_3 - s\ ^5F^0_2$
2382.18	1	41965.54	
2381.36	7	41979.99	$a\ ^3H_6 - p\ ^3G^0_5$
2380.46	7	41995.86	$a\ ^5S_2 - t\ ^5P^0_1$
2379.95	10	42004.86	$a\ ^5S_2 - t\ ^5P^0_2$
2379.85	10*ws*	42006.62	$a\ ^5D_3 - s\ ^5F^0_3$
2379.56	8	42011.74	$a\ ^5D_1 - y\ ^5S^0_2$
2379.17	1	42018.63	
2378.07	20	42037.89	$a\ ^3H_5 - p\ ^3G^0_4$
2377.94	10*rh*	42040.36	
2375.98	7	42075.04	$a\ ^3H_4 - p\ ^3G^0_3$
2375.41	40*wh*	42085.13	
2375.06	5	42091.34	$a\ ^5D_2 - s\ ^5F^0_1$
2373.69	50*rh*	42115.63	$a\ ^5D_3 - s\ ^5F^0_4$
2373.12	1*w*, Al?	42125.74	
2372.88	20*r*	42130.00	$a\ ^5D_2 - s\ ^5F^0_2$
2371.18	2	42160.20	$a\ ^3H_4 - p\ ^3G^0_4$
2370.66	3	42169.45	$a\ ^5D_3 - w\ ^3D^0_3$
2370.37	35*r*	42174.61	$a\ ^5D_2 - s\ ^5F^0_3$
2368.49	12	42208.09	$a\ ^5D_1 - s\ ^5F^0_1$
2368.46	3	42208.62	
2367.86	10	42219.31	$a\ ^5S_2 - t\ ^5P^0_3$
2367.29	3	42229.48	$a\ ^5S_2 - y\ ^5S^0_2$
2366.81	100*r*	42238.04	$a\ ^7S_3 - x\ ^7P^0_2$
2366.31	50	42246.97	$a\ ^5D_1 - s\ ^5F^0_2$
2366.14	25	42250.00	$a\ ^5D_4 - u\ ^5D^0_4$
2365.91	125*r*	42254.11	$a\ ^7S_3 - x\ ^7P^0_3$
2365.13	5	42268.04	$a\ ^5D_0 - s\ ^5F^0_1$
2364.73	150*r*	42275.19	$a\ ^7S_3 - x\ ^7P^0_4$
2362.19	15	42320.64	$a\ ^5D_4 - u\ ^5D^0_3$
2361.59	2*wh*	42331.39	
2355.98	1	42432.18	
2354.93	1*w*	42451.11	
2354.30	15	42462.46	$a\ ^5D_3 - u\ ^5D^0_4$
2352.93	5*wh*	42487.19	
2350.82	1*w*	42525.31	
2350.40	12	42532.91	$a\ ^5D_2 - u\ ^5D^0_3$
2349.83	4	42543.23	
2349.06	1	42557.17	
2348.92	25	42559.71	$a\ ^5D_2 - u\ ^5D^0_2$
2348.46	1*w*	42568.04	
2346.53	3*wh*	42603.05	
2345.91	1*wh*	42614.31	
2344.34	1	42642.85	$a\ ^5D_4 - w\ ^3F^0_3$
2344.04	1	42648.30	$a\ ^7S_3 - x\ ^5D^0_2$
2343.68	4*w*	42654.85	
2342.54	3*w*	42675.61	
2342.11	5*w*	42683.45	
2341.17	20	42700.58	$a\ ^5D_2 - u\ ^5D^0_1$
2339.71	4	42727.22	$a\ ^5D_2 - u\ ^5D^0_2$

TABLE 1. *Wavelengths and term combinations of* Cr I—Continued

d, diffuse; *h*, hazy; *H*, very hazy; *l*, shaded longward; *s*, shaded shortward; *r*, reversed; *R*, strongly reversed; *w*, wide; *W*, very wide; *Z*, Zeeman pattern in table 2.

Wavelength λ_{air}	Intensity	Wave No.	Term combination	Wavelength λ_{air}	Intensity	Wave No.	Term combination
2339.27	15	42735.26	$a\ ^5D_2-u\ ^5D^\circ_1$	2160.50	4	46270.99	$a\ ^5D_2-q\ ^5F^\circ_1$
2338.34	2	42752.25	$a\ ^5D_4-w^3F^\circ_4$	2158.00	15	46324.59	$a\ ^5D_2-q\ ^5F^\circ_2$
2337.82	4	42761.76		2157.74	30	46330.17	$a\ ^5D_3-q\ ^5F^\circ_3$
2333.33	8	42844.04	$a\ ^5D_1-u\ ^5D^\circ_2$	2155.09	15	46387.14	$a\ ^5D_1-q\ ^5F^\circ_1$
2332.98	7	42850.47	$a\ ^5D_1-u\ ^5D^\circ_0$	2154.44	25	46401.13	$a\ ^5D_2-q\ ^5F^\circ_2$
2332.71	1	42855.43	$a\ ^5D_3-w^3F^\circ_3$	2152.57	15	46441.43	$a\ ^5D_1-q\ ^5F^\circ_2$
2330.71	8	42892.20		2152.27	10	46447.91	$a\ ^5D_0-q\ ^5F^\circ_1$
2329.63	10	42912.08	$a\ ^5D_0-u\ ^5D^\circ_1$	2150.25	1	46491.54	$a\ ^5D_4-w^3H^\circ_5$
2327.26	3	42955.78		2148.02	10	46539.80	$a\ ^5S_2-s\ ^5P^\circ_3$
2326.21	2*w*	42975.16		2144.24	1	46621.83	$a\ ^5D_4-v\ ^3H^\circ_5$
2324.45	2*w*	43007.70		2106.35	3	47460.38	
2324.22	1	43011.96		2095.83	8*h*	47698.58	$a\ ^7S_3-w^7P^\circ_2$
2322.97	2	43035.10	$a\ ^5S_2-u\ ^5D^\circ_2$	2095.40	10*h*	47708.36	$a\ ^7S_3-w^7P^\circ_3$
2320.39	3	43082.94		2095.00	12*h*	47717.47	$a\ ^7S_3-w^7P^\circ_4$
2311.46	4	43249.38		2084.08	10	47967.46	
2307.71	1	43319.65	$a\ ^5D_2-w^3P^\circ_1$				
2305.60	2	43359.29	$a\ ^5D_2-w^3P^\circ_2$	2049.31	8	48781.20	$a\ ^5D_4-u\ ^3G^\circ_5$
2305.23	2	43366.25	$a\ ^5D_1-w^3P^\circ_2$	2043.06	10	48930.41	$a\ ^5D_4-p\ ^5F^\circ_3$
2299.42	1	43475.81	$a\ ^5D_1-w^3P^\circ_1$	2042.72	8	48938.55	$a\ ^5D_3-u\ ^3G^\circ_4$
2298.34	1	43496.24	$a\ ^5D_0-w^3P^\circ_1$	2039.30	35	49020.61	$a\ ^5D_4-p\ ^5F^\circ_2$
				2038.98	1	49028.30	$a\ ^5D_4-t\ ^3F^\circ_4$
2293.86	1	43581.18					
2291.74	10	43621.49		2038.21	7	49046.83	$a\ ^5D_3-4^\circ_3$
2288.11	3	43690.69		2037.72	1	49058.62	$a\ ^5D_2-u\ ^3G^\circ_3$
2286.37	20	43723.94	$a\ ^5D_4-t\ ^5D^\circ_3$	2036.34	8	49091.86	$a\ ^5D_3-p\ ^5F^\circ_3$
2285.88	25	43733.30		2034.24	35	49142.53	$a\ ^5D_3-p\ ^5F^\circ_4$
				2032.95	5	49173.71	$a\ ^5D_2-p\ ^5F^\circ_2$
2284.67	25	43756.46	$a\ ^5D_4-t\ ^5D^\circ_4$				
2284.50	7	43759.72		2032.65	1	49180.96	$a\ ^5D_2-t\ ^3F^\circ_3$
2281.71	20*w*	43813.22		2031.27	15	49214.37	$a\ ^5D_2-4^\circ_2$
2276.31	18	43917.15	$a\ ^5D_3-t\ ^5D^\circ_2$	2030.15	1	49241.52	$a\ ^5D_2-t\ ^3F^\circ_2$
2276.01	15	43922.94		2029.42	15	49259.23	$a\ ^5D_2-p\ ^5F^\circ_3$
				2028.33	10	49285.70	$a\ ^5D_1-p\ ^5F^\circ_1$
2275.31	25	43936.45	$a\ ^5D_2-t\ ^5D^\circ_3$				
2273.62	18	43969.10	$a\ ^5D_3-t\ ^5D^\circ_4$	2028.13	12	49290.56	$a\ ^5D_1-p\ ^5F^\circ_2$
2271.29	3*w*	44014.21		2026.44	12	49331.66	
2268.13	18	44075.52	$a\ ^5D_2-t\ ^5D^\circ_1$	2025.86	15	49345.78	$a\ ^5D_0-p\ ^5F^\circ_1$
2267.64	15	44085.04	$a\ ^5D_2-t\ ^5D^\circ_2$	2005.76	10	49840.21	$a\ ^5D_4-r\ ^5D^\circ_3$
				2004.94	8	49860.59	$a\ ^5D_4-s\ ^3F^\circ_4$
2267.07	6	44096.13					
2266.66	18	44104.10	$a\ ^5D_2-t\ ^5D^\circ_3$	2003.55	5	49895.18	$a\ ^5D_4-s\ ^3F^\circ_3$
2264.00	5	44155.92		2000.60	20	49968.74	$a\ ^5D_3-r\ ^5D^\circ_2$
2262.32	15	44188.70	$a\ ^5D_1-t\ ^5D^\circ_0$	1999.95	35	49985.00	$a\ ^5D_4-r\ ^5D^\circ_4$
2262.15	7	44192.02	$a\ ^5D_1-t\ ^5D^\circ_1$	1997.25	12	50052.56	$a\ ^5D_3-r\ ^5D^\circ_3$
2261.68	18	44201.40	$a\ ^5D_1-t\ ^5D^\circ_2$	1996.65	10	50067.59	$a\ ^5D_2-r\ ^5D^\circ_1$ $a\ ^5D_2-s\ ^3F^\circ_2$
2259.08	12	44252.07	$a\ ^5D_0-t\ ^5D^\circ_1$				
2228.22	18	44864.88	$a\ ^5D_4-r\ ^5F^\circ_5$				
2220.42	10	45022.47	$a\ ^5D_3-r\ ^5F^\circ_4$	1996.44	5	50072.86	$a\ ^5D_3-s\ ^3F^\circ_4$
2214.31	8	45146.69	$a\ ^5D_2-r\ ^5F^\circ_3$	1995.04	5	50107.98	$a\ ^5D_3-s\ ^3F^\circ_3$
				1993.90	15	50136.62	$a\ ^5D_2-r\ ^5D^\circ_2$
2210.38	7	45226.95	$a\ ^5D_1-r\ ^5F^\circ_2$	1993.45	8	50147.94	$a\ ^5D_1-r\ ^5D^\circ_0$
2208.76	5	45260.11	$a\ ^5D_0-r\ ^5F^\circ_1$	1992.00	5	50184.43	$a\ ^5D_1-r\ ^5D^\circ_1$
2205.20	15	45333.17	$a\ ^5D_4-s\ ^5D^\circ_4$				
2198.32	22	45475.03	$a\ ^5D_4-s\ ^5D^\circ_4$	1991.47	6	50197.78	$a\ ^5D_3-r\ ^5D^\circ_4$
2194.90	18	45545.88	$a\ ^5D_3-s\ ^5D^\circ_3$	1990.57	15	50220.47	$a\ ^5D_2-r\ ^5D^\circ_3$
				1989.62	8	50244.44	$a\ ^5D_0-r\ ^5D^\circ_1$
2191.64	8	45613.63	$a\ ^5D_2-s\ ^5D^\circ_2$	1989.27	15	50253.28	$a\ ^5D_1-r\ ^5D^\circ_2$
2188.09	6	45687.62	$a\ ^5D_2-s\ ^5D^\circ_1$	1988.35	4	50276.52	$a\ ^5D_2-s\ ^3F^\circ_2$
2186.87	5	45713.10	$a\ ^5D_2-s\ ^5D^\circ_3$				
2185.99	4	45731.49	$a\ ^5D_1-s\ ^5D^\circ_2$				
2181.53	4	45825.00	$a\ ^5D_4-s\ ^5P^\circ_3$	λ_{vac}			
2176.19	3	45937.42	$a\ ^5D_3-s\ ^5P^\circ_3$	1916.23	2	52185.8	$a\ ^5D_4-q\ ^3D^\circ_3$
2171.44	4	46037.90	$a\ ^5D_3-s\ ^5P^\circ_2$	1912.79	4	52274.2	$a\ ^5D_3-q\ ^5D^\circ_2$
2167.68	4	46117.75	$a\ ^5D_4-q\ ^5F^\circ_4$	1911.30	7	52320.4	$a\ ^5D_4-q\ ^5D^\circ_4$
2162.47	30	46228.85	$a\ ^5D_4-q\ ^5F^\circ_3$	1909.72	2	52363.7	$a\ ^5D_2-q\ ^5D^\circ_1$
2162.25	10	46233.55	$a\ ^5D_3-q\ ^5F^\circ_2$	1908.46	4	52398.3	$a\ ^5D_3-q\ ^5D^\circ_2$

TABLE 1. *Wavelengths and term combinations of* Cr I—Continued

d, Double; *h*, hazy; *H*, very hazy; *l*, shaded longward; *s*, shaded shortward; *r*, reversed; *R*, strongly reversed; *w*, wide; *W*, very wide; *Z*, Zeeman pattern in table 2.

Wavelength $\lambda_{vac.}$	Intensity	Wave No.	Term combination	Wavelength $\lambda_{vac.}$	Intensity	Wave No.	Term combination
1907. 28	2	52430. 7	$a\ ^5D_1-q\ ^5D^0_2$	1888. 17	3	52961. 3	$a\ ^5D_3-o\ ^5F^0_4$
1906. 67	2	52447. 5	$a\ ^5D_0-q\ ^5D^0_1$	1887. 85	1	52970. 3	$a\ ^5D_1-o\ ^5F^0_2$
1903. 57	1	52532. 9	$a\ ^5D_2-q\ ^5D^0_3$	1887. 60	3	52977. 3	$a\ ^5D_2-o\ ^5F^0_3$
1903. 30	1	52540. 3	$a\ ^5D_0-q\ ^5D^0_1$	1886. 34	10	53012. 7	$a\ ^5D_3-r\ ^5P^0_3$
1902. 43	3	52564. 4	$a\ ^5D_1-q\ ^5D^0_2$ $a\ ^5D_2-q\ ^5D^0_3$	1883. 11	1	53103. 5	$a\ ^5D_3-r\ ^5P^0_2$
				1881. 87	5	53138. 6	$a\ ^5D_2-r\ ^5P^0_1$
1895. 78	1	52748. 7	$a\ ^5D_4-o\ ^5F^0_4$	1880. 39	1	53180. 5	$a\ ^5D_2-r\ ^5P^0_2$
1893. 59	1	52809. 7	$a\ ^5D_3-o\ ^5F^0_3$				
1892. 01	1	52853. 8	$a\ ^5D_2-o\ ^5F^0_2$				
1890. 78	6	52888. 2	$a\ ^5D_4-o\ ^5F^0_5$				
1889. 20	1	52932. 5	$a\ ^5D_0-o\ ^5F^0_1$				

TABLE 2. *Zeeman effect of* Cr I

Wavelengths	Magnetic patterns	Wavelengths	Magnetic patterns	Wavelengths	Magnetic patterns
6661. 10	(0.00) 1.50†	5272. 01	(0.00) 0.93†	4823. 90	(0.000) 1.323
6362. 87	(0.29 **0.72**)†	5264. 16	(1.00) 1.53, 2.24†	4816. 13	(0.000) 2.285
6330. 13	(0.00) 1.82†	5261. 76	(0.00) 1.09†	4814. 25	(0.00) 1.10†
6102. 70	(0.00) 1.02†	5255. 12	(0.00) 1.32†	4810. 71	(0.00) 0.71†
5796. 74	(0.00) 0.87†	5254. 92	(0.00) 1.47†	4810. 58	(0.00) 1.30†
5791. 00	(0.00) 1.05*A*†	5247. 58	(0.00) 2.50†	4801. 02	(0.00) 1.38*B*†
5753. 66	(0.00) 1.01†	5243. 38	(0.00) **1.04,** 2.07†	4792. 49	(**0.000,** 0.288, 0.568) 0.683, 0.967, 1.255, **1.545**
5712. 77	(0.00) 1.50†	5238. 97	(0.00) 1.22†	4766. 63	(0.00) 0.77†
5712. 62	(0.00) 1.16†	5225. 05	(0.00) 1.67†	4764. 28	(0.00) 1.07*A*†
5702. 30	(0.00) 1.04†	5224. 97	(0.00) 1.64†	4756. 09	(0.000*w*) 0.988*w*
5698. 32	(0.00) 1.08†	5221. 76	(0.00) 1.36†	4752. 06	(0.000) 1.004
5694. 72	(0.00) 0.98*A*†	5208. 42	P–B	4745. 31	(0.000) 1.006
5664. 04	(0.00) 1.01†	5206. 02	P–B	4737. 33	(0.000) 1.135
5628. 64	(0.00) 0.93†	5204. 50	P–B	4730. 69	(**0.000,** 0.180, 0.375) 0.679, 0.863, 1.047, **1.234**
5480. 50	(0.00) 1.07†	5200. 20	(**0.00,** 0.99) **1.02,** 2.07†	4729. 71	(0.000) 1.184
5463. 93	(0.00) 0.99*A*†	5193. 49	(0.00) 0.80†	4727. 13	(0.00) 1.22†
5442. 40	(0.00) 0.82†	5192. 01	(0.00) 1.37*A*†	4724. 40	(?) 1.26†
5409. 78	P–B	5177. 42	(0.00) 1.50†	4718. 43	(0.000*D*) 0.999*A*
5405. 79	(**0.00,** 0.48)†	5161. 78	(0.00) 2.52†	4708. 02	(0.000*D*) 0.880*A*
5405. 00	(0.00) 1.53†	5144. 67	(?) 1.53, 2.58†	4700. 60	(0.00) 1.50†
5400. 58	(0.00) 1.50†	5139. 60	(0.00) 0.79†	4698. 61	(0.00) 0.37†
5395. 81	(0.00) 1.01*A*†	5072. 93	(0.00 . . .) **0.95,** 2.01†	4698. 46	(0.00) 0.89†
5390. 38	(0.00) 1.49†	5067. 73	(0.00) 0.94*A*†	4697. 04	(0.00 . . .) **1.06,** 1.32†
5387. 57	(0.00) 1.49†	5065. 92	(?) 1.63*D*†	4693. 94	(0.00) 1.02†
5386. 96	(0.00) 1.50†	5051. 90	(0.00) 0.86†	4689. 38	(0.00 . . .) **0.51,** 0.94†
5371. 48	(0.00) 1.10†	5018. 17	(0.00) 1.07†	4680. 86	(0.000) 0.654
5370. 36	(0.00) 1.01†	5013. 31	(0.00) 1.13†	4669. 34	(?) 1.65†
5368. 53	(0.00) 0.96†	4985. 95	(0.00) 1.12†	4666. 51	(0.00) 1.87†
5348. 30	P–B	4964. 92	(0.00) 2.24†	4666. 20	(0.00) 0.58†
5345. 77	P–B	4954. 81	(**0.00,** 0.25) 0.41†	4652. 15	(**0.000,** 0.340, 0.670) **0.824,** 1.172, 1.511, 1.841, 2.174
5340. 46	(0.00) 1.67†	4942. 49	(0.00) 1.87†	4651. 28	(**0.00,** 1.02) **0.51,** 1.53, 2.57†
5312. 88	(0.47) 1.87†	4936. 34	(0.00) 0.43*A*†	4646. 15	(**0.000,** 0.167, 0.334, 0.508) **0.998,** 1.170, 1.335, 1.505, 1.674, 1.839, 2.008
5300. 74	(0.00) 1.97†	4930. 18	(0.00) 1.20†		
5298. 29	P–B	4922. 28	(0.00) 1.07†	4639. 52	(0.00) 2.16†
5297. 99	(0.00) 1.17†	4903. 25	(?) 0.38, **0.86**	4626. 18	(1.008) 1.504, 2.515
5296. 69	(**0.00,** 1.00) **0.50,** 1.53 . . . †	4887. 01	(0.00) 0.86†	4625. 91	(0.00) 1.27†
5292. 57	(0.00) 1.45†	4885. 77	(0.00) 0.61†		
5285. 64	(0.00) 1.40†	4870. 79	(0.00) 0.75†		
5275. 21	(0.00) 1.21†	4861. 84	(0.00) 0.99†		
5273. 46	(0.00) 1.56†	4836. 85	(0.000) 2.350		

TABLE 2. *Zeeman effect of* Cr I—Continued

Wavelengths	Magnetic patterns
4624.56	(0.00) 1.04†
4622.47	(0.00) 1.36†
4619.54	(0.000) 1.518
4616.12	(0.336, **0.672**) 1.166, **1.502, 1.838**, 2.173
4613.36	(0.000) 2.508
4611.96	(0.00) 0.54†
4600.74	(0.169, 0.337, **0.508**) 1.170, 1.333, **1.503, 1.669**, 1.842, 2.004
4600.11	(0.68) 1.63†
4595.60	(0.121) 1.013*D*
4591.40	(**0.00**, 0.33) 1.76, **2.24**†
4586.15	(0.00) 1.44†
4580.04	(**0.000**, 0.508) **1.496**, 2.005, 2.516
4575.11	(0.000) 0.815
4569.63	(0.77) 1.75†
4565.51	(**0.000**, 0.165, 0.340) 1.277, 1.509, 1.670, 1.836, **2.000**
4564.16	(0.000) 1.020
4545.95	(0.164, **0.332**) 1.668, **1.836, 2.003**, 2.174
4542.64	(0.00) 1.12†
4527.45	(0.00) 1.26†
4526.46	(0.00) 1.32†
4521.14	(0.000) 0.968
4515.44	(0.000) 1.488
4506.84	(0.000) 0.956
4500.29	(0.27) 0.84†
4498.73	(0.000) 1.455
4496.85	(**0.000**, 0.332, 0.669) **0.999**, 1.335, 1.670, 2.005, 2.361
4492.31	(**0.00**, 0.60) **1.01**, 1.54†
4488.06	(0.00) 1.37†
4482.88	(0.54) 1.49, 2.08†
4458.54	(0.00) 1.09†
4432.16	(0.000) 1.497
4430.48	(0.00) 1.14†
4424.29	(0.00) 1.16*A*†
4413.86	(0.00) 1.16*A*†
4410.97	(0.00) 1.04†
4403.51	(0.000) 1.003
4391.76	(?) 1.56, 2.07, **2.57**†
4387.51	(0.00) 1.04†
4384.97	(0.277, 0.450, **0.604**) 0.910, 1.051, 1.201, **1.348, 1.497**, 1.650, 1.799, 1.936
4382.54	(0.00) 1.22†
4381.11	(0.00) 1.16†
4377.54	(0.00) 1.16†
4376.80	(0.000) 1.166
4375.34	(0.000) 0.824*A*
4373.65	(0.00) 0.99†
4373.25	(**0.00**, 1.52) 0.00, 1.52, **3.11**†
4363.13	(0.000) 0.830
4359.65	(0.506, **1.006**) 0.502, **1.002, 1.502**, 2.010
4351.77	(**0.000**, 0.098, 0.200, 0.304, 0.409) **0.988**, 1.102, 1.207, 1.309, 1.409, 1.504, 1.603, 1.698
4351.05	(1.499) 0.000, 1.499
4344.51	(**0.000**, 0.148, 0.303, 0.457) **0.892**, 1.050, 1.206, 1.355, 1.498, 1.645, 1.786
4343.17	(?) **1.28**, 1.96†
4340.14	(0.00) 1.38†
4339.74	(0.00) 0.00†
4339.45	(0.00) 0.75*A*†
4337.57	(**0.00**, 0.47) **0.48**, 0.97, 1.48†
4325.07	(0.00) 0.87†
4323.52	(0.00) 1.02†
4320.61	(0.00) 1.65†
4309.73	(0.00) 1.58†
4301.18	(0.000) 1.043*A*
4300.52	(0.000) 0.967
4299.97	(0.00) 0.94†
4297.75	(0.00) 0.96†
4295.77	(0.00) 1.69†
4291.97	(0.00) 0.87†
4289.73	(**0.000**, 0.334, 0.674) **1.329**, 1.668, 2.000, 2.330, 2.667
4284.91	(0.000) 1.005
4280.42	(0.00) 0.90†
4271.07	(0.00) 1.18†
4268.79	(0.00) **0.70**, 1.16†
4263.15	(0.00) 1.20†
4255.50	(0.00) 1.22†
4254.33	(**0.000**, 0.255, 0.503, 0.756) **0.998**, 1.248, 1.500, 1.748, 2.002, 2.256, 2.505
4240.71	(0.000) 1.155*A*
4238.96	(0.00) 1.45†
4232.23	(0.00) 0.78†
4230.49	(0.00) 0.86†
4226.75	(0.000) 1.006, 1.060
4224.52	(0.00) 0.87†
4221.58	(0.00) 0.68†
4217.65	(0.00) 1.11†
4211.34	(0.00) 1.22†
4209.76	(0.000) 1.127
4209.37	(0.00) 1.04†
4206.91	(0.00) 1.03†
4204.48	(0.000) 0.955
4203.59	(0.00) 0.38†
4200.10	(0.00) 1.24†
4194.96	(0.00) 2.01†
4193.66	(0.00) 0.92†
4192.11	(0.000) 0.948
4191.27	(0.00) 0.92†
4190.66	(0.00) 0.98†
4190.15	(0.00) 1.18†
4179.27	(0.00) 0.90†
4175.96	(0.00) 1.58†
4172.78	(0.00) 1.14†
4170.21	(0.000) 1.046
4169.84	(0.000) 1.105*A*
4165.52	(0.000) 1.030
4163.63	(0.00) 1.18
4161.43	(0.000) 1.046*A*
4152.78	(0.00) 0.96†
4142.19	(0.00) 1.39†
4137.92	(0.00) 1.28†
4134.39	(0.00) 0.69†
4131.36	(0.000) 0.995
4129.20	(0.00) 1.22†
4128.39	(0.00) 1.20†
4126.51	(0.00) 1.31†
4125.44	(0.00) 1.10†
4123.39	(0.00) 1.18†
4122.16	(0.000) 1.017
4121.82	(0.000*d*?) 1.041
4121.26	(0.00) 1.02†
4104.86	(0.00) 0.81†
4103.84	(0.00) 1.32†
4092.18	(0.00) 0.89†
4090.30	(0.00) 1.14†
4077.68	(0.000) 0.890*B*
4077.09	(0.000) 0.655
4076.07	(0.000) 1.021
4074.86	(0.000) 1.123
4067.83	(0.00) 1.07†
4066.93	(0.000) 0.848
4065.71	(0.000) 1.029*A*
4060.65	(0.00) 0.96†
4058.78	(0.000) 0.849
4057.83	(0.00) 0.90†
4057.21	(0.00) 0.86†
4056.78	(0.00) 0.98†
4056.05	(0.00) 0.37*A*†
4051.32	(0.000) 0.997
4049.08	(0.00) 1.00†
4048.78	(0.00) 1.04†
4039.10	(0.14) 1.17†
4025.01	(0.00) 1.07†
4022.27	(0.00) 0.65†
4018.22	(0.00) 1.57†
4012.48	(0.00) 0.92†
4001.44	(0.00) 1.07†
3999.68	(0.00) 1.08†
3992.85	(0.00) 1.69†
3989.98	(0.00) 1.16*A*†
3981.24	P-B
3979.80	(0.00) 1.56†
3971.27	P-B
3958.08	(0.000) 1.160
3941.50	(0.000) 1.497
3930.27	(0.00) 1.57†
3928.65	(0.000) 1.500
3926.66	(0.000) 1.703
3921.03	(0.000) 1.510
3919.16	(0.000) 1.503
3916.25	(0.000) 1.502
3915.85	(0.00) 1.19†
3912.01	(0.00) 1.94†
3910.72	(0.00) 1.26†
3908.76	(0.000) 1.500
3907.26	(0.00) 1.76†
3903.17	(0.000) 1.405, 1.600
3902.91	(0.00) 1.499
3897.66	(0.000) 1.018
3894.04	(0.000) 1.500

TABLE 2. *Zeeman effect of* Cr I—Continued

Wavelengths	Magnetic patterns
3891. 93	(0.000) 0.989*A*
3890. 83	(**0.000,** 0.292) **0.992,** 1.269
3886. 80	(0.000) 1.501
3885. 24	(**0**.000) 1.494
3885. 20	(0.000) 1.502
3883. 29	(0.000) 1.497
3879. 23	(0.00) **0.50,** 1.83†
3874. 55	(0.00) 1.18†
3862. 54	(0.00) 1.71†
3857. 63	P–B
3855. 30	(0.00) 2.57†
3854. 23	P–B
3853. 19	P–B
3852. 22	(0.000) 1.505
3849. 54	(0.00) 1.62†
3849. 35	(0.00) 1.24†
3841. 28	(**0.000,** 0.303, 0.594) **0.729,** 1.022, 1.296, 1.573, 1.866
3831. 03	(0.000) 1.508
3823. 52	(0.000) 1.502
3820. 46	(0.00) 1.16†
3819. 57	(0.00*W*) 0.00†
3817. 85	(0.00) 1.27†
3814. 63	(0.000) 0.750
3812. 26	(0.000) 1.057
3807. 92	(0.00) 1.46†
3806. 83	(0.000) 1.207
3804. 80	(0.000) 1.494
3801. 19	(0.00) 0.86†
3797. 71	(0.00) 1.47†
3747. 25	(0.00) 1.04†
3742. 97	(0.00) 1.35†
3733. 44	P–B
3689. 65	(0.000) 1.108
3681. 69	(0.000) 1.500
3676. 32	(0.057) 1.487
3653. 92	(0.00) 0.63†
3646. 16	P–B
3615. 65	(**0.000,** 0.344, 0.704, 1.053) **0.603,** 0.946, 1.307, 1.646
3612. 61	(0.627) 0.524
3608. 41	(0.00) 0.60†
3605. 32	(**0.000,** 0.329, 0.664) 1.342, 1.669, 2.008, 2.342, **2.674**
3601. 65	(0.00) 1.46†
3599. 40	(0.000) 1.456
3593. 48	(0.074, 0.166, **0.258**) 1.743, 1.845, **1.929, 2.016,** 2.107, 2.203
3582. 61	(0.492, 0.752, **1.084**)?
3578. 68	(**0.000,** 0.256, 0.509, 0.764) **1.002,** 1.250, 1.505, 1.758, 2.008, 2.266, 2.511
3574. 80	(0.00) 1.38†
3562. 28	(0.000) 1.177
3559. 78	(0.000) 1.512
3550. 63	(0.000) 1.474
3532. 89	(**0.000,** 0.264) **0.844,** 1.177
3527. 09	(0.000) 1.014
3518. 40	(0.000) 1.188*B*
3510. 53	(0.000) 1.016
3508. 09	(0.443, **0.586**)?
3494. 96	(0.000) 1.027
3488. 44	(**0.000,** 0.157, 0.315, 0.474, 0.635) 0.963, 1.116, 1.277, 1.440, **1.585**
3481. 54	(0.000) 1.181
3481. 30	(0.33) 1.12†
3476. 17	(0.000) 1.190
3472. 76	(0.075, 0.219, 0.384, **0.503**)?
3468. 74	(0.000) 0.697
3467. 71	(0.000) 1.032
3450. 81	(0.000) 1.002
3443. 78	(0.201) 0.847*D*
3415. 31	(0.000) 1.230
3412. 26	(0.000) 1.063
3396. 02	(0.000) 0.992
3365. 52	(0.000) 0.889
3351. 97	(0.354, 0.650, **0.996**) 1.006, 1.326, **1.628, 1.985,** 2.209, 2.513
3346. 79	(0.000) 0.922
3346. 72	(0.000) 1.013
3343. 34	(0.00) 1.05†
3332. 88	(0.215, **0.304**) 1.012*D*
3330. 60	(0.000) 0.782
3329. 06	(0.125) 1.213
3326. 59	(0.000) 0.674
3259. 98	(0.348, 0.526, 0.722, 0.841, **1.080**) 0.201, 0.379, 0.559, 0.737, **0.894, 1.081,** 1.268, 1.439, 1.607, 1.784
3257. 83	(0.58) 1.17†
3253. 26	(0.000) 1.130
3251. 83	(0.137) 1.067
3251. 58	(0.155)?
3247. 28	(0.00) 0.31*A*†
3245. 54	(0.203, 0.331, **0.461**) 0.570, 0.681, **0.810, 0.932,** 1.056, 1.172
3244. 12	(0.322, **0.501**) 1.731
3237. 73	(0.260, 0.412, **0.557**) 0.687, 0.811, **0.930, 1.059,** 1.172, 1.272
3233. 24	(. . ., 0.351) **0.849,** 1.502
3229. 21	(0.000) 1.040
3219. 62	(0.000) 1.919
3211. 32	(0.000*d*?) 0.937*B*
3198. 12	(**0.000,** 0.175, 0.358) **0.947,** 1.137, 1.329, 1.469
3192. 12	(**0.000,** 0.672, 1.319) **0.000,** 0.672, 1.319
3167. 44	(0.000) 0.548
3163. 76	(0.000*w*) **1.027,** 1.164
3160. 62	
3159. 58	(0.000*D*) 0.718*A*
3155. 16	(0.000) 0.995
3153. 55	(**0.000,** 0.194, 0.391) **1.073,** 1.283
3152. 89	(0.135) 1.119
3148. 44	(0.000*C*) 0.911*B*
3144. 39	(0.000) 0.487
3141. 88	(0.090) 1.062
3119. 70	(0.000) 0.848
3119. 25	(0.068) 1.133
3110. 87	(0.113) 1.090
3109. 34	(0.238*B*) 0.813*D*
3104. 71	(**0.000,** 0.231, 0.448)
3095. 38	(0.000) 0.817
3087. 53	(0.000) 1.201
3080. 71	(0.391, **0.579**)?
3077. 84	(0.000*W, D*) 1.258, **1.375**
3073. 68	(0.000) 1.228
3071. 30	(0.000) 1.099
3065. 06	(**0.000,** 0.116, 0.225) 1.010*B*
3061. 81	(0.000) 1.191
3061. 64	(0.000) 1.042
3058. 16	(0.097)?
3053. 87	(**0.000,** 0.173, 0.330, 0.459) **1.011,** 1.164, 1.324
3052. 22	(**0.000,** 0.204, 0.408, 0.621) 1.267, 1.476, **1.696**
3039. 77	(0.000) 1.239
3039. 73	(0.120) 1.104
3037. 05	(0.142, 0.300, 0.472, **0.636**) 0.895, 1.044, 1.206, **1.360, 1.512,** 1.662, 1.823, 1.955
3034. 19	(0.201, 0.343, **0.492**) 1.432
3031. 50	(0.000) 0.900
3031. 35	(**0.000,** 1.456) 0.000, 1.456, **2.952**
3030. 25	(0.230, 0.480, **0.741**) 0.734, 1.013, **1.257, 1.501,** 1.729, 1.987
3029. 16	(**0.000,** 0.932) **0.547.** 1.492, 2.463
3024. 36	(0.380*B*) 1.397*D*
3021. 58	(0.438) 0.919*A*
3020. 67	(1.492) 0.000, 1.492
3018. 83	(0.00*W*) 1.89*B*†
3018. 49	(0.939) 1.541, 2.552
3017. 59	(0.00*W*) **0.865,** 1.034, 1.190, 1.345, 1.540, 1.692, 1.852
3015. 20	(0.00) 0.00†
3014. 93	(**0.000,** 0.248, 0.451) **0.757,** 1.011, 1.264, 1.502
3014. 76	(0.00) 1.58†
3013. 72	(0.00) 1.26†
3013. 03	(0.000) 2.468
3011. 11	(0.000) 0.983
3005. 06	(0.000) 1.491
3003. 79	(0.000) 1.024
3000. 88	(0.000) 1.501
2998. 78	(**0.000,** 0.474) **1.546,** 2.010, 2.512
2998. 12	(0.000), 1.176
2996. 57	(0.000) 1.498
2995. 09	(0.48, **0.94**) 1.07, 1.51, **1.97,** 2.47†
2994. 06	(0.76, **1.41**) 0.67, 1.29, **2.07,** 2.78†
2991. 88	(0.000) 1.501
2991. 40	(0.000) 1.039

TABLE 2. *Zeeman effect of* Cr I—Continued

Wavelengths	Magnetic patterns	Wavelengths	Magnetic patterns
2988. 64	(**0.000**, 0.358, 0.700) **0.950**, 1.307, 1.637, 2.017, 2.358	2739. 40	(0.000) 0.942
2986. 47	(0.000) 1.484	2736. 46	(**0.00**, 0.52) **1.58**, 1.95†
2986. 13	(0.00) 1.52†	2731. 90	(0.25) 1.90†
2986. 01	(0.000) 1.502	2726. 50	(0.00) 1.02†
2985. 85	(0.000) 1.492	2716. 18	(0.00) 0.78†
2984. 82	(0.000) 1.206	2706. 53	(0.000) 0.810
2984. 01	(0.000) 1.033	2705. 41	(0.000) 1.049
2981. 42	(0.000) 0.965	2704. 74	(0.000) 1.214
2980. 78	(0.000) 1.534	2702. 52	(0.000) 1.151
2975. 48	(0.000) 1.511	2701. 99	(0.000) 1.027
2971. 10	(0.000) 1.515	2688. 04	(0.000) 0.559
2967. 64	(0.000) 1.483	2654. 41	(0.000) 1.122
2939. 44	(0.000) 1.130	2642. 12	(0.000) 1.094
2935. 53	(0.000) 1.002	2626. 60	(0.000) 1.704
2913. 72	(0.00) 1.03†	2622. 87	(0.161) 1.473
2911. 15	(0.000) 1.501	2620. 48	(0.000) 1.734
2910. 89	(0.000) 1.497	2591. 84	(0.000*D*) 1.049*A*
2909. 05	(0.000) 1.496	2579. 14	(0.000) 0.919
2905. 48	(0.000) 1.497	2578. 27	(0.000) 0.975
2904. 67	(0.000) 0.668	2577. 66	(0.456*B*) . . .
2896. 76	(0.000) 1.507	2572. 15	(0.126) 0.882
2894. 17	(0.000) 1.505	2571. 74	(0.000) 1.134
2893. 25	(0.000) 1.496	2566. 55	(0.00) 1.45†
2891. 42	(0.000) 1.166	2560. 70	(0.70) 1.81†
2889. 29	(0.000) 1.497	2557. 14	(0.000) 0.933
2889. 22	(0.000) 1.486	2549. 55	(0.96) **1.51**, 2.38†
2886. 99	(0.000) 1.496	2545. 64	(0.000) 2.464
2881. 14	(0.000) 1.038	2528. 56	(0.000) 1.452
2879. 27	(0.000) 1.504	2527. 11	(0.260) 1.423
2871. 63	(0.000) 1.509	2519. 51	(0.000*D*) 1.088*A*
2849. 30	(0.000) 1.138	2516. 92	(0.246) 1.482
2840. 89	(0.161) 1.183	2508. 97	(0.00) 1.59†
2831. 04	(0.000) 0.678	2508. 11	(0.00) 1.52†
2826. 73	(0.00) 1.38†	2506. 82	(0.000) 0.452
2795. 82	(0.000) 1.075	2504. 31	(0.00*D*) 0.73*A*
2790. 28	(0.000) 0.988	2496. 30	(0.00) 1.149
2787. 84	(0.000) 0.984	2492. 57	(0.000) 0.972
2780. 70	(0.00) 1.19†	2491. 35	(0.00) 0.00†
2775. 67	(0.00)	2408. 72	(0.00) 0.89†
2771. 45	(0.000) 1.200	2408. 60	(0.00) 1.22†
2769. 90	(0.000) 0.939*A*		
2767. 53	(0.000) 1.094		
2759. 67	(0.000) 1.228		
2742. 16	(0.000) 1.064		
2741. 08	(0.000) 0.993		

TABLE 3. *Paschen-Back interaction in the a $^5S-z\,^5P^\circ$ group of* Cr I

Term combination No-field wavelength	Observed Zeeman components and intensities		Theoretical Zeeman components and intensities		Polarization and transition
$a\,^5S_2-z\,^5P_3^\circ$ 5208.415	5211.092	10	5211.107	8.8	$\sigma+1\rightarrow+2$
	5210.775	12	5210.760	9.4	$\sigma\ \ 0\rightarrow+1$
	5210.411	10	5210.414	10.0	$\sigma-1\rightarrow\ \ 0$
	5209.990	12	5209.984	10.5	$\sigma-2\rightarrow-1$
	5209.509	15	5209.503	11.0	$\sigma-3\rightarrow-2$
	5209.243	10	5209.238	14.0	$\pi+2\rightarrow+2$
	5208.940	8	5208.942	8.8	$\pi+1\rightarrow+1$
	5208.623	10	5208.595	7.6	$\pi\ \ 0\rightarrow\ \ 0$
	5208.248	6	5208.249	6.2	$\pi-1\rightarrow-1$
	5207.829	10	5207.819	4.4	$\pi-2\rightarrow-2$
	5207.344	8	5207.343	11.0	$\sigma+3\rightarrow+2$
	5207.074	7	5207.073	4.7	$\sigma+2\rightarrow+1$
	5206.790	7	5206.777	2.0	$\sigma+1\rightarrow\ \ 0$
	5206.456	6	5206.430	1.3	$\sigma\ \ 0\rightarrow-1$
	5206.081	4	5206.084	0.7	$\sigma-1\rightarrow-2$
$a\,^5S_2-z\,^5P_2^\circ$ 5206.021	5208.420	5	5208.436	6.5	$\sigma+1\rightarrow+2$
	5208.420	5	5208.328	5.5	$\sigma\ \ 0\rightarrow+1$
	5208.268	5	5208.286	4.4	$\sigma-1\rightarrow\ \ 0$
	5207.706	7	5207.708	3.1	$\sigma-2\rightarrow-1$
	5206.332	8	5206.299	6.7	$\pi+2\rightarrow+2$
	5206.245	7	5206.271	11.1	$\pi+1\rightarrow+1$
	5206.210	5	5206.163	12.5	$\pi\ \ 0\rightarrow\ \ 0$
	5206.112	2	5206.121	13.7	$\pi-1\rightarrow-1$
	5205.551	15	5205.543	14.8	$\pi-2\rightarrow-2$
	5204.157	5	5204.134	9.9	$\sigma+2\rightarrow+1$
	5204.098	6	5204.106	4.0	$\sigma+1\rightarrow\ \ 0$
	5204.098	6	5203.998	3.5	$\sigma\ \ 0\rightarrow-1$
	5203.944	7	5203.956	2.5	$\sigma-1\rightarrow-2$
$a\,^5S_2-z\,^5P_1^\circ$ 5204.505	5206.724	6	5206.749	0.4	$\sigma-1\rightarrow\ \ 0$
	5206.279	7	5206.368	0.7	$\sigma\ \ 0\rightarrow+1$
	5205.890	7	5205.909	0.9	$\sigma+1\rightarrow+2$
	5204.590	15	5204.584	3.7	$\pi-1\rightarrow-1$
	5204.123	15	5294.203	5.1	$\pi\ \ 0\rightarrow\ \ 0$
	5203.735	18	5203.744	6.2	$\pi+1\rightarrow+1$
	5202.424	30	5202.419	10.6	$\sigma-1\rightarrow-2$
	5201.950	25	5202.038	10.3	$\sigma\ \ 0\rightarrow-1$
	5201.575	15	5201.579	10.0	$\sigma+1\rightarrow\ \ 0$

TABLE 4. *Even terms of* Cr I

Electron configuration	Term symbol	Level	Interval	Observed g	Electron configuration	Term symbol	Level	Interval	Observed g
$3d^5(a\,^6S)4s$	$a\,^7S_3$	0.00		2.007	$3d^4\,4s^2$	$a\,^3P_0$	23163.27		
						$^3P_1$	23512.00	348.73	
$3d^5(a\,^6S)4s$	$a\,^5S_2$	7593.16		2.006		$^3P_2$	24093.16	581.16	
$3d^4\,4s^2$	$a\,^5D_0$	7750.78	60.04	0.000	$3d^4\,4s^2$	$a\,^3H_4$	23933.90		
	$^5D_1$	7810.82	116.65	1.501		$^3H_5$	24056.11	122.21	
	$^5D_2$	7927.47	167.74	1.496		$^3H_6$	24200.23	144.12	
	$^5D_3$	8095.21	212.36	1.501					
	$^5D_4$	8307.57		1.497					
$3d^5(a\,^4G)4s$	$a\,^5G_2$	20517.40			$3d^5(b\,^4D)4s$	$b\,^5D_0$	24277.06		
	$^5G_3$	20520.92	3.52			$^5D_1$	24286.54	9.48	
	$^5G_4$	20523.69	2.77			$^5D_2$	24299.89	13.35	
	$^5G_5$	20523.94	0.25			$^5D_3$	24303.94	4.05	
	$^5G_6$	20519.60	−4.34			$^5D_4$	24282.34	−21.60	
$3d^5(a\,^4P)4s$	$a\,^5P_3$	21840.84	−7.04	1.6	$3d^5(a\,^4G)4s$	$a\,^3G_3$	24833.86		
	$^5P_2$	21847.88	−9.06	1.847		$^3G_4$	24897.55	63.69	
	$^5P_1$	21856.94		2.500		$^3G_5$	25038.61	141.06	

TABLE 4. *Even terms of* Cr I—Continued

Electron configuration	Term symbol	Level	Interval	Observed g
$3d^4\,4s^2$	$a\ ^3F_2$	24940.61		
	$^3F_3$	25106.34	165.73	
	$^3F_4$	25177.39	71.05	
$3d^5(a\ ^4P)4s$	$b\ ^3P_0$	27163.20		
	$^3P_1$	27176.22	13.02	
	$^3P_2$	27223.05	46.83	
$3d^4\,4s^2$	$b\ ^3G_3$	27597.22		
	$^3G_4$	27703.84	106.62	
	$^3G_5$	27816.88	113.04	
$3d^5(b\ ^4D)4s$	$a\ ^3D_3$	28637.00		
	$^3D_2$	28682.18	−45.18	
	$^3D_1$	28679.43	2.75	
$3d^5(a\ ^2D)4s$	$b\ ^3D_3$	31009.00		
	$^3D_2$	31028.33	−19.33	
	$^3D_1$	31048.85	−20.52	
$3d^5(a\ ^2I)4s$	$a\ ^3I_7$	31048.00		
	$^3I_8$	31049.33	−1.33	
	$^3I_5$	31055.35	−6.02	
$3d^5(b\ ^4F)4s$	$a\ ^5F_1$	31352.42		
	$^5F_2$	31355.21	2.79	
	$^5F_3$	31364.33	9.12	
	$^5F_4$	31377.96	13.63	
	$^5F_5$	31393.40	15.44	
$3d^4\,4s^2$	$a\ ^1G_4$	31987.06		
$3d^4\,4s^2$	$a\ ^1I_6$	32097.36		
$3d^5(a\ ^2F)4s$	$b\ ^3F_2$	33040.10		
	$^3F_3$	33060.74	20.64	
	$^3F_4$	33113.27	52.53	
$3d^5(a\ ^2I)4s$	$b\ ^1I_6$	33762.74		
$3d^4\,4s^2$	$c\ ^3D_1$	33906.65		
	$^3D_2$	33935.65	29.00	
	$^3D_3$	33934.88	−0.77	
$3d^5$	$c\ ^5D_4$	35398.02		
	$^5D_3$	35501.26	−103.24	
	$^5D_2$	35572.94	−71.68	
	$^5D_1$	35618.51	−45.57	
	$^5D_0$	35640.69	−22.18	
$3d^5(b\ ^4F)4s$	$c\ ^3F_2$	35807.90		
	$^3F_3$	35813.73	5.83	
	$^3F_4$	35862.82	49.09	
$3d^5(b\ ^2H)4s$	$b\ ^3H_4$	35870.53		
	$^3H_5$	35884.40	13.87	
	$^3H_6$	35934.02	49.62	
$3d^5(b\ ^2F)4s$	$d\ ^3F_2$	36558.55		
	$^3F_3$	36552.13	−6.42	
	$^3F_4$	36577.73	25.60	
$3d^5(a\ ^6S)5s$	$e\ ^7S_3$	36895.73		
$3d^5(b\ ^2G)4s$	$c\ ^3G_3$	37205.88		
	$^3G_4$	37244.17	38.29	
	$^3G_5$	37233.50	−10.67	
$3d^5(a\ ^6S)5s$	$e\ ^5S_2$	37883.34		
$3d^5(b\ ^2H)4s$	$a\ ^1H_5$	38537.68		
$3d^5(b\ ^2G)4s$	$b\ ^1G_4$	39158.63		
$3d^5(a\ ^6S)4d$	$e\ ^7D_1$	42253.42		
	$^7D_2$	42254.52	1.10	
	$^7D_3$	42256.26	1.74	
	$^7D_4$	42258.37	2.11	
	$^7D_5$	42261.06	2.69	
$3d^5(a\ ^6S)4d$	$e\ ^5D_4$	44050.87		
	$^5D_3$	44068.72	−17.85	
	$^5D_2$	44080.90	−12.18	
	$^5D_1$	44088.92	−8.02	
	$^5D_0$	44092.80	−3.88	
$3d^5(a\ ^6S)6s$	$f\ ^7S_3$	45643.38		
$3d^5(a\ ^6S)6s$	$f\ ^5S_2$	45967.81		
$3d^44s(a\ ^6D)5s$	$f\ ^7D_1$	46448.60		
	$^7D_2$	46524.84	76.24	
	$^7D_3$	46637.21	112.37	
	$^7D_4$	46783.06	145.85	
	$^7D_5$	46958.98	175.92	
$3d^5(a\ ^6S)5d$	$g\ ^7D_1$	47700.18		
	$^7D_2$	47700.95	0.77	
	$^7D_3$	47702.30	1.35	
	$^7D_4$	47704.66	2.36	
	$^7D_5$	47709.80	5.14	
$3d^44s(a\ ^6D)5s$	$f\ ^5D_0$	48488.23		
	$^5D_1$	48507.56	19.33	
	$^5D_2$	48558.57	51.01	
	$^5D_3$	48661.59	103.02	
	$^5D_4$	48824.50	162.91	
$3d^5(a\ ^6S)7s$	$g\ ^7S_3$	49177.83		
$3d^5(a\ ^6S)7s$	$g\ ^5S_2$	49321.51		
$3d^5(a\ ^6S)8s$	$h\ ^5S_2$	51035.68		
$3d^44s(a\ ^6D)4d$	$e\ ^7G_1$	53148.35		
	$^7G_2$	53177.87	29.52	
	$^7G_3$	53228.49	50.62	
	$^7G_4$	53298.90	70.41	
	$^7G_5$	53393.50	94.60	
	$^7G_6$	53517.85	124.35	
	$^7G_7$	53662.64	144.79	
$3d^44s(a\ ^6D)4d$	$h\ ^7D_1$	--------		
	$^7D_2$	53195.03		
	$^7D_3$	53284.34	89.31	
	$^7D_4$	53375.46	91.12	
	$^7D_5$	53627.75	252.29	
$3d^44s(a\ ^6D)4d$	$e\ ^7F_0$	--------		
	$^7F_1$	53215.40		
	$^7F_2$	53279.80	64.40	
	$^7F_3$	53384.72	104.92	
	$^7F_4$	53526.22	141.50	
	$^7F_5$	53706.06	179.84	
	$^7F_6$	53927.47	221.41	

TABLE 4. *Even terms of* Cr I—Continued

Electron configuration	Term symbol	Level	Interval	Observed g	Electron configuration	Term symbol	Level	Interval	Observed g
	$e\ ^5F_1$	54296.76	86.60		$3d^4\,4s(b\ ^4P)5s$	$e\ ^5P_1$	61558.17	129.39	
	$^5F_2$	54383.36	92.93			$^5P_2$	61687.56	162.61	
	$^5F_3$	54476.29	96.55			$^5P_3$	61850.17		
	$^5F_4$	54572.84	87.47			$f\ ^7F_0$	------		
	$^5F_5$	54660.31				$^7F_1$	------		
	$g\ ^5D_0$	54646.20	25.70			$^7F_2$	------		
	$^5D_1$	54671.90	146.65		$3d^3\,4p(z\ ^6F^\circ)4p$	$^7F_3$	62034.44	154.39	
$3d^4\,4s(a\ ^4D)5s$	$^5D_2$	54818.55	168.27			$^7F_4$	62188.83	283.97	
	$^5D_3$	54986.82	222.19			$^7F_5$	62472.80	185.58	
	$^5D_4$	55209.01				$^7F_6$	62658.38		
	$e\ ^3D_1$	54804.69	169.95			$f\ ^5G_2$	62646.60	15.36	
$3d^4\,4s(a\ ^4D)5s$	$^3D_2$	54974.64	230.15			$^5G_3$	62661.96	9.04	
	$^3D_3$	55204.79			$3d^3(a\ ^4G)4d$	$^5G_4$	62671.00	19.96	
	$e\ ^3G_2$	57350.65	10.59			$^5G_5$	62690.96	−17.04	
	$^5G_3$	57361.24	11.54			$^5G_6$	62673.92		
$3d^3(a\ ^4G)5s$	$^5G_4$	57372.78	10.15			$e\ ^5H_3$	64712.04	39.38	
	$^5G_5$	57382.93	6.39			$^5H_4$	64751.42	50.66	
	$^5G_6$	57389.32			$3d^4\,4s(a\ ^4H)5s$	$^5H_5$	64802.08	34.22	
	$e\ ^3G_3$	57984.94	7.21			$^5H_6$	64836.30	103.98	
	$^3G_4$	57992.15	−1.92			$^5H_7$	64940.28		
	$^3G_5$	57990.23							

TABLE 5. *Odd terms of* Cr I

Electron configuration	Term symbol	Level	Interval	Observed g	Electron configuration	Term symbol	Level	Interval	Observed g
	$z\ ^7P^\circ_2$	23305.01	81.34	2.334		$z\ ^5D^\circ_0$	33338.20	85.59	−0.003
$3d^5(a\ ^6S)4p$	$^7P^\circ_3$	23386.35	112.49	1.92	$3d^4\,4s(a\ ^6D)4p$	$^5D^\circ_1$	33423.79	118.32	1.499
	$^7P^\circ_4$	23498.84		1.752		$^5D^\circ_2$	33542.11	129.44	1.497
	$z\ ^7F^\circ_0$	24971.21	39.43			$^5D^\circ_3$	33671.55	144.51	1.497
	$^7F^\circ_1$	25010.64	78.56			$^5D^\circ_4$	33816.06		1.499
	$^7F^\circ_2$	25089.20	116.82						
$3d^4\,4s(a\ ^6D)4p$	$^7F^\circ_3$	25206.02	153.60			$z\ ^3P^\circ_0$	33762.56	134.70	
	$^7F^\circ_4$	25359.62	189.02		$3d^4\,4s(a\ ^4D)4p$	$^3P^\circ_1$	33897.26	293.23	
	$^7F^\circ_5$	25548.64	222.76			$^3P^\circ_2$	34190.49		
	$^7F^\circ_6$	25771.40							
	$z\ ^5P^\circ_1$	26787.50	−8.78	1.670		$z\ ^3F^\circ_2$	35897.87	136.35	
$3d^5(a\ ^6S)4p$	$^5P^\circ_2$	26796.28	−5.65	1.830	$3d^4\,4s(a\ ^4D)4p$	$^3F^\circ_3$	36034.22	177.93	
	$^5P^\circ_3$	26801.93		2.512		$^3F^\circ_4$	36212.15		
	$z\ ^7D^\circ_1$	27300.19	81.99			$z\ ^3D^\circ_1$	38597.06	133.61	
	$^7D^\circ_2$	27382.18	118.19		$3d^4\,4s(a\ ^4D)4p$	$^3D^\circ_2$	38730.67	180.66	
$3d^5\,4s(a\ ^6D)4p$	$^7D^\circ_3$	27500.37	149.34			$^3D^\circ_3$	38911.33		
	$^7D^\circ_4$	27649.71	175.74						
	$^7D^\circ_5$	27825.45				$y\ ^5F^\circ_1$	40906.46	64.83	0.004
						$^5F^\circ_2$	40971.29	114.97	1.28
	$y\ ^7P^\circ_2$	27728.87	91.36	2.341	$3d^5\,4s(a\ ^4D)4p$	$^5F^\circ_3$	41086.26	138.52	1.246
$3d^4\,4s(a\ ^5D)4p$	$^7P^\circ_3$	27820.23	115.03	1.929		$^5F^\circ_4$	41224.78	168.69	1.360
	$^7P^\circ_4$	27935.26		1.761		$^5F^\circ_5$	41393.47		------
	$y\ ^5P^\circ_1$	29420.90	163.72	2.513		$x\ ^5P^\circ_1$	40930.31	52.66	2.455
$3d^4\,4s(a\ ^6D)4p$	$^5P^\circ_2$	29584.62	240.13	1.836	$3d^4\,4s(a\ ^4D)4p$	$^5P^\circ_2$	40982.97	60.38	1.76
	$^5P^\circ_3$	29824.75		1.669		$^5P^\circ_3$	41043.35		1.640
	$z\ ^5F^\circ_1$	30787.30	71.52	0.002					
	$^5F^\circ_2$	30858.82	106.64	0.997		$y\ ^5D^\circ_0$	41224.80	64.37	−0.001
$3d^4\,4s(a\ ^6D)4p$	$^5F^\circ_3$	30965.46	140.91	1.245	$3d^4\,4s(a\ ^4D)4p$	$^5D^\circ_1$	41289.17	119.86	1.503
	$^5F^\circ_4$	31106.37	173.98	1.345		$^5D^\circ_2$	41409.03	166.07	1.504
	$^5F^\circ_5$	31280.35		1.396		$^5D^\circ_3$	41575.10	207.09	1.503
						$^5D^\circ_4$	41782.19		1.500

TABLE 5. *Odd terms of* Cr I—Continued

Electron configuration	Term symbol	Level	Interval	Observed g
$3d^4\,4s(a\,{}^4\mathrm{H})4p$	$z\,{}^5\mathrm{H}^0_3$	42025. 60	54. 21	
	${}^5\mathrm{H}^0_4$	42079. 81	73. 93	
	${}^5\mathrm{H}^0_5$	42153. 74	98. 43	
	${}^5\mathrm{H}^0_6$	42252. 17	135. 15	
	${}^5\mathrm{H}^0_7$	42387. 32		
$3d^4\,4s(b\,{}^4\mathrm{P})4p$	$x\,{}^5\mathrm{D}^0_0$	42218. 37	74. 59	−0. 003
	${}^5\mathrm{D}^0_1$	42292. 96	145. 86	1. 501
	${}^5\mathrm{D}^0_2$	42438. 82	209. 44	1. 494
	${}^5\mathrm{D}^0_3$	42648. 26	260. 31	1. 498
	${}^5\mathrm{D}^0_4$	42908. 57		1. 497
$3d^5(a\,{}^6\mathrm{S})5p$	$x\,{}^7\mathrm{P}^0_2$	42238. 04	16. 07	
	${}^7\mathrm{P}^0_3$	42254. 11	21. 09	
	${}^7\mathrm{P}^0_4$	42275. 20		
$3d^5(a\,{}^4\mathrm{G})4p$	$z\,{}^5\mathrm{G}^0_2$	42515. 35	23. 46	
	${}^5\mathrm{G}^0_3$	42538. 81	26. 04	
	${}^5\mathrm{G}^0_4$	42564. 85	24. 40	
	${}^5\mathrm{G}^0_5$	42589. 25	16. 56	
	${}^5\mathrm{G}^0_6$	42605. 81		
$3d^4\,4s(b\,{}^4\mathrm{P})4p$	$z\,{}^5\mathrm{S}^0_2$	43124. 88		
$3d^5(a\,{}^4\mathrm{P})4p$	$w\,{}^5\mathrm{P}^0_1$	44125. 90	61. 02	
	${}^5\mathrm{P}^0_2$	44186. 92	72. 44	
	${}^5\mathrm{P}^0_3$	44259. 36		
$3d^4\,4s(a\,{}^4\mathrm{H})4p$	$z\,{}^5\mathrm{I}^0_4$	44246. 70	61. 26	
	${}^5\mathrm{I}^0_5$	44307. 96	85. 14	
	${}^5\mathrm{I}^0_6$	44393. 10	121. 34	
	${}^5\mathrm{I}^0_7$	44514. 44	152. 11	
	${}^5\mathrm{I}^0_8$	44666. 55		
$3d^4\,4s(a\,{}^4\mathrm{H})4p$	$y\,{}^5\mathrm{G}^0_2$	44299. 98	73. 36	
	${}^5\mathrm{G}^0_3$	44373. 34	161. 12	
	${}^5\mathrm{G}^0_4$	44534. 46	57. 00	
	${}^5\mathrm{G}^0_5$	44591. 46	154. 80	
	${}^5\mathrm{G}^0_6$	44746. 26		
$3d^4\,4s(b\,{}^4\mathrm{P})4p$	$v\,{}^5\mathrm{P}^0_1$	44666. 74	208. 45	
	${}^5\mathrm{P}^0_2$	44875. 19	238. 03	
	${}^5\mathrm{P}^0_3$	45113. 22		
$3d^4\,4s(a\,{}^4\mathrm{F})4p$	$x\,{}^5\mathrm{F}^0_1$	45201. 84	23. 36	
	${}^5\mathrm{F}^0_2$	45225. 20	30. 31	
	${}^5\mathrm{F}^0_3$	45255. 51	30. 57	
	${}^5\mathrm{F}^0_4$	45286. 08	20. 37	
	${}^5\mathrm{F}^0_5$	45306. 45		
$3d^5(a\,{}^4\mathrm{G})4p$	$z\,{}^3\mathrm{H}^0_6$	45348. 73	−5. 45	
	${}^3\mathrm{H}^0_5$	45354. 18	−4. 45	
	${}^3\mathrm{H}^0_4$	45358. 63		
$3d^5(a\,{}^4\mathrm{G})4p$	$y\,{}^5\mathrm{H}^0_3$	45566. 02	48. 86	
	${}^5\mathrm{H}^0_4$	45614. 88	48. 40	
	${}^5\mathrm{H}^0_5$	45663. 28	44. 08	
	${}^5\mathrm{H}^0_6$	45707. 36	34. 13	
	${}^5\mathrm{H}^0_7$	45741. 49		
$3d^5(a\,{}^4\mathrm{P})4p$	$y\,{}^3\mathrm{P}^0_0$	45722. 59	−3. 39	
	${}^3\mathrm{P}^0_1$	45719. 20	15. 12	
	${}^3\mathrm{P}^0_2$	45734. 32		
$3d^5(a\,{}^4\mathrm{G})4p$	$y\,{}^3\mathrm{F}^0_2$	45966. 45	33. 91	
	${}^3\mathrm{F}^0_3$	46000. 36	57. 84	
	${}^3\mathrm{F}^0_4$	46058. 20		
$3d^5(a\,{}^4\mathrm{P})4p$	$y\,{}^3\mathrm{D}^0_1$	46077. 09	32. 17	
	${}^3\mathrm{D}^0_2$	46109. 26	65. 14	
	${}^3\mathrm{D}^0_3$	46174. 40		
$3d^5\,(a\,{}^4\mathrm{P})4p$	$w\,{}^5\mathrm{D}^0_0$	46081. 27	217. 05	
	${}^5\mathrm{D}^0_1$	46298. 32	51. 18	
	${}^5\mathrm{D}^0_2$	46349. 50	18. 85	
	${}^5\mathrm{D}^0_3$	46368. 35	54. 11	
	${}^5\mathrm{D}^0_4$	46422. 46		
$3d^5\,(a\,{}^4\mathrm{G})4p$	$w\,{}^5\mathrm{F}^0_1$	46678. 35	−1. 29	
	${}^5\mathrm{F}^0_2$	46677. 06	11. 18	
	${}^5\mathrm{F}^0_3$	46688. 24	32. 30	
	${}^5\mathrm{F}^0_4$	46720. 54	−15. 56	
	${}^5\mathrm{F}^0_5$	46704. 98		
$3d^4\,4s(a\,{}^4\mathrm{H})4p$	$z\,{}^5\mathrm{G}^0_2$	46846. 77	58. 26	
	${}^5\mathrm{G}^0_3$	46905. 03	80. 84	
	${}^5\mathrm{G}^0_4$	46985. 87		
$3d^4\,4s(c\,{}^4\mathrm{D})4p$	$u\,{}^5\mathrm{P}^0_3$	46878. 61	−89. 09	
	${}^5\mathrm{P}^0_2$	46967. 70	−54. 05	
	${}^5\mathrm{P}^0_1$	47021. 75		
$3d^4\,4s(b^4\,\mathrm{G})4p$	$x\,{}^5\mathrm{G}^0_2$	47047. 47	78. 23	
	${}^5\mathrm{G}^0_3$	47125. 70	64. 17	
	${}^5\mathrm{G}^0_4$	47189. 87	38. 93	
	${}^5\mathrm{G}^0_5$	47228. 80	−6. 53	
	${}^5\mathrm{G}^0_6$	47222. 27		
$3d^5\,(a\,{}^4\mathrm{G})4p$	$y\,{}^3\mathrm{G}^0_3$	47048. 48	6. 43	
	${}^3\mathrm{G}^0_4$	47054. 91	0. 40	
	${}^3\mathrm{G}^0_5$	47055. 31		
$3d^4\,4s(b\,{}^4\mathrm{P})4p$	$z\,{}^3\mathrm{S}^0_1$	47088. 40		
$3d^4\,4s(a\,{}^4\mathrm{H})4p$	$z\,{}^3\mathrm{I}^0_5$	47586. 06	44. 37	
	${}^3\mathrm{I}^0_6$	47630. 43	62. 20	
	${}^3\mathrm{I}^0_7$	47692. 63		
$3d^4\,4s(b\,{}^4\mathrm{G})4p$	$x\,{}^5\mathrm{H}^0_3$	47621. 31	67. 20	
	${}^5\mathrm{H}^0_4$	47688. 51	105. 31	
	${}^5\mathrm{H}^0_5$	47793. 82	148. 47	
	${}^5\mathrm{H}^0_6$	47942. 29	197. 89	
	${}^5\mathrm{H}^0_7$	48140. 18		
$3d^5\,(b\,{}^4\mathrm{D})4p$	$v\,{}^5\mathrm{F}^0_1$	47629. 66	1. 85	
	${}^5\mathrm{F}^0_2$	47631. 51	4. 74	
	${}^5\mathrm{F}^0_3$	47636. 25	3. 59	
	${}^5\mathrm{F}^0_4$	47639. 84	4. 92	
	${}^5\mathrm{F}^0_5$	47644. 76		
$3d^5\,(a\,{}^6\mathrm{S})6p$	$w\,{}^7\mathrm{P}^0_2$	47697. 44	11. 15	
	${}^7\mathrm{P}^0_3$	47708. 59	10. 49	
	${}^7\mathrm{P}^0_4$	47719. 08		
$3d^5\,(b\,{}^4\mathrm{D})4p$	$v\,{}^5\mathrm{D}^0_0$	47788. 08	−15. 78	
	${}^5\mathrm{D}^0_1$	47772. 30	13. 80	
	${}^5\mathrm{D}^0_2$	47786. 10	28. 30	
	${}^5\mathrm{D}^0_3$	47814. 40	52. 08	
	${}^5\mathrm{D}^0_4$	47866. 48		
$3d^4\,4s(b\,{}^4\mathrm{G})4p$	$u\,{}^5\mathrm{F}^0_1$	47877. 55	40. 38	
	${}^5\mathrm{F}^0_2$	47917. 93	56. 60	
	${}^5\mathrm{F}^0_3$	47974. 53	39. 87	
	${}^5\mathrm{F}^0_4$	48014. 40	−28. 64	
	${}^5\mathrm{F}^0_5$	47985. 76		
$3d^4\,4s(c\,{}^4\mathrm{D})4p$	$t\,{}^5\mathrm{F}^0_1$	48210. 04	7. 79	
	${}^5\mathrm{F}^0_2$	48217. 83	34. 08	
	${}^5\mathrm{F}^0_3$	48251. 91	−209. 08	
	${}^5\mathrm{F}^0_4$	48042. 80		
	${}^5\mathrm{F}^0_5$	. . .		
$3d^4\,4s(b\,{}^4\mathrm{P})4p$	$x\,{}^3\mathrm{P}^0_0$	48226. 36	104. 94	
	${}^3\mathrm{P}^0_1$	48331. 30	127. 37	
	${}^3\mathrm{P}^0_2$	48458. 67		

TABLE 5. *Odd terms of* Cr I—Continued

Electron configuration	Term symbol	Level	Interval	Observed g
$3d^4\,4s(a\,^4H)4p$	$y\,^3H_4^\circ$	48288.37	22.02	
	$^3H_5^\circ$	48310.39	134.96	
	$^3H_6^\circ$	48445.35		
$3d^4\,4s(a\,^4F)4p$	$x\,^3G_3^\circ$	48515.08	47.08	
	$^3G_4^\circ$	48562.16	224.23	
	$^3G_5^\circ$	48786.39		
	1_3°	48636.14		
$3d^4\,4s(b\,^4P)4p$	$x\,^3D_1^\circ$	48839.90	187.68	
	$^3D_2^\circ$	49027.58	283.28	
	$^3D_3^\circ$	49310.86		
$3d^4\,4s(b\,^4G)4p$	$w\,^3G_3^\circ$	49370.70	83.24	
	$^3G_4^\circ$	49453.94	84.12	
	$^3G_5^\circ$	49538.06		
$3d^4\,4s(a\,^4F)4p$	$w\,^5G_2^\circ$	49466.77	52.95	
	$^5G_3^\circ$	49519.72	53.31	
	$^5G_4^\circ$	49573.03	44.58	
	$^5G_5^\circ$	49617.61	17.55	
	$^5G_6^\circ$	49635.16		
$3d^5\,(a\,^4P)4p$	$y\,^3S_1^\circ$	49477.04		
$3d^4\,4s(a\,^6D)5p$	$t\,^5P_1^\circ$	49588.97	9.11	
	$^5P_2^\circ$	49598.08	214.38	
	$^5P_3^\circ$	49812.46		
$3d^5(b\,^4D)4p$	$x\,^3F_4^\circ$	49620.69	−29.53	
	$^3F_3^\circ$	49650.22	−2.54	
	$^3F_2^\circ$	49652.76		
$3d^5(a\,^4P)4p$	$y\,^5S_2^\circ$	49822.59		
$3d^4\,4s(a\,^6D)5p$	$s\,^5F_1^\circ$	50018.80	38.81	
	$^5F_2^\circ$	50057.61	44.43	
	$^5F_3^\circ$	50102.04	108.83	
	$^5F_4^\circ$	50210.87	42.10	
	$^5F_5^\circ$	50253.27		
$3d^5(b\,^4D)4p$	$w\,^3D_1^\circ$	50105.54	78.56	
	$^3D_2^\circ$	50184.10	80.38	
	$^3D_3^\circ$	50264.48		
$3d^4\,4s(c\,^4D)4p$	$u\,^5D_4^\circ$	50557.56	−70.55	
	$^5D_3^\circ$	50628.11	−26.65	
	$^5D_2^\circ$	50654.76	−8.01	
	$^5D_1^\circ$	50662.77	1.57	
	$^5D_0^\circ$	50661.20		
$3d^4\,4s(a\,^4F)4p$	$w\,^3F_3^\circ$	50890.15	60.27	
	$^3F_2^\circ$	50950.42	109.37	
	$^3F_4^\circ$	51059.79		
$3d^5(b\,^4D)4p$	$w\,^3P_0^\circ$	51176.88	69.99	
	$^3P_1^\circ$	51246.87	39.65	
	$^3P_2^\circ$	51286.52		
$3d^5(a\,^2I)4p$	$z\,^1H_5^\circ$	51401.24		
$3d^4\,4s(a\,^4F)4p$	$t\,^5D_0^\circ$	51999.62		
	$^5D_1^\circ$	52003.06	3.44	
	$^5D_2^\circ$	52012.44	9.38	
	$^5D_3^\circ$	52031.72	19.28	
	$^5D_4^\circ$	52064.27	32.55	
$3d^5(a\,^2I)4p$	$y\,^3I_5^\circ$	52591.94	68.67	
	$^3I_6^\circ$	52660.61	17.27	
	$^3I_7^\circ$	52677.88		

Electron configuration	Term symbol	Level	Interval	Observed g
	2_1°	52720.07		
$3d^4\,4s(b\,^4G)4p$	$x\,^3H_3^\circ$	52914.94	29.55	
	$^3H_5^\circ$	52885.39	−78.05	
	$^3H_4^\circ$	52963.44		
$3d^5(b\,^4F)4p$	$r\,^5F_1^\circ$	53011.65	25.87	
	$^5F_2^\circ$	53037.52	36.38	
	$^5F_3^\circ$	53073.90	43.64	
	$^5F_4^\circ$	53117.54	54.79	
	$^5F_5^\circ$	53172.33		
$3d^4\,4s(a\,^6D)5p$	$s\,^5D_0^\circ$	--------		
	$^5D_1^\circ$	--------	-------	
	$^5D_2^\circ$	53541.25	-------	
	$^5D_3^\circ$	53640.74	99.49	
	$^5D_4^\circ$	53782.77	142.03	
$3d^4\,4s(a\,^2H)4p$	$v\,^3G_3^\circ$	53804.84	122.75	
	$^3G_4^\circ$	53927.59	150.54	
	$^3G_5^\circ$	54078.13		
$3d^4\,4s(a\,^4D)5p$	$s\,^5P_1^\circ$	53963.05	69.58	
	$^5P_2^\circ$	54032.63	100.25	
	$^5P_3^\circ$	54132.88		
$3d^4\,4s(a\,^4D)5p$	$q\,^5F_1^\circ$	54198.23	53.96	
	$^5F_2^\circ$	54252.19	76.76	
	$^5F_3^\circ$	54328.95	96.34	
	$^5F_4^\circ$	54425.29	111.24	
	$^5F_5^\circ$	54536.53		
$3d^5(a\,^2I)4p$	$z\,^3K_8^\circ$	54316.83	88.11	
	K_7°	54404.94	93.33	
	K_8°	54498.27		
$3d^4\,4s(a\,^2H)4p$	$w\,^3H_4^\circ$	54736.55	62.63	
	$^3H_5^\circ$	54799.18	87.64	
	$^3H_6^\circ$	54886.82		
$3d^4\,4s(a\,^2H)4p$	$z\,^1I_6^\circ$	54800.26		
$3d^5(a\,^2I)4p$	$v\,^3H_4^\circ$	54810.94	118.78	
	$^3H_5^\circ$	54929.72	−63.15	
	$^3H_6^\circ$	54866.57		
$3d^5(a\,^2D)4p$	$v\,^3D_1^\circ$	54956.59	196.04	
	$^3D_2^\circ$	55152.63	299.01	
	$^3D_3^\circ$	55451.64		
$3d^5(a\,^2I)4p$	$z\,^1K_7^\circ$	54970.23		
$3d^4\,4s(b\,^2F)4p$	$v\,^3F_2^\circ$	54992.93	108.94	
	$^3F_3^\circ$	55101.87	105.53	
	$^3F_4^\circ$	55207.40		
$3d^5(a\,^2F)4p$	$u\,^3F_4^\circ$	55120.77	−231.95	
	$^3F_3^\circ$	55352.72	−120.95	
	$^3F_2^\circ$	55473.67		
$3d^5(a\,^2I)4p$	$y\,^1I_6^\circ$	55516.69		
$3d^4\,4s(a\,^2H)4p$	$x\,^3I_5^\circ$	55686.46	54.65	
	$^3I_6^\circ$	55741.11	57.99	
	$^3I_7^\circ$	55799.10		
$3d^5(b^2\,H)4p$	$u\,^3H_6^\circ$	55908.12	33.14	
	$^3H_5^\circ$	55874.98	−40.52	
	$^3H_4^\circ$	55915.50		
$3d^4\,4s(a\,^2H)4p$	$y\,^1H_5^\circ$	55945.08		

TABLE 5. *Odd terms of* Cr I—Continued

Electron configuration	Term symbol	Level	Interval	Observed g
$3d^5(b\ ^4F)4p$	$v\ ^5G^0_2$	56155. 12		
	$^5G^0_3$	56209. 81	54. 69	
	$^5G^0_4$	56279. 56	69. 75	
	$^5G^0_5$	56361. 86	82. 30	
	$^5G^0_6$	56449. 10	87. 24	
$3d^5(a\ ^2D)4p$	$v\ ^3P^0_2$	56591. 88		
	$^3P^0_1$	56722. 60	−130. 72	
	$^3P^0_0$	56802. 50	−79. 90	
$3d^5(a\ ^2G)4p$	$u\ ^3G^0_5$	56985. 67		
	$^3G^0_4$	57033. 60	47. 93	
	$^3G^0_3$	57088. 25	54. 65	
$3d^5(b\ ^2S)4p$	$u\ ^3P^0_2$	57087. 70		
	$^3P^0_1$	57132. 59	−44. 89	
	$^3P^0_0$	57154. 59	−22. 00	
$3d^4\ 4s(a\ ^6D)6p$	$p\ ^5F^0_1$	57096. 62		
	$^5F^0_2$	57100. 66	4. 04	
	$^5F^0_3$	57186. 60	85. 94	
	$^5F^0_4$	57237. 50	50. 90	
	$^5F^0_5$	57327. 66	90. 16	
	4^0_3	57141. 85		
$3d^5(c\ ^2F)4p$	$t\ ^3F^0_2$	57220. 67		
	$^3F^0_3$	57276. 42	55. 75	
	$^3F^0_4$	57335. 47	59. 05	
$3d^4\ 4s(b\ ^2F)4p$	$t\ ^3G^0_3$	57557. 03		
	$^3G^0_4$	57587. 36	30. 33	
	$^3G^0_5$	57702. 36	115. 00	
$3d^4\ 4s(a\ ^4D)5p$	$r\ ^5D^0_0$	57958. 42		
	$^5D^0_1$	57995. 04	36. 62	
	$^5D^0_2$	58063. 80	68. 76	
	$^5D^0_3$	58147. 76	83. 96	
	$^5D^0_4$	58292. 62	144. 86	
$3d^5(a\ ^2D)4p$	$s\ ^3F^0_2$	58162. 84		
	$^3F^0_3$	58202. 65	39. 81	
	$^3F^0_4$	58167. 89	−34. 76	
$3d^4\ 4s(a\ ^2P)4p$	$u\ ^3D^0_1$	58725. 28		
	$^3D^0_2$	58860. 23	134. 95	
	$^3D^0_3$	59122. 15	261. 92	
$3d^4\ 4s(a\ ^2G)4p$	$t\ ^3H^0_4$	58728. 29		
	$^3H^0_5$	58754. 58	26. 29	
	$^3H^0_6$	58775. 36	20. 78	
$3d^5(a\ ^2F)4p$	$t\ ^3D^0_1$	58870. 20		
	$^3D^0_2$	58772. 03	−98. 17	
	$^3D^0_3$	58924. 12	152. 09	
$3d^4\ 4s(a\ ^2G)4p$	$r\ ^3F^0_2$	59357. 90		
	$^3F^0_3$	59417. 01	59. 11	
	$^3F^0_4$	59487. 71	70. 70	
$3d^5(b\ ^2H)4p$	$w\ ^3I^0_4$	59806. 27		
	$^3I^0_5$	59884. 27	78. 00	
	$^3I^0_7$	59957. 46	73. 19	
$3d^5(b\ ^2H)4p$	$x\ ^1H^0_5$	60005. 60		
$3d^4\ 4s(a\ ^2P)4p$	$x\ ^3S^0_1$	60084. 09		
$3d^4\ 4s(a\ ^6D)6p$	$q\ ^5D^0_0$	60241. 5		
	$^5D^0_1$	60291. 04	49. 5	
	$^5D^0_2$	60374. 94	83. 90	
	$^5D^0_3$	60493. 42	118. 48	
	$^5D^0_4$	60627. 96	134. 54	
$3d^5(d\ ^2G)4p$	$q\ ^3F^0_2$	60253. 00		
	$^3F^0_3$	60326. 04	73. 04	
	$^3F^0_4$	60367. 38	41. 34	
$3d^5\ 4s(b\ ^2I)4p$	$v\ ^3I^0_5$	60427. 63		
	$^3I^0_6$	60527. 55	99. 92	
	$^3I^0_7$	60656. 97	129. 42	
$3d^5(b\ ^2H)4p$	$x\ ^1I^0_6$	60441. 42		
$3d^5(b^2H)4p$	$s\ ^3G^0_3$	60467. 85		
	$^3G^0_4$	60503. 94	−36. 09	
	$^3G^0_5$	60518. 16	−14. 22	
$3d^5(b^2F)4p$	$s\ ^3D^0_1$	60615. 84		
	$^3D^0_2$	60629. 87	−14. 03	
	$^3D^0_3$	60678. 12	−48. 25	
$3d^4 4s(a^4D)6p$	$o\ ^5F^0_1$	60683. 53		
	$^5F^0_2$	60781. 25	97. 72	
	$^5F^0_3$	60904. 84	123. 59	
	$^5F^0_4$	61056. 41	151. 57	
	$^5F^0_5$	61184. 95	139. 43	
$3d^4 4s(c^3G)4p$	$p\ ^3F^0_2$	. . .		
	$^3F^0_3$	60819. 50	141. 08	
	$^3F^0_4$	60960. 58		
$3d^4 4s(c^3G)4p$	$s\ ^3H^0_4$	60870. 63		
	$^3H^0_5$	61008. 07	137. 44	
	$^3H^0_6$	61191. 64	183. 57	
$3d^4 4s(a^4D)6p$	$r\ ^5P^0_1$	61065. 96		
	$^5P^0_2$	61107. 95	41. 99	
	$^5P^0_3$	61198. 68	90. 73	
$3d^5(b^2F)4p$	$r\ ^3G^0_3$	61078. 28		
	$^3G^0_4$	61123. 20	44. 92	
	$^3G^0_5$	61161. 35	38. 15	
$3d^4 4s(a^2P)4p$	$t\ ^3P^0_2$	61387. 86		
	$^3P^0_1$	61527. 34	139. 48	
	$^3P^0_0$	61675. 72	148. 38	
$3d^4 4s(c^2G)4p$	$q\ ^3G^0_3$	61930. 05		
	$^3G^0_4$	61976. 50	46. 55	
	$^3G^0_5$	62037. 60	61. 10	
$3d^4 4s(b^2I)4p$	$r\ ^3H^0_4$	62762. 06		
	$^3H^0_5$	62830. 26	68. 20	
	$^3H^0_6$	62903. 03	72. 77	
	$q\ ^3H^0_4$	63116. 80		
	$^3H^0_5$	63144. 36	27. 56	
	$^3H^0_6$	63182. 94	38. 58	
$3d^5(d^2G)4p$	$p\ ^3H^0_4$	63841. 81		
	$^3H^0_5$	63927. 27	85. 46	
	$^3H^0_6$	63997. 86	70. 59	
$3d^5(d^2G)4p$	$p\ ^3G^0_3$	66008. 95		
	$^3G^0_4$	66094. 06	85. 11	
	$^3G^0_5$	66180. 34	86. 28	

TABLE 6. CrO *band-heads*

Wave-length	In-tensity	Wave number	Wave-length	In-tensity	Wave number
11035. 8	2	9058. 9	6396. 12	25	15630. 17
10985. 26	3	9100. 6	6394. 46	40	15634. 23
10941. 25	3	9137. 2	6364. 40	10	15708. 07
10179. 95	2	9820. 6	6295. 59	4	15879. 75
9317. 2	1	10729. 9	6244. 35	10	16010. 06
8675. 7	2	11523. 3	6119. 98	15	16335. 41
8360. 07	5	11958. 34	6058. 54	25	16501. 07
8338. 18	8	11989. 73	6055. 00	10	16510. 72
8173. 36	3	12231. 51	6053. 45	8	16514. 94
8028. 3	2*h*	12452. 52	6051. 76	50	16519. 56
7842. 8	5	12747. 05	6025. 01	15	16592. 90
7369. 3	10	13566. 08	5885. 84	15	16985. 23
7327. 4	5	13643. 65	5806. 74	10	17216. 60
7213. 4	4	13859. 27	5794. 50	15	17252. 97
7190. 1	2	13904. 19	5744. 72	12	17402. 47
7172. 5	3	13938. 30	5673. 06	20	17622. 29
6829. 37	4	14638. 61	5635. 96	30	17738. 30
6772. 23	20	14762. 12	5564. 15	20	17967. 22
6453. 32	10	15491. 63	5550. 76	8	18010. 56
6397. 87	30	15625. 89	5546. 48	8	18024. 46

TABLE 7. *Series in* Cr I

$3d^5\,ns$ series		$3d^5\,np$ series	$3d^5\,nd$ series
^7S terms	^5S terms	$^7P^\circ$ terms	^7D terms
$a\ ^7S_3$ 54570 $e\ ^7S_3$ 17674 $f\ ^7S_3$ 8927 $g\ ^7S_3$ 5392	$a\ ^5S_2$ 46977 $e\ ^5S_2$ 16687 $f\ ^5S_2$ 8602 $g\ ^5S_2$ 5249 $h\ ^5S_2$ 3534	$z\ ^7P^\circ_4$ 31071 $x\ ^7P^\circ_4$ 12295 $w\ ^7P^\circ_4$ 6851	$e\ ^7D_5$ 12310 $g\ ^7D_5$ 6861
$L=31071$ cm^{-1} $\alpha=+0.5161$ $\beta=-0.0980$	$L=27782$ cm^{-1} $\alpha=+0.5772$ $\beta=-0.0488$	$L=54570$ cm^{-1} $\alpha=+1.0196$ $\beta=-0.1399$	$L=31071$ cm^{-1} $\alpha=+2.0038$ $\beta=-0.0181$

TABLE 8. *Classification of some infrared lines of* Cr I

Term combination	Calculated wave number	Calculated wavelength	Observed wavelength and intensity R. and B [4]	Solar wavelength and intensity G. M. and McM [45]
	cm^{-1}	*A*	*A*	*A*
$e\ ^7S_3-x\ ^7P^\circ_4$	5342. 31	18718. 50	18717. 0(20)	
$e\ ^7S_3-x\ ^7P^\circ_3$	5358. 38	18662. 36	18654. 2(30)	
$e\ ^7S_3-x\ ^7P^\circ_2$	5379. 47	18589. 19	18583. 5(30)	
$e\ ^5S_2-w\ ^5P^\circ_1$	6242. 56	16019. 16	----------	16021. 7?+atm.
$e\ ^5S_2-w\ ^5P^\circ_2$	6303. 58	15864. 00	15860. 5(30)	15863. 7(12)+atm.
$e\ ^5S_2-w\ ^5P^\circ_3$	6376. 02	15683. 77	15680. 0(30)	15683. 6(4)

TABLE 9. *Theoretical and observed terms of* Cr I

Electron configuration $1s^2 2s^2 2p^6 3s^2 3p^6 +$	Theoretical and observed terms
$3d^5\,4s$	^{7,5}**S** ^{5,3}(**GFDP**) ^{3,1}(**IGFDS**) ^{3,1}(**HGF**DP) ^{3,1}D
$3d^4\,4s^2$	^{5}**D** ^{3}(**HGFDP**) ^{1}(**IGFDS**) ^{3}(FP) ^{1}(GDS)
$3d^6$	^{5}**D** ^{3}(HGFDP) ^{1}(IGFDS) ^{3}(FP) ^{1}(GDS)
$3d^5\,4p$	^{7,5}**P**° ^{5,3}(**HGF**)° ^{5,3}(**GFD**)° ^{5,3}(**FDP**)° ^{5,3}(**DPS**)° ^{3,1}(**KIH**)° ^{3,1}(**HGF**)° ^{3,1}(**GFD**)° ^{3,1}(**FDP**)° ^{3,1}**P**° ^{3,1}(**IHG**)° ^{3,1}(**HGF**)° ^{3,1}(**GFD**)° ^{3,1}(FDP)° ^{3,1}(DPS)° ^{3,1}(FDP)°
$3d^4\,4s\,4p'_4$	^{7,5}(**FDP**)° ^{5,3}(**FDP**)° ^{5,3}(**IHG**)° ^{3,1}(**IHG**)° ^{5,3}(**HGF**)° ^{3,1}(HGF)° ^{5,3}(**GFD**)° ^{3,1}(GFD)° ^{5,3}(**FDP**)° ^{3,1}(FDP)° ^{5,3}(**DPS**)° ^{3,1}(**DPS**)° ^{3,1}(**HGF**)° ^{3,1}(KIH)° ^{3,1}(GFD)° ^{3,1}(FDP)° ^{3,1}P° ^{5,3}(GFD)° ^{3,1}(GFD)° ^{5,3}(DPS)° ^{3,1}(DPS)° ^{3,1}(HGF)° ^{3,1}(FDP)° ^{3,1}P°
$3d^5\,ns$	^{7,5}**S** ^{5,3}(**GFDP**), etc.
$3d^5\,np$	^{7,5}**P**° ^{5,3}(HGF)° ^{5,3}(GFD)° ^{5,3}(FDP)° ^{5,3}(DPS)°, etc.
$3d^5\,nd$	^{7,5}**D** ^{5,3}(IHGFD), etc.
$3d^4\,4s\,ns$	^{7,5}**D** ^{5,3}**D** ^{5,3}(**HGFDP**), etc.
$3d^4\,4s\,np$	^{7,5}(**FDP**)° ^{5,3}(**FDP**)°
$3d^4\,4s\,nd$	^{7,5}(**GFDPS**) ^{5,3}(GFDPS), etc.
$3d^4\,4p^2$	^{7,5,3}(FDP) ^{3}(GFDPS) ^{5}D, etc.

5. References

[1] K. W. Meissner, Ann. Physik [IV] **50,** 713 (1916).
[2] C. C. Kiess and W. F. Meggers, BS Sci. Pap. **16,** 51 (1920) S372.
[3] L. Stüting, Z. wiss. Phot. **7,** 73 (1909).
[4] H. M. Randall and E. F. Barker, Astrophys. J. **49,** 54 (1919).
[5] R. Richter, Dissertation (Göttingen, Germany, 1914).
[6] W. Miller, Ann. Physik [IV] **24,** 105 (1907).
[7] M. Catalán, Phil. Trans. Roy. Soc. (London) [A] **223,** 127 (1922).
[8] H. Gieseler, Ann. Physik [IV] **69,** 147 (1922).
[9] C. C. and H. K. Kiess, Science **56,** 666 (1922).
[10] M. A. Catalán, Compt. rend. **176,** 84, 1063 (1923).
[11] M. A. Catalán, Anales soc. espan. fis. quim. **21,** 84 (1923).
[12] H. Gieseler, Z. Physik **22,** 228 (1924).
[13] W. F. Meggers, C. C. Kiess, and F. M. Walters, Jr., J. Opt. Soc. Am. and Rev. Sci. Instr. **9,** 355 (1924).
[14] A. S. King, Astrophys. J. **41,** 86 (1915).
[15] J. E. Purvis, Proc. Cambridge Phil. Soc. [I] **14,** 41 (1906).
[16] W. Miller, Dissertation (Göttingen, Germany, 1906); Ann. Physik [IV] **24,** 105 (1907).
[17] W. Hartmann, Dissertation (Halle, Germany, 1907).
[18] H. D. Babcock, Astrophys. J. **33,** 217 (1911), and unpublished.
[19] R. Richter, Dissertation (Göttingen, Germany, 1914).
[20] A. S. King, Astrophys. J. **60,** 282 (1924).
[21] H. Gieseler and W. Grotrian, Z. Physik **22,** 245 (1924).
[22] R. V. Zumstein, Phys. Rev. **27,** 562 (1926).
[23] E. O. Hulburt, Phys. Rev. **24,** 129 (1924).
[24] A. W. Smith and M. Muskat, Phys. Rev. **29,** 663 (1927).
[25] C. C. Kiess, BS J. Research **5,** 775 (1930) RP229.
[26] M. A. Catalán and P. M. Sancho, Anales soc. espan. fis. quim. **29,** 327 (1931).
[27] C. C. Kiess, J. Research NBS **15,** 79 (1935) RP812.
[28] C. C. Kiess, J. Research NBS **47,** 385 (1951) RP2266.
[29] IAU Transactions **6,** 100 (1938).
[30] A. S. King, Astrophys. J. **41,** 167 (1915); **60,** 282 (1924).
[31] R. Frerichs, Ann. Physik [IV] **81,** 807 (1926).
[32] J. S. V. Allen and C. E. Hesthal, Phys. Rev. **47,** 926 (1935).
[33] A. J. Hill and R. B. King, J. Optical Soc. Am. **41,** 315 (1951).
[34] H. N. Russell, Proc. Nat. Acad. Sci. **11,** 322 (1925).
[35] A. Sommerfeld, Atombau und Spektrallinien, 4te Auflage, S. 670 (F. Vieweg und Sohn, Braunschweig, Germany, 1924).
[36] C. C. Kiess and G. Shortley, J. Research NBS **42,** 183 (1949) RP1961.
[37] H. Gieseler, Z. Physik **22,** 242 (1924).
[38] H. Gieseler, Z. Physik **22,** 228 (1924).
[39] C. E. Moore, Atomic Energy Levels, NBS Circ. 467 (1952).
[40] A. G. Shenstone, Phil. Trans. Roy. Soc. London [A] **235,** 195 (1936).
[41] D. N. Davis, Astrophys. J. **106,** 28 (1947).
[42] R. Mecke and M. Guillery, Phys. Z. **28,** 514 (1927).
[43] W. F. C. Ferguson, J. Research NBS **8,** 381 (1932) RP423.
[44] C. Ghosh, Z. Physik **78,** 521 (1932).
[45] L. Goldberg, O. C. Mohler, and R. F. McMath, Astrophys. J. **109,** 28, (1949).

WASHINGTON, March 10, 1953.

U. S. GOVERNMENT PRINTING OFFICE: 1953

UNIVERSITY OF MICHIGAN
GENERAL LIBRARY
DOCUMENTS DIVISION
1276 ANN ARBOR MICH

Journal of Research of the National Bureau of Standards Vol. 55, No. 5 November 19

Contents

		Page
Metal ultrasonic delay lines. Russell W. Meiss, John H. Darr, and John D. Grimsley.	RP2453	209
A radio-frequency permeameter. Peter H. Haas.	RP2454	221
On mildly nonlinear partial difference equations of elliptic type. Lipman Bers.	RP2455	229
Determination of glucose by means of sodium chlorite. Herbert F. Launer, William K. Wilson, and Joseph E. Flynn.	RP2456	237
Description and analysis of the first spectrum of Chromium, Cr I. Carl C. Kiess.	RP2457	245

Single copies of the above Research Papers are available for sale by the Superintendent of Documents, U.S. Government Printing Office, Washington 25, D.C. Subscription price $4.50 a year; $1.25 additional for foreign mailing. Remittance should be sent directly to the Superintendent of Documents, and not to the National Bureau of Standards. Reprints of these papers may be purchased from the Superintendent of Documents at 5 cents each.

PRINTED AT THE GOVERNMENT PRINTING OFFICE, WASHINGTON, D.C.